

Hydrologic Modelling of Humber River Basin

by

HASAB-UL ALAM CHOWDHURY

A Thesis submitted to the

School of Graduate Studies

in partial fulfillment of the requirements for the degree of

Master of Engineering

Faculty of Engineering and Applied Science

Memorial University of Newfoundland

May 2019

St. John's, Newfoundland

ABSTRACT

The physiographic features of Newfoundland create many challenges for hydrological analysis of watersheds on the island. The most recent glaciations have deepened valleys and altered drainage networks due to the deposition of glacial drift material. The Humber River Basin (HRB), located on the west coast of Newfoundland, is the second largest river basin (7068 Km²) on the island, and several communities within the basin are subject to flooding due to extreme events. It is expected that the magnitude and frequency of extreme events will increase with climate change, and impact analyses are required to assess vulnerability of communities within the basin to climate change. For proper assessment, a hydrologic model is indispensable for the watershed in this complex terrain. The present study analyzed the streamflow derived from the drainage basin by cold regions hydrological simulation. The Cold Regions Hydrological Modelling platform (CRHM) was used to create a hydrological model for HRB boreal regions with physically-based modules were also sequentially linked in CRHM to simulate snow processes, frozen soils, variable contributing area and wetland storage and runoff generation. Nine “research basins” (RBs) were defined and each was divided into thirteen hydrological response units (HRUs): forest, forest wetland, roads, settlement, cropland, trees, treed wetland, water, grassland unmanaged, other land, wetland, wetland shrub, wetland herb etc. Model observation data such as temperature, relative humidity, wind speed and precipitation were collected from Environment Canada weather stations. Various model parameters were estimated by using SRTM digital elevation model (DEM), the advanced very high-resolution radiometer (AVHRR) land cover data, and stream network and wetland inventory GIS data. Some parameters were collected from Lower Smoky River Basin datasets. Model simulations were conducted for 2001-2010 and calibration was performed. The model performance for streamflow was evaluated against field observations and it could capture the timing and magnitude of basin discharge but underestimated the peak discharge.

ACKNOWLEDGEMENTS

I express my sincere gratitude and indebtedness to my supervisor Dr. Joseph A. Daraio, Assistant Professor, Faculty of Engineering and Applied Science, Memorial University of Newfoundland, for his dynamic guidance, continuous support and effective appreciation during this study. His devotion to this study has made the process of completing the study and the realization of this dissertation truly enjoyable.

I express my deep sense of gratitude to Dr. Kevin Shook for his encouragement, technical assistance and guidance. I highly appreciate for his advice, assistance and kindness in providing all possible help.

I thank all my friends, especially my roommates, for always being there for me. I gratefully acknowledge my parents and family members for motivating me to complete my research and their loving concern, continuous encouragement and support, without which the work would not have been completed.

Finally, I am grateful to the Almighty who has given me the opportunity and strength to complete this research work.

Table of Contents

| | |
|--|------|
| ABSTRACT | ii |
| ACKNOWLEDGEMENTS | iii |
| Table of Contents | iv |
| List of Tables | ix |
| List of Figures | xiii |
| List of Abbreviations | xx |
| List of Appendices | xxiv |
| Chapter 1 Introduction | 1 |
| 1.1 Background | 1 |
| 1.2 Study Objectives | 2 |
| 1.3 Organization of Thesis | 2 |
| Chapter 2 Literature Review | 4 |
| 2.1 Hydrological Modelling | 4 |
| 2.2 Hydrological Modelling for Humber River Basin | 5 |

| | |
|--|----|
| 2.2.1 Streamflow Synthesis and Reservoir Regulation Model (SSARR)..... | 5 |
| 2.2.2 Dynamic Regression Model..... | 9 |
| 2.2.3 Rainfall-Runoff Routing Model..... | 12 |
| 2.2.4 Artificial Neural Network Model (ANN) | 14 |
| 2.2.5 WATFLOOD Flood Forecasting Model | 20 |
| 2.3 Hydrological processes in Canada..... | 24 |
| 2.4 Cold Regions Hydrological Model (CRHM)..... | 26 |
| 2.5 Hydrological Modelling for Cold Regions | 28 |
| Chapter 3 Site Description and Data Collection and Preparation | 33 |
| 3.1 Study Area | 33 |
| 3.1.1 Physiography | 35 |
| 3.1.2 Surficial Geology | 36 |
| 3.1.3 Climate | 37 |
| 3.1.4 Forest Cover | 38 |
| 3.2 Availability of Data | 39 |
| 3.3 Basin Data | 40 |

| | |
|--|-----------|
| 3.3.1 Surface Elevation Data | 40 |
| 3.3.2 Land Cover Data | 42 |
| 3.4 Meteorological and Hydrometric Data Collection | 45 |
| 3.4.1 Meteorological Data | 45 |
| 3.4.2 Water Level Data for Routing | 52 |
| 3.4.3 Hydrometric Data for model Assessment | 53 |
| 3.4.4 Snow Survey Data | 54 |
| 3.5 Data Interpolation and Quality | 54 |
| Chapter 4 Methodology and Model Setup | 59 |
| 4.1 Modelling Approach | 59 |
| 4.2 Watershed Delineation and Selection of Sub-basins for Modelling | 61 |
| 4.3 Precipitation Station over Humber River sub-basins | 66 |
| 4.4 Sub-basin Characterization and Typing | 67 |
| 4.5 Land Use Map and Hydrological Response Unit and Sub-basins Structure and Parameterization | 68 |
| 4.6 Aspect Map | 69 |

| | |
|---|------------|
| 4.7 Slope Map..... | 71 |
| 4.8 Blowing snow module parameters | 72 |
| 4.9 Albedo parameters | 72 |
| 4.10 Soil parameters..... | 72 |
| 4.11 Routing parameters..... | 74 |
| 4.12 Model Calibration | 78 |
| 4.12.1 Automatic Calibration using Shuffled Complex Evolution Optimization | 78 |
| 4.12.2 Manual Calibration | 80 |
| Chapter 5 Results and Discussion | 82 |
| 5.1 Streamflow Simulation at Gauge Locations | 82 |
| 5.2 Streamflow prediction and comparison | 85 |
| 5.3 Model Calibration Results..... | 87 |
| 5.3.1 Parameter Estimation from optimization..... | 88 |
| 5.3.2 Streamflow Calibration | 89 |
| 5.4 Model Validation Results | 107 |
| 5.5 Simulations for Entire Basin | 114 |

| | |
|---|------------|
| 5.6 Winter snowpack prediction and comparison..... | 117 |
| 5.7 Discussion..... | 125 |
| Chapter 6 Conclusion and Recommendation..... | 128 |
| 6.1 Conclusions | 128 |
| 6.2 Recommendations | 132 |
| References..... | 134 |
| Appendix..... | 142 |

List of Tables

| | |
|---|----|
| Table 3. 1 Humber River Basin main meteorological station of precipitation | 48 |
| Table 3. 2 Humber River Basin main meteorological station of Temperature, Relative Humidity and Wind Speed..... | 50 |
| Table 3. 3 Hydrometric stations in Humber River..... | 53 |
| Table 3. 4 Station data quality for temperature, relative humidity and wind speed were assessed by the percentage of missing data. All numbers in % of record from January, 2001 to December, 2010..... | 55 |
| Table 3. 5 Precipitation Station data quality was assessed by the percentage of missing data. All numbers in % of record from January, 2001 to December, 2010. | 55 |
| Table 3. 6 Spatial interpolation equations based on correlations (temperature, relative humidity, wind speed) between stations (Pomeroy et al., 2013). | 56 |
| Table 3. 7 Spatial interpolation equations based on double mass curves (precipitation) between stations (Pomeroy et al., 2013). | 57 |
| Table 4.1 Area of the 9 modelled sub-basins..... | 65 |
| Table 4.2 Station influence over sub-basins | 67 |

| | |
|---|-----|
| Table 5. 1 The Model bias index (MB), model efficiency index (NSE), and root mean square error (RMSE) of simulated streamflow (January 2001 to December 2010) | 87 |
| Table 5. 2 Optimized parameters for the observed and simulated streamflow of Sub-basin 1..... | 89 |
| Table 5. 3 Optimized parameters for the observed and simulated streamflow of Sub-basin 4..... | 89 |
| Table 5. 4 Model bias index (MB), model efficiency index (NSE), and root mean square error (RMSE) of simulated streamflow (September 2001 to December 2005) | 103 |
| Table 5. 5 Model efficiency index (NSE), and root mean square error (RMSE) of simulated streamflow at Sheffield Brook at Trans-Canada Highway | 107 |
| Table 5. 6 Model bias index (MB), model efficiency index (NSE), and root mean square error (RMSE) of simulated streamflow | 113 |
| Table 5. 7 Model bias index (MB), model efficiency index (ME), and root mean square error (RMSE) of simulated SWE..... | 124 |
| | |
| Table A. 1 Forms of Dynamic Regression Model for Humber River Basin (Picco, 1997) | 143 |
| | |
| Table F. 1 HRU areas for the sub-basin 1..... | 163 |

| | |
|--|-----|
| Table F. 2 HRU areas for the sub-basin 2..... | 163 |
| Table F. 3 HRU areas for the sub-basin 3..... | 164 |
| Table F. 4 HRU areas for the sub-basin 4..... | 164 |
| Table F. 5 HRU areas for the sub-basin 5..... | 164 |
| Table F. 6 HRU areas for the sub-basin 6..... | 165 |
| Table F. 7 HRU areas for the sub-basin 7..... | 165 |
| Table F. 8 HRU areas for the sub-basin 8..... | 165 |
| Table F. 9 HRU areas for the sub-basin 9..... | 166 |
| Table F. 10 HRU elevation, aspect and slope for the sub-basin 1 | 166 |
| Table F. 11 HRU elevation, aspect and slope for the sub-basin 2 | 167 |
| Table F. 12 HRU elevation, aspect and slope for the sub-basin 3 | 167 |
| Table F. 13 HRU elevation, aspect and slope for the sub-basin 4 | 167 |
| Table F. 14 HRU elevation, aspect and slope for the sub-basin 5 | 168 |
| Table F. 15 HRU elevation, aspect and slope for the sub-basin 6 | 168 |
| Table F. 16 HRU elevation, aspect and slope for the sub-basin 7 | 169 |
| Table F. 17 HRU elevation, aspect and slope for the sub-basin 8 | 169 |
| Table F. 18 HRU elevation, aspect and slope for the sub-basin 9 | 169 |
| Table F. 19 Blowing snow module parameters in the Humber River Basin (HRB) (Pomeroy et. al., 2013)..... | 171 |
| Table F. 20 Albedo and canopy parameters in the Humber River Basin (HRB) (Pomeroy et. al., 2013) | 172 |

Table F. 21 Soil parameters in the Humber River Basin (HRB). K_{s_gw} , K_{s_Upper} and K_{s_lower} are the saturated hydraulic conductivity in the groundwater, upper and lower of soil layers, respectively. λ is the pore size distribution index. $Soil_{rechr_max}$, $Soil_{moist_max}$ and g_{w_max} are the water storage capacity for the recharge, soil of both recharge and lower and groundwater layers, respectively. S_{d_max} is the depression storage capacity. (Pomeroy et. al., 2013) 173

List of Figures

| | |
|---|----|
| Figure 2. 1 Schematics of SSARR Model | 7 |
| Figure 2. 2 Dynamic Regression Model Building Cycle step by step | 11 |
| Figure 2. 3 Architecture of a Standard Three Layer Neural Network Model (Cai, 2010) | 16 |
| Figure 2. 4 The microstructure of a neuron in the network | 17 |
| Figure 2. 5 Major Hydrological Processes of WATFLOOD Model | 21 |
| Figure 2. 6 Grouped Response Unit and Runoff Routing Concept | 22 |
| Figure 3. 1 Humber River Basin | 34 |
| Figure 3. 2 General Location of Study Area..... | 36 |
| Figure 3. 3 Contour map (m) of the River Basin | 38 |
| Figure 3. 4 DEM for Humber River Basin | 41 |
| Figure 3. 5 Land Cover Map (GeoTIFF) for Humber River Basin | 44 |
| Figure 3. 6 Humber River sub-basins with meteorological stations having Daily Precipitation | 47 |
| Figure 3. 7 Humber River sub-basins with meteorological stations having hourly Temperature, Relative Humidity and Wind Speed | 51 |

| | |
|---|----|
| Figure 3. 8 Humber River sub-basins with Water Survey of Canada hydrometric station locations | 52 |
| Figure 4. 1 Cold Regions Hydrological Cycle (Marsh et al., n.d.) | 60 |
| Figure 4. 2 Flow Chart of Watershed Delineation Methodology | 63 |
| Figure 4. 3 Humber River sub-basins, ArcGIS-derived stream network. Colors are used to distinguish sub-basins and have no other meaning and green dots are the pour points.... | 64 |
| Figure 4. 4 Thiessen Polygon for Precipitation Station over Humber River sub-basins, ArcGIS-derived Thiessen Polygon | 66 |
| Figure 4. 5 HRU generation for the Humber River modelled sub-basins | 69 |
| Figure 4. 6 Aspect of slopes in the Humber River Basin calculated from the DEM..... | 70 |
| Figure 4. 7 Slope angle in the Humber River Basin, calculated from the DEM | 71 |
| Figure 4. 8 Routing sequence between HRUs within the modelled sub-basins in the Humber River Basin and Sub-basin 1 and Sub-basin 2 are shown here, rest Sub-basins are almost same..... | 76 |
| Figure 4. 9 Routing sequence between the modelled sub-basins in the Humber River Basin | 77 |
| Figure 4. 10 Flow Chart of the shuffled complex evolution (SCE) method (Duan et. Al., 1993) | 80 |

| | |
|---|----|
| Figure 5. 1 Streamflow gauge of study area | 83 |
| Figure 5. 2 Time series plot of Upper Humber River near Reidville | 83 |
| Figure 5. 3 Time series plot of Sheffield Brook near Trans-Canada Highway | 84 |
| Figure 5. 4 Time series plot of Humber Village Bridge at downstream of Deer Lake..... | 84 |
| Figure 5. 5 Daily, Monthly and Annual Streamflow (September 2001 to December 2005) at Upper Humber River at Reidville | 90 |
| Figure 5. 6 Seasonal Streamflow (September 2001 to December 2005) at Upper Humber River at Reidville | 91 |
| Figure 5. 7 Daily and Monthly Streamflow (September 2001 to December 2002) at Upper Humber River at Reidville | 92 |
| Figure 5. 8 Daily, Monthly and Annual Streamflow (September 2001 to December 2003) at Upper Humber River at Reidville | 93 |
| Figure 5. 9 Seasonal Streamflow (September 2001 to December 2003) at Upper Humber River at Reidville | 94 |
| Figure 5. 10 Daily, Monthly and Annual Streamflow (September 2003 to December 2005) at Upper Humber River at Reidville | 95 |
| Figure 5. 11 Seasonal Streamflow (September 2003 to December 2005) at Upper Humber River at Reidville | 96 |

| | |
|--|-----|
| Figure 5. 12 Daily, Monthly and Annual Streamflow (September 2001 to December 2005) at Sheffield Brook near Trans-Canada Highway | 97 |
| Figure 5. 13 Seasonal Streamflow (September 2001 to December 2005) at Sheffield Brook near Trans-Canada Highway..... | 98 |
| Figure 5. 14 Daily, Monthly and Annual Streamflow (September 2001 to December 2002) at Sheffield Brook near Trans-Canada Highway | 99 |
| Figure 5. 15 Daily, Monthly and Annual Streamflow (September 2001 to December 2003) at Sheffield Brook near Trans-Canada Highway | 100 |
| Figure 5. 16 Seasonal Streamflow (September 2001 to December 2003) at Sheffield Brook near Trans-Canada Highway..... | 101 |
| Figure 5. 17 Daily, Monthly and Annual Streamflow (September 2003 to December 2005) at Sheffield Brook near Trans-Canada Highway | 102 |
| Figure 5. 18 Seasonal Streamflow (September 2003 to December 2005) at Sheffield Brook near Trans-Canada Highway..... | 103 |
| Figure 5. 19 Streamflow (2001-2010) at Sheffield Brook near Trans-Canada Highway | 104 |
| Figure 5. 20 Streamflow (2001) at Sheffield Brook near Trans-Canada Highway | 105 |
| Figure 5. 21 Streamflow (2003) at Sheffield Brook near Trans-Canada Highway | 105 |

| | |
|---|-----|
| Figure 5. 22 Streamflow (2009) at Sheffield Brook near Trans-Canada Highway | 106 |
| Figure 5. 23 Streamflow (2001-2003) at Sheffield Brook near Trans-Canada Highway | 106 |
| Figure 5. 24 Streamflow (2007-2008) at Sheffield Brook near Trans-Canada Highway | 107 |
| Figure 5. 25 Daily, Monthly and Annual Streamflow (September 2005 to December 2010) at Upper Humber River at Reidville | 108 |
| Figure 5. 26 Seasonal Streamflow (September 2005 to December 2010) at Upper Humber River at Reidville | 109 |
| Figure 5. 27 Daily, Monthly and Annual Streamflow (September 2005 to December 2010) at Sheffield Brook near Trans-Canada Highway | 110 |
| Figure 5. 28 <i>Seasonal</i> Streamflow (September 2005 to December 2010) at Sheffield Brook near Trans-Canada Highway..... | 111 |
| Figure 5. 29 Daily, Monthly and Annual Streamflow (September 2001 to December 2010) at Humber River Bridge..... | 112 |
| Figure 5. 30 <i>Seasonal</i> Streamflow (September 2001 to December 2010) at Humber River Bridge..... | 113 |
| Figure 5. 31 Streamflow (September 2001 to December 2010) at outlet of Sub-basin 3115 | |

| | |
|--|-----|
| Figure 5. 32 Streamflow (September 2001 to December 2010) at outlet of Sub-basin 5116 | |
| Figure 5. 33 Streamflow (September 2001 to December 2010) at outlet of Sub-basin 6116 | |
| Figure 5. 34 Streamflow (September 2001 to December 2010) at outlet of Sub-basin 7116 | |
| Figure 5. 35 Streamflow (September 2001 to December 2010) at outlet of Sub-basin 8117 | |
| Figure 5. 36 Ground Snow Station over Humber River Basin | 118 |
| Figure 5. 37 Observed SWE (September 2001 to December 2010) at Cormack Weather Station (Daily, Monthly and Annual) at Forest HRU and Simulated SWE at Forest HRU of Sub-basin 2 | 119 |
| Figure 5. 38 Observed SWE (September 2001 to December 2010) at Cormack Weather Station (<i>Seasonal</i>) at Forest HRU and Simulated SWE at Forest HRU of Sub-basin 2. | 120 |
| Figure 5. 39 Observed SWE (September 2001 to December 2005) at Deer Lake Airport Weather Station (Daily, Monthly and Annual) at Forest HRU and Simulated SWE at Forest HRU of Sub-basin 9..... | 121 |
| Figure 5. 40 Observed SWE (September 2001 to December 2005) at Deer Lake Airport Weather Station (<i>Seasonal</i>) at Forest HRU and Simulated SWE at Forest HRU of Sub-basin 9 | 122 |

| | |
|---|-----|
| Figure 5. 41 Observed SWE (September 2001 to December 2010) at South Brook Pasadena Weather Station (Daily, Monthly and Annual) at Forest HRU and Simulated SWE at Forest HRU of Sub-basin 9..... | 123 |
| Figure 5. 42 Observed SWE (September 2001 to December 2010) at South Brook Pasadena Weather Station (Seasonal) at Forest HRU and Simulated SWE at Forest HRU of Sub-basin 9..... | 124 |
| Figure E.1 Flowchart of physically-based hydrological modules used in the Humber River Basin Model (HRB)..... | 182 |

List of Abbreviations

| | |
|--------|---|
| AML | Arc Macro Language |
| ANN | Artificial Neural Network |
| AOGCM | Atmospheric-Ocean Coupled Global Model |
| APC1 | First Generation Adjusted Precipitation for Canada |
| APC2 | Second Generation Adjusted Precipitation for Canada |
| AVHRR | Advanced Very High-Resolution Radiometer |
| BOREAS | Boreal Ecosystem-Atmosphere Study |
| BPNN | Back Propagation Neural Network |
| CaLDAS | Canadian Land Data Assimilation System |
| CaPA | Canadian Precipitation Analysis |
| CDCD | Canadian Daily Climate Data |
| CGIAR | Consultative Group on International Agricultural Research |
| CMC | Canadian Meteorological Center |
| CSI | Consortium for Special Information |
| CV | Coefficient of Variation |

| | |
|---------|--|
| DA | Drainage Area |
| DDS | Dynamically Dimensioned Search |
| DEM | Digital Elevation Model |
| EBSM | Energy-Budget Snowmelt Model |
| EC | Environment Canada |
| ECMWF | European Center for Medium-Range Weather Forecast |
| EVAP | Evaporation module of CRHM |
| FIFE | First ISLSCP Field Experiment |
| GCM | Global Climate Model or Global Circulation Model |
| GEM | Global Environmental Multiscale |
| GR | Global Reanalysis |
| GRNN | General Regression Neural Network |
| GRU | Group Response Unit |
| GUI | Graphical User Interface |
| HEC-HMS | Hydrologic Engineering Center Hydraulic Modelling System |
| HRU | Hydrological Response Unit |

| | |
|--------|--|
| ISLSCP | International Satellite Land Surface Climatology Project |
| MAP | Mesoscale Alpine Program |
| MSC | Meteorological Service of Canada |
| NARR | North American Regional Reanalysis |
| NASA | National Aeronautics and Space Administration |
| NCEP | National Centre for Environmental Prediction |
| NCER | National Centre for Atmospheric Research |
| NHN | National Hydro Network |
| NL | Newfoundland and Labrador |
| NNGR | NCEP-NCAR Global Reanalysis |
| NOAA | National Oceanic and Atmospheric Administration |
| NTDB | National Topographic Database |
| NTS | National Topographic System |
| OI | Optimum Interpolation |
| PS | Pattern Search |
| QPF | Quantitative Precipitation Forecast |

| | |
|---------|---|
| RCM | Regional Climate Model |
| RMCQ | Réseau Météorologique Coopératif du Québec |
| SD | Standard Deviation |
| SRTM | Shuttle Radar Topographical Mission |
| SSARR | Streamflow Synthesis and Reservoir Regulation |
| SWAT | Soil and Water Assessment Tool |
| SWBD | Shoreline and Waterbodies Database |
| USGS | United States Geological Survey |
| UZS | Upper Zone Storage |
| WMO | World Meteorological Organization |
| WRMD | Water Resources Management Division |
| WSC | Water Survey of Canada |
| WSCSSDA | WSC Sub-Sub-Drainage Areas |

List of Appendices

| | |
|--|-----|
| Appendix A Forms of Dynamic Regression Model | 143 |
| Appendix B Missing precipitation data | 145 |
| Appendix C Meteorological Observation of Humber River Basin..... | 148 |
| Appendix D Annual Averages of Meteorological Observation Stations..... | 158 |
| Appendix E Watershed Delineation..... | 162 |
| Appendix F Area of Hydrological Response Unit and Sub-basins Structure and Parameterization | 163 |
| Appendix G CRHM Hydrological Module for Humber River Basin..... | 175 |
| Appendix H List of Symbols | 191 |

Chapter 1 Introduction

1.1 Background

The physiographic features of Newfoundland create many challenges to the study of watersheds on the island (Jasim, 2014). Communities along the river basin are facing problem due to the increase in development and subsequent damage of extreme events in recent decades (Cai, 2010; Picco, 1997). During winter, the basin is covered by snow (Jasim, 2014) and most of the part of Upper Humber River is affected by snowfall (Cai, 2010). As a result, at spring, the streamflow is highly influenced by snowmelt (Jasim, 2014). Snowmelt contributes the most to the floods usually occurring during the spring freshet, which together with heavy rainfall can result in even more severe flooding because of rain-on-snow processes (Fang *et. al.*, 2016). In recent years, climate change, impact is very significant, and this makes the appropriate water management and storage plans difficult (Jasim, 2014; Singh *et. al.*, 2014). Basin drainage characteristics are fundamental in understanding various hydrological processes in hydrology (Altaf *et. al.*, 2013). Therefore, there is an urgent need for the evaluation of water resources and watershed analysis because it plays a primary role in the sustainability of livelihood and regional economies (Singh *et. al.*, 2014). To assess the impact of climate change, cold regions hydrological modelling is indispensable for analyzing of hydrological processes of the large watershed of Newfoundland (Ellis *et al.*, 2010).

1.2 Study Objectives

The main objective of this study is to create a cold regions hydrologic model which will be used for snow simulation and predicting the impact of climate change. The other objectives are:

- (i) To delineate the large watershed and update the boundary of the watershed;
- (ii) To create a cold regions hydrologic model for streamflow prediction in the Humber River basin;
- (iii) To calibrate and validate the model with Water Survey of Canada gauged data;
- (iv) To compute the hydrological process such as snow water equivalent (SWE), snowmelt, snow accumulation etc.

1.3 Organization of Thesis

There are six chapters in the thesis. The first chapter is introduction and the background of the study, the study area, the availability of data and objectives of the study are presented. Chapter 2 reviews the previous literature related to the study area. It includes a brief description of previous studies of Humber River Basin and the studies and applications of cold regions hydrological modelling (CRHM). Chapter 3 describes the procedure of data collection and data preparation for the analysis of the watershed. In Chapter 4, the methodology of the model setup, modules, catchment delineation and selection of model parameters are presented. The results, model calibration, validation and discussion on

hydrological simulations are given in Chapter 5. The conclusion and recommendations are given in Chapter 6.

Chapter 2 Literature Review

2.1 Hydrological Modelling

Hydrological study of a basin is very important for analyzing various problems such as snowmelt, snow accumulation, and flood risk assessment, flood forecasting and hydrodynamic and morphologic assessment. It is related to the development of a region because rainfall, runoff, snowfall, water level and discharge are all water resources related issues (Cai, 2010).

Hydrologic simulation and prediction of streamflow and snow water equivalent are very important for hydrologists for preparing responses to flooding events. Simulation of snow generally depends on hydrologic models with varying levels of complexity and completeness, and the level of complexity and uncertainty of a model depends on its components (Cai, 2010). It is difficult to measure and simulate each interaction between air, water and land use due to the lack of data (Jasim, 2014), but reliable hydrological models can nevertheless simulate the complex interactions among hydrological inputs, landscape properties, and initial parameters (Dornes, 2009).

The flow characterization of a river basin is estimated by precipitation-runoff relationships that are based on a collection of principles set out in mathematical equations. Those models are normally called conceptual rainfall-runoff models. Various physical parameters such as drainage area and stream slope, and process parameters such as depths of the water table, interflow rates, and coefficients of infiltration, percolation and soil storage along with the

weather and precipitation inputs are required. There are various hydrological models based on specific regions and purposes and the probability of success or failure is dependent on the quality of data available. The Streamflow Synthesis and Reservoir Regulation (SSARR) Model, the Systeme Hydrologique European (SHE) Model, the Institute of Hydrology Distributed Model (IHDM), the Kinematic Wave Model, the Lambert ISO Model, and TOPMODEL are few of the name of hydrological models (Cai, 2010).

2.2 Hydrological Modelling for Humber River Basin

The Water Resources Management Division (WRMD) of Newfoundland and Labrador's Department of Environment and Conservation has used several models for flow forecasting on the Humber River Basin over the last few decades. Various hydrological models used in recent studies of the Humber River basin include Streamflow Synthesis and Reservoir Regulation (SSARR) model, statistically based dynamic regression model (Picco, 1997), rainfall-runoff routing model (Cai,2010), statistically based Artificial Neural Network (ANN) model (Cai, 2010) and Watflood flood forecasting model (Jasim, 2014). These models are briefly described below.

2.2.1 Streamflow Synthesis and Reservoir Regulation Model (SSARR)

A deterministic mathematical model, the SSARR model, generates surface runoff by considering the hydrologic parameters was first implemented in the Pacific North West during 1956 by the US Corps of Engineers for planning, design and operation of water resources management, as well as to simulate and predict flows for controlled and natural

reservoirs. During 1973, the model was used in the Saint John River basin in New Brunswick, Canada. The Humber River Basin possess similar geographic, climatic and operational characteristics, and thus the same model was used to generate streamflow for the largest river basin of western Newfoundland. The model was chosen for various reasons such as its simple structure and use readily available data, its fast simulation time and low computational time, the available model parameters from the Saint John River basin in New Brunswick, the excellent reservoir routing capability, the variable computational time steps, its availability to compute the areal distribution of snowmelt, and its efficiency in practical application and wide use for forecasting flood in various regions (Picco, 1997).

The main component of the hydrologic cycle was described in a closed system in a very simplified way in the SSARR model. Water budget is defined by meteorological inputs and runoff, soil storage and evapotranspiration are the output from the model (Picco, 1997). SSARR, a continuous hydrological model along with routing and having a real distribution of meteorological input, can simulate snowmelt. The input data includes the rainfall, snowmelt interception, soil moisture, interflow, groundwater recharge, evapotranspiration, and the various time dependent processes. These components have a relation to the huge number of flexible hydrometeorological parameters to represent the process (Picco, 1997).

The Humber River watershed includes 11 sub-basins, two reservoirs and one lake. A weighted average of meteorological station data, along with area-elevation relationships, were used and adjusted during calibration by the snowmelt and routing coefficients (Picco, 1997).

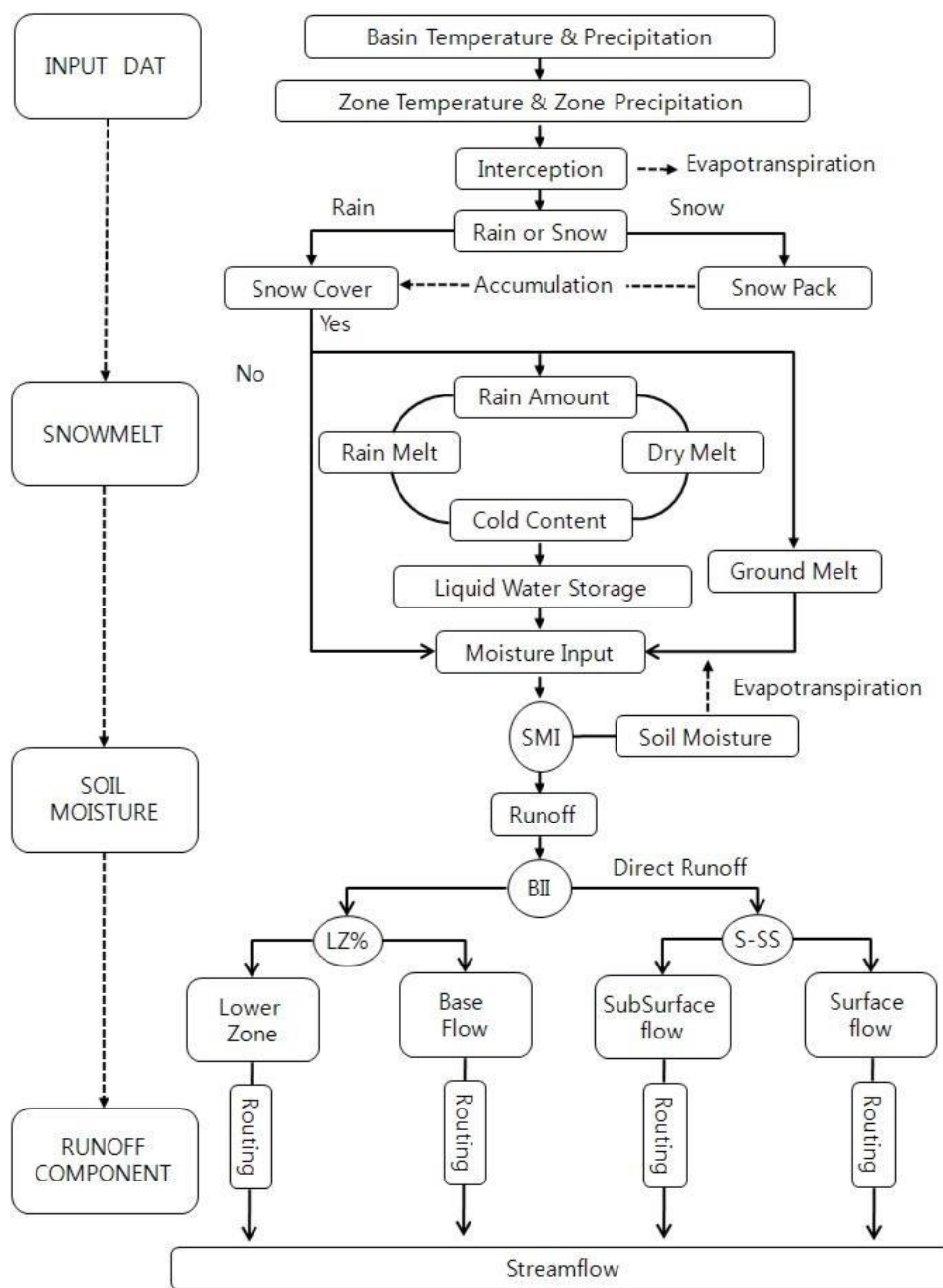


Figure 2. 1 Schematics of SSARR Model

The model performed well for a peak discharge simulation of the Reidville and Village Bridge. But, the result from the model underestimated the runoff from the precipitation and

snowmelt event during winter and overestimated the snowmelt in spring. Thus, the model has a limited capacity for simulating snow, making it less useful for the Upper Humber River which is significantly affected by snow during winter. The SSARR model also cannot perform well for snow simulation and hampers the accuracy of the forecasts (Picco, 1997). The discharge was calculated in sub-basin scale with the routing facilities and a hydrograph at the outlet point within a homogeneous hydrologic environment, and the variation of discharge was also considered in the model for hydroelectric generation and flood control. A schematic representation of SSARR is presented in Figure 2.2.

The model can consider reservoir routing at any location, and inflows are derived from single or multiple tributaries of the upstream river basin. Streamflow routing method, called storage-flow relationship, in natural river channels can also solve the routing equations in unsteady flow conditions. The streamflow and channel storage are related to each other along the river system. Reservoir outflows are determined by considering the natural and human effects, including the basic hydrologic elements, channel storage effects and other water control elements within the streamflow simulation process (Picco, 1997).

To determine the probability of predicting flows during the high flow events, the Humber River basin model was developed between 1984 and 1985. The result showed that accurate flow simulation was achieved by improving the data collection network, and devices were installed to record real time precipitation and temperature data (Cai, 2010).

WRMD developed a newer version of the SSARR Model by using the daily average temperature and total daily precipitation. Today, the model is practically obsolete due to its cumbersome results and technical difficulties (Picco, 1997).

2.2.2 Dynamic Regression Model

The statistical model named dynamic regression model was developed on a Forecast Pro Software package called Business Forecast Systems Inc, 1993 for the Humber River Basin to develop flow forecasts for the downstream portion of the basin. Since 2008, WRMD has been using the statistically based Dynamic Regression Model on an interim basis until a replacement model can be developed (Jasim, 2014).

The statistical method was used to analyze historical climate data and greater efficiency was obtained by using real time hydro-meteorological data. This is a linear time series model and lagged flows and precipitation were considered as inputs (Picco, 1997).

The model combines time-series based dynamic features with explanatory variables with its single equation regression. A long dataset is required to support a correlation-based model and it can be selected if long, stable datasets are available and there is an accurate fit of explanatory variables. The performance of the model was increased by additional explanatory variables, such as daily average temperature and daily total precipitation (Picco, 1997).

The dynamic regression model was developed for the five gauged sub-basins within the Humber River Basin and the model was able to predict a reasonably accurate flow forecast

as it used few coefficients. Hydrometric and climate data from the nearest stations were used and the closest station data were used for missing data (Picco, 1997).

The model was developed by following several steps and an initial model with an independent variable. The closest precipitation station was selected as the runoff variable is dependent on precipitation. The regression coefficients were fitted in the next step. Diagnostics were performed with the significant variables which were checked for lagged variables and autoregressive terms until a satisfactory result was achieved. There were inter-annual and intra-annual variations between some time series such as temperatures being high in summer and low in winter and climate change trends. The model building continued with a simple regression to the best fitting of data. The Goodness of fit tests were also performed for the model (Picco, 1997).

The ordinary least squares dynamic model takes the form shown in equation 2.1.

$$\phi(b)Y_t = \beta Z_t + \epsilon_t \quad (2.1)$$

where $\phi(b)$ = autoregressive polynomial, Y_t = dependent variable at time t, β = coefficient of i 'th exogenous variable $Z_t(i)$, Z_t = vector of exogeneous variables at time t, ϵ_t = errors where the errors are NID $(0, \sigma^2)$, i.e. normally and independently distributed with variance σ^2 .

Goodrich (1989) also used a Cochrane-Orcutt model to improve the model dynamics. He replaced Equation 2.1 with the following pair of equations:

$$\phi(b)Y_t = \beta Z_t + \omega_t \quad (2.2)$$

$$R(b)\omega_t = \epsilon_t \quad (2.3)$$

where $R(b) =$ polynomial in the backward shift operator,

$\omega_t =$ raw residual at time.

These two equations can be written into a single equation as a combined form:

$$R(b)(\phi(b)Y_t - \beta Z_t) = \epsilon_t \quad (2.4)$$

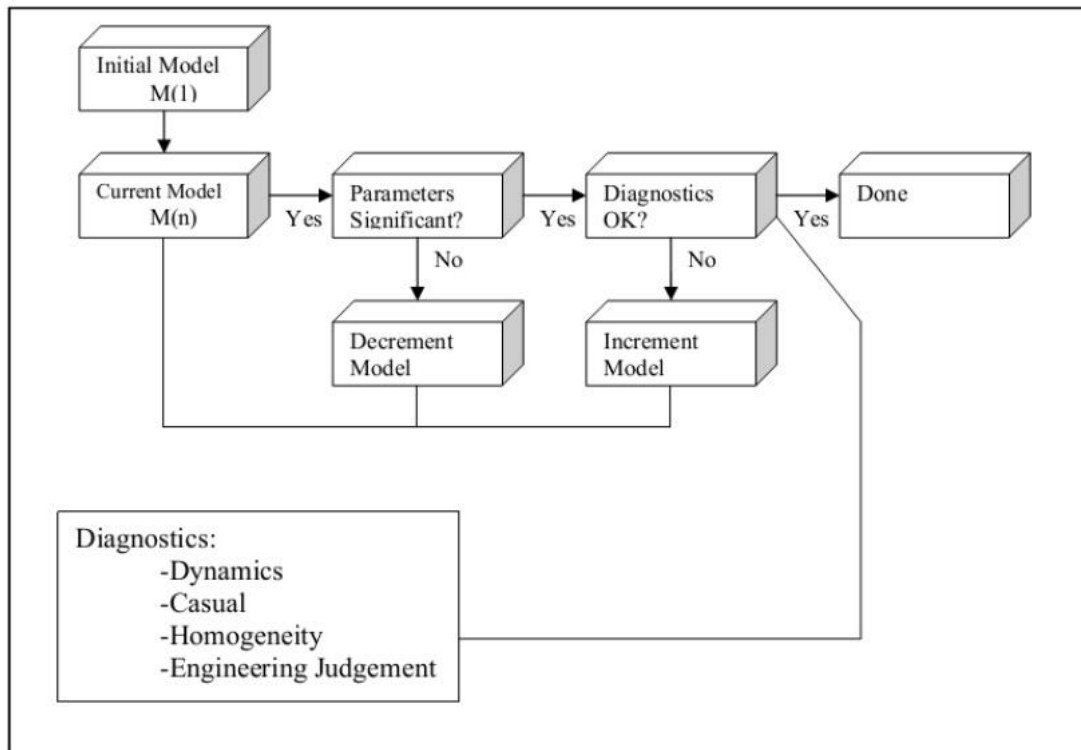


Figure 2. 2 Dynamic Regression Model Building Cycle step by step

Then, the one, two and three day forecasts were generated using the dynamic regression model. The model performed better than the SSARR model for generating flow simulations with less data in calibration but cannot consider the snowmelt effect from the upper Humber River watershed. The model cannot work with any nonlinear hydrologic effects (Picco, 1997).

2.2.3 Rainfall-Runoff Routing Model

An in-house Routing Model was developed using a series of water balance equations by WRMD engineers. This method was implemented on three different spreadsheets to simulate flow over the Upper Humber River at Black Brook, Reidville and Deer Lake. The calibration was performed with a trial-and-error method for estimating model parameters. Upper Humber Basin is affected by snowfall and the model was not able to calculate the snowmelt effectively. At Upper Humber River at Black Brook, the effective rainfall data were used (Cai,2010). Effective rainfall is defined as the amount of rainfall that reaches the land surface. It can be calculated using equation 2.5:

$$ER = OR - I(\text{If Observed Rainfall} \geq \text{Interception}) \quad (2.5)$$
$$= 0 (\text{If Observed Rainfall} < \text{Interception})$$

where ER = Effective Rainfall, OR = Observed Rainfall and I = Interception.

Deer Lake has inflow from Reidville and Grand Lake outlet, and the water level and outflow of Deer Lake were also calculated. The model calculated the water level of Deer Lake (WL_D) using equations 2.10 and 2.11:

$$NI[t - 1] = F_R[t] + I_G[t] + I_D[t] + O_G[t] \quad (2.6)$$

where I_G = Local Inflow below Grand Lake = $\frac{199}{2108} * F_R$

I_D = Local Inflow to Deer Lake = $\frac{640}{2108} * F_R$

O_G = Outflow of Grand Lake.

$$WL_D[t] = WL_D[t - 1] + \frac{NI[t-1]}{Lake\ Area} \quad (2.7)$$

The outflow at Humber Village Bridge at the outlet of Deer Lake was calculated based on the water level of Deer Lake at day t, according to equation 2.12

$$F_v[t] = 251.5 * WL_D[t] - 1.092 \quad (2.8)$$

Here, F_v = Flow at Village Bridge

The model's mean absolute error was calculated by comparing the calculated and observed flows. The model's performance was better for the downstream part than the upstream of the basin and it was in a satisfactory range at Deer Lake and the Humber Village Bridge station. Its performance at Black Brook was poor and the model was not able to compute the snowmelt effect from the upper Humber Basin. In addition, the model also had

inaccuracy in forecasting and there did not exist any document for the proper calibration of model parameters (Cai, 2010).

2.2.4 Artificial Neural Network Model (ANN)

The lower accuracy of deterministic model, SSARR model will be overcome by the statistical model, the dynamic regression model. The dynamic regression model generates forecast and it was more accurate than SSARR, but its performance is not good for snowmelt impact from the Upper Humber Basin. As a result, to provide accurate forecast for snowmelt simulations for the Upper Humber basin with easier calibration, WRMD seeks a better model. In the last 20 years, the Artificial Neural Network (ANN) model, an advanced computation and simulation model, has been widely used in the field of hydrological modelling and a non-conceptual flow forecast model based on an ANN was proposed for this basin. The ANN model is also used in many areas of research and practical applications. A non-parametric approach named the General Regression Neural Network (GRNN) and a parameter-based model with calibration, the Back Propagation Neural Network (BPNN) model was considered. To analyze the proper input and parameters for better optimization, Design of Experiment (DOE) was also used (Cai, 2010).

ANN is analogous to the human brain and operates as a human brain signal and consists of neurons and connections like a biological neural system to simulate a route that can link the input X to the output Y. The human brain reacts to the things people see, hear, and feel that stimulate the brain in real life. In engineering applications, the function of an ANN

establishes the relationship between the inputs and outputs from a given set of input data to predict output, such as the human brain process. The model's performance will be strong when it faces a similar situation in the future. The model was used for the Humber River basin for its abilities to use field recorded data without regression analysis, simultaneously identify the effects of fixed and random variables, generate a predicted value for the response variable for any combination of input variables, bring random variables to the response variable into interactions, perform parallel computations and simulate a nonlinear system. There are few limitations of ANN model such as computational time, overfitting, forecast error, hidden neurons and difficult to optimize the model (Cai, 2010).

The neuron network's standard three layers, input layer, hidden layer, and output layer, are shown in the Figure2.3. The ANN architecture is a combination of neurons and connections. Neurons have an intermediate value that combines the weighted sum of all its inputs. The input signals are received by neurons and a neuron computes outputs using its output function and puts the results through to their neighboring neurons for the next step of processing (Cai,2010).

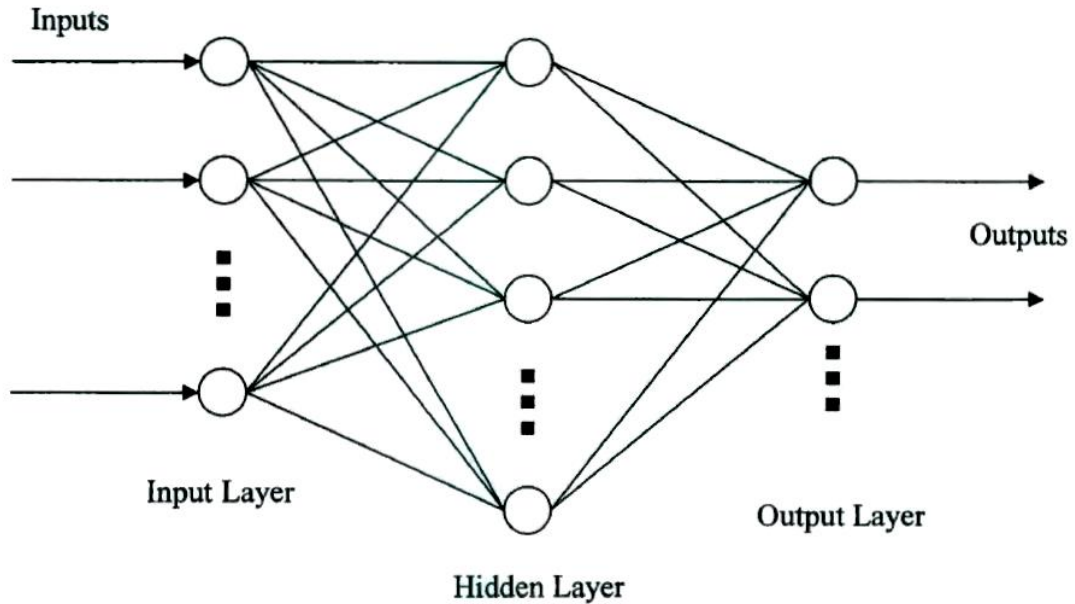


Figure 2. 3 Architecture of a Standard Three Layer Neural Network Model (Cai, 2010)

The input is computed by the formula,

$$I = \sum W_{ij}X_{ij} \quad (2.9)$$

where X is the input, W is the weight of each input, and I is the weighted sum, i is the number of input sources and j is the number of target neurons. A transfer function f(I) was used to pass I value for logistic, linear, Gaussian or a hyperbolic tangent transfer function (Cai,2010).

A set of data in the ANN model is represented by Network training which is an adjustment of the connection weights or network structure. ANN can be divided into different categories based on architectures and training algorithms and the Back Propagation Neural

Network (BPNN) and General Regression neural network (GRNN) are most commonly used for river flow forecasting (Cai, 2010) and are discussed below (Cai,2010).

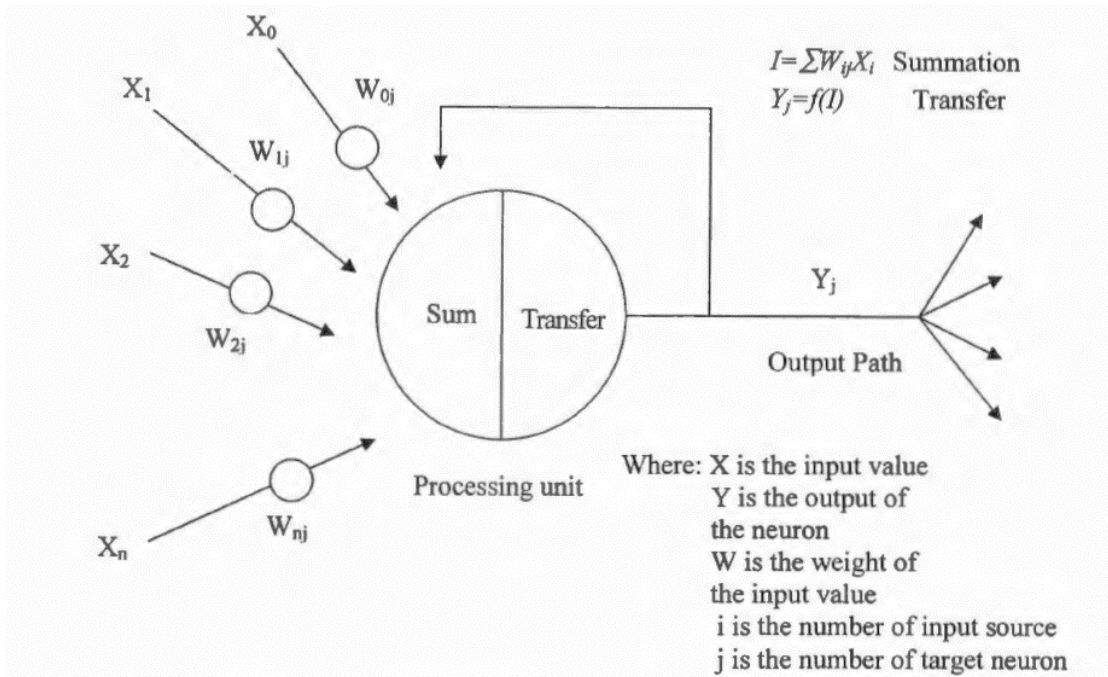


Figure 2. 4 The microstructure of a neuron in the network

2.3.4.1 Back Propagation Neural Network

The Backpropagation Neural Network model was used to forecast daily flows. There are several steps for the computation of flows by the model. The data are stored in the input neurons which transmit the data to the hidden neurons across the links. The transmitted values are multiplied by weights on each link and a transfer function creates activity for the hidden neurons by the weighted sum. Hidden neurons transmit output layers to activate and the procedure was repeated. Then, the output neurons are obtained by an activation function to get the activation level which is considered as the final solution of the network.

The logistic function is usually used as an activation function in BPNN. The common numeric ranges are from 0 to 1 and -1 to 1 for the network (Cai,2010).

The sigmoid function is an activation function usually used for back propagation and is given below.

$$f(I) = \frac{1}{1+e^{-I}} \quad (2.10)$$

where $I_i = \sum_{j=1}^n W_{ij}X_j$

The delta rule is used for weight updates and is given below.

$$\Delta w_{ij} = \beta E f(I) + \alpha \Delta w_{ij}^{previous} \quad (2.11)$$

where $\alpha = \text{momentum factor}$, $\beta = \text{learning rate}$

$$\text{The error of the output layer is } E_{ij}^{output} = y_j^{desired} - y_j^{actual} \quad (2.12)$$

$$\text{The error of the hidden layer is } E_i^{hidden} = \frac{df(I_i^{hidden})}{dI} \sum_{j=1}^n w_{ij} E_j^{output} \quad (2.13)$$

In BPNN, the errors of the current layer are calculated based on the errors of the backward layer.

2.3.4.2 General Regression Neural Network (GRNN)

BPNN does have number of limitations, and GRNN works better for many types of problems than BPNN. GRNN is used for quick training on sparse datasets and its patterns

are compared based on the distance of network connections between each other. GRNN also consists of the same three-layer structure as BPNN. The output is proportional to the inputs in the training set of the network. This proportion can be defined as,

$$W_i(x, y) = \frac{\exp(-\frac{d_i^2}{2\sigma^2})}{\sum_{j=1}^n \exp(-\frac{d_j^2}{2\sigma^2})} \quad (2.14)$$

where d_i is the computed distance, and σ is the spreading factor or smoothing factor of the transfer function.

The calculation of the distance of new patterns from the training patterns is a critical step to run GRNN. There are two methods for the calculation. The first method, Vanilla or Euclidean Distance, computes a root of the sum of the squared difference between the pattern and the weight vector for that neuron. Second, the City Block Distance Metric calculates the sum of the absolute values of the differences in all dimensions between the pattern and the weight vector for that neuron with a faster computation time than Euclidean Distance, but the method has poor accuracy (Cai,2010).

The Euclidean Distance is expressed as,

$$d = \sqrt{(p_1 - q_1)^2 + (p_2 - q_2)^2 + \dots + (p_n - q_n)^2} = \sqrt{\sum_{i=1}^n (p_i - q_i)^2} \quad (2.15)$$

Therefore, the forecast model was developed for a one day forecast of the streamflow of the study area by using the ANN model for three hydrometric stations at the Upper Humber River at Black Brook, Reidville and Humber River Village Bridge. The model was assessed

by goodness of fit computations which assessed Nash-Sutcliffe efficiency, correlation coefficient r , mean squared error, mean absolute error and the percentage of outliers. ANN predicts more accurate result than the in-house routing model developed by WRMD and slightly better results than the Dynamic Regression model. The results from the ANN model were in the considerable range for the lower part of the river basin and the result was not satisfactory for the Upper Humber river station at Black Brook as it was highly influenced by snowmelt runoff. The model could perform well only for a one day forecast while a two-day forecast was acquired by two steps and the model performance was hampered due to the errors with forecasted input factors from several sources (Cai, 2010).

2.2.5 WATFLOOD Flood Forecasting Model

The first four models could not consider the snowmelt runoff, and Upper Humber River is affected by snowfall. The ANN model could predict an accurate forecast only for one day (Cai, 2010). To eliminate the damage of flood, optimize the renewable energy from hydroelectric power plant, and predict the flood level, it is indispensable to develop an advanced flow forecasting model to overcome the limitations of previous models. WATFLOOD, a continuous model was able to simulate the entire annual hydrologic cycle including the snowmelt period for the large watershed of Newfoundland. A gridded hydrological model uses a square grid system for all input and output information in a given watershed with gridded precipitation data from rain gauges, radar or numerical weather models. The study used gridded meteorological inputs such as precipitation data from APC2 (Second Generation Adjusted Precipitation for Canada), NARR (North American

Regional Reanalysis) and CaPA (Canadian Precipitation Analysis) based on 30 years. The study identified appropriate sets of precipitation and temperature data based on the objective function for model calibration and validation. Remotely sensed land cover images for the land cover information including land surface elevation and land cover, and model forcing (precipitation, temperature and climate normal's) data were also used for the simulation. There were 16 different land cover classes called Grouped Response Units, or GRUs, in addition to an impervious class and hydrologic characteristics were expressed by its own set of parameter values. The lack of observed data during the snowmelt period is overcome by the simulation in the study as the accuracy of the model's predictions relies on input data (Jasim, 2014).

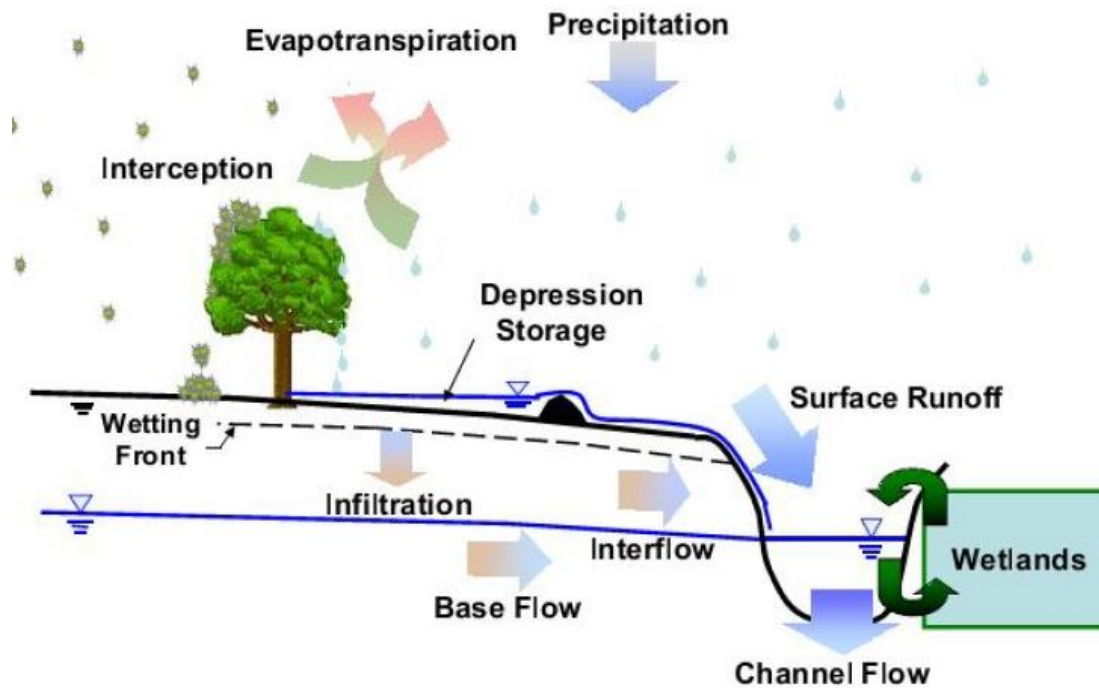


Figure 2. 5 Major Hydrological Processes of WATFLOOD Model

WATFLOOD, a leading hydrological model of Canada is a physically-based, mesoscale, large domain fully distributed hydrological model that follows the rules of the hydrologic budget of a watershed for each hydrologically significant landcover class. The model was first developed by Dr. Nicholas Kouwen of the University of Waterloo in 1972 for long term hydrologic simulations and flood forecasting by considering physical processes including interception, infiltration, evaporation, transpiration, snow accumulation and ablation, interflow, recharge, baseflow and overland flow, wetland and channel routing with effects on runoff and streamflow. The WATFLOOD model is used for both research and practical applications including augmenting flow records, dam safety studies, atmospheric community uses, state variable estimation, environmental assessments, real time flow forecasting and non-point source pollution modelling (Jasim, 2014).

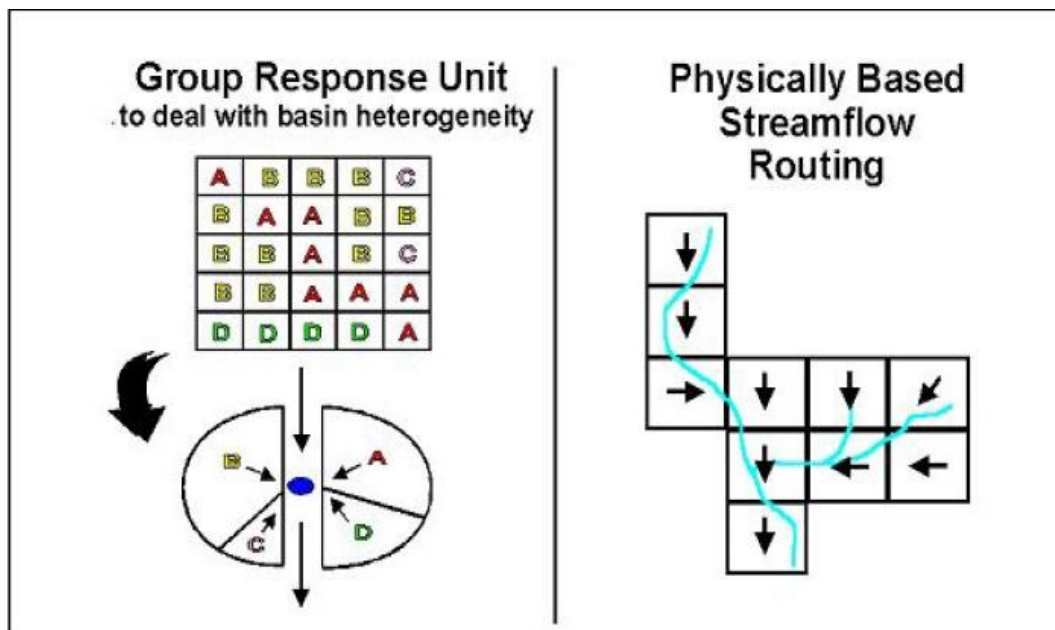


Figure 2. 6 Grouped Response Unit and Runoff Routing Concept

The main advantage of the WATFLOOD model were its fast computing time and that requires only temperature and precipitation as input data. The result is distributed output data which can be further evaluated using other sets of data. The evaluation of internal components for testing hydrologic models is crucial as different process descriptions often lead to very similar outflow hydrographs, without identifying specific problem sources in the (Jasim, 2014).

In the study, the streamflow simulation was performed for eight stream gauges at various locations including Reidville, Humber River Village Bridge, Black Brook, Lewaseechjeech Brook, Sheffield Brook, Glide Brook, Boot Brook, and South Brook at Pasadena. The model showed satisfactory Nash-Sutcliffe efficiency values at several gauge locations including Reidville, Humber River at Village Bridge and Black Brook where discharges are important for flood forecasting (Jasim, 2014).

The disadvantages of the model was, it cannot rely on APC2 data because of its production lag (only data up to 2011 is available). The updated data were necessary to generate useful forecasts. WATFLOOD calculates soil moisture in the upper layer of soil as a depth of water (UZS) by multiplying soil moisture content with the porosity of soil layer as it does not calculate soil moisture directly. The simulated UZS computed using MAP rain gauge precipitation data and radar data fit well with the measured soil moisture at all six measurement sites. The model was also useful for checking datasets and erroneous points as some problems existed in the dataset (recorded precipitation, soil moisture contents and streamflows) (Jasim, 2014).

The physically-based models performs well for predicting the streamflow but shows poor performance for hydrological processes (soil moisture, evaporation, snow accumulation and snowmelt, and groundwater flow). So, streamflow calibration and validation are not enough for physically-based models and several methods of calibration-validation of hydrological processes of the water budget were needed. The validation of the soil moisture and evaporation processes was performed by the data from BOREAS (1998) and soil moisture was measured at various depths for 20 sites. The evaporation data were collected from eddy correlation flux measurement towers and snow accumulation data were used from the Columbia River basin in British Columbia for the validation of evaporation and snow accumulation. The validation result showed that the WATFLOOD model performance was accurate for the major hydrological processes. Additionally, WATFLOOD is capable of accurately modelling the rainfall-runoff processes for increasing rainfall intensities with respect to peak flow, basin lag and time to peak flow (Jasim, 2014).

2.3 Hydrological processes in Canada

now accumulation and snowmelt flood is a common natural disaster in forested, central and eastern portions of southern Canada. Approximately 36% of mean Canadian annual precipitation is snowfall, and snowmelt and ice cover are most common on many rivers in April. Sometimes, the flow rate exceeds the capacity due to the accumulation of rain water on saturated ground. This overflow of water from waterbodies when submerges land normally not covered by water called flood. Canada is vulnerable for various types of natural hydrological hazards such as snowmelt, heavy summer rainfall and ice jams in the

streams. The accumulated snow melt events produce rapid streamflow increases and creates a significant flood hazards generated by rain-on-snow. It is also associated with flooding. The greater impermeability of the soil surface in the watershed along with a small area with intense rainfall is responsible for floods. By contrast, large watersheds with frozen soil and relative infiltration potential are mostly susceptible to snowmelt floods. The hydrological disaster creates the demand for hydrological modelling of snow accumulation and flood studies. In the hydrologic cycle, water flows from land and rivers to oceans and evaporates from oceans to atmosphere, condenses and then returns to the land surface and then to rivers again. Generally, it is expressed in terms of the movement of water in the atmosphere on, above and below the earth's surface. There are various processes in hydrologic cycle and precipitation, runoff and evaporation are the fundamentals between all of them. For hydrologic studies, the rainfall-runoff relationship plays very significant role for modelling the movement of water. A hydrologic model can easily present the vital processes of hydrological cycle in a simplified way. The models are developed based on mathematical principles and called conceptual rainfall-runoff models. There are several types of hydrologic models such as index models, deterministic models, stochastic models and physically-based distributed models. The first-generation hydrologic models, the SSARR model and MUSKINGUM routing method, used unit hydrographs for depicting basin response for given runoff depth, snowmelt and rainfall input. Later, the hydrologic forecast become more accurate with the availability of remotely-sensed data. Figure 2.1 shows the basic hydrological processes in a hydrologic model. Again, some hydrologic responses cannot be measured in the field, and in the absence of those data, rainfall-runoff

models help to predict hydrologic responses. The model requires the rainfall and runoff information as well as evaporation, interception, snowmelt and catchment physical characteristics (Jasim, 2014).

2.4 Cold Regions Hydrological Model (CRHM)

As snowmelt runoff contributes significantly to the drainage area (Jasim, 2014), WRMD seeks a better model for the Upper Humber River basin for accurate predictions of snowmelt runoff simulations along with easier calibration. This is very difficult in subarctic and arctic environments as the basin is ungauged in nature. This research is an attempt to apply a new approach, a CRHM model for the simulation of snowmelt runoff and snow water equivalent for large watersheds in boreal environments with limited data. Calibration is not needed to produce restricted for the high level of confidence in the process representations of the modules and good flexibility of the model structure (Krogh et al., 2013; Pomeroy et al., 2007).

The advantages of CRHM model is that it has flexible spatial representation from lumped to distributed approaches, HRU can be placed in landscapes to analyze snow redistribution processes, and episodic drainage from both poorly drained, and dry sites can be simulated. The model platform can be used to create many models of a basin for inter comparison, testing of new algorithms, evaluation of model structures, and estimation of predictive uncertainty. However, the parameter is not available in Canada due to the lack of observations and a reliable inventory model and thus the model is less spatially detailed

than the distributed models such as Systeme Hydrologique Europeen (SHE) (Pomeroy et al., 2007; Zhou et al., 2014).

The structure of the CRHM model is modular object-oriented and uses physically-based algorithms. The existing algorithms can be modified, or new algorithms can be developed and added as modules to the module library for specific applications. The basin model can be created in the CHRM platform, which is a basic difference with most hydrological models (Pomeroy et al., 2007).

There are various components of CRHM models such as observations including time-series meteorological data and surface observations of streamflow, snowpack, or soil moisture, parameters including spatial data of the basin area, elevation, and cover type and those are evaluated by using a GIS interface in basin delineation, characterization and parameterization of a hydrologic response unit (HRU). Modules represent the algorithms implemented in the hydrological or physical processes globally and groups is a collection of modules executed in sequence for all HRUs in specific individual modules for a complex set of processes. In addition, its structure is a parallel collection of modules and used to compare sets of algorithms, and customize models. Variables and states are created by the declarations in the modules. Variables include meteorological inputs (precipitation, temperature, wind speed) and States are HRU conditions such as soil moisture, snow water equivalent, and albedo (Pomeroy et al., 2007).

2.5 Hydrological Modelling for Cold Regions

CRHM models were used for various cold region studies in Canada in recent years and these studies are briefly described below.

The most important hydrological event of the year of Needleleaf forests is snowmelt and most of these areas include mountainous and boreal regions of the northern hemisphere. To study the cold regions hydrology due to snow processes in a Needleleaf environment, the model was developed from field investigations in cold region environments, with modest data and parameter requirements, and was used to analyze the cold regions hydrologic cycle (Ellis et al., 2010).

In addition, for better performance analysis, the accumulated snow and melt from the simulations were compared to observation data collected at paired forest and clearing sites of varying latitudes, elevations, forest cover densities, and climates. The result of CRHM is satisfactory in characterizing variations in snow accumulation between forests and clearing sites from the performance analysis. But the simulations of the mean and maximum seasonal SWE showed some systematic bias at forest sites, clearing sites, or both due to errors in observations or model parameterization (Ellis et al., 2010).

On the other hand, a study was conducted on the radiation and snowmelt dynamics of Needleleaf forest cover where runoff is the main contributor to spring river flows in western North America. The effect of Needleleaf forest cover on radiation and snowmelt timing was determined by field observations in pine and spruce forests and clearing sites

of varying slopes and aspects at the eastern Canadian Rocky Mountain headwater basin. The simulated result was compared with the open clearing sites and shortwave radiation showed a deviation in melt timing under forest cover with different aspects. Longwave radiation to snow showed an improved result at the dense spruce forest sites as longwave radiation was a dominant part of total energy for snowmelt (Ellis et al., 2011).

The Canadian prairies are affected by drought and warmer temperatures, lower precipitation, and lower soil moisture, and sparser vegetation than in normal conditions is common in those regions. CRHM is also a helpful tool to analyze the snowmelt processes to drought. The blowing snow sublimation, lower precipitation, higher air temperature and lower initial soil moisture caused reduced snowfall which affects snowmelt runoff. The drought condition was accelerated with environmental changes such as Infiltration, soil moisture storage change, evaporation snow accumulation and snow cover duration (Fang et al., 2007).

The lowering of winter precipitation and raising winter air temperature from actual meteorological observations were inputs in the model. Lower fall soil moisture and vegetation height parameters, sensitivity of snow accumulation, snow cover duration, sublimation of blowing snow, evaporation, infiltration into frozen soils, soil moisture storage change, snowmelt runoff and streamflow discharge were estimated as output from the simulation (Fang et al., 2007).

Canadian prairies are dominant features in the Smith Creek Basin area and CRHM was used to predict the snowmelt derived streamflow of the research basin located at east central Saskatchewan, Canada. The basin was divided into five representative basins and each representative basin was sub-divided into seven hydrological response units to simulating snow processes, frozen soil, variable contributing areas and wetland storage and runoff generation by physically-based modules without calibration. The simulated data was compared with field observations for snowpack, soil moisture and streamflow. The model performance was assessed by root mean square differences (RMSD) and the result stands within a considerable range. Finally, the estimated results suggest that the prediction of snow hydrology is possible without calibration with physically-based models along with high resolution geospatial data (Fang et al., 2010).

In addition, to assess the sensitivity of snowmelt hydrology in Marmot Creek, Alberta, a model was developed by considering the slope effects on snow redistribution, interception and energetics with minimal calibration. The basin was divided into four representative basins and each representative basin was sub-divided into eight hydrological response units for snowmelt sensitivity analysis. 40 forest disturbance scenarios were compared with the land cover for four simulation years and forest disturbances due to fire and clear-cutting affected the massive part of the basin areas with higher elevations and were generally more than twice as effective as pine beetle in increasing snowmelt or streamflow. Peak daily streamflow discharges were generated corresponding to forest cover disturbance much

better than the seasonal streamflow volumes and increased by forest removal on south-facing slopes and level sites (Pomeroy et al., 2012).

A study was conducted using CRHM along with two other models to simulate snowcover ablation and snowmelt runoff with limited data in subarctic environments, of Wolf Creek Research Basin, Yukon Territory. Spatial data, observations and landscape units (topography and vegetation) based on previous research were used. The comparisons between three models showed that CRHM simulations with proper solar radiation worked better for initial snowcover, snowcover ablation and snowmelt runoff in a complex subarctic environment. The model accuracy for snowcover ablation was increased by including the spatially distributed information (Dornes et al., 2009).

A devastating flood occurred in Southern Alberta at Marmot Creek Research Basin in late 2013. To simulate the flood, a physically-based modular hydrological model was developed using the CRHM platform by considering hydrological processes such as snow redistribution, sublimation, melt, runoff over frozen and unfrozen soil, evapotranspiration, subsurface runoff on hillslopes, groundwater recharge and discharge and streamflow routing. The simulation was not calibrated, and the streamflow was only compared with observation data for eight hydrological years. The model results were used to analyze the various hydrological processes due to extreme flood runoff generation. A flood sensitivity analysis was performed and sensitivity to changing precipitation and land cover was assessed by varying the precipitation amount. The model was then used to determine the responses of hydrological processes during the 2013 flood from different ecozones such as

alpine, tree line, montane forest and large and small forest clearings in Marmot Creek (Fang et al., 2016, Whitfield et al., 2016).

Another study was performed to assess impact of climate warming and permafrost thaw induced changes to surface water systems in streamflow over recent decades in northwestern Canada. The study area was a wetland-dominated and continental permafrost at Scotty Creek, NWT, Canada where permafrost is discontinuous and occurs below tree-covered peat plateaus. The model was set up for understanding the behavior of permafrost thawing and estimate basin runoff from the plateaus using the CRHM and evaluating the impact of changes primary runoff on the basin discharge. There was also an assessment for other flow and storage processes, such as secondary runoff and the routing of water through connected bogs and channel fens, and hydrograph simulation for basins with thawing permafrost plateaus (Quinton and Baltzer, 2013).

Chapter 3 Site Description and Data Collection and Preparation

The study was conducted in the Humber River Basin (HRB), which is located nearest to the City of Corner Brook and it has an estimated gross area of about 7068 Km² based on ArcGIS hydrology module basin delineation. To setup CRHM model requires observation data files that contain continuous daily precipitation and hourly air temperature, humidity (relative humidity or dew point), and wind speed data. This chapter contains details of the data which include land surface characterization: land surface elevation and land cover. It also includes observation data: precipitation, temperature, relative humidity and wind speed, streamflow and other associated data (water level for routing). Hourly solar radiation data or daily observations of sunshine hours are not mandatory, but CRHM has a provision to work with solar radiation data. Therefore, if reliable solar radiation data are not available, CRHM can estimate radiation derived from the day of year, latitude, and elevation, adjusted for cloud cover using the daily temperature range (Shook and Pomeroy, 2012).

3.1 Study Area

The Humber River (HR) basin, located on the west coast of Newfoundland, is the second largest river basin (7068 Km²) on the island (Jasim, 2014). The study area of the HR watershed lies between geographic latitudes 48° and 50° N and longitudes 56° and 59° W with an elevation range from 0m to 806m above mean sea level (Figure1). The watershed includes the Upper Humber River, with an area of 2110 Km², and Grand Lake, with an

area of 5030 Km². The length of the river reach is 153 Km, originating from the Gros Morne National Park and the location of outfall is at the Bay of Islands (Jasim, 2014). Grand Lake and Deer Lake are the two largest water bodies of the study area. The hydroelectric power plant in Deer Lake covers almost half of the basin area (Picco, 1997). Another hydroelectric generating station is located on the eastern side of Grand Lake (Jasim, 2014).

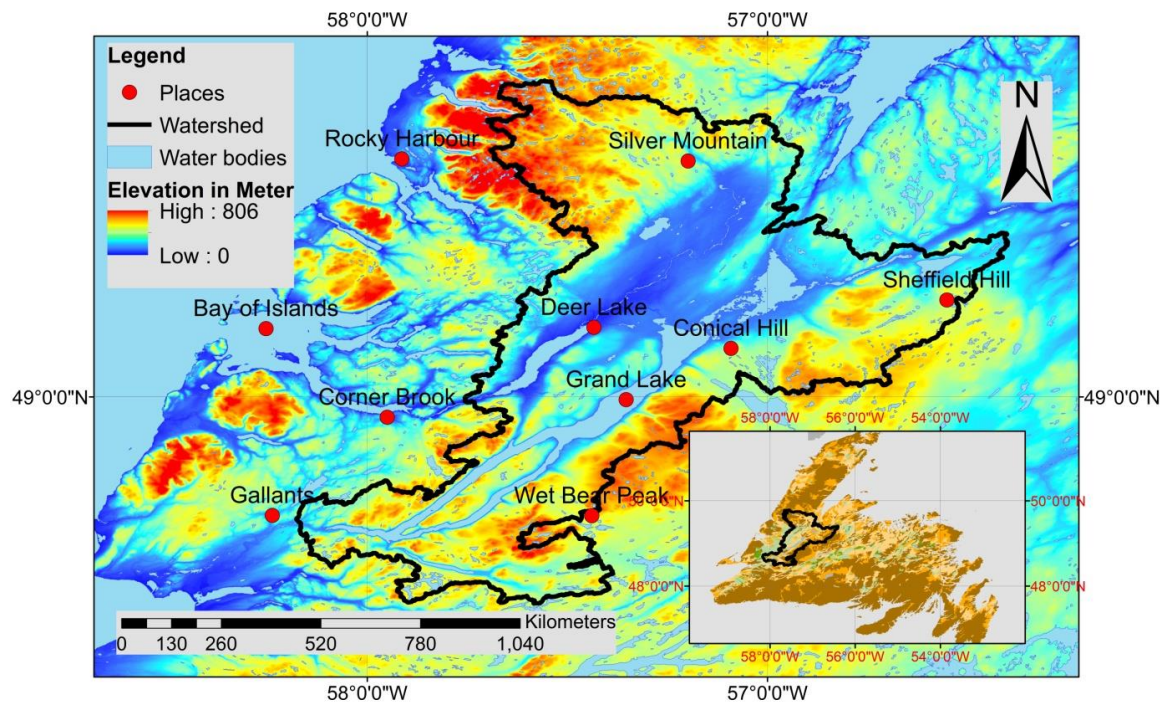


Figure 3. 1 Humber River Basin

Other smaller lakes are Hinds Lake, Adies Lake, Birchy Lake and Sandy Lake. Due to Grand Lake's controlled water levels above the natural level, Grand Lake, Sandy Lake and

Birchy Lake form one connected lake (Jasim, 2014). The stations over the lake area need accurate flow forecast information to operate safely and efficiently (Jasim, 2014).

3.1.1 Physiography

The Newfoundland Highlands is the dominant physiographic region of Humber River Basin and is divided into four sub-regions called the Great Northern Highlands, the Blow Me Down Mountains, the Atlantic Uplands of Newfoundland and the Grand Lake Lowlands (Picco, 1997).

The Great Northern Highlands' geographic position is northward along the Great Northern Peninsula from Bonne Bay and the Lomond River Valley. It is a barren mountainous high land with elevations ranging from 180 to 800 m. The Upper Humber River and the Main River flow along the highland slope in a southeastwardly direction. The Blow Me Down Highlands are located at the coast along the Gulf of St. Lawrence in the Bay of Islands to Trout River with abruptly rising highland with elevations ranging from 550 m to 700 m. On the contrary, the Atlantic Upland, a barren forest upland is situated between Grand Lake and Red Indian Lake and extending northward to the Burlington Peninsula with elevations ranging from 400 m to 600 m. The largest water bodies consist of Grand Lake, Sandy Lake

and Deer Lake, are the central part of the basin and dominant features of Grand Lake Lowlands (Picco, 1997).

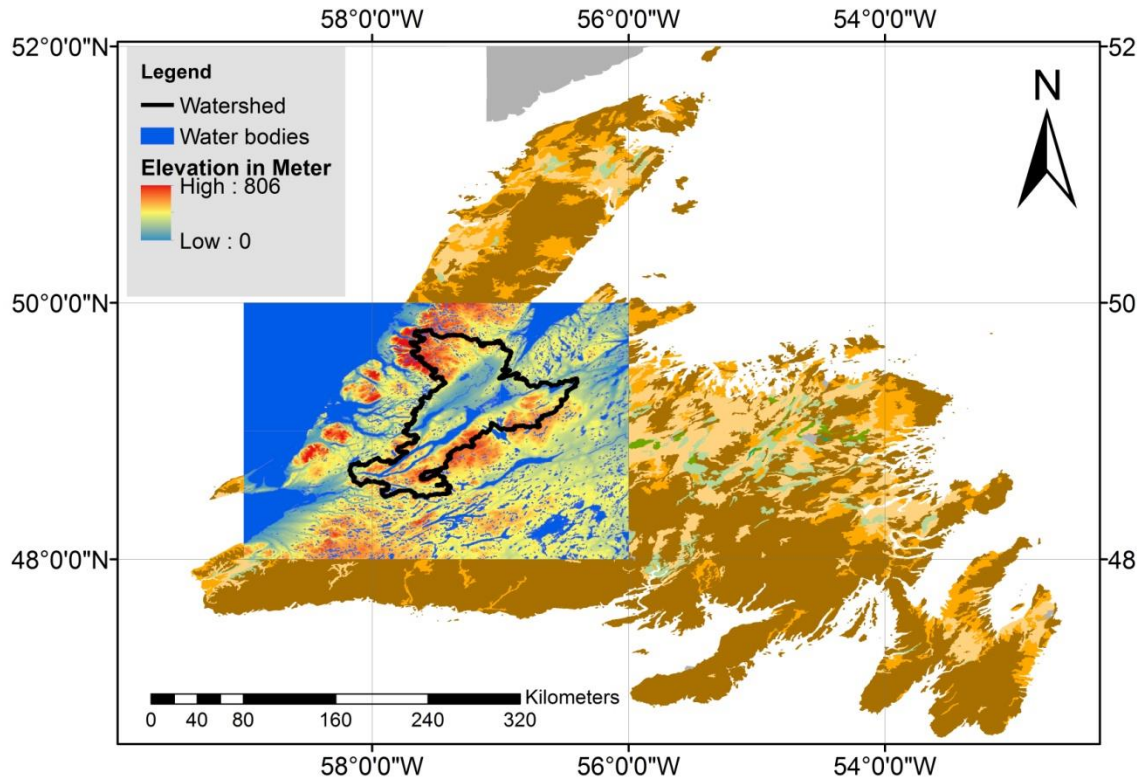


Figure 3. 2 General Location of Study Area

3.1.2 Surficial Geology

The basic pattern of surficial geology of the large watershed are bed rock, glacial tills, sands, gravels and organic soils. Bedrock is the dominant between all of them and forms extensive rock plains, knolls and ridges and covered by a thin layer of soils by vegetation of forest, scrub or peat bog. The bed rock encompasses the area of the Long-Range

Mountains, the Mountain Slopes, the Topsail Uplands and the Burlington Peninsula. It consists excessive soil moisture, adverse relief, steepness, stoniness and shallowness and are not suitable for agriculture. The glacial tills are found in irregular thickness with moraine deposit overlying the bedrock. The grey silty sand or sandy silt is found in the Long-Range Mountains and Topsail Uplands, and red clayey silt is found in the surface of the Humber River Valley. Deposits of ice contact sand and gravel are found in various till cover local areas having similarity of the lithology of underlying bedrock. The sand and gravel are deposited in the stream and river valleys and the greater percentage of sand and gravel deposits are found in the Deer Lake, Upper Humber River Valley, and the Sandy Lake-Birchy Lake areas. The area of poor surface drainage and unfertile Topsail Uplands at the southern Grand Lake have deposits of peats. High moor bogs and string bogs are accumulated on the highland plateaus of the Long-Range Mountains within the watershed (Picco, 1997).

3.1.3 Climate

The climate of the study area is characterized by a temperate, marine climate influenced by the Gulf of St. Lawrence to the west and long-range mountains to the east. The average annual temperature ranges from 2.9⁰C at BaieVerte to a high of 5.1⁰C at Corner Brook and the maximum precipitation is 1470mm at western coast of Woody Point and minimum precipitation is 943.5mm at Badger which is 80Km far away from coastal belt. Precipitation is influenced by orographic effects, with the lowest amounts during the months of April-May and the highest amounts during the fall season (Picco, 1997).

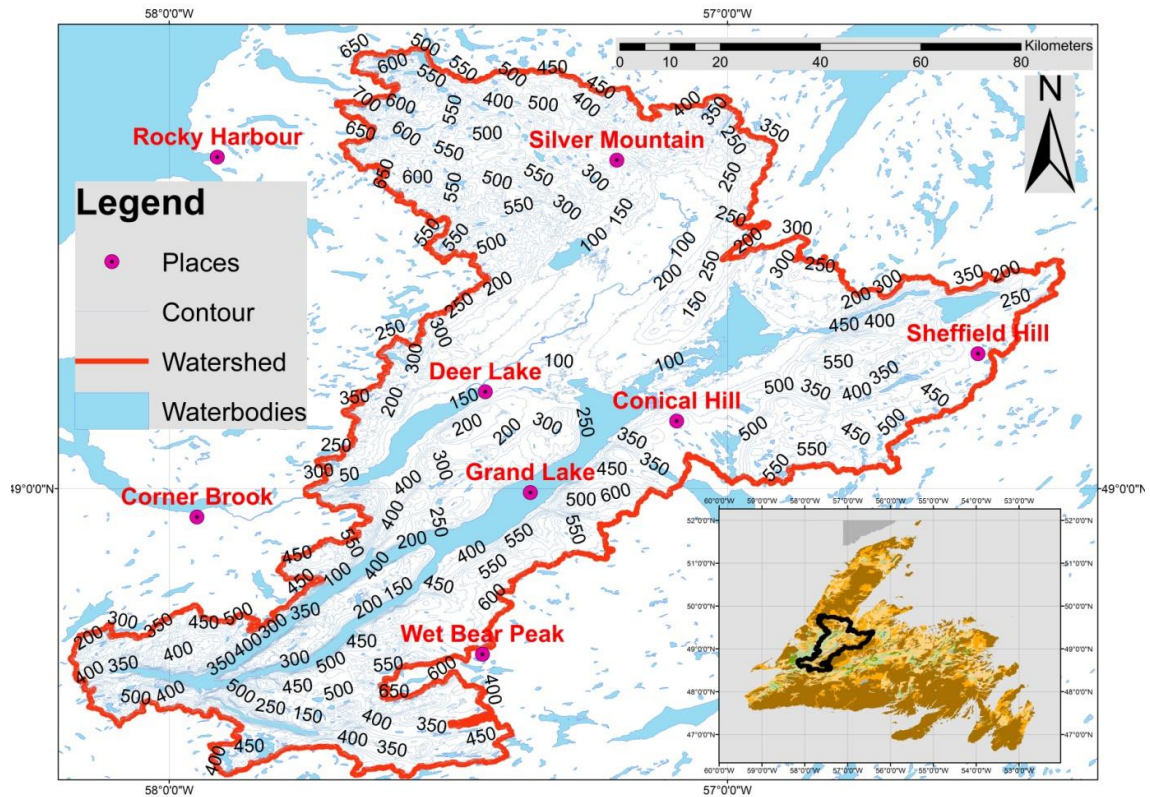


Figure 3. 3 Contour map (m) of the River Basin

3.1.4 Forest Cover

The Boreal Forest Region of Canada is the dominant forest; the Forest Boreal Region and the Forest and Barren Boreal Region are two sub-divisions. Four major classes of forest cover mature forest, scrub land, barren and peat bog, are seen in the basin, and mature forest cover is the dominant feature between all of them. The significant tree species are White Spruce, Black Spruce, Balsam Fir, White Pine, Yellow Birch, White Birch, Trembling Aspen and Balsam Poplar. Figure 3 illustrates the forest and vegetative cover within the basin. Forest covers the thickest glacial till layer above the bedrock and a major

part of the tree cover is sparse due to the thin veneer till soils and exposed bedrock. The downstream part of Deer Lake at Steady Brook has highest density of treed land and Balsam Fir, Black Spruce, Softwood Scrub and White Birch are dominant species. Softwood and hardwood scrub lands, rock barrens and peat bogs are also seen at the other areas of the watershed (Picco,1997).

3.2 Availability of Data

Flood forecasting were performed from 1995 by Water Resources Management Division of the Department of Environment and Labor for the residents living in the downstream sections and for the safe and efficient operation of the Deer Lake Power Company's hydroelectric development (Picco,1997). There are 8 hydrometric stations and 13 climate stations in operation both around and within the Humber River basin, but not all stations provide continuous hourly or daily data records. The data for this study were collected from Environment Canada Climate stations and Water Survey of Canada Hydrometric stations. Therefore, only 10 complete years of data were used, and missing data were filled up by temporal or spatial equations. For simulated flow, only three of the observed hydrometric stations named Reidville, Sheffield Brook near Trans-Canada Highway and the Humber Village Bridge were used. The study area does have climate and hydrometric records but there were insufficient concurrent data available to incorporate into model development (Cai, 2010).

3.3 Basin Data

The dominant factors of land use change are economic, technological, institutional, cultural, agricultural and globalized expansion by humans to meet their various needs. The world's landscape has changed as a result of various natural processes, and has had impact on local hydrology and environments. This makes it crucial to develop a hydrological model (Jasim, 2014). Land surface elevation and land cover information are used to generate the basin data required by CRHM model (Pomeroy et al., 2007; Pomeroy et al., 2013). Data used in this study are described in the following section.

3.3.1 Surface Elevation Data

The Base Features of the study area were derived hydrologically from surface elevation data for simulating the surface hydrology of the basin. Digital Elevation Models (DEMs) accurately replicate both landscape form and processes to support modelling of hydrological processes. To efficiently determine the hydrological processes, topographic accuracy, methods of preparation and grid size are important. The hydrologically corrected DEMs performed well for simulating basin cold regions hydrology and the response of performance improved the model results (Jarihaniet. al., 2015).

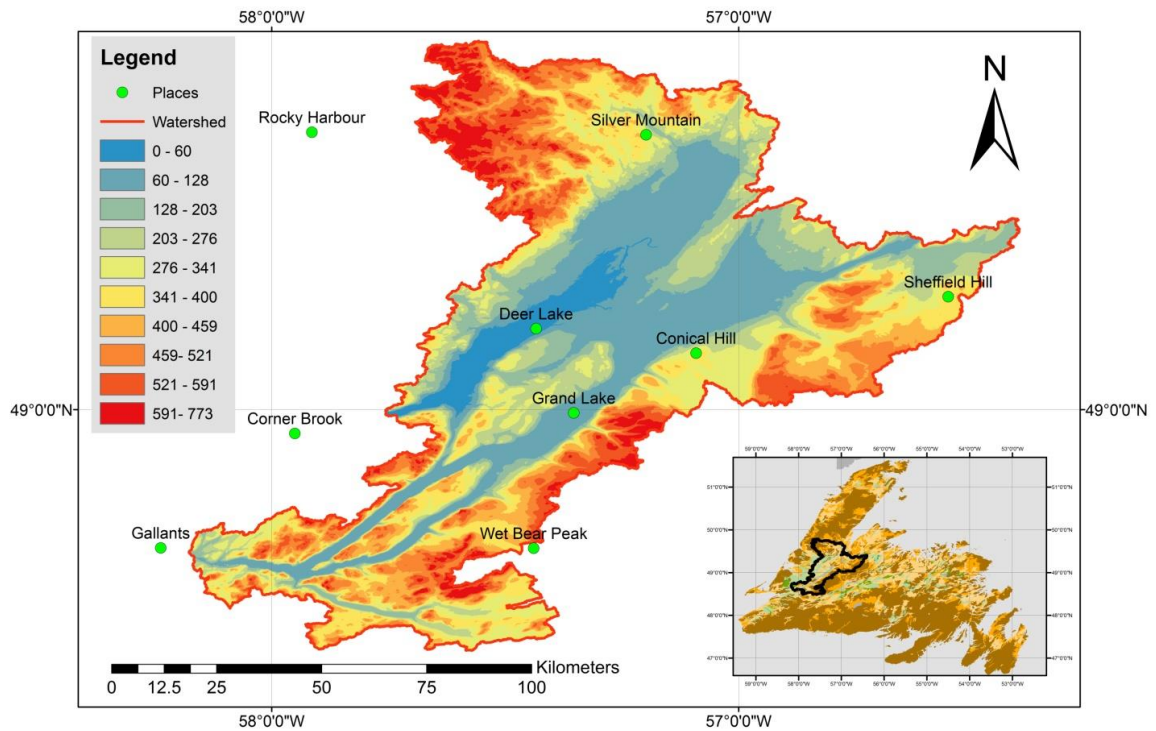


Figure 3. 4 DEM for Humber River Basin

The land's topography is expressed in terms of Digital Elevation Model (DEM) and various types of GIS terrain analysis help to provide elevation, aspect, slope, and to delineate the basin (Jasim, 2014; Pomeroy *et. al.*, 2013). In DEMs terrain is represented by a grid of squares and each square is associated with a single elevation value. In this study, a DEM from the United States Geological Survey (USGS) was used (<https://earthexplorer.usgs.gov/>) and DEM data were provided by the National Aeronautics and Space Administration (NASA) by Shuttle Radar Topography Mission (SRTM). Elevation datasets have missing data problems and typically those points occur over waterbodies, desert regions and mountains. Therefore, the original SRTM 30m DEM was used to produce the original point and contour data. The SRTM 30m DEM has the

resolution of 30m. The DEM tiles can be downloaded in 1-degree x 1-degree tiles in both ASCII or GeoTiff format and then mosaic to merge the whole study area. In this study, the GeoTiff format with WGS84 datum was used. The downloaded DEM data was cropped using ArcGIS in the required area for the study (Jasim, 2014).

3.3.2 Land Cover Data

Land cover changes affect the local hydrology, which in turn impacts the climate. The characterization of land cover is also very significant for the development of a hydrological model (Jasim, 2014; Pomeroy et al., 2013). The spatial representation was based on landscape units, topography and vegetation, and HRU are defined as spatial units (Pomeroy *et al.*, 2007).

Therefore, land cover data are required for the CRHM Model for generating a hydrologic response unit to simulate the hydrological cycle (Pomeroy *et al.*, 2007). The forest cover map was produced by the Earth Observation for Sustainable Development (EOSD) project for agricultural and forest areas of Canada and for Northern Territories with the collaboration of the Canadian Space Agency (CSA) and in partnership with the provincial and territorial governments, Water Information Service (NLWIS) of Agriculture and Agri-Food Canada (AAFC) and the Canadian Centre of Remote Sensing (CCRS). On the other hand, the land cover information was derived from vectorization of raster thematic data originating from classified Landsat 5 and Landsat 7 ortho-images and closest as possible to the source (original raster data).

In the present study, AVHRR land cover data (downloaded from http://www.agr.gc.ca/atlas/rest/services/imageservices/landuse_2010/ImageServer) were used for HRU classification. The data are based on a latitude-longitude coordinate system in raster format. Land was classified across Canada with a spatial resolution of 30 meters during the year 1990, 2000 and 2010. The classification system of land use maps is based on the Intergovernmental Panel on Climate Change (IPCC) and consist of: Forest, Water, Cropland, Grassland, Settlement and Other land. The land use classifications of 2010 were used for HRU identification. The land use maps of 2010 were developed with high-accuracy and high-resolution for the annual National Inventory Report (NIR) to the United Nations Framework Convention on Climate Change (UNFCCC).

CRHM requires land use data to be incorporated with its sub-basin. The HRU areas were calculated and pre-processed using ArcGIS toolsets. The land use data were obtained from GeoTIFF format (Figure 3.2) and land use classes were directly generated from classified GeoTIFFs (Jasim, 2014). The dominant land cover in the Humber River Basin consist of Boreal forest and wetland, and a considerable amount of area is natural waterbodies, native grassland and cropland. AVHRR land cover data consists of 13 types of land use classifications and requires a large number of hydrologic parameters. Owing to the limited number of parameters available in this study area, the parameters for boreal forest regions were selected from the Lower Smoky River Basin (Pomeroy et al., 2013).

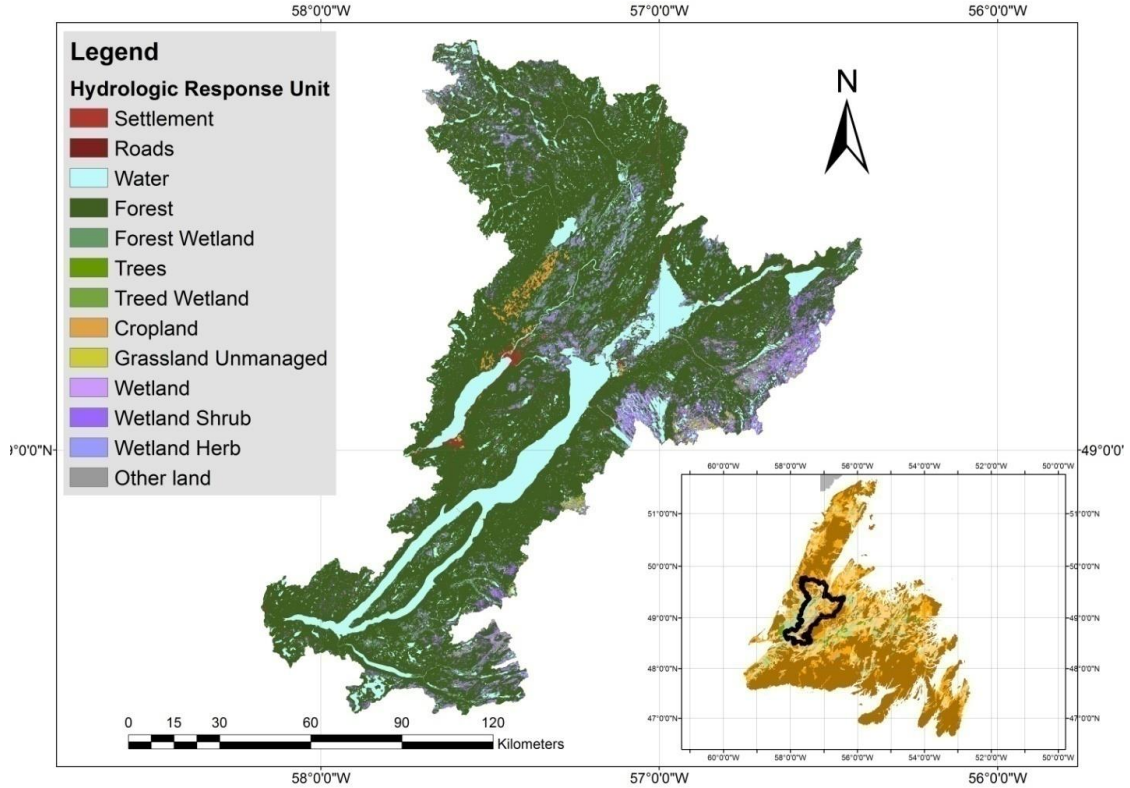


Figure 3. 5 Land Cover Map (GeoTIFF) for Humber River Basin

Waterbodies and Watercourses were collected from the National Topographic Data Base (NTDB) and the National Hydro Network (NHN) in vector datasets which included lakes, water courses and channels (Geogatis, Natural Resource Canada). The NTDB maps also include other features such as urban areas, vegetation, roads, railways, reservoirs, rivers, streams, canals, islands, waterfalls and human constructions (e.g. dams) as well as a linear drainage network (Pomeroy et al., 2013).

3.4 Meteorological and Hydrometric Data Collection

The spring snowmelt runoff is the main annual streamflow event in the basin. The frozen soils and wind redistribution of snow develop over the winter, and snowmelt and meltwater runoff normally occur in the early spring with the peak basin streamflow. Instrumentation at HRB consists of a streamflow gauge, main meteorological station, network of 12 rain gauge stations, and network of two wetland water level stations. The observation files required to run the CRHM model contain continuous daily or hourly precipitation (rainfall and snowfall) and hourly air temperature, humidity (relative humidity or dew point), and wind speed data. Hourly solar radiation data or daily observations of sunshine hours are not mandatory to set up the model, but is recommended for enhanced analysis. CRHM estimates radiation using calculated clear-sky solar radiation derived from the day of year, latitude, and elevation, and is adjusted for cloud cover using the daily temperature range when reliable radiation data is not available. The gaps of all meteorological observations were filled using temporal or spatial interpolation. For gaps of three hours or less, temporal interpolation is used for filling. For longer gaps, spatial interpolation from adjacent stations is used (Pomeroy et al., 2013). Other meteorological, snow depth and soil moisture data can be used to analyze and evaluate the performance of CRHM simulations.

3.4.1 Meteorological Data

The climate variables were recorded from various Environment Canada climate stations. CRHM requires at least temperature, relative humidity, wind speed and precipitation data

for simulating streamflow. In this study, those data were the most crucial. Data for a 10-year period spanning from 2001 to 2010 were sought for the study. It should be noted that not all of the stations selected for this study contain the entire 10-year dataset. A brief description of the selected meteorological stations and the datasets is given below.

The main meteorological station data were collected from January, 2001 to December, 2010 from Environment Canada National Climate Data. The data includes measurements of air temperature, relative humidity, wind speed, snow depth, rainfall, snowfall and total precipitation. Information Archive weather stations (downloaded from http://climate.weather.gc.ca/historical_data/search_historic_data_e.html) in or near the Humber River Basin were used for any missing variables. Hourly records of air temperature (t , °C), relative humidity (rh , %), wind speed (u , m/s) and daily precipitation (ppt , mm) were used to create observation files for CRHM (Jasim, 2014; Pomeroy et al., 2013).

3.4.1.1 Precipitation Data

The precipitation data from 12 stations near the Humber River basin were selected for setting up the model. Precipitation data was obtained directly from Environment Canada. Table 3.1 summarizes the rainfall stations and includes location, latitude (°), longitude (°), elevation and period of available data. Figure 3.3 shows the location of the precipitation stations selected for the study. Each data file collected from Environment Canada contains

all the daily adjusted precipitation data available for a station. These data were then combined, formatted and written in the observation format required by CRHM.

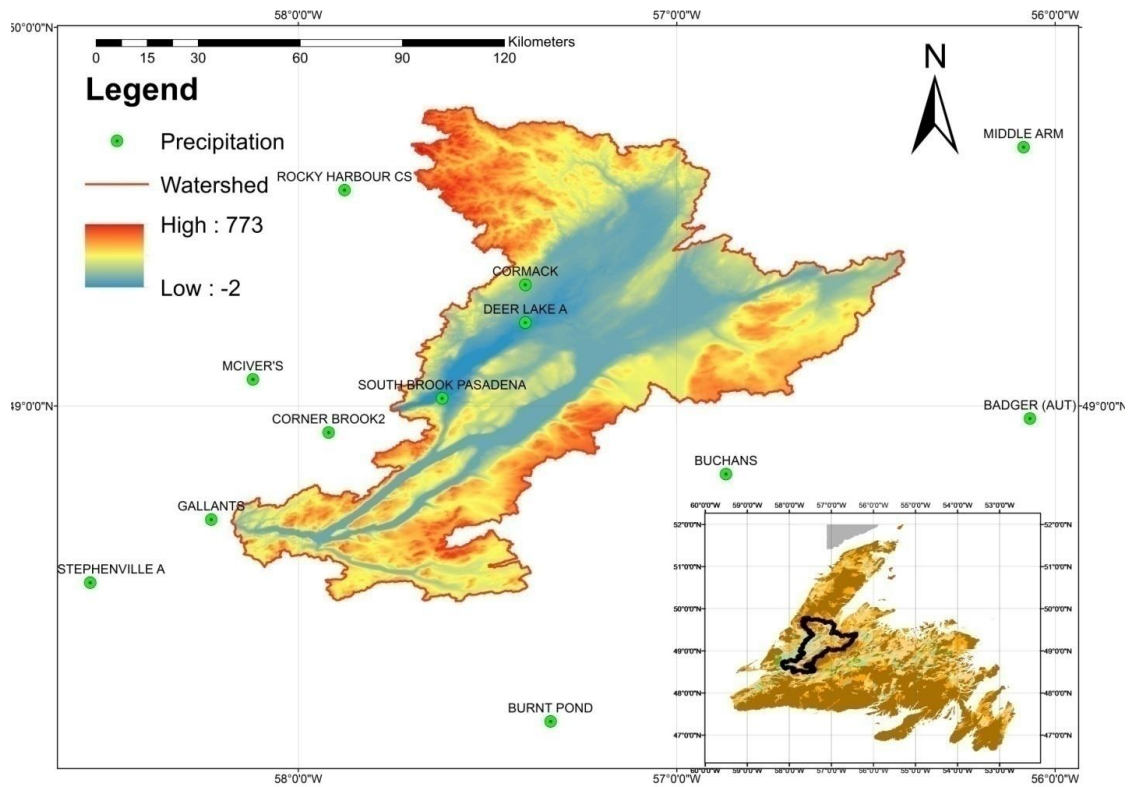


Figure 3. 6 Humber River sub-basins with meteorological stations having Daily Precipitation

Table 3. 1 Humber River Basin main meteorological station of precipitation

| Station | Province | Latitude (°) | Longitude (°) | Elevation (m a.s.l) | Period of Record Daily ppt |
|-------------------|-----------------|---------------------|----------------------|----------------------------|-------------------------------------|
| Badger AUT | NL | 48°58'00.000" N | 56°04'00.000" W | 102.70 m | 1 January, 2001 - 31 December, 2010 |
| Buchans | NL | 48°49'00.000" N | 56°52'00.000" W | 269.70 m | 1 January, 2001 - 31 December, 2010 |
| Burnt Pond | NL | 48°10'00.000" N | 57°20'00.000" W | 298.70 m | 1 January, 2001 - 31 December, 2010 |
| Cormack | NL | 49°19'00.000" N | 57°24'00.000" W | 153.90 m | 1 January, 2001 - 31 December, 2010 |
| Corner Brook | NL | 48°56'00.000" N | 57°55'00.000" W | 151.80 m | 1 January, 2001 - 31 December, 2010 |
| Deer Lake Airport | NL | 49°12'33.000" N | 57°23'40.000" W | 21.90 m | 1 January, 2001 - 31 December, 2010 |
| Gallants | NL | 48°42'00.000" N | 58°14'00.000" W | 143.00 m | 1 January, 2001 - 31 December, 2010 |
| Mcivers | NL | 49°04'00.000" N | 58°07'00.000" W | 49.50 m | 1 January, 2001 - 31 December, 2010 |
| Middle Arm WS | NL | 49°41'00.000" N | 56°05'00.000" W | 47.80 m | 1 January, 2001 - 31 December, 2010 |

| Station | Province | Latitude (°) | Longitude (°) | Elevation (m a.s.l) | Period of Record Daily ppt |
|----------------------|-----------------|---------------------|----------------------|----------------------------|-------------------------------------|
| Rocky Harbour CS | NL | 49°34'12.000" N | 57°52'40.000" W | 67.70 m | 1 January, 2001 - 31 December, 2010 |
| South Brook Pasadena | NL | 49°01'00.000" N | 57°37'00.000" W | 38.10 m | 1 January, 2001 - 31 December, 2010 |
| Stephenville Airport | NL | 48°32'00.000" N | 58°33'00.000" W | 24.70 m | 1 January, 2001 - 31 December, 2010 |

3.4.1.2 Temperature Data

Historical temperature data obtained from station observations from National Climate Data and Information Archive Environment Canada. Five temperature stations are selected around the basin boundary. In this study, data were sought for the period of January, 2001 to December, 2010. Table 3.2 summarizes the gauges with their location, latitude (°), longitude (°), elevation and period of data collected. The temperature data were hourly recorded. These data were then combined, formatted and written in the observation file required by CRHM. Figure 3.4 shows the location of the weather stations and table 3.2 shows the elevation variations among the stations used.

Table 3. 2 Humber River Basin main meteorological station of Temperature, Relative Humidity and Wind Speed

| Station | Province | Latitude (°) | Longitude (°) | Elevation (m a.s.l) | Period of Record of Hourly t, rh, u |
|-------------------------------|----------|-----------------|-----------------|---------------------|-------------------------------------|
| Badger AUT | NL | 48°58'00.000" N | 56°04'00.000" W | 102.70 m | 1 January, 2001 - 31 December, 2010 |
| Corner Brook Weather Station | NL | 48°56'00.000" N | 57°55'00.000" W | 151.80 m | 1 January, 2001 - 31 December, 2010 |
| Deer Lake Airport | NL | 49°12'33.000" N | 57°23'40.000" W | 21.90 m | 1 January, 2001 - 31 December, 2010 |
| Rocky Harbour Climate Station | NL | 49°34'12.000" N | 57°52'40.000" W | 67.70 m | 1 January, 2001 - 31 December, 2010 |
| Stephenville Airport | NL | 48°32'00.000" N | 58°33'00.000" W | 24.70 m | 1 January, 2001 - 31 December, 2010 |

3.4.1.3 Relative Humidity Data

Historical hourly records of relative humidity data were collected from five stations for setting up the model. Data was obtained from National Climate Data and Information Archive Environment Canada. Table 3.2 summarizes the relative humidity stations and includes location, latitude (°), longitude (°), elevation and period of available data. In the

present study, data were sought for the period of January, 2001 to December, 2010. These data were then combined, formatted and written in the observation file required by CRHM.

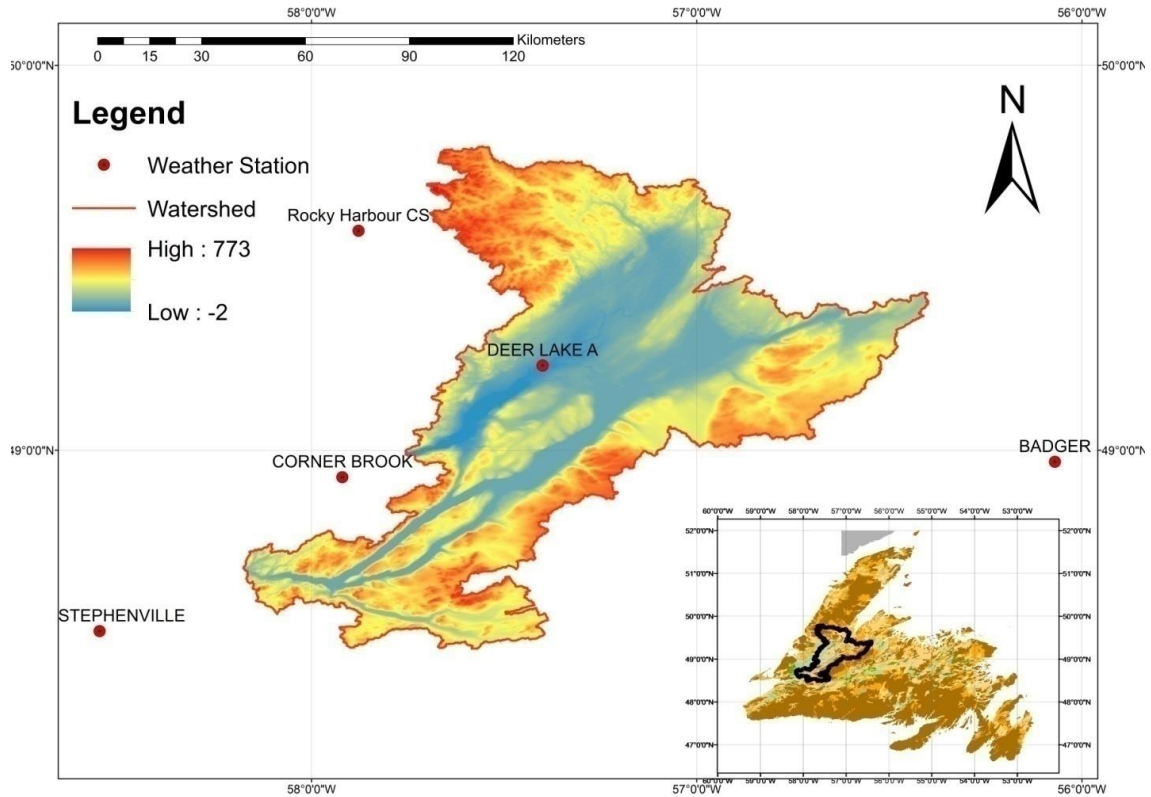


Figure 3. 7 Humber River sub-basins with meteorological stations having hourly Temperature, Relative Humidity and Wind Speed

3.4.1.4 Wind Speed Data

Wind speed data for setting up the model were collected from five stations. The data were obtained directly from National Climate Data and Information Archive Environment Canada. Table 3.2 summarizes the wind speed stations and includes location, latitude (°), longitude (°), elevation and period of available data. Then the data file collected from

Environment Canada contains all the hourly records available for a station were combined, formatted and written in the observation format required by CRHM.

3.4.2 Water Level Data for Routing

Water Level data were collected from archived hydrometric data from the Water Survey of Canada (downloaded from https://wateroffice.ec.gc.ca/search/historical_e.html). There are only two stream gauges for measuring water level data in the study area. Figure 3.5 shows the locations of the water level data stations.

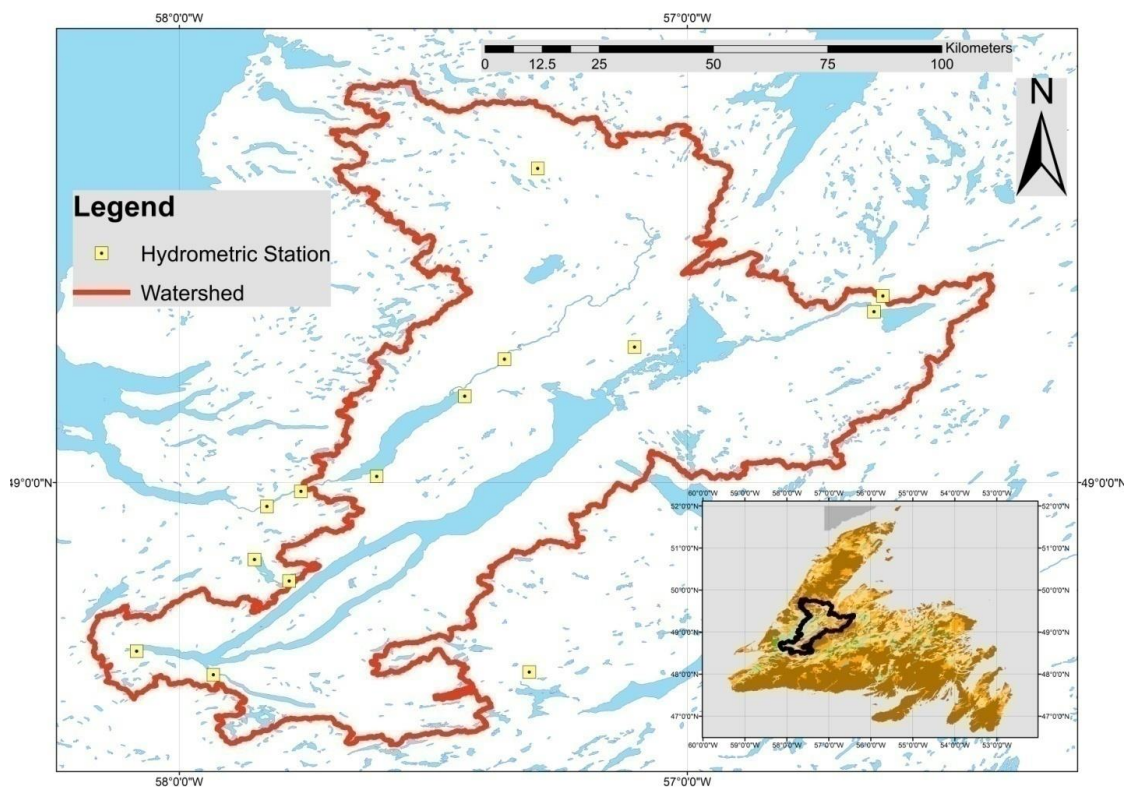


Figure 3. 8 Humber River sub-basins with Water Survey of Canada hydrometric station locations

3.4.3 Hydrometric Data for model Assessment

Observed hydrometric data, primarily streamflow data, were used to assess model performance. The archived data were collected from hydrometric stations in or near the Humber River basin. (downloaded from https://wateroffice.ec.gc.ca/search/historical_e.html) These data were acquired from the Water Survey of Canada. The data were collected by the National Hydrometric Program. Regression values were calculated using the observed and simulated streamflow values. In this study, daily streamflow data were sought for the period of 2001 to 2010. Table 3.3 summarizes the gauges and includes the following information: ID, latitude (°), longitude (°) and period of data collected.

Table 3. 3 Hydrometric stations in Humber River

| Station Name | Latitude (°) | Longitude (°) | Station ID |
|---|--------------|---------------|------------|
| Boot Brook at Trans-Canada Highway | 49°16'00" N | 57°06'14" W | 02YK008 |
| Copper Pond Brook near Corner Brook Lake | 48°48'23" N | 57°47'01" W | 02YL011 |
| Corner Brook Lake at Lake Outlet | 48°50'55" N | 57°51'07" W | 02YL009 |
| Deer Lake near Generating Station | 49°10'12" N | 57°26'17" W | 02YL007 |
| Grand Lake East of Grand Lake Brook | 48°40'06" N | 58°05'02" W | 02YK010 |
| Humber River at Humber Village Bridge | 48°58'58" N | 57°45'38" W | 02YL003 |
| Indian Brook Diversion above Birchy Lake | 49°22'02" N | 56°36'54" W | 02YM004 |
| Lewaseechjeech Brook at Little Grand Lake | 48°37'19" N | 57°55'59" W | 02YK002 |
| Sheffield Brook near Trans-Canada Highway | 49°20'10" N | 56°37'57" W | 02YK005 |
| South Brook at Pasadena | 49°00'44" N | 57°36'41" W | 02YL004 |
| Star Brook above Star Lake | 48°37'38" N | 57°18'40" W | 02YN004 |

| Station Name | Latitude (°) | Longitude (°) | Station ID |
|---|---------------------|----------------------|-------------------|
| Steady Brook above Confluence To Humber River | 48° 57' 11" N | 57° 49' 39" W | 02YL012 |
| Upper Humber River near Reidville | 49° 14' 34" N | 57° 21' 36" W | 02YL001 |
| Upper Humber River above Black Brook | 49° 37' 05" N | 57° 17' 40" W | 02YL008 |

3.4.4 Snow Survey Data

Archived snow survey data were acquired from the 12 precipitation stations. The stations have significant data gaps and no continuous data records for ground snow. The snow depth or ground snow data was recorded at the stations on a daily basis. Measured snow depth will be used to assess the performance of CRHM by regression analysis (Pomeroy et al., 2013).

3.5 Data Interpolation and Quality

CRHM hourly observation data for temperature, relative humidity and wind speed were assembled from the five meteorological stations during the period of October 2001 to July 2010. Precipitation data from twelve stations were collected for the same period. Two CRHM observation files were created for hourly and daily data (Pomeroy et al., 2013).

The Deer Lake Airport station is the only station which has complete and continuous data records. The other meteorological stations had missing hourly records for air temperature, relative humidity and wind speed, and for daily precipitation. Table 3.4 and table 3.5 summarizes the percentage of missing data in the model simulation period. An example of missing precipitation data from the stations is shown in Figure 3.6, which demonstrates a

gap in the data by a flag value of -1. Missing data can strongly effect the accuracy of model simulations, and should be considered when evaluating the model's performance. Continuous data means that there must be an observation for each time interval (daily or hourly) without gaps or substantial errors. Since all meteorological observations have gaps, these gaps must be filled by temporal or spatial interpolation. For gaps of three hours or less, temporal interpolation is used for infilling, whilst for longer gaps spatial interpolation from adjacent stations were used. Other meteorological data, as well as snowpack and soil moisture data, can be used to diagnose and evaluate CRHM simulations (Pomeroy et al., 2013).

Table 3. 4 shows station data quality for temperature, relative humidity and wind speed that were assessed using a percentage of missing data. All numbers in % of record from January, 2001 to December, 2010.

| Station | Temperature | Relative Humidity | Wind Speed |
|-------------------------------|--------------------|--------------------------|-------------------|
| Badger AUT | 1 | 1 | 1 |
| Corner Brook Weather Station | 1.5 | 1.5 | 5 |
| Deer Lake Airport | 0 | 0 | 0 |
| Rocky Harbour Climate Station | 1.5 | 3 | 1 |
| Stephenville Airport | 0 | 0 | 0 |

Table 3. 5 Precipitation Station data quality was assessed by the percentage of missing data. All numbers in % of record from January, 2001 to December, 2010.

| Station | Precipitation |
|----------------|----------------------|
| Badger AUT | 7.5 |
| Buchans | 30 |

| Station | Precipitation |
|----------------------|----------------------|
| Burnt Pond | 50 |
| Cormack | 0 |
| Corner Brook | 5 |
| Deer Lake Airport | 0 |
| Gallants | 41 |
| Mcivers | 35 |
| Middle Arm WS | 21 |
| Rocky Harbour CS | 6 |
| South Brook Pasadena | 51 |
| Stephenville Airport | 0 |

Hourly meteorological data gaps were infilled using spatial or temporal interpolation to create continuous records of hourly air temperature, relative humidity and wind speed. Gaps shorter than 3 hours were infilled by averaging the last and next data points and infilling the gap with the average. Data gaps longer than 3 hours were infilled using spatial interpolation from the spatial correlations calculated between the stations with gaps and Deer Lake Airport station data. This is shown in table 3.6 and table 3.7. The daily precipitation data gaps were filled using double mass curve ratiometric equations developed between stations, and no bias was introduced. Special care was taken when infilling gaps in precipitation so as not to introduce a cumulative bias in seasonal precipitation (Pomeroy et al., 2013).

Table 3. 6 Spatial interpolation equations based on correlations (temperature, relative humidity, wind speed) between stations (Pomeroy et al., 2013) and the coefficients (x, y and r^2) are shown below.

| Stations | Equations <i>Temperature = x t_{DeerLakeAirport} + y</i> <i>Relative Humidity = x rh_{DeerLakeAirport} + y</i> <i>Wind Speed = x u_{DeerLakeAirport} + y</i> |
|------------------|---|
| Badger AUT | 1.037; -0.318; 0.930 0.875; 7.867; 0.671 0.519; 2.606; 0.392 |
| Corner Brook | 0.972; 0.117; 0.956 0.746; 18.24; 0.773 0.585; 3.865; 0.366 |
| Rocky Harbour CS | 1.037; -0.318; 0.930 0.875; 7.867; 0.671 0.519; 2.606; 0.392 |
| Stephenville | 0.86; 1.719; 0.919 0.512; 38.36; 0.399 0.784; 11.32; 0.36 |

Table 3. 7 Spatial interpolation equations based on double mass curves (precipitation) between stations (Pomeroy et al., 2013) and the coefficients (z and r^2) are shown below.

| Stations | Equations precipitation = $z ppt_{DeerLakeAirport}$ |
|-----------------|--|
| Badger AUT | 0.884; 0.989 |
| Buchans | 1.118; 0.985 |
| Burnt Pond | 1.169; 0.971 |
| Cormack WS | 1.162; 0.986 |
| Corner Brook WS | 0.835; 0.990 |
| Gallants | 1.234; 0.994 |

| Stations | Equations precipitation = $z ppt_{DeerLakeAirport}$ |
|----------------------|---|
| Mcivers | 0.936; 0.983 |
| Middle Arm WS | 0.660; 0.984 |
| Rocky Harbour CS | 1.091 ; 0.989 |
| South Brook Pasadena | 0.66 ; 0.984 |
| Stephenville Airport | 1.155; 0.988 |

Chapter 4 Methodology and Model Setup

4.1 Modelling Approach

Climate change along with the irregular frequency and intensity of precipitation (rainfall and snowfall) make appropriate water management and storage plans difficult. Therefore, there is an urgent need to evaluate water resources and watershed analysis because they play a primary role in the sustainability of livelihood and regional economies (Singh *et al.*, 2014). The Humber River Basin Model was developed by using the Cold Regions Hydrological Model platform (CRHM), a physically-based, distributed, modular, object-oriented model originally developed to study the cold climate of continental Canada. The cold regions hydrological processes in a modelling platform were developed by the University of Saskatchewan in collaboration with Environment Canada based on 50 years of research in the central and western provinces and northern territories. The regions include prairie, parkland, boreal forest, subarctic, arctic and high elevation forest, and tundra environments (Pomeroy *et al.*, 2007).

The model incorporates an appropriate structure, spatial resolution and selected parameters over small to medium-sized basins (including the water balance, streamflow, soil moisture and snow accumulation) with physically-based algorithms for simulating the hydrological cycle (Pomeroy *et al.*, 2007). It has since given rise to physically-based object-oriented modelling system to develop the hydrological processes of significant uncertainty including snow redistribution by wind, snow interception, sublimation, snowmelt,

infiltration into frozen soils, hillslope water movement over permafrost, actual evaporation, and radiation exchange to complex surfaces. Warming in those regions are due to increased agriculture, forestry, and mining developments (Pomeroy et al., 2007).

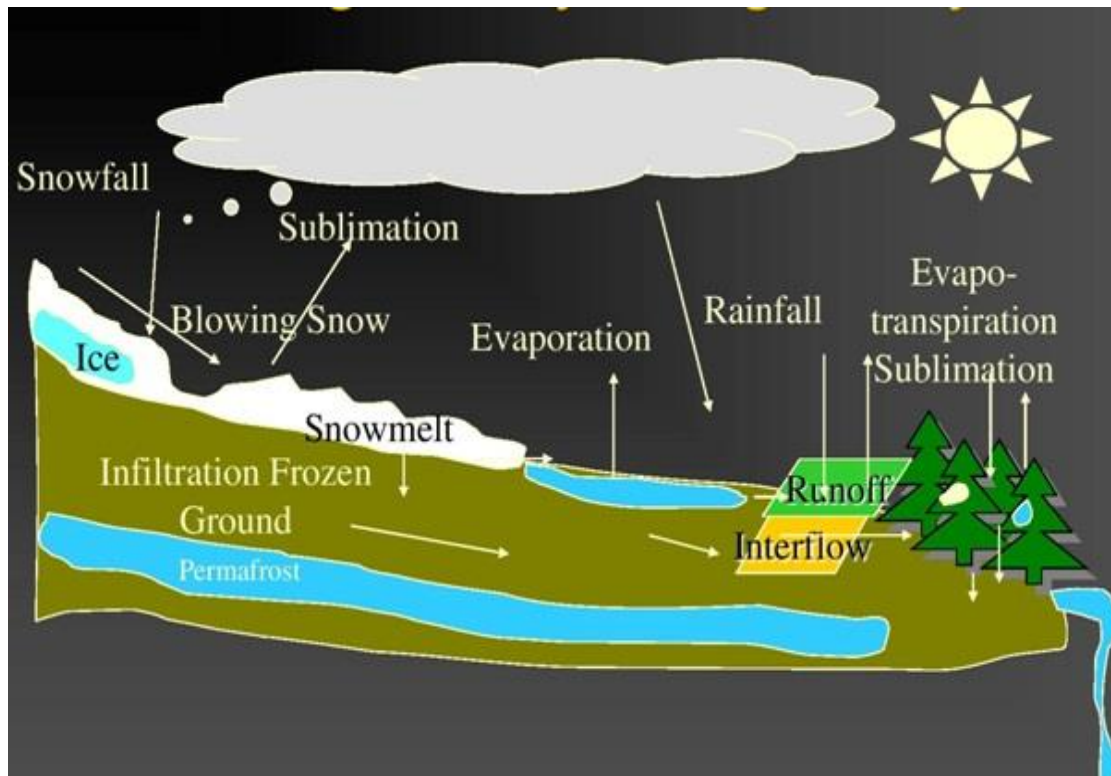


Figure 4. 1 Cold Regions Hydrological Cycle (Marsh et al., n.d.)

CRHM can be used for useful natural phenomena such as calculation of solar radiation using diurnal temperature ranges, direct and diffuse radiation to slopes, longwave radiation in complex terrain, blowing snow, sub-canopy turbulent and radiative transfer, sublimation, energy balance snowmelt, sub-surface flow, depression storage fill and spill, saturation excess overland flow and routing of surface, hydrological drought, sub-surface and streamflow. The model operates on the spatial unit of the hydrological response unit

(HRU) optimal for modelling basins' hydrological behavior. For a specific application, existing algorithms can be modified, or new algorithms can be developed and added to the module library (Dornes et al., 2008).

CRHM does not require calibration with gauged flows for its physically-based algorithms, and was therefore suitable for parameterization in ungauged basins. CRHM can be executed with a wide range of time steps, but the hourly time step is preferred. Parameters are selected from soil and land cover characteristics, vegetation cover, drainage networks, and other basin information. Some unmeasured parameter values can be transferred from hydrologically similar basins. Input parameters can be entered and edited directly in the user interface or obtained from GIS files, and from other formats such as ASCII. Calibration of unknown parameters against gauged flows is possible using trial and error (Pomeroy et al., 2013).

4.2 Watershed Delineation and Selection of Sub-basins for Modelling

A watershed is an area of surface which contributes major runoff to the single outlet as concentrated drainage. A larger watershed can be subdivided into smaller watersheds called sub-basins (Altaf et. al., 2013; Ariza-Villaverde et. al., 2015). In the present study, hydrological conditions of the watershed was analyzed by assessing the drainage pattern for information about permeability, storage capacity of the rocks and yield of the basin. Georeferencing was completed by taking ground control points (GCPs) by using the WGS 84 datum. Land use, land cover, topography, slope, and delineation of the drainage map of

the large basin were generated from an integrated use of USGS Shuttle Radar Topographic Mission (SRTM) 30m Digital Elevation Model (DEM). In addition, analysis of flow direction and flow accumulations were performed by filling DEM sinks. Subwatershed boundaries were derived by defining a pour point for each subwatershed. The stream length, area, and perimeter of the watershed were calculated by the geometry of the watershed polygons, and the length of the watershed was calculated by summing the length of the main stream channel and the distance from the top of the main channel to the watershed mouth (Altaf et. al., 2013; Bera et. al., 2014; Singh et. al., 2014).

Watersheds can be delineated from a DEM by computing the flow direction of the land surface. After that, the assessment of drainage pattern of a basin within the watershed is analyzed by background information about the hydrological conditions. An integrated use of satellite data, and DEM from USGS were used to generate topographic features and extract various drainage parameters (ArcGIS 10.1, n.d.; Hadley, 1961; Jasim, 2014; Johnston et. al., 2009).

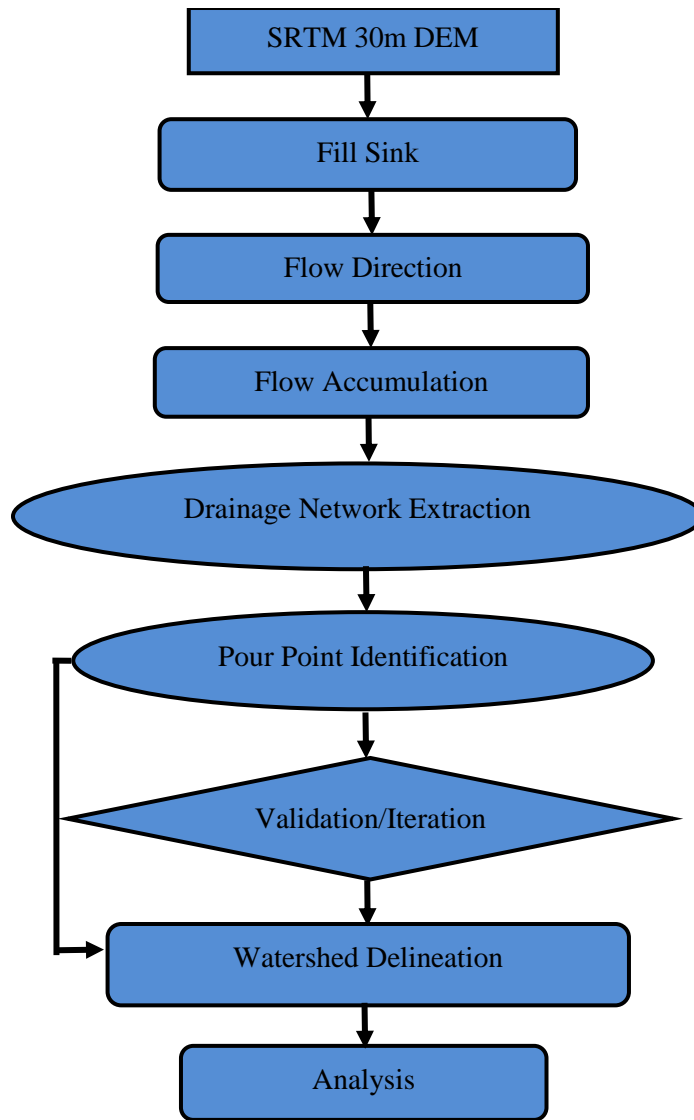


Figure 4. 2 Flow Chart of Watershed Delineation Methodology

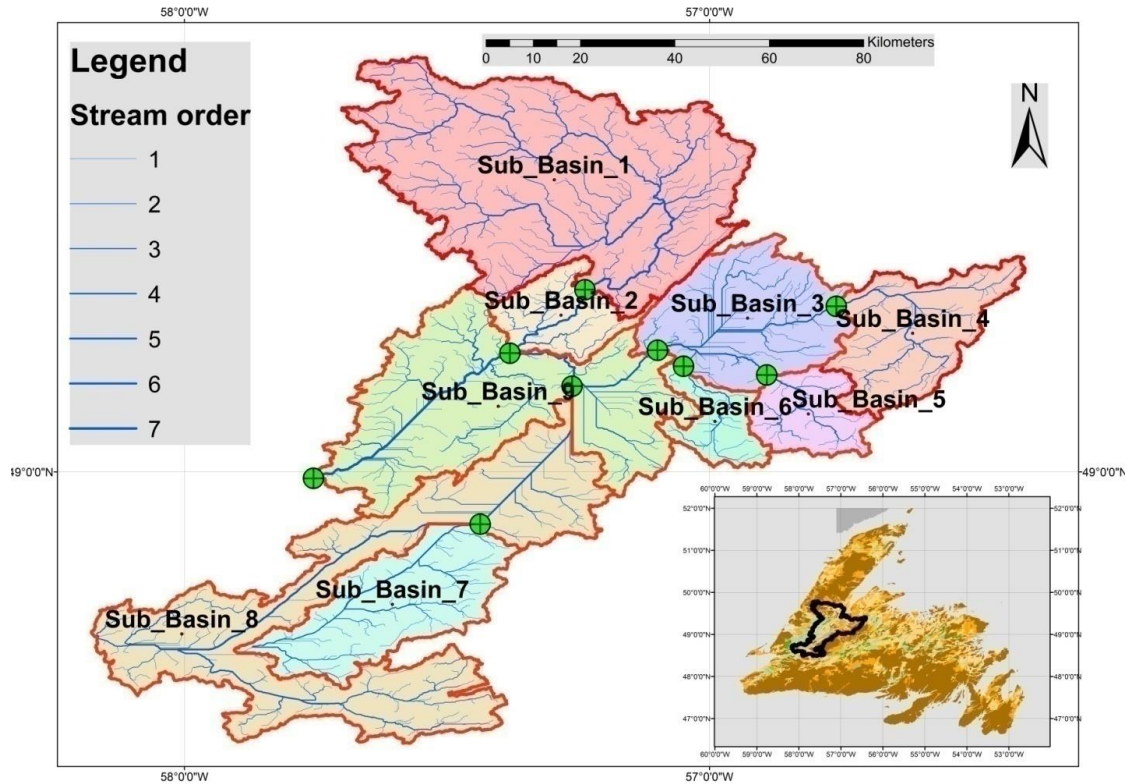


Figure 4. 3 Humber River sub-basins, ArcGIS-derived stream network. Colors are used to distinguish sub-basins and have no other meaning and green dots are the pour points

ArcView GIS terrain preprocessing was carried out using the DEM to delineate sub-basins, which assists in the sub-basin setup for CRHM modelling. In total, 9 sub-basins were delineated; sub-basin delineation for CRHM was mainly based on the location of the stream network. It was performed in an iterative way because there were not enough Water Survey of Canada stream gauge stations for the study period and irregular drainage patterns. The Humber River sub-basins delineated in this manner are shown in Figure 4.4 along with meteorological stations and hydrometric stations. Data acquired from hydrometric stations

reporting on a daily basis and can be used for streamflow routing, while other stations provide data that can only be accessed well after the measurement time.

For modelling of large basins such as HRB, a set of physically-based modules were assembled with several HRUs to represent a sub-basin, which was considered a “representative basin” (RB) having the same modules but differing parameter sets. The HRB was divided into nine sub-basins represented by nine RBs (Fig). Finally, the routing was performed along the main stream through lakes, wetlands and channel for streamflow generation (Fang et. al., 2010).

There were 9 sub-basins, 3 sub-basins had hydrometric stations and need to be modelled. Those are named Sub-Basins 1 to 9 and are shown in Figure 4.5. Those modelled sub-basins encompass 7068 Km² in area. The area for each of those 9 modelled sub-basins is listed in table 4.1.

Table 4.1 Area of the 9 modelled sub-basins

| Sub-Basin | Area(km²) |
|------------------|-----------------------------|
| Sub-Basin-1 | 1868 |
| Sub-Basin-2 | 257 |
| Sub-Basin-3 | 638 |
| Sub-Basin-4 | 490 |
| Sub-Basin-5 | 238 |
| Sub-Basin-6 | 181 |

| Sub-Basin | Area(km ²) |
|-------------|------------------------|
| Sub-Basin-7 | 620 |
| Sub-Basin-8 | 1530 |
| Sub-Basin-9 | 1247 |

4.3 Precipitation Station over Humber River sub-basins

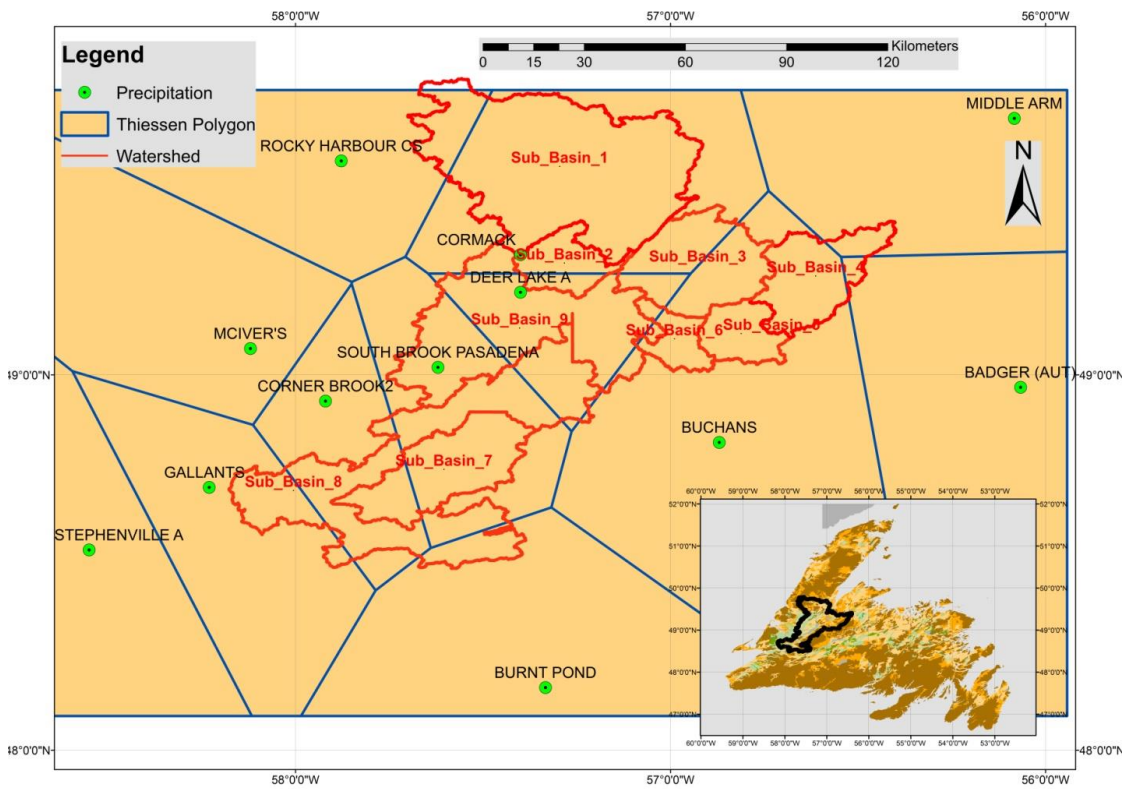


Figure 4. 4 Thiessen Polygon for Precipitation Station over Humber River sub-basins, ArcGIS-derived Thiessen Polygon

The daily station data were spatially interpolated to each of 9 modelled Humber River sub-basins using the Thiessen Polygon Analysis. Locations of the sub-basin, precipitation

stations, and Thiessen polygon analyses are shown in the figure 4.6. The polygons were derived from ArcGIS and used to calculate the weighted precipitation of the stations.

Table 4.2 Station influence over sub-basins

| Sub-Basin | Temperature, Humidity, Wind Speed | Relative Precipitation |
|------------------|---|--|
| Sub-Basin-1 | Rocky Harbour CS | Cormack WS |
| Sub-Basin-2 | Deer Lake Airport | Cormack WS |
| Sub-Basin-3 | Deer Lake Airport | Buchans, Cormack WS, Deer Lake Airport |
| Sub-Basin-4 | Badger AUT | Buchans, Badger AUT, Middle Arm WS |
| Sub-Basin-5 | Badger AUT | Buchans |
| Sub-Basin-6 | Deer Lake Airport | Buchans |
| Sub-Basin-7 | Corner Brook Weather Station | Corner Brook Weather Station, South Brook Pasadena |
| Sub-Basin-8 | Corner Brook Weather Station, Stephenville Airport, Deer Lake Airport | Corner Brook Weather Station, Gallants, South Brook Pasadena |
| Sub-Basin-9 | Deer Lake Airport | Deer Lake Airport, South Brook Pasadena |

4.4 Sub-basin Characterization and Typing

The spatial variability of land cover attributes and drainage conditions in the basin were expressed by HRU. CRHM was originally used to create hydrological models for smaller watersheds in western Canada; and mainly in a sub-arctic, boreal forest, mountain, or prairie setting. However, the Humber River Basin is diverse and large, almost 7068 km², and flows through a boreal forest towards the Bay of Islands. Some tributary streams originate in the forests of the boreal plain over the basin. To model this basin, 13 types of HRU were introduced among the nine and the region as a whole was classed as a boreal

forest. The 9 modelled sub-basins were then classified into HRU types by using AVHRR land cover information. There are 13 classes presented in the AVHRR land cover data for the modelled sub-basins: forest, forest wetland, roads, settlement, cropland, trees, treed wetland, water, grassland unmanaged, other land, wetland, wetland shrub, wetland herb, etc.

4.5 Land Use Map and Hydrological Response Unit and Sub-basins Structure and Parameterization

The hydrological processes can be described as calculations of single sets of parameters and state variables such as soil moisture, and horizontal fluxes in vertical and horizontal directions. (Pomeroy et al., 2007).

Hydrological response units (HRUs) are based on the combination of vegetation, soils, drainage, waterbody, and topographic parameter information. The 13 AVHRR land cover classes (Figure 3.5) were generalized to HRUs, and the HRU generation process is shown in Figure 4.8. As noted earlier, these 9 modelled sub-basins were in the boreal forest ecoregion of the Humber River Basin. Figure 3.5 shows the HRUs mapped on to the modelled sub-basins in the Humber River Basin. The corresponding area, elevation, aspect, and slope for the HRUs were computed using ArcGIS terrain analysis profile tool and ArcGIS hydrology tool. Tables F.1 to F.9 present the HRU area for these different types of sub-basins (Pomeroy et al., 2013; Fang et. al., 2010). Tables F.10 to F.18 present the HRU area, elevation, aspect, and slope for these different types of sub-basins.

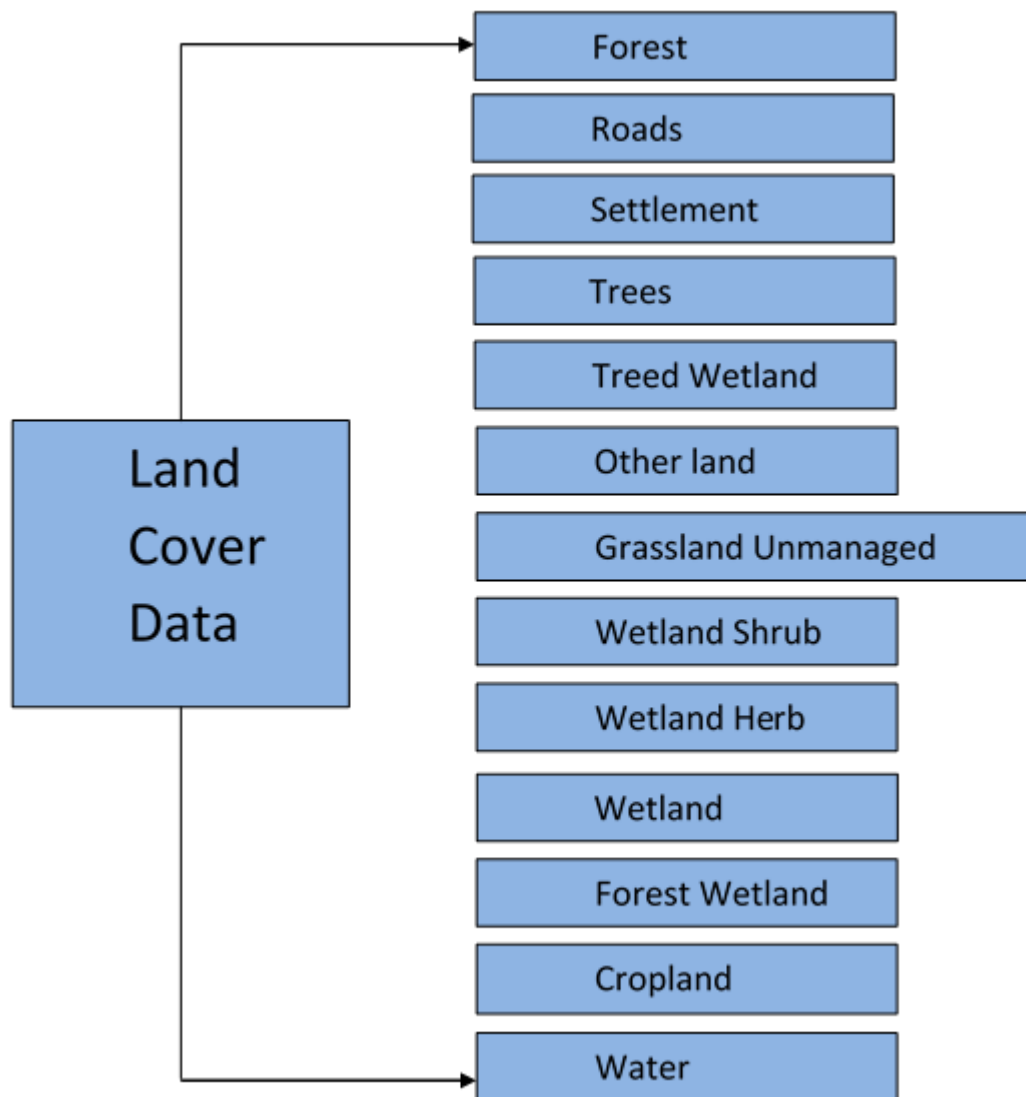


Figure 4. 5 HRU generation for the Humber River modelled sub-basins

4.6 Aspect Map

The slope direction of the maximum rate of change in value from each cell to its neighbours is identified by aspect. The values of the output raster will be the compass direction of the aspect. The compass direction is shown by the values of each cell in the output raster and

indicates the direction the cell's slope faces. It is measured clockwise in degrees from 0 (due north) to 360 (again due north) and flat areas without downslope direction are given a value of -1 (ArcGIS 10.1, n.d.).

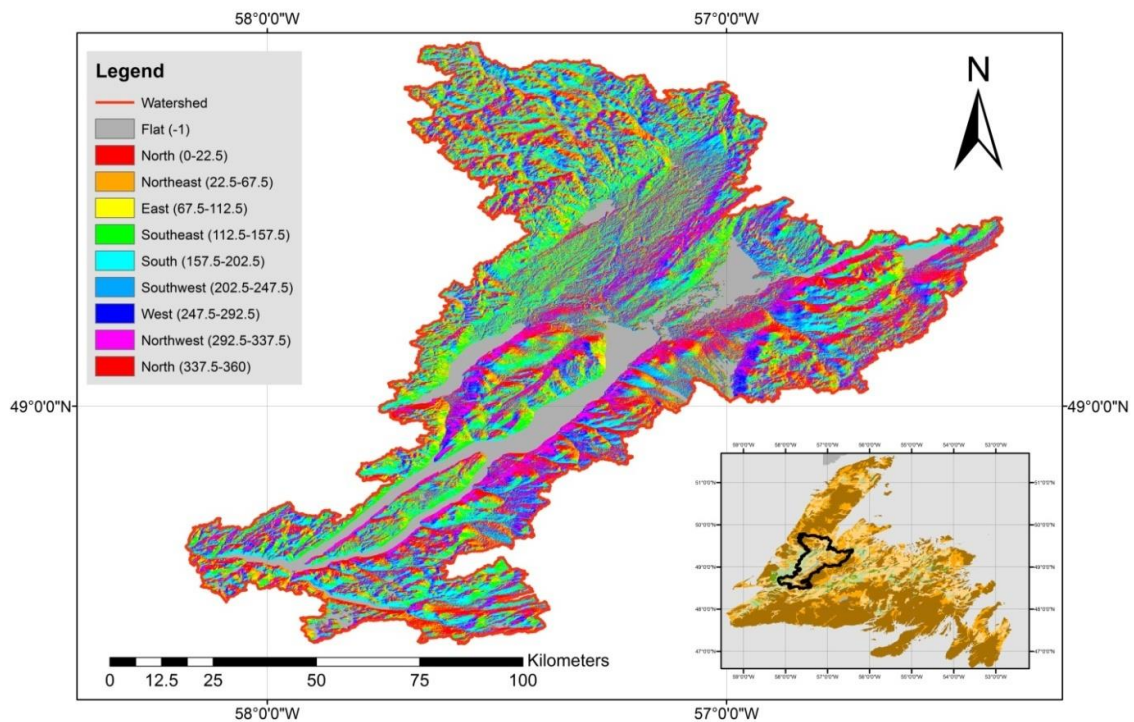


Figure 4. 6 Aspect of slopes in the Humber River Basin calculated from the DEM

The distribution of vegetation type and the impact of the sun on local climate can be determined by aspect map, which was itself determined by mountain slope face. The hottest time of day in the afternoon is shown by the west-facing slope, which will be warmer than a sheltered, east-facing slope. The aspect map derived from SRTM DEM represents the compass direction of the aspect. 0 degrees is true north, and the 90-degree aspect is to the east (Altaf et. al., 2013; Singh et. al., 2014).

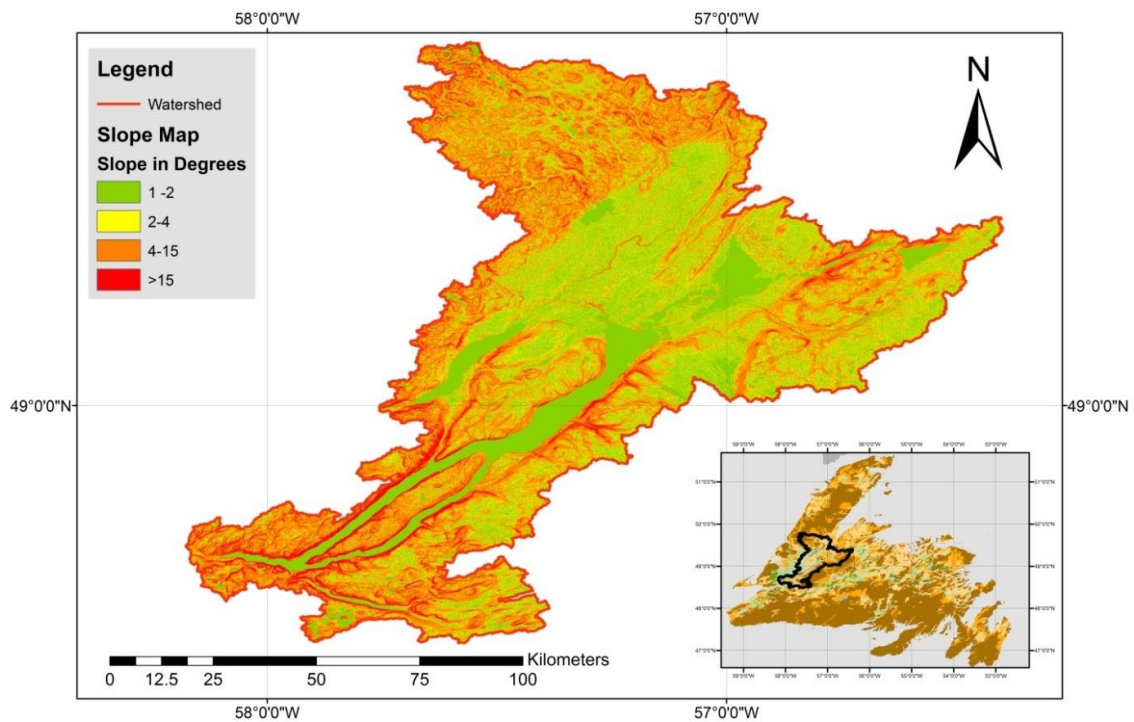


Figure 4. 7 Slope angle in the Humber River Basin, calculated from the DEM

4.7 Slope Map

The ArcGIS slope tool calculates the maximum rate of change in value from that cell to its neighbours. The maximum change in elevation over the distance between the cell and its eight neighbours identifies the steepest downhill. The flat terrain has a lower slope value and it is higher when steeper than terrain. The output slope raster is calculated in degrees (ArcGIS 10.1, n.d.). The measure of change in surface value over distance is called slope, which can be expressed in degrees or as a percentage. The maximum difference and gradient can in turn be determined by calculating the slope. To extract elevation from remote sensing data, point or contour lines are interpolated. DEM cell value is referenced

to a common datum (Singh et. al., 2014). The classified slope values in degrees are shown in the slope map at the Figure 4.10 (below).

4.8 Blowing snow module parameters

Table F.19 shows the values of blowing snow module parameters for the HRUs. Fetch distance is the upwind distance that blowing snow travels without disrupting its flow. These values were collected for the Lower Smoky River basin in the boreal forest region. Values of vegetation height, stalk density, and stalk diameter were set for these HRUs to represent them in the prairie and mountain forest environments during fall and winter. Those parameter values were also used here (Pomeroy et al., 2013; Fang et. al., 2010).

4.9 Albedo parameters

Table F.20 presents the values of albedo and canopy parameters for HRUs. For the albedo parameters, the measured values in the boreal forest environment by Granger and Pomeroy (1997) were used for the different HRUs. The albedo of fresh snow was considered to 0.85 based on measurements in the Canadian Rockies and northern prairies. The leaf area index (LAI), was set to 0.1 for the boreal ecoregion HRU (Pomeroy et al., 2013; Fang et. al., 2010).

4.10 Soil parameters

Table F.21 lists the values of soil parameters for HRUs of Humber River Basin. The drainage factors for lateral flow in soil layers, the groundwater layer, and the vertical flow

of excess soil water to groundwater were calculated by Brooks and Corey (1964) relationship using saturated hydraulic conductivity and pore size distribution parameters (Pomeroy et al., 2013).

Field data collection for soil was not performed in this study of the Humber River Basin. Soil samples were instead collected from the Smith Creek Research Basin and the Lower Smoky River Basin. The data were collected by field transects located near the rain gauge and water level stations of and were later used to determine the soil moisture and porosity, soil properties and vegetation during the fall of 2007 and 2008. These transects were selected to represent characteristic basin land uses: summer fallow, grain stubble, grassland, woodland, wetland, and drainage channel. Vegetation height, type, and density were recorded from the same field transects. (Fang et. al., 2010).

The groundwater storage capacity of the region is relatively unknown; an estimated value of 500 mm was set in the prairies, foothills, and mountains of western Canada. Surface depressional storage capacities were collected from the prairie environment of Smith Creek Research Basin and the data were used for agricultural ecoregion HRUs (Pomeroy et al., 2013).

$$rech_{ssr_K} = cK_{s_upper} \left(\frac{soil_{rech}}{soil_{rech_max}} \right)^{(3+2/\lambda)} \tan(\theta) \frac{soil_{rech_max}}{1000} \quad (4.1)$$

$$lowerr_{ssr_K} = cK_{s_lower} \left(\frac{soil_{lower}}{soil_{lower_max}} \right)^{(3+2/\lambda)} \tan(\theta) \frac{soil_{lowerr_max}}{1000} \quad (4.2)$$

$$gW_K = cK_{s_gW} \tan(\theta) \frac{gW}{1000} \quad (4.3)$$

$$soil_{gW_K} = cK_{s_lower} \left(\frac{soil_{moist}}{soil_{moist_max}} \right)^{(3+2/\lambda)} \quad (4.4)$$

where K_{s_gW} [ms^{-1}], K_{s_upper} [ms^{-1}], and K_{s_lower} [ms^{-1}] are the saturated hydraulic conductivities of the groundwater, recharge, and lower of soil layers, respectively. $soil_{rechr}$ [mm] and $soil_{moist}$ [mm] are the storage of water in recharge and entire soil (i.e. recharge and lower layers) layers, respectively; $soil_{lower}$ [mm] is the storage of water in the lower layer and is the difference between $soil_{rechr}$ [mm] and $soil_{moist}$ [mm], and c [-] is a units conversion factor from [ms^{-1}] to [$mmDay^{-1}$] equal to 86.4×106 (Fang et al., 2013).

4.11 Routing parameters

Figures 4.9 and 4.10 respectively demonstrate the routing sequences between HRUs and within the sub-basins. The routing sequence within the sub-basin from upland HRUs to the wetland HRUs and then to the channel HRUs is adopted from the sequence used in the CRHM modelling study (Pomeroy et al., 2010); the routing distribution parameter is used to partition the amount of runoff between HRUs; the values of the routing distribution parameters were estimated by applying the Hack's law length-area relationship (Fang et al., 2010).

The routing sequence between sub-basins follows the channel flow order from the upstream part to the downstream part of the basin, using Muskingum routing method. Flow travel times were calculated from the routing length and average flow velocity. For routing between HRUs within sub-basins varies from sub-basins to sub-basins. The routing

sequences of sub-basin 1 and sub-basin 2 were shown in figure 4.11. Routing lengths for the ‘main river valley’ HRU were determined from the channel length by GIS analysis. Manning’s equation (Chow, 1959) was used to estimate the average streamflow velocity, which requires longitudinal channel slope, Manning’s roughness coefficient, and hydraulic radius as parameters. The longitudinal channel slope of a HRU or a sub-basin was estimated from the average slope of the HRU or sub-basin. The average slope was derived from the terrain pre- processing GIS using the Humber River Basin DEM. The hydraulic radius was determined from the lookup table using channel shape and channel depth as criteria. For routing between sub-basins, channel shape was set as rectangular. The dimensionless weighting factor controls the level of attenuation, ranging from 0 (maximum attenuation) to 0.5 (no attenuation); a medium value of 0.25 was assigned (Pomeroy et al., 2013; Fang et. al., 2010).

$$v = \frac{1}{n} R^{\frac{2}{3}} S^{\frac{1}{2}} \quad (4.5)$$

$$K = \text{Travel time} = t = \frac{L}{v} \quad (4.6)$$

$$C_0 + C_1 + C_2 = 1.0 \quad (4.7)$$

$$Q_n = C_0 I_n + C_1 I_{n-1} + C_2 Q_{n-1} \quad (4.8)$$

$$C_0 = \frac{-Kx+0.5 \Delta t}{K-Kx+0.5\Delta t} \quad (4.9)$$

$$C_1 = \frac{Kx+0.5 \Delta t}{K-Kx+0.5\Delta t} \quad (4.10)$$

$$C_2 = \frac{K-Kx-0.5 \Delta t}{K-Kx+0.5\Delta t} \quad (4.11)$$

Where v is the velocity, R is the hydraulic Radius, S is channel slope and L is the length of the channel. C_0, C_1, C_2 are Muskingum routing coefficient and I is the inflow of the channel.

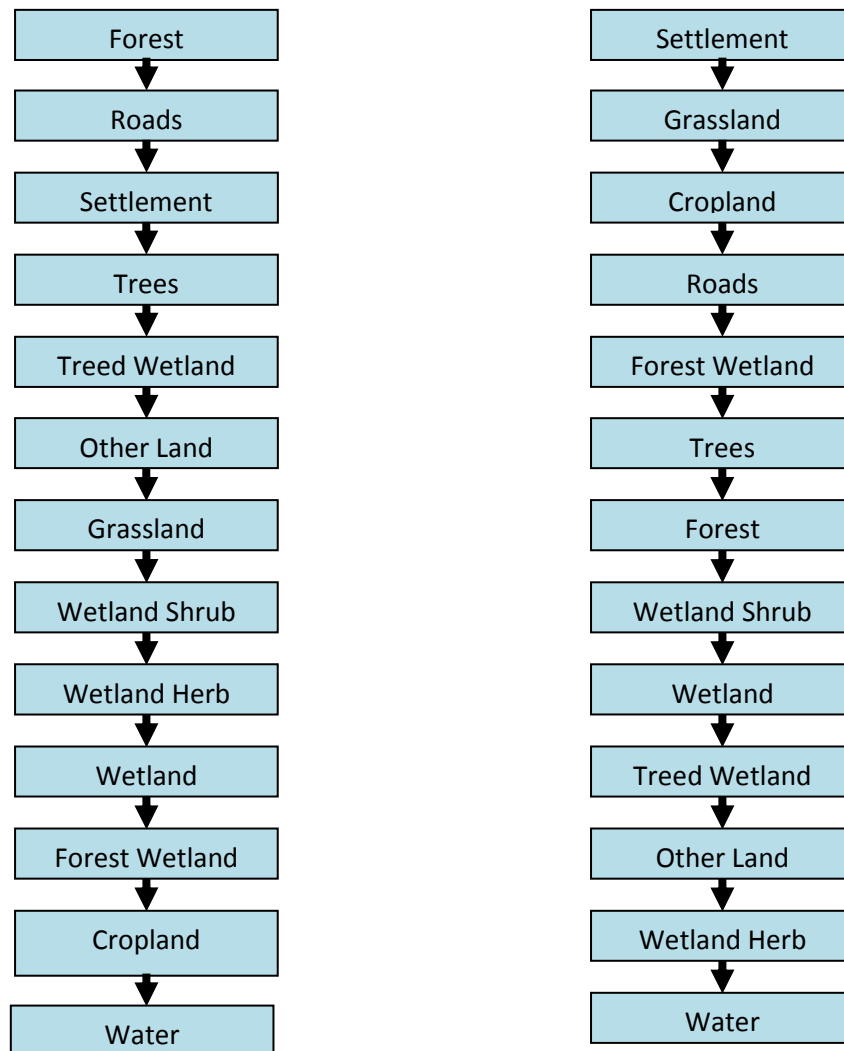


Figure 4. 8 Routing sequence between HRUs within the modelled sub-basins in the Humber River Basin and Sub-basin 1 and Sub-basin 2 are shown here, rest Sub-basins are almost same

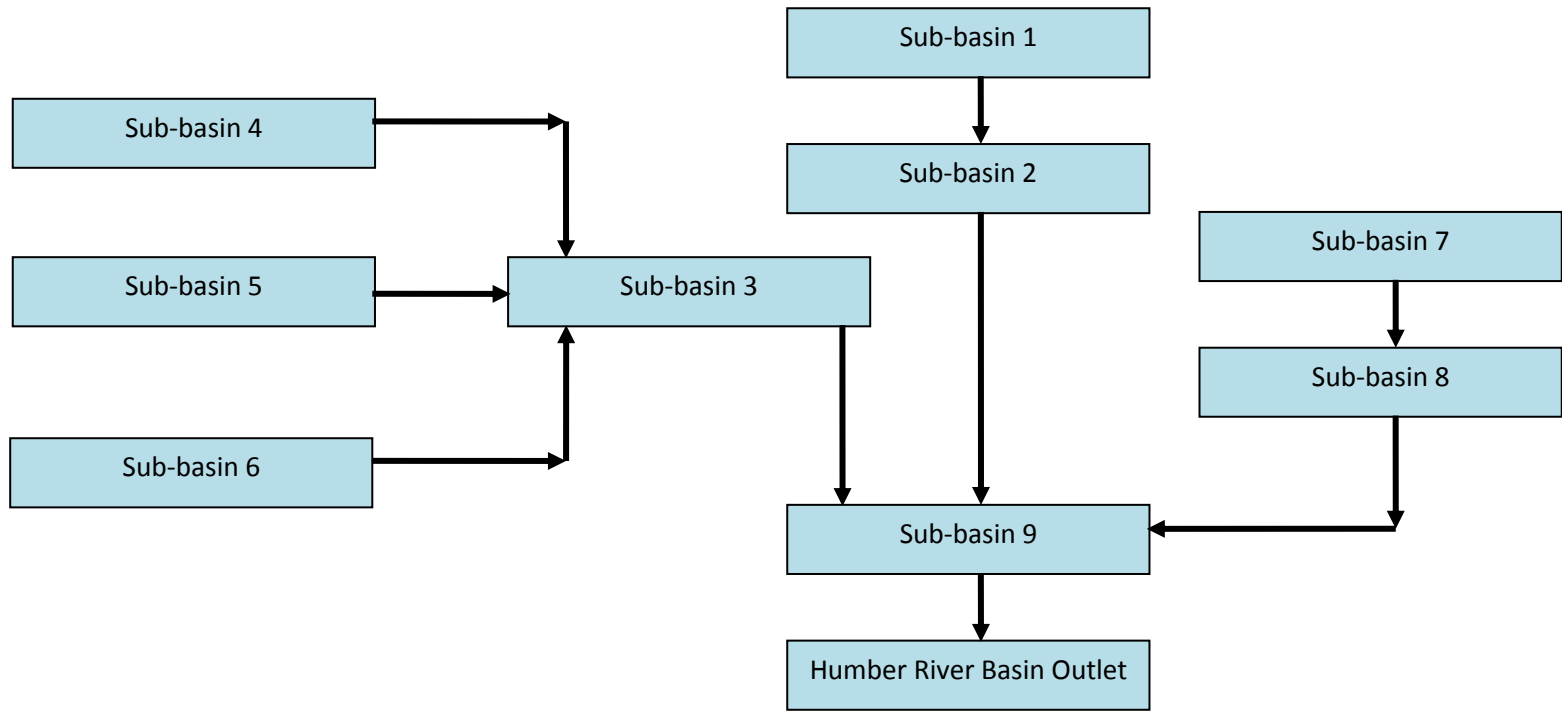


Figure 4. 9 Routing sequence between the modelled sub-basins in the Humber River Basin

4.12 Model Calibration

CRHM works successfully in uncalibrated runs in cold regions, but CRHM was never intended to be used with calibration, and the calibration is difficult. For the study area, the CRHM model was set up as a non-calibrated model. But after a complete model set-up, the model simulated results showed underestimated NSE values. Therefore, the model was calibrated with the Water Survey of Canada Hydrometeorological data for the period of September 2001 to December 2005.

The details of the stations including their location, drainage area and available data period were presented in Chapter 4. The simulated results were compared with the observed streamflow at the two gauge locations by using MB and RMSE as objective functions and are shown in Chapter 5.

4.12.1 Automatic Calibration using Shuffled Complex Evolution Optimization

There are no optimization routines available in the CRHM model and an optimization routine was developed using Shuffled Complex Evolution (SCE) Optimization in R environment. In this study, a calibration function was developed, and the function was optimized by SCE global algorithms. There are eleven Optimized parameters for thirteen land cover classes. Most of the parameters are related to the soil moisture module and four parameters are from the routing module.

Automatic calibration procedures were applied to the HRU to estimate the effective values of the parameters. Parameter sets were found using the SCE (Duan *et. al.*, 1993) global optimization algorithm. Automatic calibration was implemented using RStudio

software. Parameter sets for the streamflow simulation were obtained after performing a huge number of independent model simulations with the SCE algorithm using a single objective function, the root mean square error (RMSE) and model bias (MB). The NSE value was also estimated to assess the performance of the model during calibration of the distributed model (Duan *et. al.*, 1993).

The SCE method is a combination of probabilistic and deterministic approaches, data clustering, systematic evolution of a complex of points in global improvement, and competitive evolution. The algorithm's performance is depending on the controlled random search CRS2 method and a multistart algorithm based on the simplex method. The algorithms are assessed by simulating 100 randomly initiated trials on eight sample problems of varying difficulty. The SCE algorithm's flowchart is illustrated below in Figure 5.5 (Duan *et. al.*, 1993).

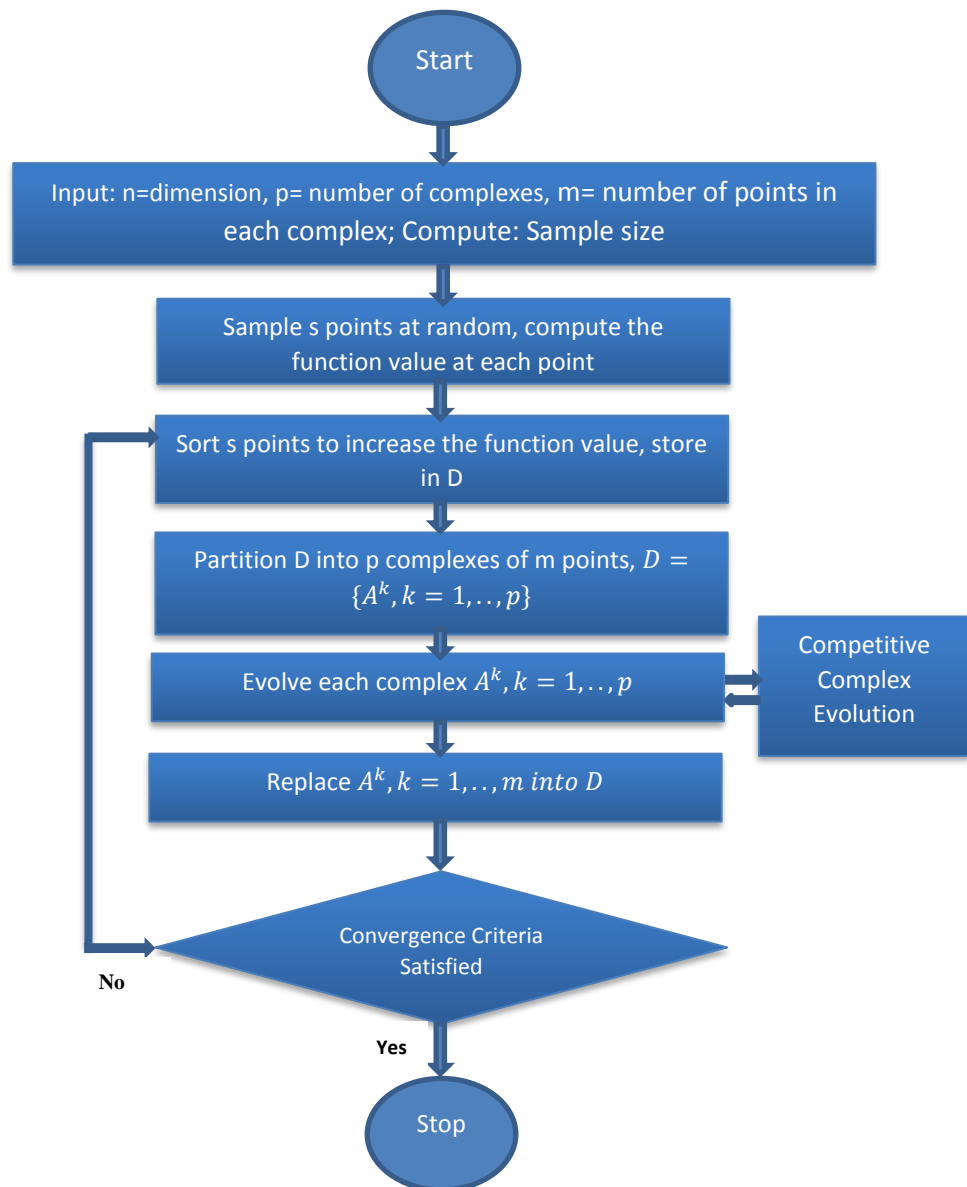


Figure 4. 10 Flow Chart of the shuffled complex evolution (SCE) method (Duan et. Al., 1993)

4.12.2 Manual Calibration

As it is hard to get good results from SCE optimization, it needs manual interference to optimize the parameters by trying different values. The parameters were adjusted

subsequently, one by one. This was also performed by the sub routine in R environments and the parameter values were fine-tuned by running the model. The manual calibration was performed for the entire study period, January 2001 to December 2010.

First, the albedo parameter was optimized and the winter snowpack events of the computed hydrographs coincide with the observed hydrographs. The soil moisture and routing parameters showed a significant effect on the timing of the spring hydrograph and the rate of melt. These parameters were set next. Several Other parameters were adjusted based on the type of land cover, precipitation and modeled runoff to match the observed hydrograph.

Chapter 5 Results and Discussion

5.1 Streamflow Simulation at Gauge Locations

Streamflow simulations conducted for the nine sub-basins of HRB were performed and compared to the Water Survey of Canada gauged discharges from January, 2001 to December, 2010 at the outlets of the three sub-basins at Upper Humber River Near Reidville, Sheffield Brook Near Trans-Canada Highway and Humber Village Bridge at the Humber River Basin outlet which is at the downstream of Deer Lake. Daily discharge data were obtained for those gauges and simulated daily averages were obtained from simulated hourly data. The discharge data from these gauges were used to evaluate the HRB discharge prediction for their corresponding sub-basins and were used to evaluate the performance of the model. The model simulation of daily discharges was compared to observed daily discharges, as shown in **Figure 5.2** to **Figure 5.4**. The simulations used to generate the integrated information about runoff generation from all surface and subsurface hydrological processes. During the starting of the simulations, the channels were choked with deep snow and ice and there was great uncertainty in some of the early season estimates of stream stage and velocity (Fang et. al., 2010).

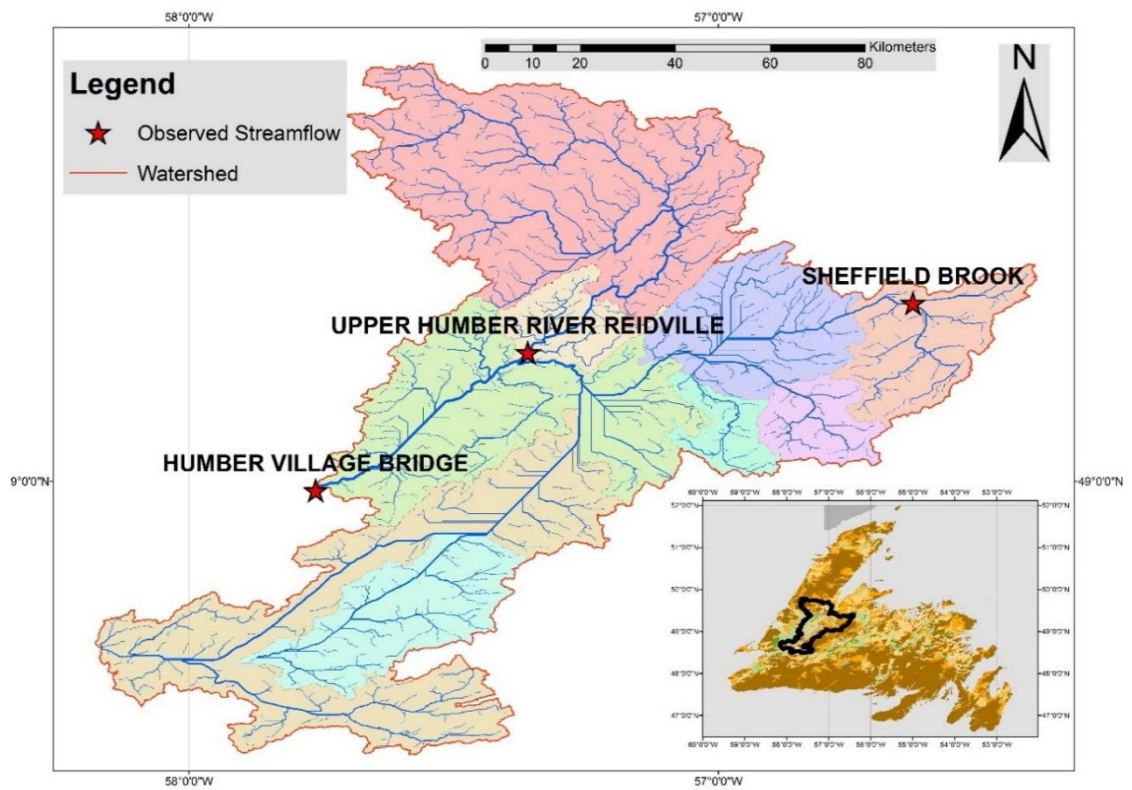


Figure 5. 1 Streamflow gauge of study area

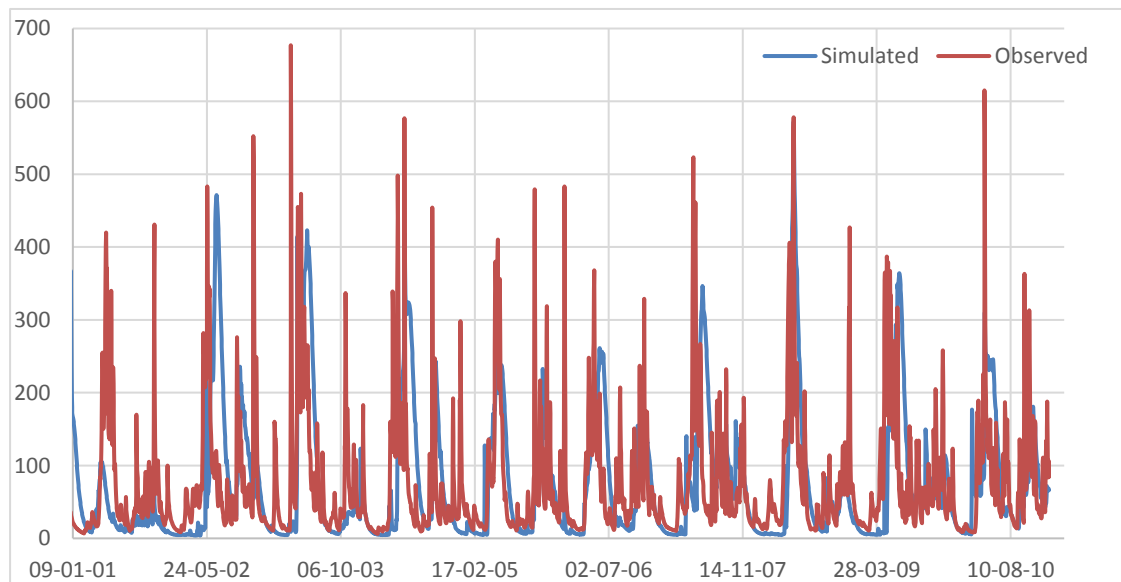


Figure 5. 2 Time series plot of Upper Humber River near Reidville

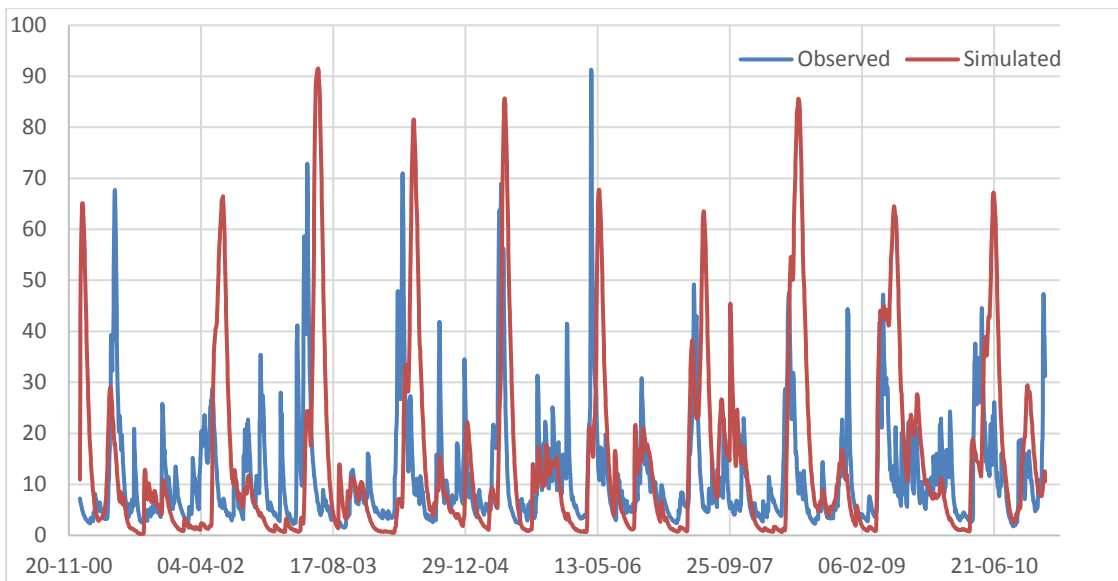


Figure 5. 3 Time series plot of Sheffield Brook near Trans-Canada Highway

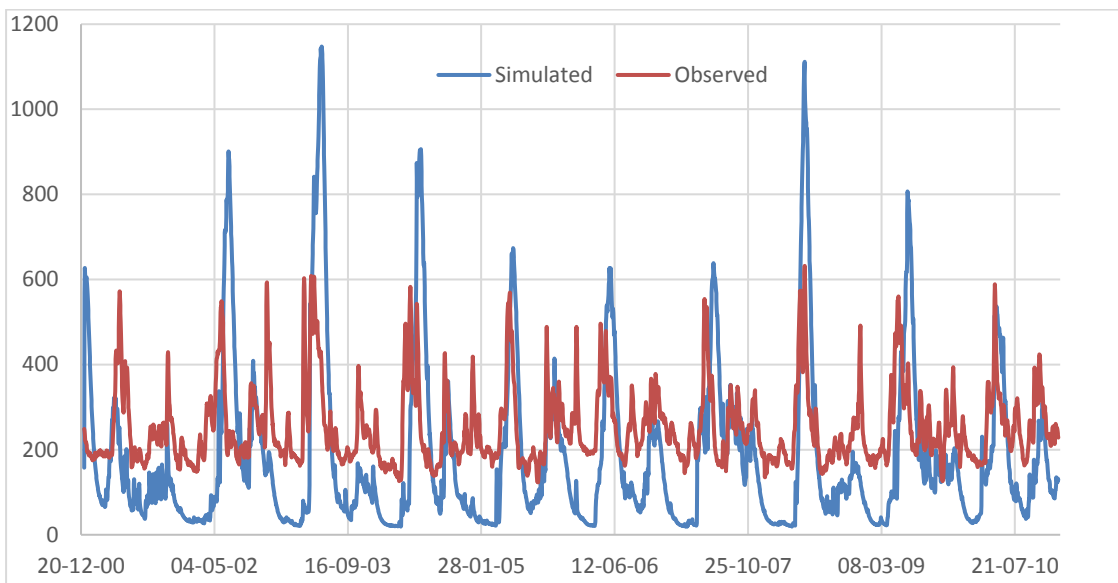


Figure 5. 4 Time series plot of Humber Village Bridge at downstream of Deer Lake

Both the precipitation and weather stations that provide forcing meteorological data for the model had substantial missing data, and model simulations of streamflow were greatly influenced. Various soil and routing parameters were also collected from the Lower Smoky River basin due to the lack of measured datasets. This greatly affects the

sub-surface and base flows during the winter snow accumulation period. Therefore, the simulated data differed from observed data during winter at the Humber Village Bridge gauge station. In contrast, there are two large reservoirs at the sub-basin 8 and sub-basin 9 where the reservoir flows were not calculated by the hydrological routing. As a result, the hydrological model could not perform well for the reservoir simulation. The simulated hydrographs for the outlet of HRB also have large spikes after the peak spring snowmelt runoff. The simulated peak spring discharges for all sub-basins are higher than the observed ones. These problems were solved by changing several model parameters which improves the model performance. The fall soil saturation fallstat parameter in the crack module was set to 35% for all HRUs to form large surface cracks to increase the amount of infiltration (Pomeroy et al., 1990). In addition, the subsurface depression storage factor and groundwater depression storage factor were also changed to improve model performance. Again, the subsurface travel time ssrKstorage in the netroute parameter in the routing module was set to 12 days for HRUs for the low velocity of interflow in mineral soils.

5.2 Streamflow prediction and comparison

Model performance was assessed by the following three measures: the model bias index (MB), the model efficiency index (ME) or Nash Sutcliffe efficiency (NSE), and the root mean square error (RMSE). These indexes provide a complementary evaluation of the model's performance. MB compares the total simulation output to the total of all observations. The NSE is a statistical measure, which indicates model performance compared to the mean of the observations that is explained by the predicted data. The

RMSE is a quantification of the absolute unit error between simulations and observations. Here, the MB is calculated as (Fang et. al., 2010)

$$MB = \frac{\sum_{i=1}^n x_{sim}}{\sum_{i=1}^n x_{obs}} \quad (5.1)$$

where x_{sim} and x_{obs} are the respective simulated and observed values at a given timestep for n number of paired simulated and observed values. Accordingly, MB values less than 1 signify an overall under-prediction by the model, and values greater than 1, an overall over-prediction by the model.

The representation of this statistical measure, NSE is given by, (Fang et. al., 2010)

$$NSE = 1 - \left[\frac{\sum_{i=1}^n (x_{sim} - x_{obs})^2}{\sum_{i=1}^n (x_{obs} - x_{avg})^2} \right] \quad (5.2)$$

where x_{avg} is the mean value of n number of x_{obs} values. The ratio between the mean square error and the variance of the observed data were represented by the second term of the equation. In Eq. (5.2), model efficiency increases as the NSE index approaches 1, which represents a perfect match between simulations and observations; 0 indicates an equal efficiency between simulations and the x_{avg} , with increasingly negative values signifying a progressively superior estimation by the x_{avg} .

In addition, The RMSE is a weighted measure of the difference between observation and simulation and has the same units as the observed and simulated values. The root mean square error (RMSE) is determined by (Fang et. al., 2010)

$$RMSE = \sqrt{\frac{1}{n} \sum_{i=1}^n (x_{sim} - x_{obs})^2} \quad (5.3)$$

Figure 5.1 to 5.3 shows the comparisons of observed and predicted daily streamflow discharge for sub-basin 2, sub-basin 4 and sub-basin 9. Simulations of the daily discharge for the sub-basin 2 and sub-basin 4 over the period of 2001–2010 were often in close range with gauged discharges, but sub-basin 9 have a gap during the winter snow accumulation period.

Table 5. 1 The Model bias index (MB), model efficiency index (NSE), and root mean square error (RMSE) of simulated streamflow (January 2001 to December 2010)

| Observation Station | MB | NSE | RMSE |
|---|-----------|------------|-------------|
| Sheffield Brook at Trans-Canada Highway | 1.3 | -2.14 | 19.37 |
| Upper Humber River near Reidville | 1 | -0.25 | 93.21 |
| Humber Village Bridge | 0.72 | -3.15 | 185.41 |

The negative NSE value underestimates for the sub-basins and calibration is needed to validate the model for the large river basin. Several parameters have no measured values and those are optimized for calibrating the model. The simulation period started in January and there would probably have been snow on the ground. The model was set up without any initial conditions (soil moisture, snowcover). As such, the simulation period was changed during the model calibration and the run was started from the fall season, September.

5.3 Model Calibration Results

Three sub-basins were selected at two stream gauge locations to simulate streamflow for the model calibration. Sub-basin 1 and sub-basin 2 were selected for the outlet at Upper Humber River at Reidville and Sub-basin 4 for the outlet point at Sheffield Brook near Trans-Canada Highway was considered for the calibration point.

5.3.1 Parameter Estimation from optimization

The model was calibrated separately for two sub-basins and two different parameter sets were obtained. The table contains these calibrated parameter sets. The results of the calibration in terms of Nash-Sutcliffe and the simulated streamflow plots are also given in Chapter 5 (Section 5.3 and 5.4).

The hydrological process was presented by physically based equations in distributed models. The landscape heterogeneity is a challenge for the parameter representation in the model. As, land surface physical characterizations are generally collected at a single point and there is no fixed rule for the model parameterization. The nonlinear nature of the natural hydrological processes made the determination of these effective parameters flexible (Pomeroy et al., 2007).

Additionally, there were no good measurements of the original soil moisture and those were estimated for better model performance within their upper and lower bounds. Parameters were spin-up during the model simulation. No initial conditions were set up as the model simulation began in the fall season before the snow accumulates (Duan *et al.*, 1993). These can be used to start the calibration and evaluation runs.

The land cover classes are used as single group parameters. The parameters were changed simultaneously in the SCE optimization. All these parameters mentioned are adjusted based on the observed fit of plotted hydrographs with the simulated hydrograph and the value of the objective function. The adjusted parameters were shown in table 5.2 and table 5.3

Table 5. 2 Optimized parameters for the observed and simulated streamflow of Sub-basin 1

| Parameters | (2001-2005) | (2001-2002) | (2001-2003) | (2003-2005) |
|-----------------------------|--------------------|--------------------|--------------------|--------------------|
| albedo Albedo_snow | 0.5 | 0.243 | 0.201 | 0.561 |
| Soil gw_K | 1 | 1.33 | 0.938 | 4.57 |
| Soil lower_ssr_K | 0.9 | 9.6 | 2.47 | 6.82 |
| Soil rechr_ssr_K | 3.2 | 3.04 | 8.3 | 2.06 |
| Soil Sd_gw_K | 7 | 5.9 | 1.32 | 1.34 |
| Soil Sd_ssr_K | 7 | 30.4 | 21.2 | 40.6 |
| Soil soil_gw_K | 30 | 4.08 | 5.48 | 1.75 |
| Netroute Kstorage | 0 | 11.8 | 14.4 | 14.1 |
| Netroute Lag | 0 | 0.328 | 7.09 | 7.1 |
| Netroute ssrKstorage | 0.8 | 12.5 | 9.68 | 2.17 |
| Netroute ssrLag | 12 | 0.32 | 9.23 | 6.73 |

Table 5. 3 Optimized parameters for the observed and simulated streamflow of Sub-basin 4

| Parameters | (2001-2005) | (2001-2002) | (2001-2003) | (2003-2005) |
|-----------------------------|--------------------|--------------------|--------------------|--------------------|
| albedo Albedo_snow | 0.4 | 0.01 | 0.273 | 0.39 |
| Soil gw_K | 1 | 5.24 | 3.11 | 0 |
| Soil lower_ssr_K | 1 | 6.2 | 6.81 | 1.35 |
| Soil rechr_ssr_K | 1.2 | 0.37 | 0.441 | 5.82 |
| Soil Sd_gw_K | 2.5 | 3.36 | 3.7 | 0 |
| Soil Sd_ssr_K | 5 | 14.2 | 6.13 | 14.1 |
| Soil soil_gw_K | 1 | 4.87 | 0.369 | 6.04 |
| Netroute Kstorage | 1 | 6.39 | 19.1 | 7.95 |
| Netroute Lag | 0 | 4.96 | 2.32 | 0.876 |
| Netroute ssrKstorage | 12 | 5.35 | 5.65 | 6.44 |
| Netroute ssrLag | 1 | 4.08 | 2.58 | 3.47 |

5.3.2 Streamflow Calibration

The model simulation was performed for the selected calibration period with the forcing data, and September 2001 to December 2005, September 2001 to December 2002, September 2001 to December 2003, and September 2003 to December 2005 were the calibration period for the forcing data. Table 5.4 summarizes the values of model

assessment from the Goodness of Fit (GOF) test and objective function obtained from the two different gauge locations.

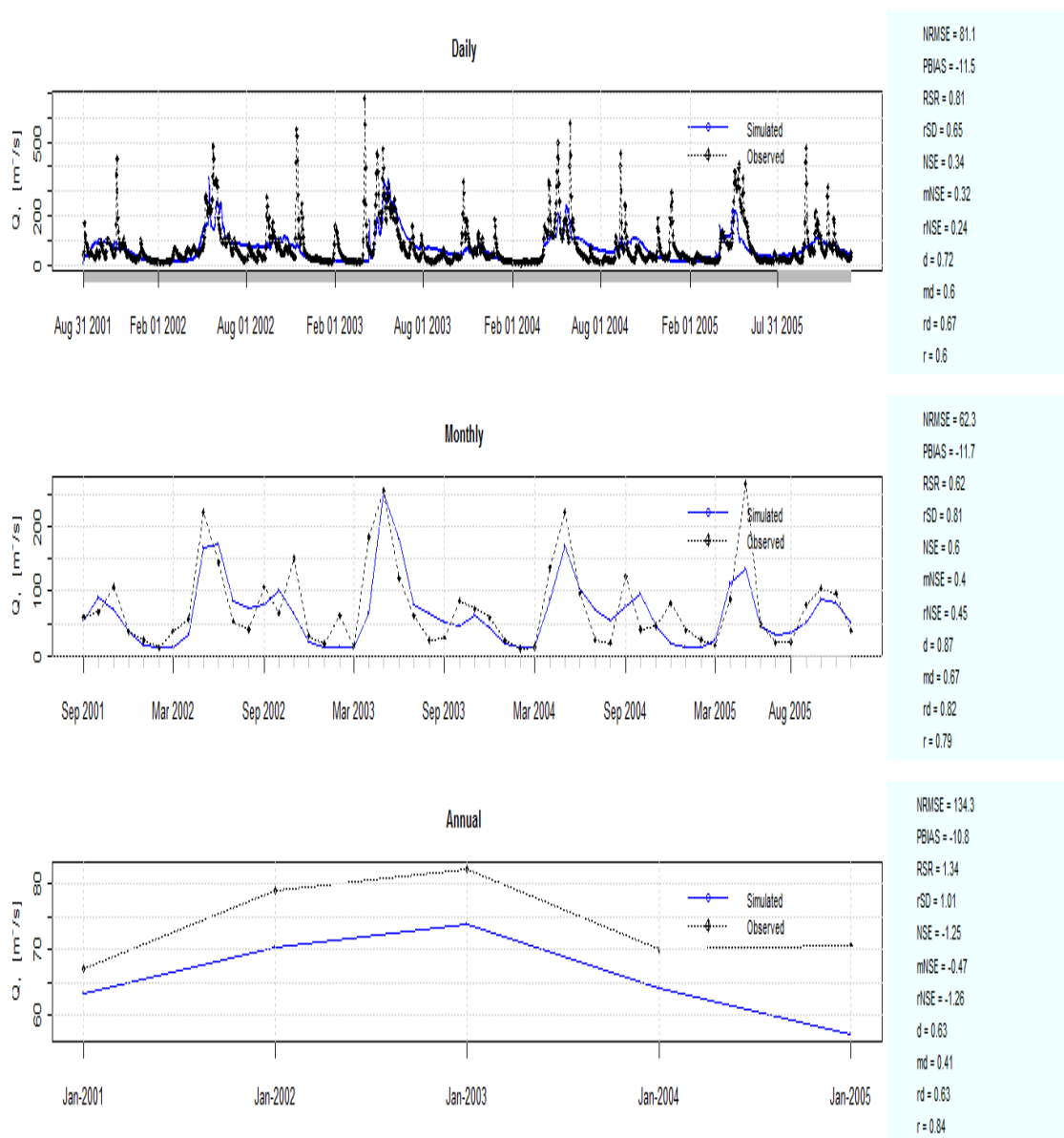


Figure 5. 5 Daily, Monthly and Annual Streamflow (September 2001 to December 2005) at Upper Humber River at Reidville

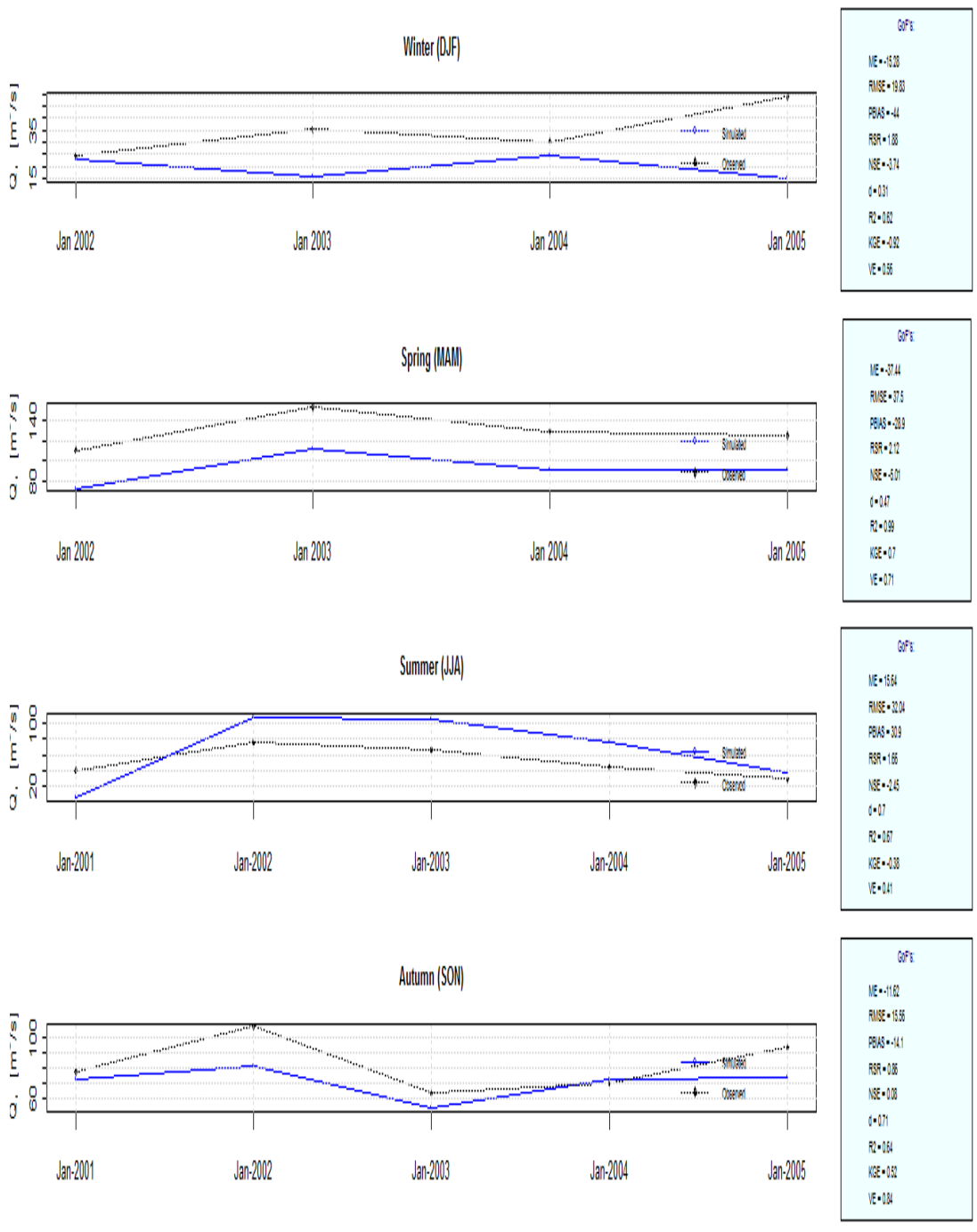


Figure 5. 6 Seasonal Streamflow (September 2001 to December 2005) at Upper Humber River at Reidville

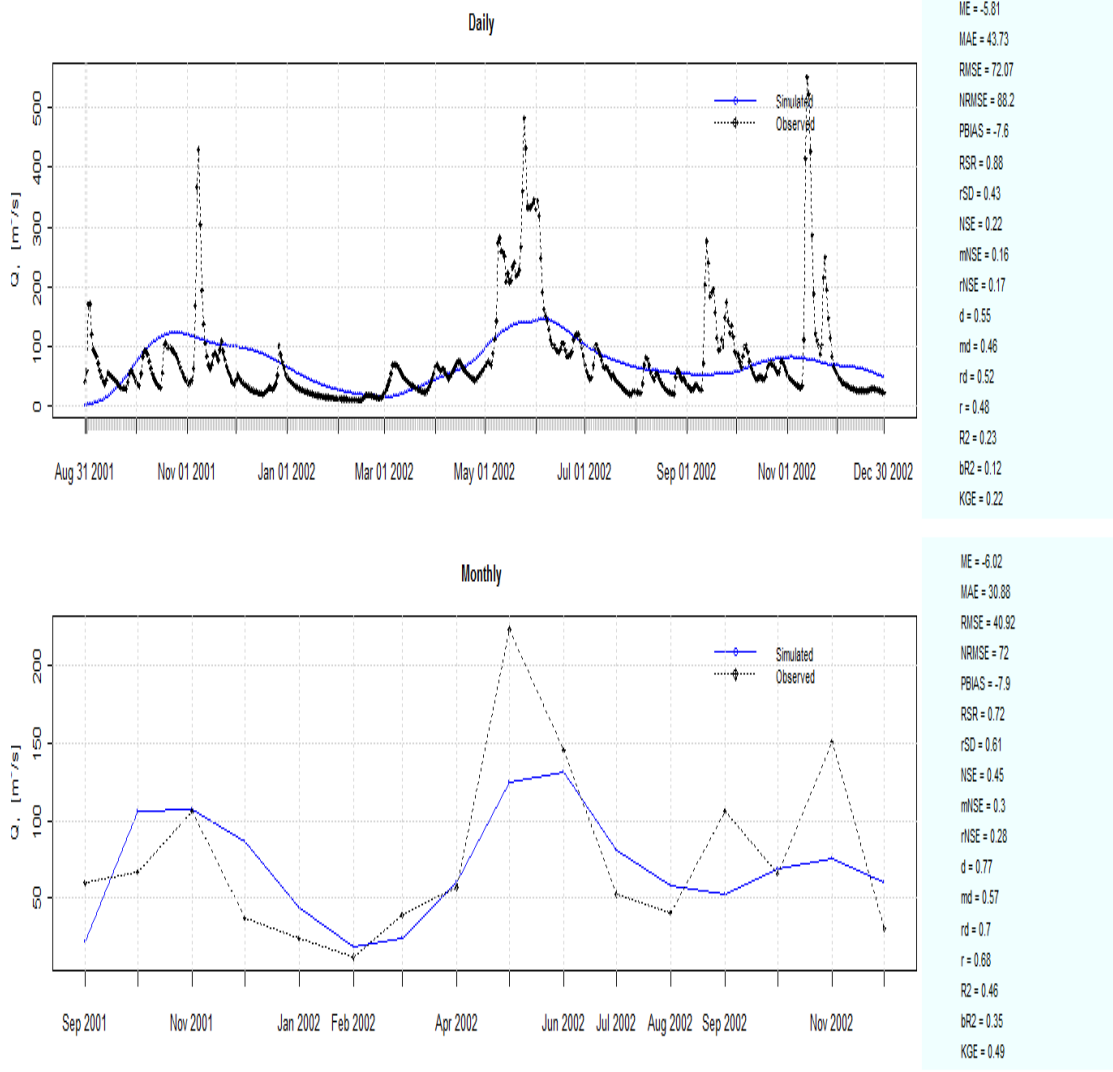


Figure 5. 7 Daily and Monthly Streamflow (September 2001 to December 2002) at Upper Humber River at Reidville

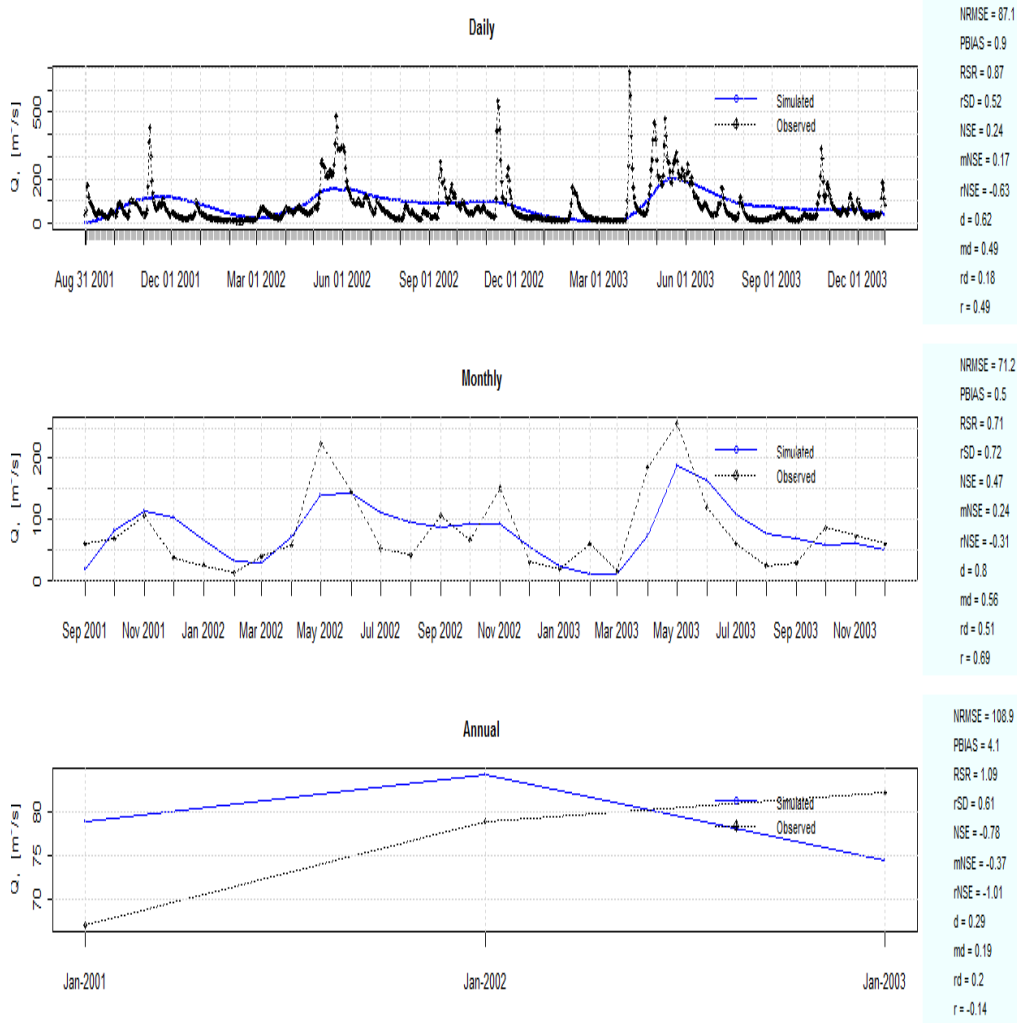


Figure 5. 8 Daily, Monthly and Annual Streamflow (September 2001 to December 2003) at Upper Humber River at Reidville

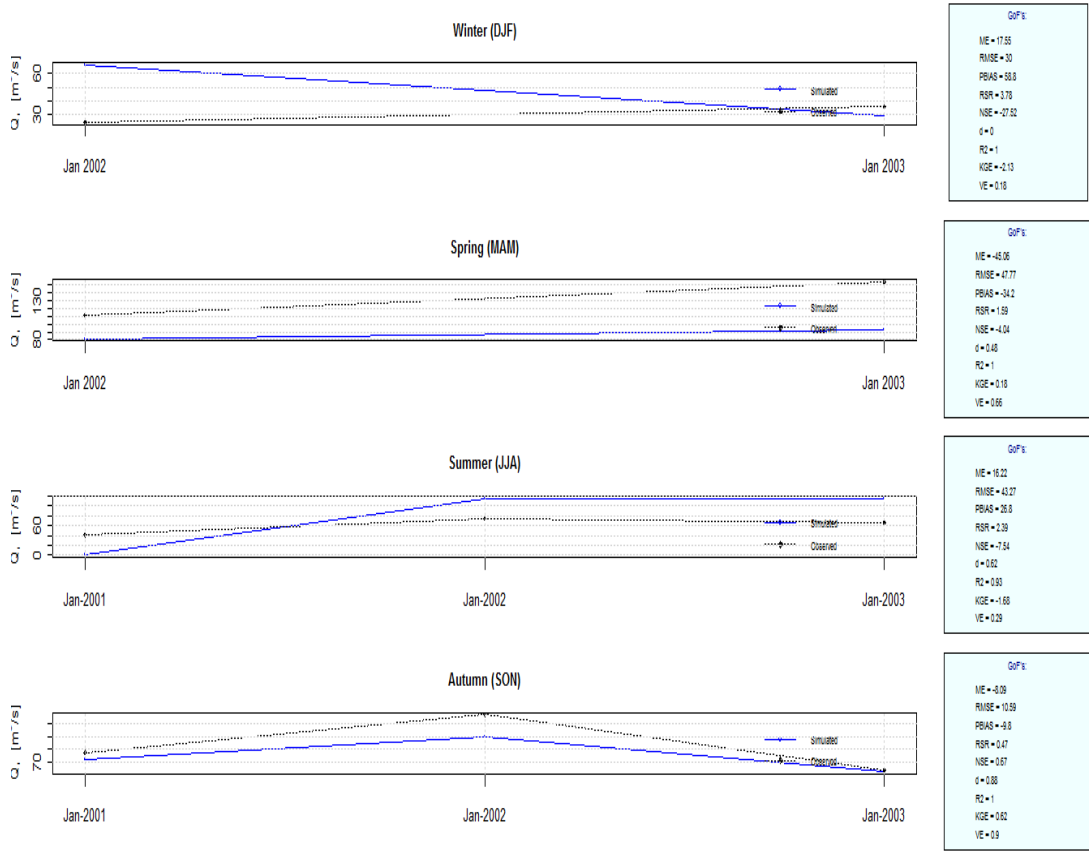


Figure 5. 9 Seasonal Streamflow (September 2001 to December 2003) at Upper Humber River at Reidville

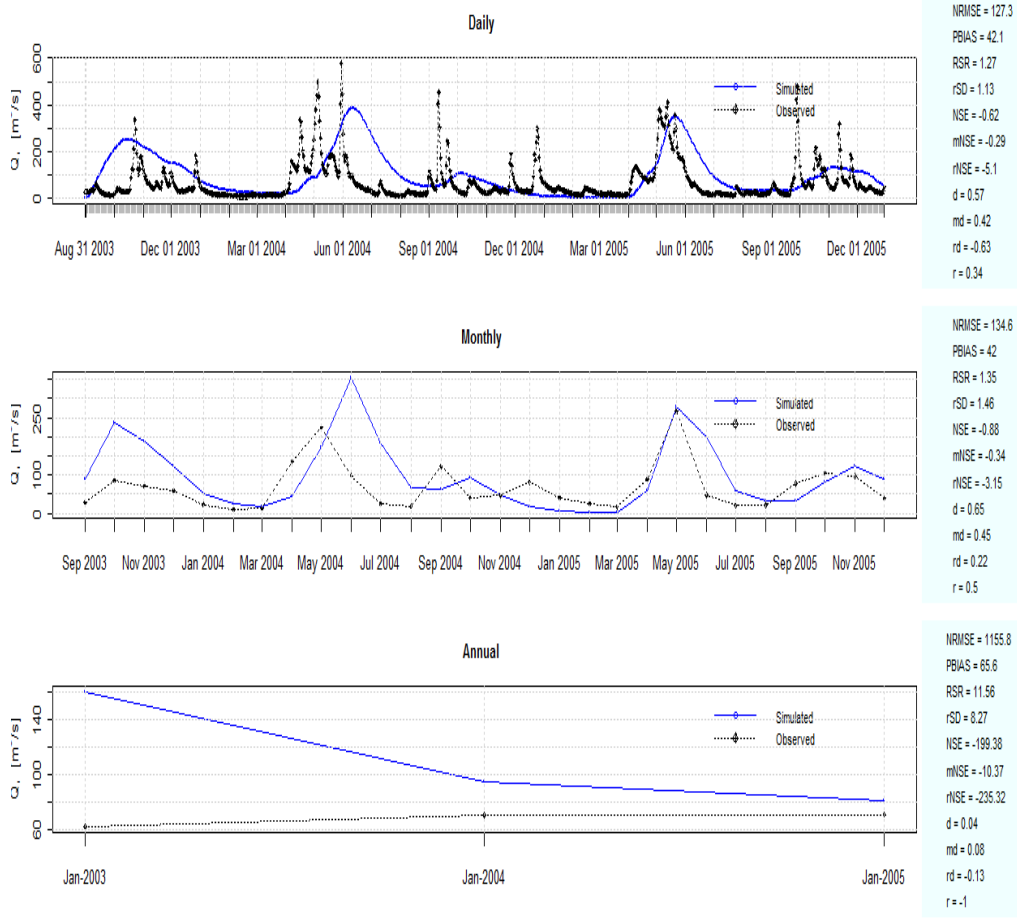


Figure 5. 10 Daily, Monthly and Annual Streamflow (September 2003 to December 2005) at Upper Humber River at Reidville

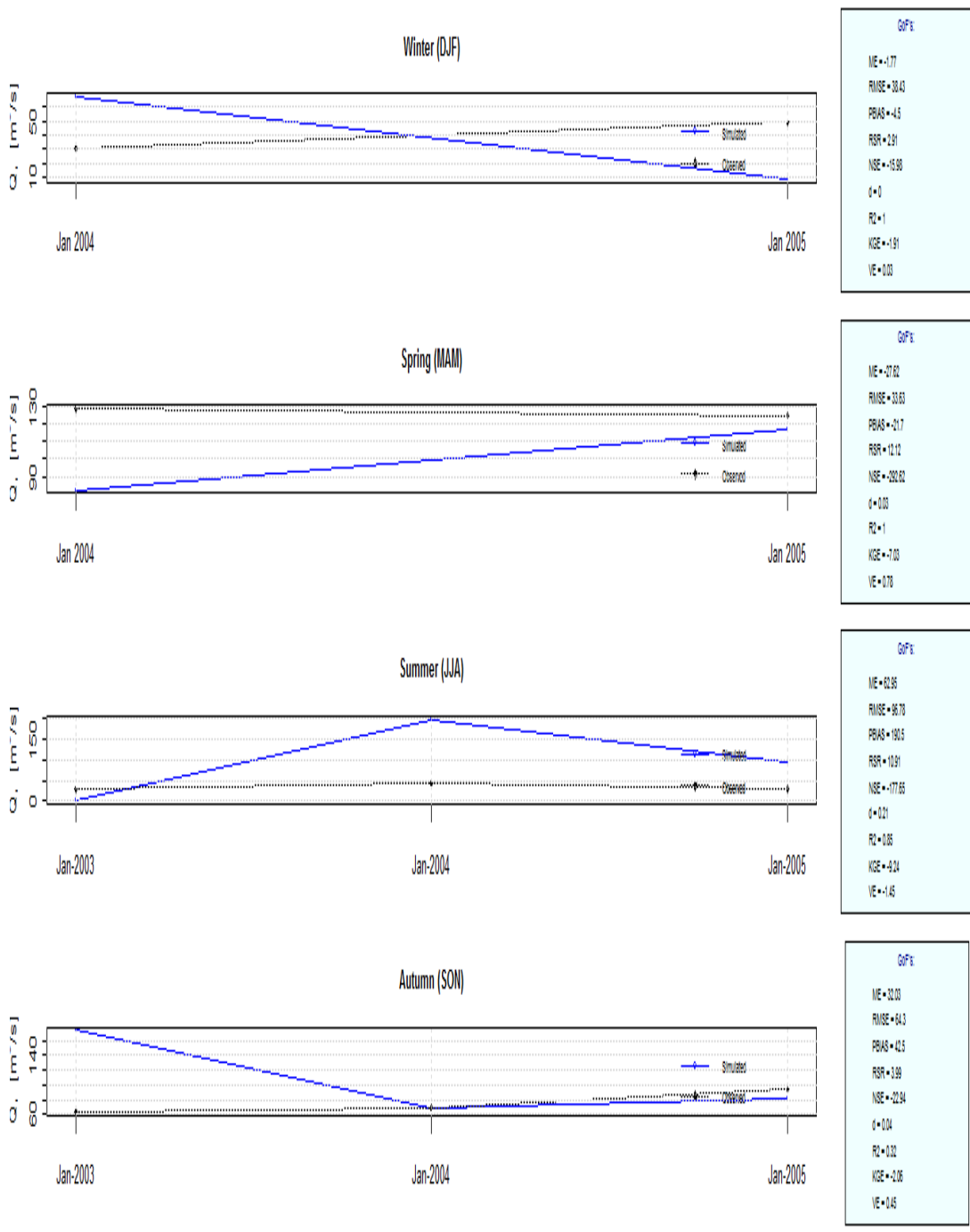


Figure 5. 11 Seasonal Streamflow (September 2003 to December 2005) at Upper Humber River at Reidville

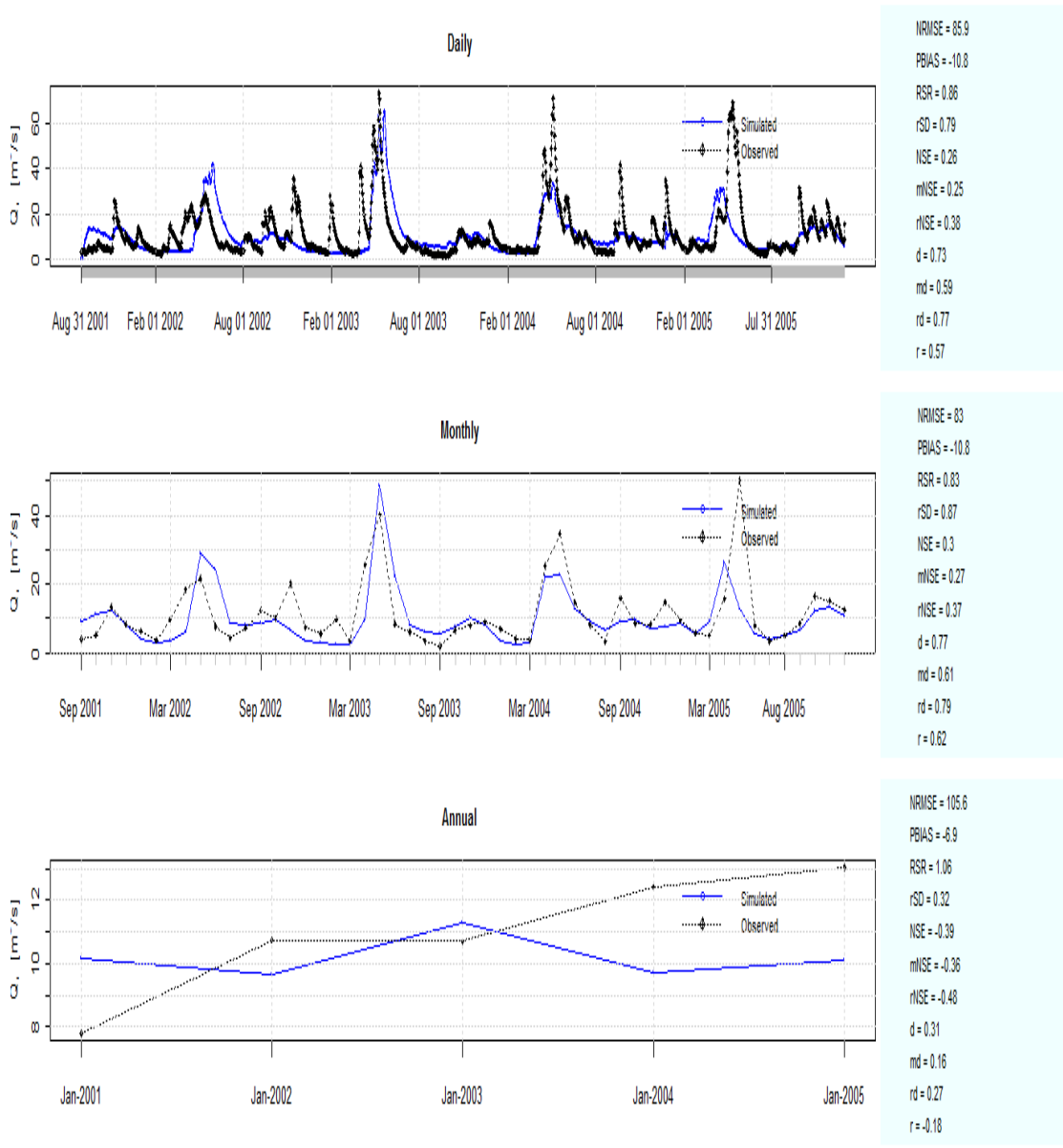


Figure 5. 12 Daily, Monthly and Annual Streamflow (September 2001 to December 2005) at Sheffield Brook near Trans-Canada Highway

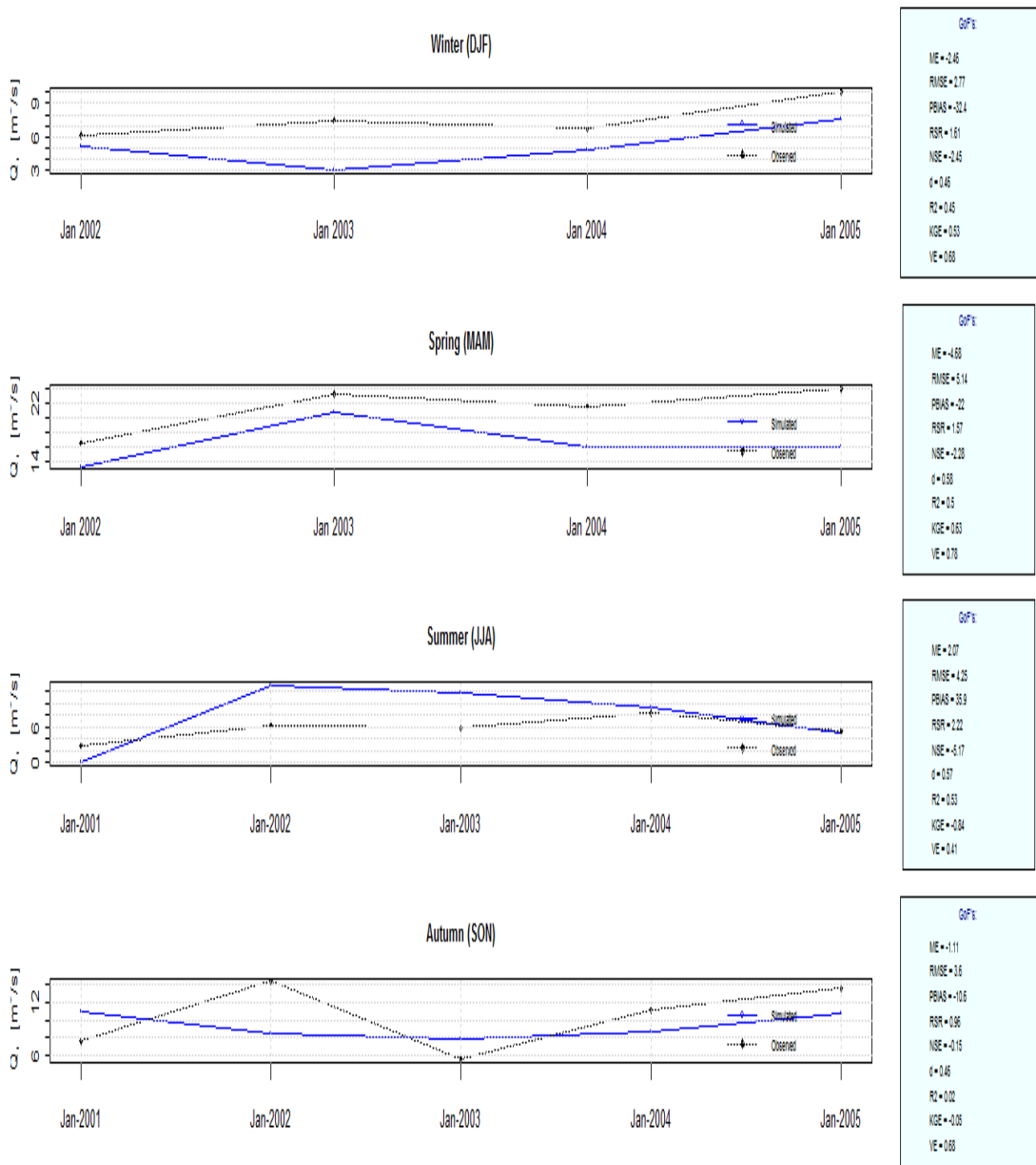


Figure 5. 13 Seasonal Streamflow (September 2001 to December 2005) at Sheffield Brook near Trans-Canada Highway

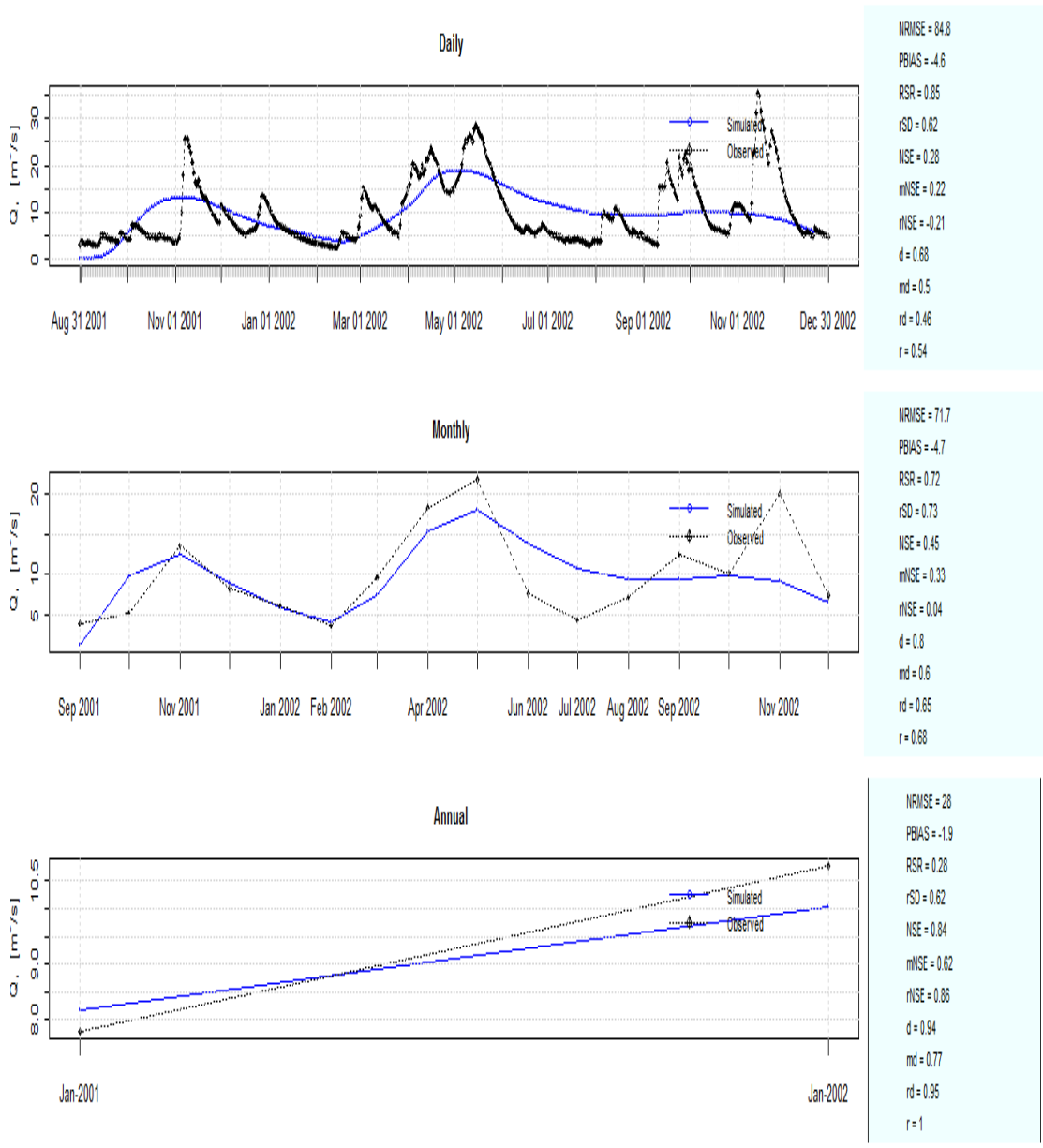


Figure 5. 14 Daily, Monthly and Annual Streamflow (September 2001 to December 2002) at Sheffield Brook near Trans-Canada Highway

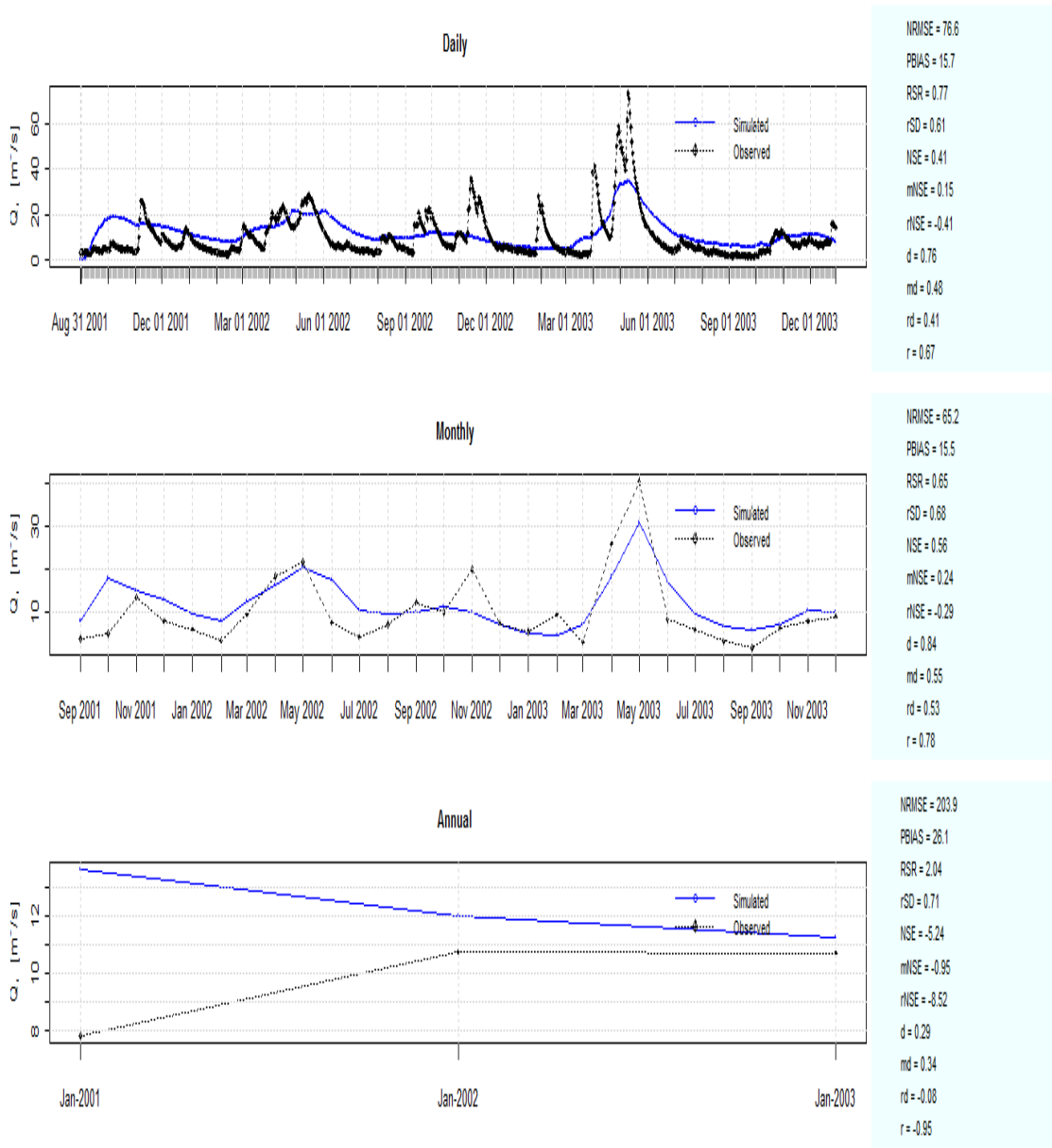


Figure 5. 15 Daily, Monthly and Annual Streamflow (September 2001 to December 2003) at Sheffield Brook near Trans-Canada Highway

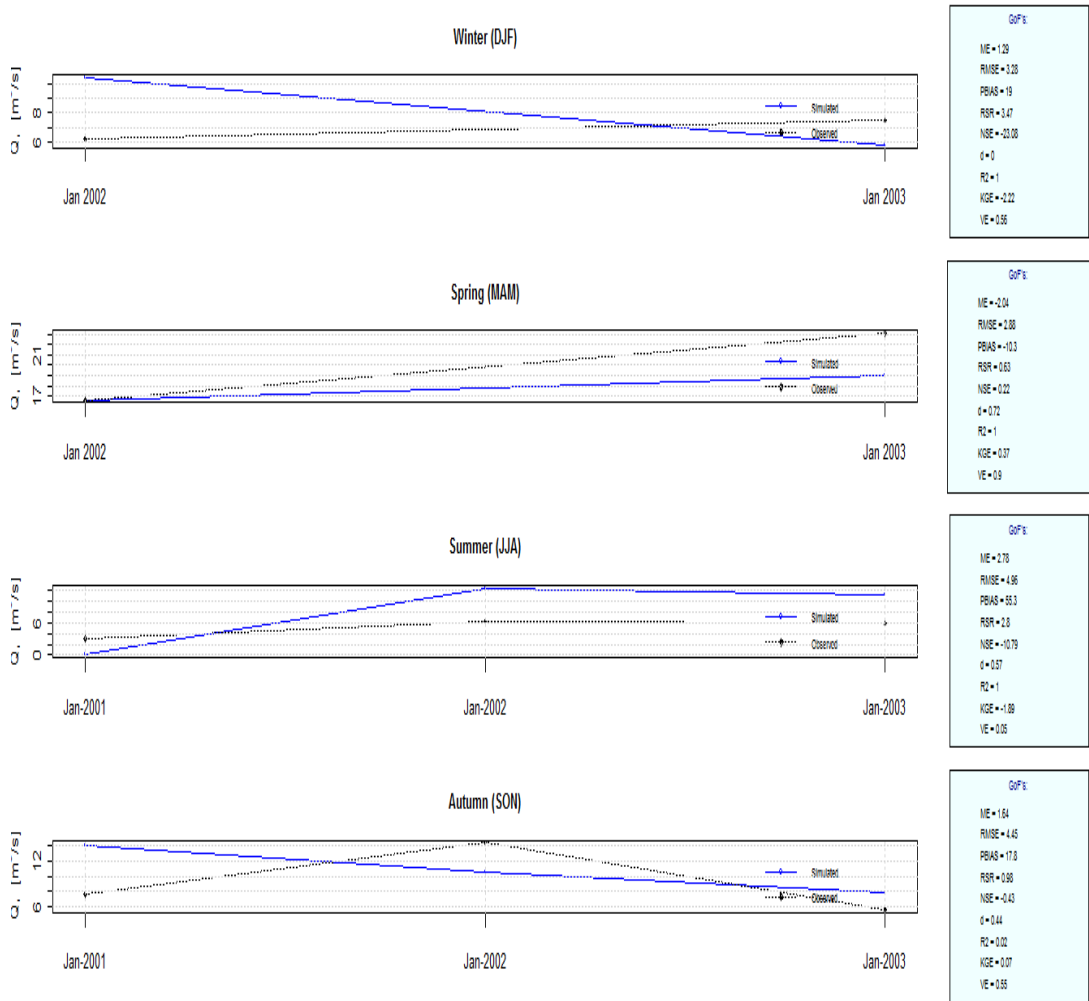


Figure 5. 16 Seasonal Streamflow (September 2001 to December 2003) at Sheffield Brook near Trans-Canada Highway

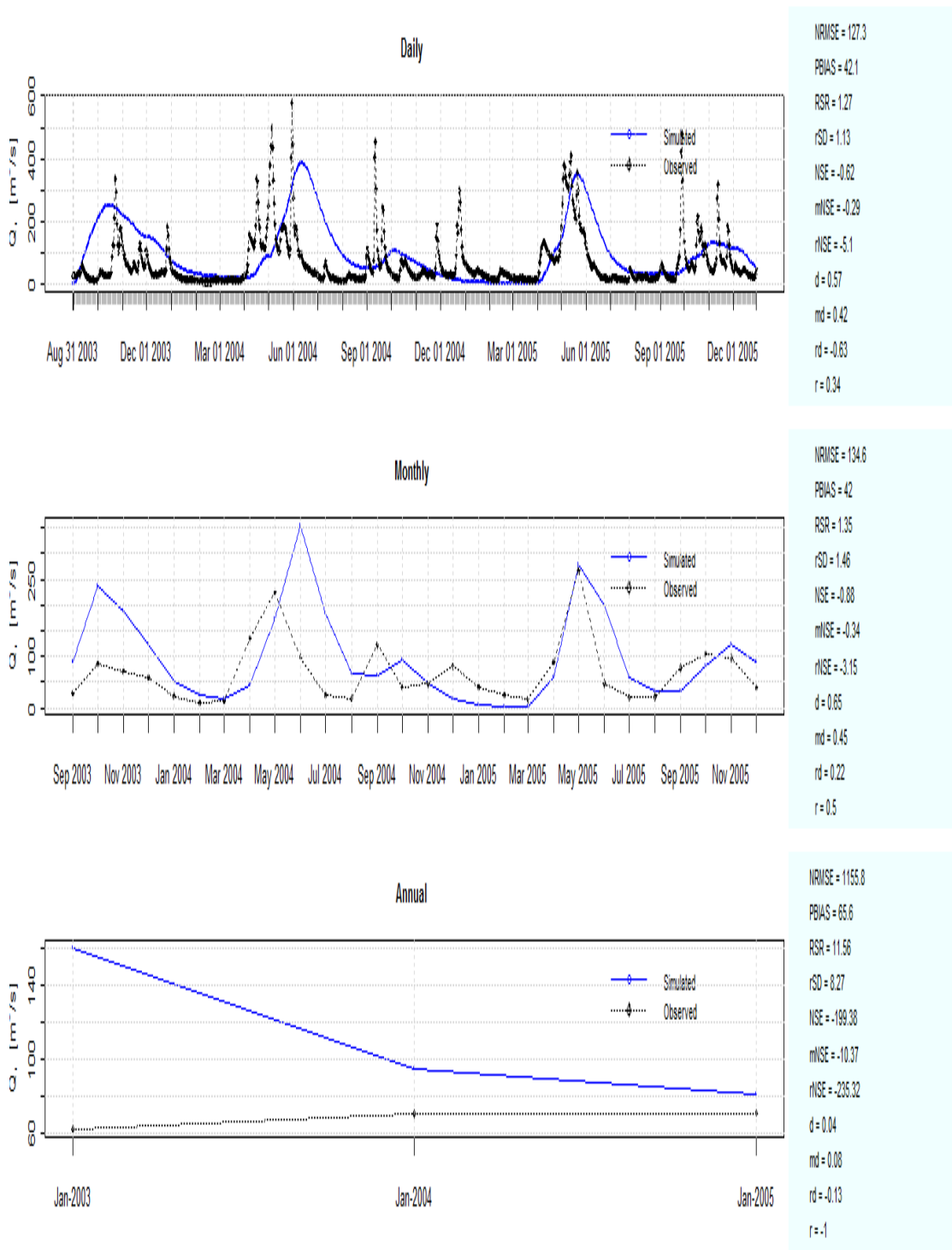


Figure 5. 17 Daily, Monthly and Annual Streamflow (September 2003 to December 2005) at Sheffield Brook near Trans-Canada Highway

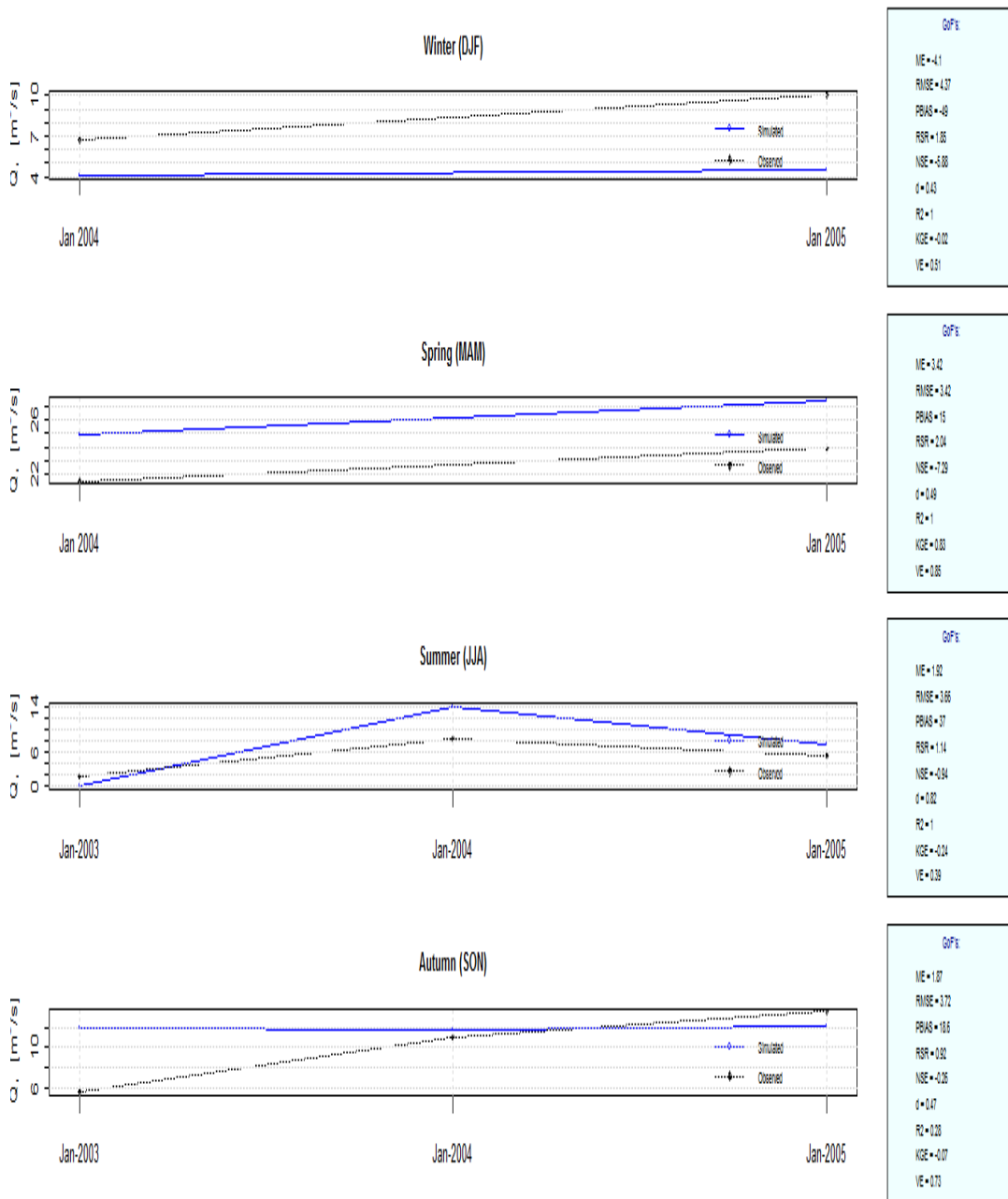


Figure 5. 18 Seasonal Streamflow (September 2003 to December 2005) at Sheffield Brook near Trans-Canada Highway

Table 5. 4 Model bias index (MB), model efficiency index (NSE), and root mean square error (RMSE) of simulated streamflow (September 2001 to December 2005)

| Observation Station | MB | NSE | RMSE |
|---|-------|-------|------|
| Sheffield Brook at Trans-Canada Highway | 0.892 | 0.261 | 6.45 |
| Upper Humber River near Reidville | 0.885 | 0.342 | 46.7 |

According to Table 5.3, the NSE value is better at Reidville than at Sheffield Brook for the calibration period. The base of the simulated hydrograph matches well with the observed data after calibration but cannot simulate peak discharge properly at Upper Humber River near Reidville (Figure 5.6 and Figure 5.7). The values which were used for calibrating model parameters are a residual value and it is one of the problems in streamflow calibration. The parameters values will also incorporate all the errors in the forcing data, the model structure, the state variables and the algorithms. However, the overall model performance is considerable as it has positive Nash values at all the locations.

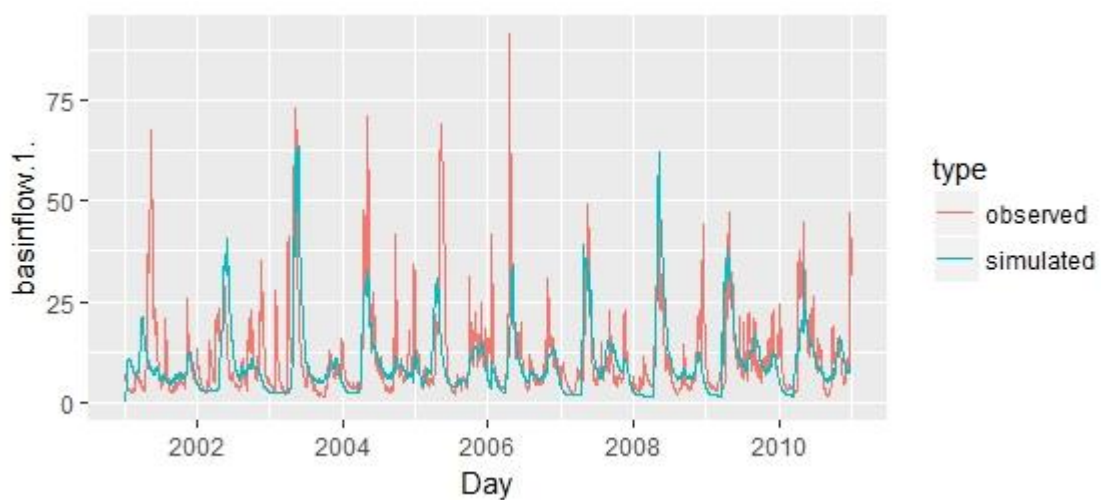


Figure 5. 19 Streamflow (2001-2010) at Sheffield Brook near Trans-Canada Highway

After manual adjustments of the above parameters with satisfactory model results, the results were plotted in segments for various years and the model performance was also assessed.

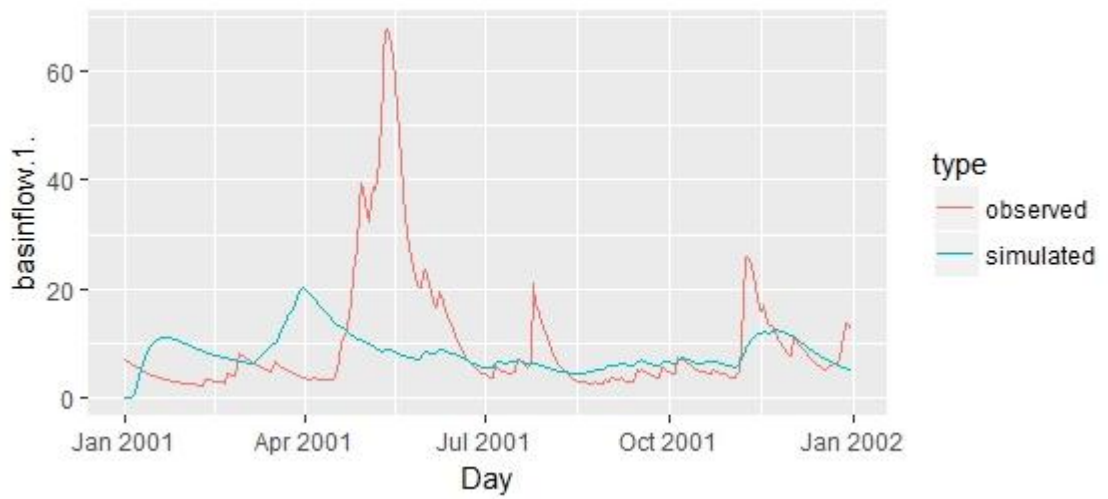


Figure 5. 20 Streamflow (2001) at Sheffield Brook near Trans-Canada Highway

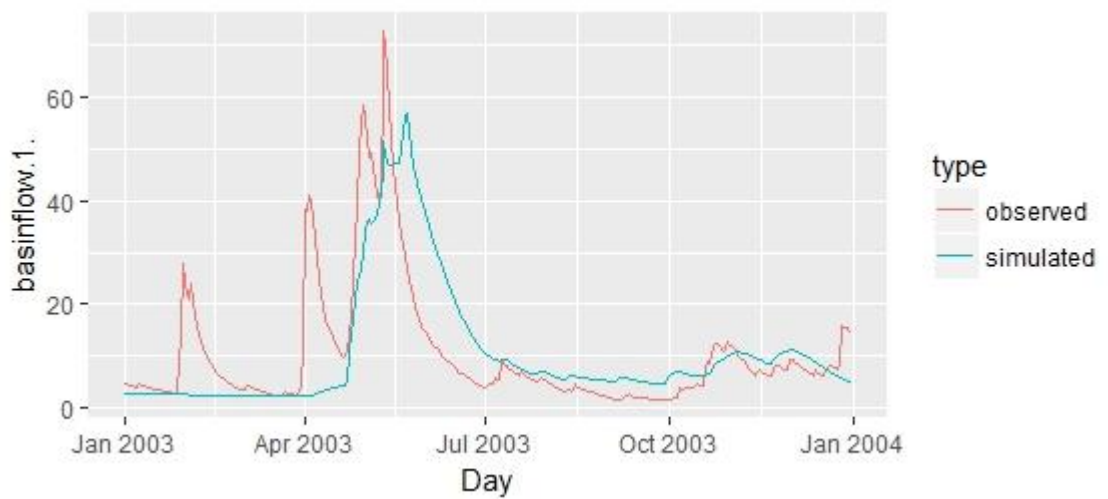


Figure 5. 21 Streamflow (2003) at Sheffield Brook near Trans-Canada Highway

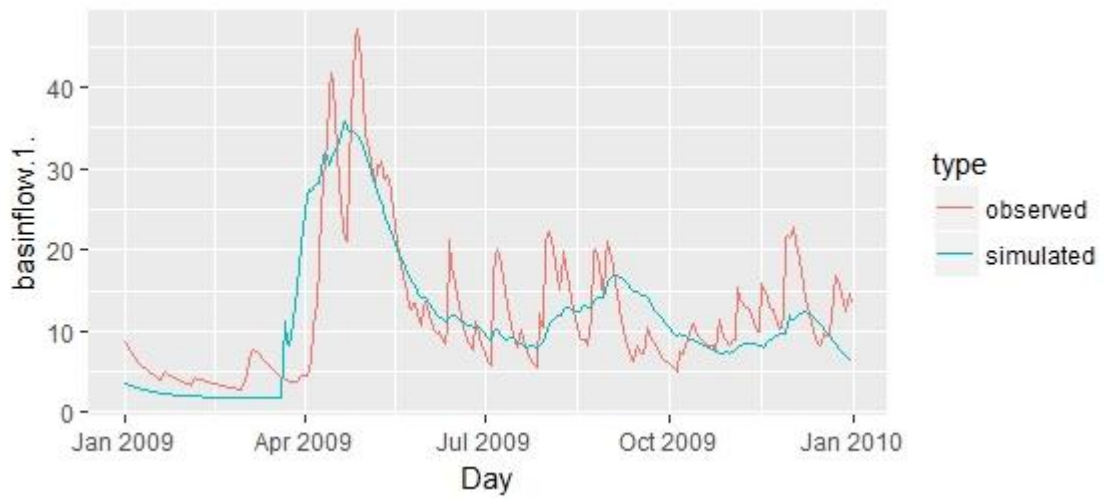


Figure 5. 22 Streamflow (2009) at Sheffield Brook near Trans-Canada Highway

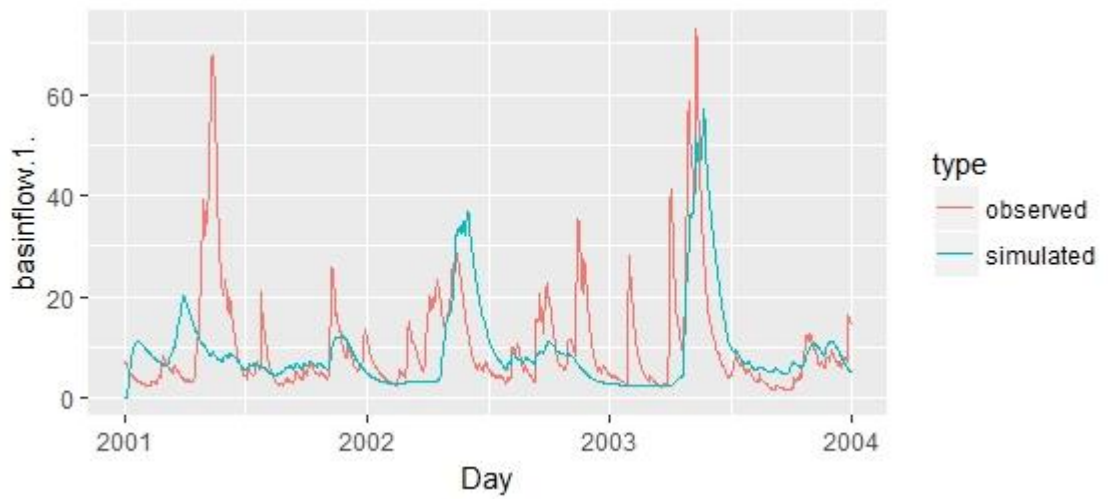


Figure 5. 23 Streamflow (2001-2003) at Sheffield Brook near Trans-Canada Highway

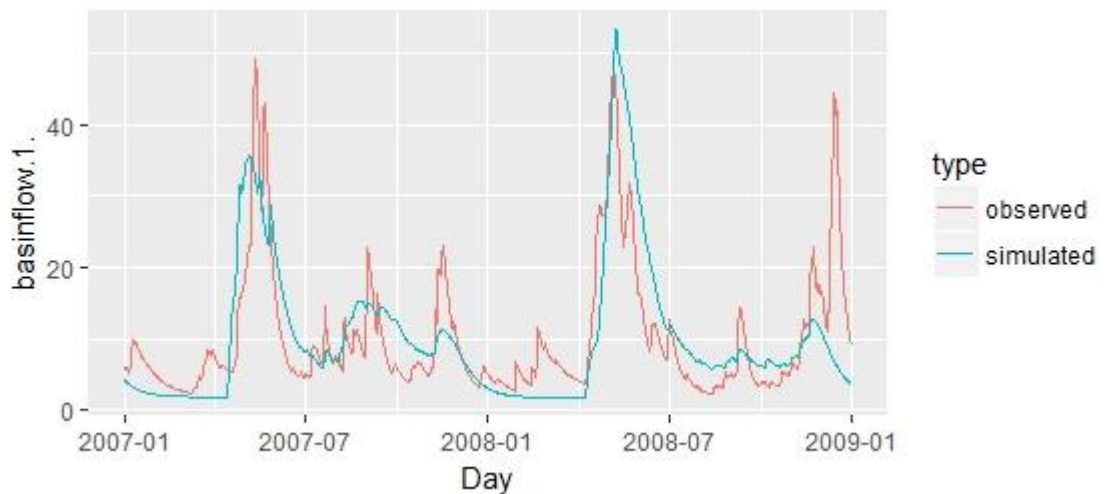


Figure 5. 24 Streamflow (2007-2008) at Sheffield Brook near Trans-Canada Highway

Table 5. 5 Model efficiency index (NSE), and root mean square error (RMSE) of simulated streamflow at Sheffield Brook at Trans-Canada Highway

| Observation Period | NSE | RMSE |
|--------------------|---------|------|
| 2001-2010 | 0.276 | 9.3 |
| 2001 | -0.0612 | 3.9 |
| 2003 | 0.388 | 3.15 |
| 2009 | 0.586 | 1.76 |
| 2001-2003 | 0.0612 | 5.78 |
| 2007-2008 | 0.429 | 3.12 |

5.4 Model Validation Results

The model was validated after obtaining satisfactory model calibration results. The parameters found by optimization were used for model validation. It was validated for the period of September 2006 to December 2010. The simulated streamflow of Humber Village Bridge at basin outlet was plotted for September 2001 to December 2010. The model performance was also assessed, and it is summarized in table 5.5.

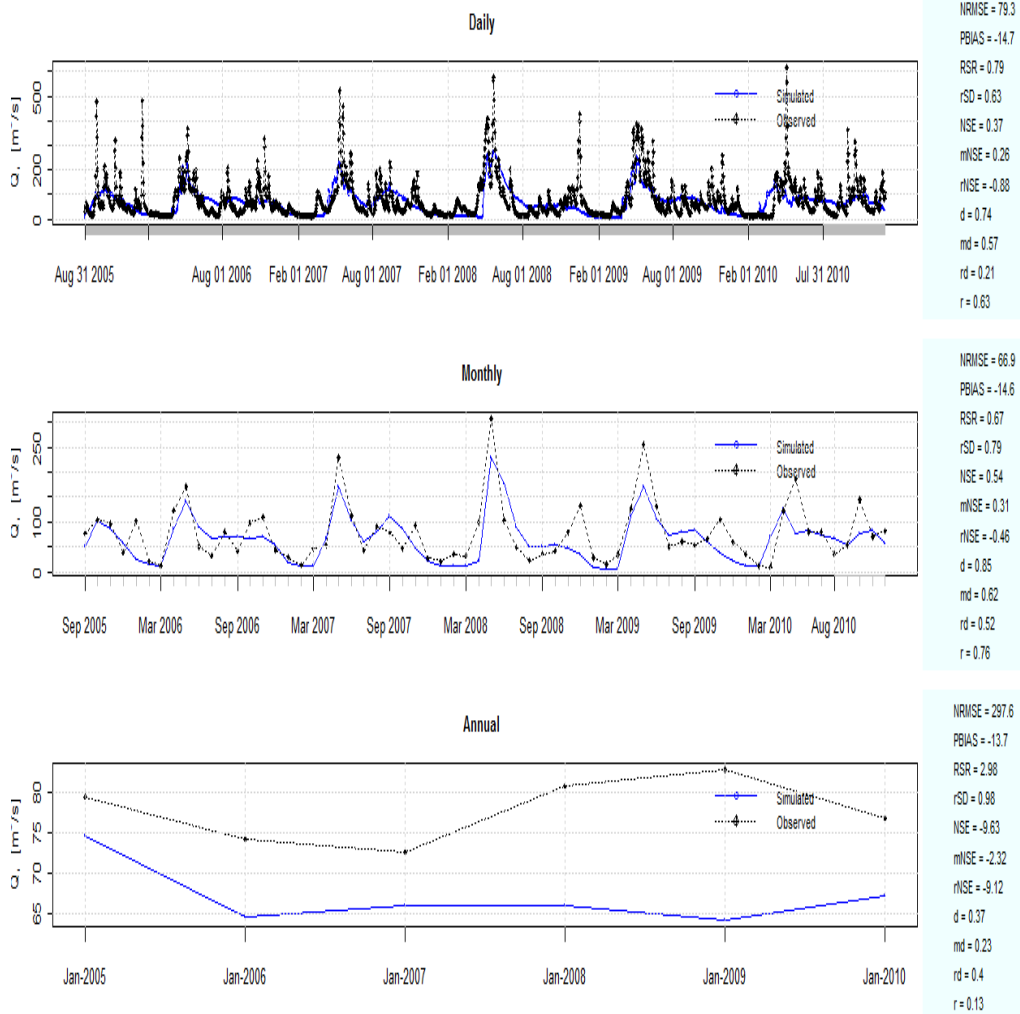


Figure 5. 25 Daily, Monthly and Annual Streamflow (September 2005 to December 2010) at Upper Humber River at Reidville

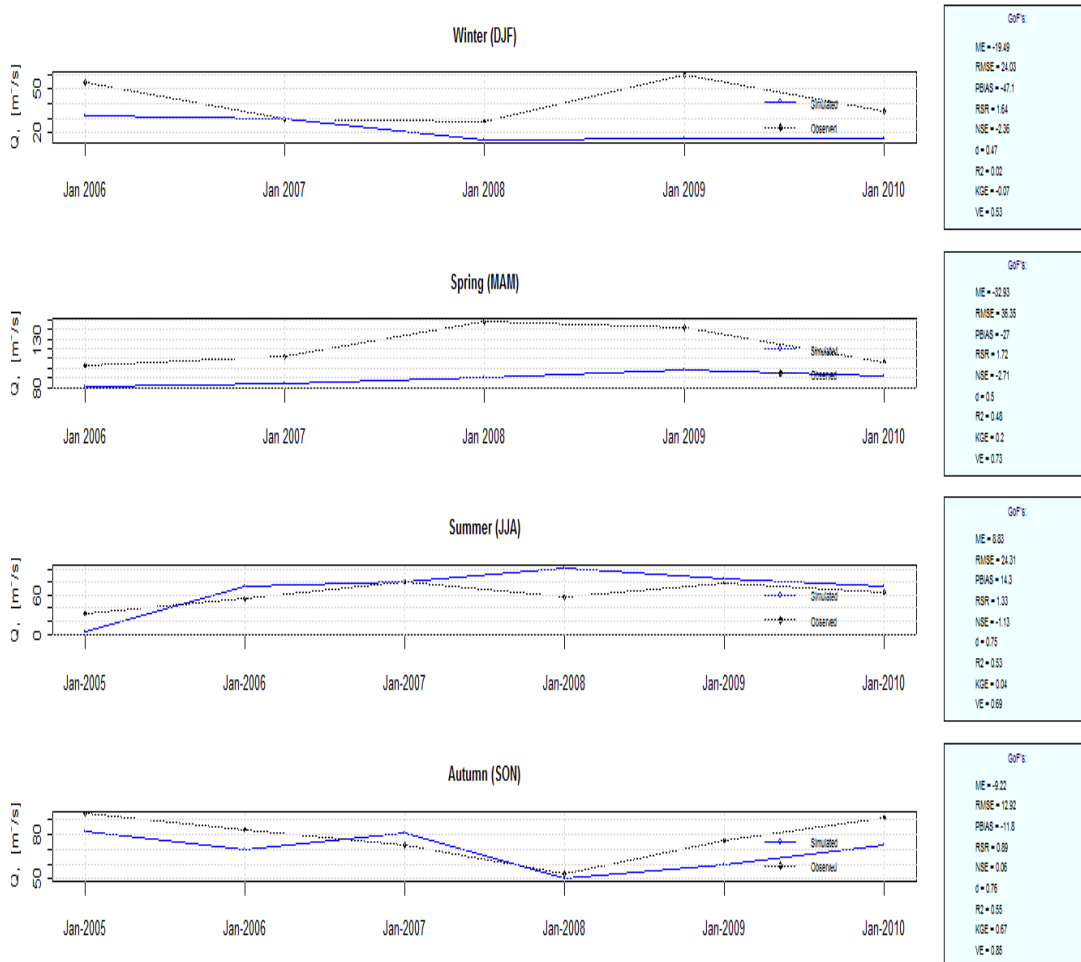


Figure 5. 26 Seasonal Streamflow (September 2005 to December 2010) at Upper Humber River at Reidville

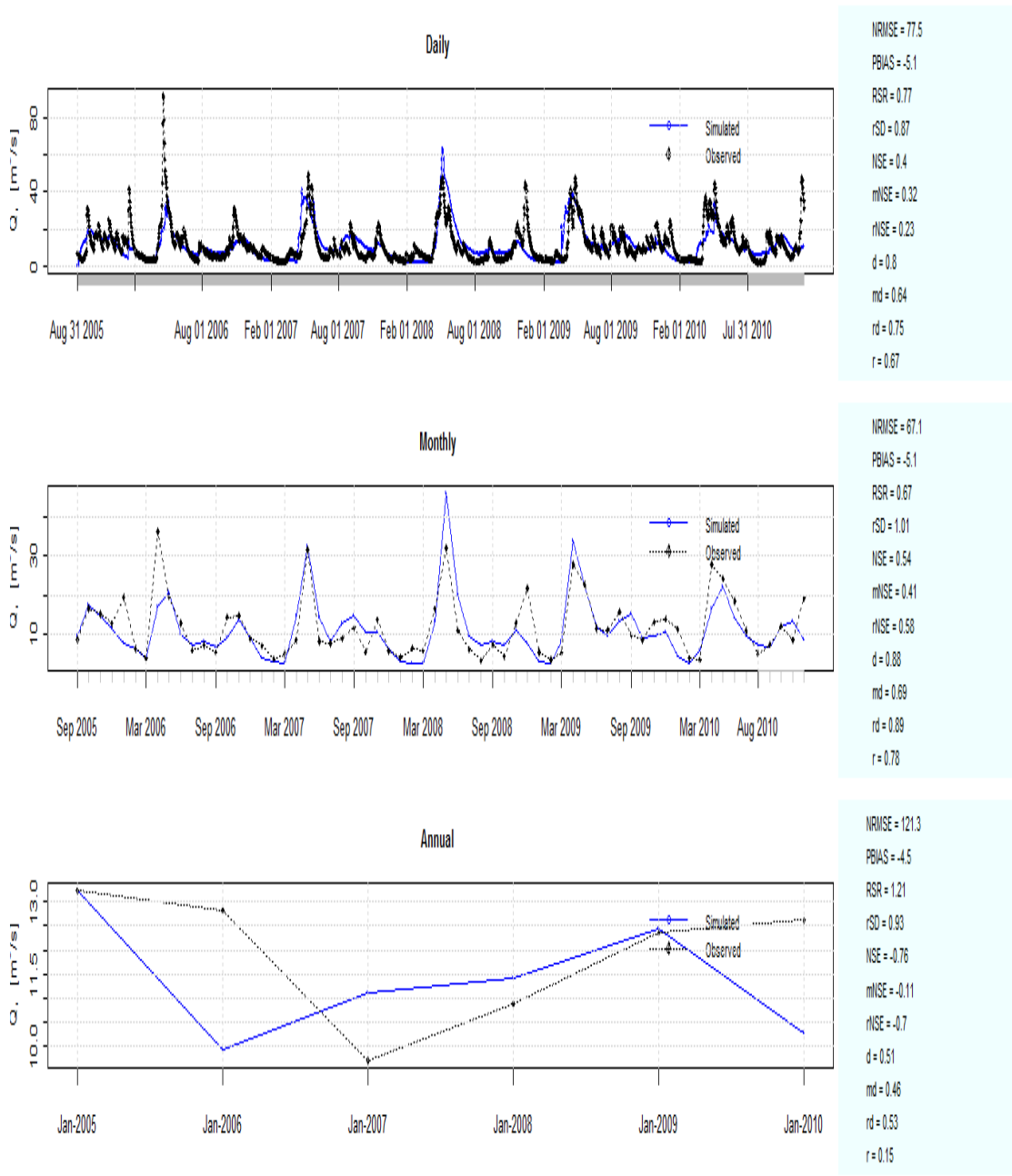


Figure 5. 27 Daily, Monthly and Annual Streamflow (September 2005 to December 2010) at Sheffield Brook near Trans-Canada Highway

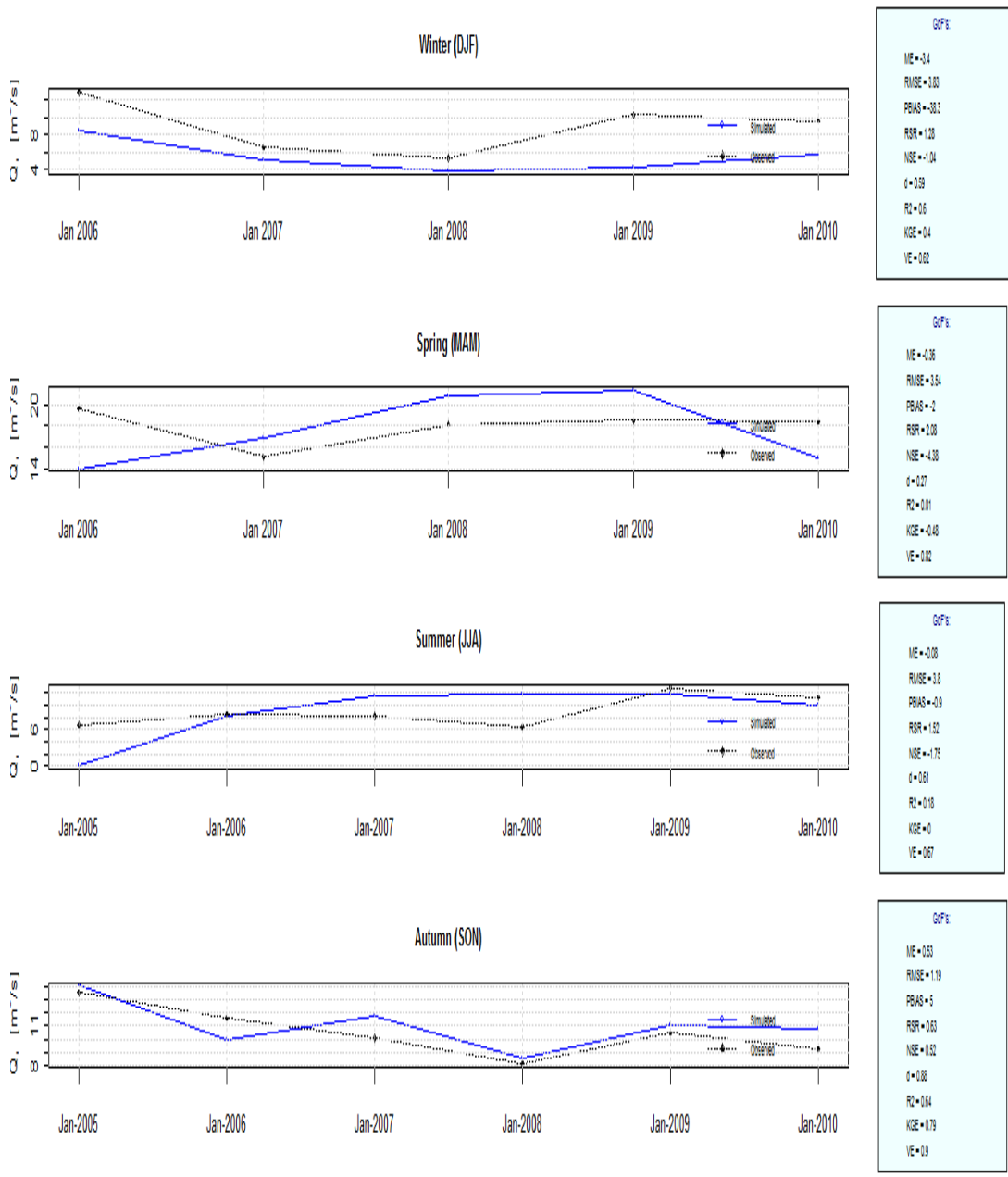


Figure 5. 28 *Seasonal Streamflow (September 2005 to December 2010) at Sheffield Brook near Trans-Canada Highway*

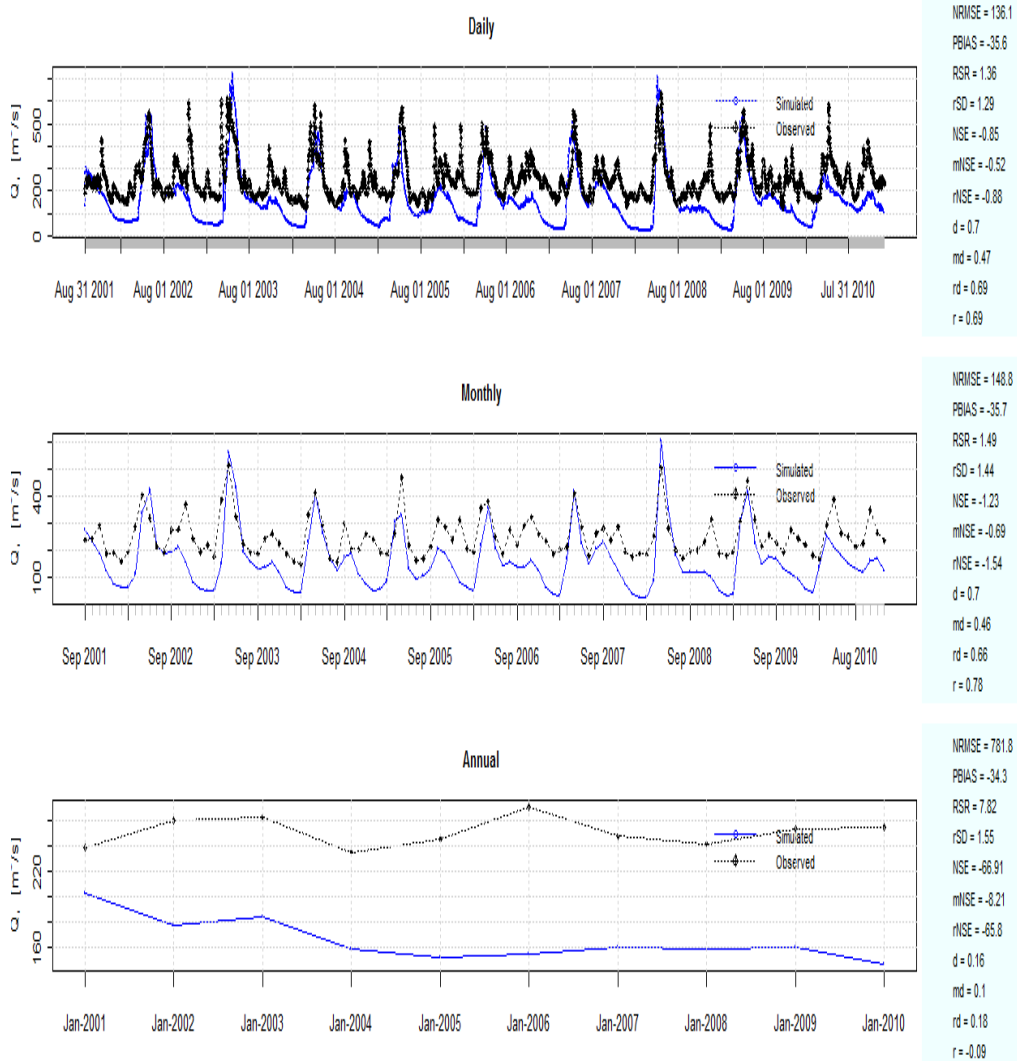


Figure 5. 29 Daily, Monthly and Annual Streamflow (September 2001 to December 2010) at Humber River Bridge

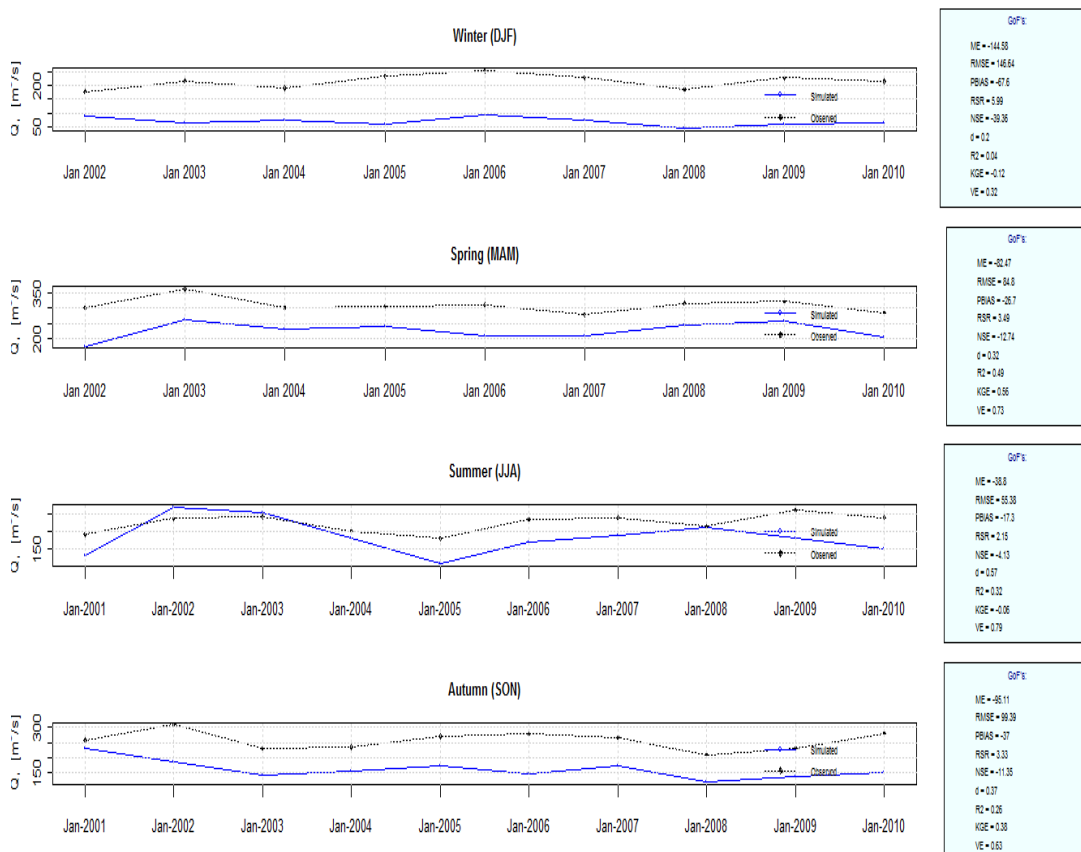


Figure 5. 30 *Seasonal* Streamflow (September 2001 to December 2010) at Humber River Bridge

Table 5. 6 Model bias index (MB), model efficiency index (NSE), and root mean square error (RMSE) of simulated streamflow

| Observation Station | MB | NSE | RMSE |
|---|-------|-------|-------|
| Sheffield Brook at Trans-Canada Highway (September 2005 to December 2010) | 0.949 | 0.399 | 5.56 |
| Upper Humber River near Reidville (September 2005 to December 2010) | 0.853 | 0.372 | 45.64 |
| Humber Village Bridge at Basin Outlet (September 2001 to December 2010) | 0.6 | -0.85 | 120 |

It is very difficult to represent the real natural hydrological process in a hydrological model perfectly. The most important aspect of the model output is the representation of results considering the main features of the hydrologic system. In this study, the main

objective was predicting streamflow and the model was validated by comparison of the predicted streamflow with observed streamflow.

The validation showed similar results to the calibration simulations. The results obtained from the validation run are provided in Section 5.4. It showed that the calibration of the model managed to develop a good understanding between observed and simulated streamflow. In all cases the volume of the simulated hydrograph is similar with the observed volume, but it fails to simulate the streamflow during winter at Humber River at Village Bridge.

5.5 Simulations for Entire Basin

The simulated hydrographs of the entire study period (September 2001 to December 2010) for Sub-basin 3, Sub-basin 5, Sub-basin 6, Sub-basin 7 and Sub-basin 8 are presented in the section. The parameters estimated for Sub-basin 4 were used for simulating the streamflow. There was no observed station at the outlet point of those Sub-basins. Only simulated hydrographs are shown below.

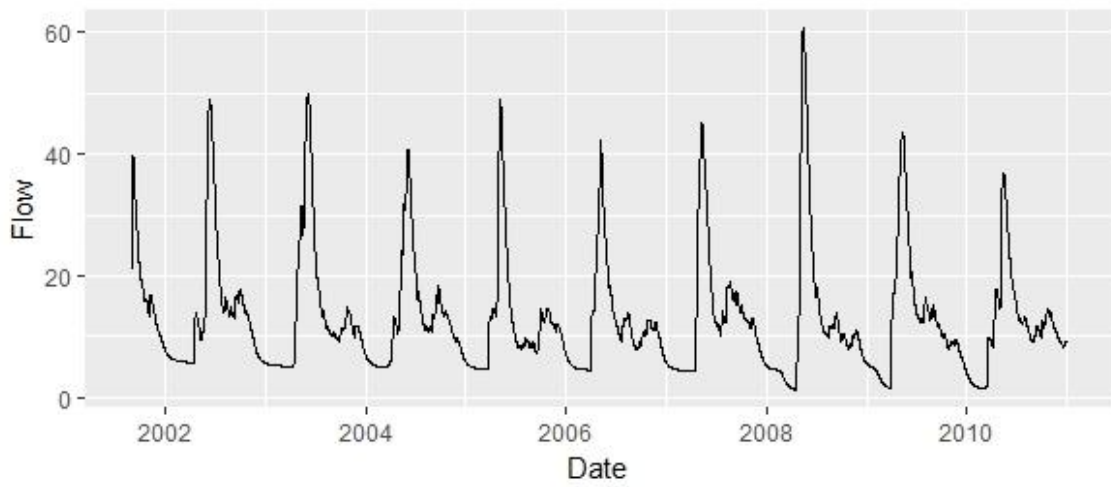


Figure 5. 31 Streamflow (September 2001 to December 2010) at outlet of Sub-basin 3

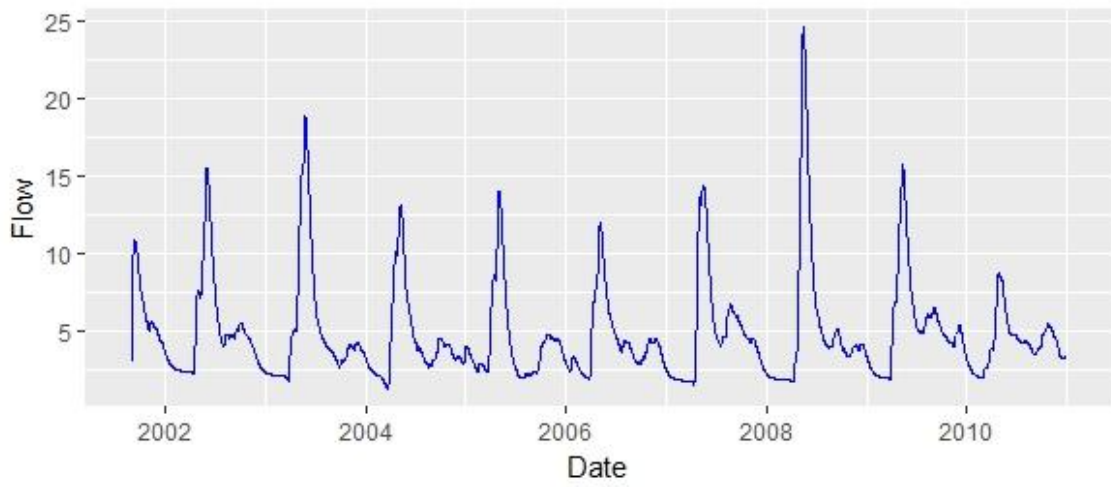


Figure 5. 32 Streamflow (September 2001 to December 2010) at outlet of Sub-basin 5

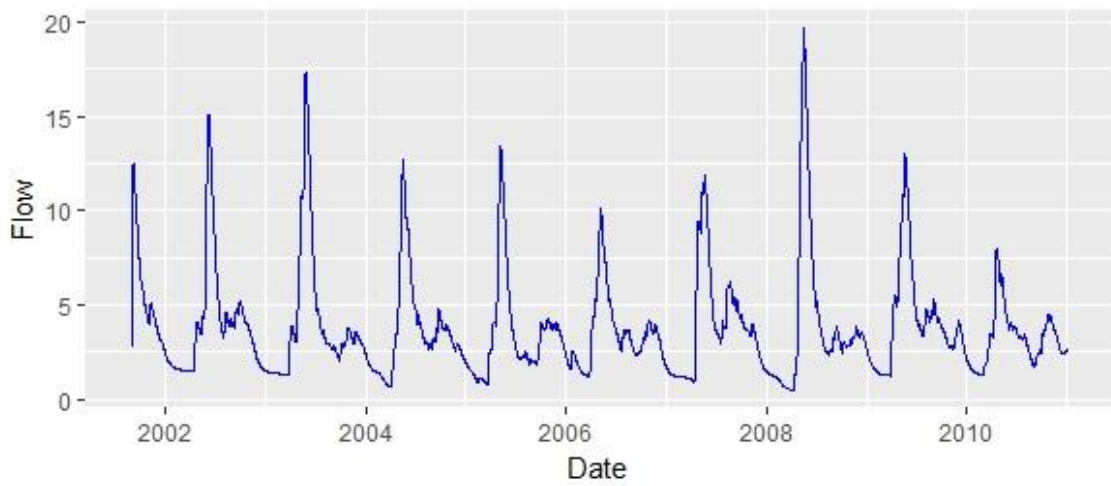


Figure 5. 33 Streamflow (September 2001 to December 2010) at outlet of Sub-basin 6

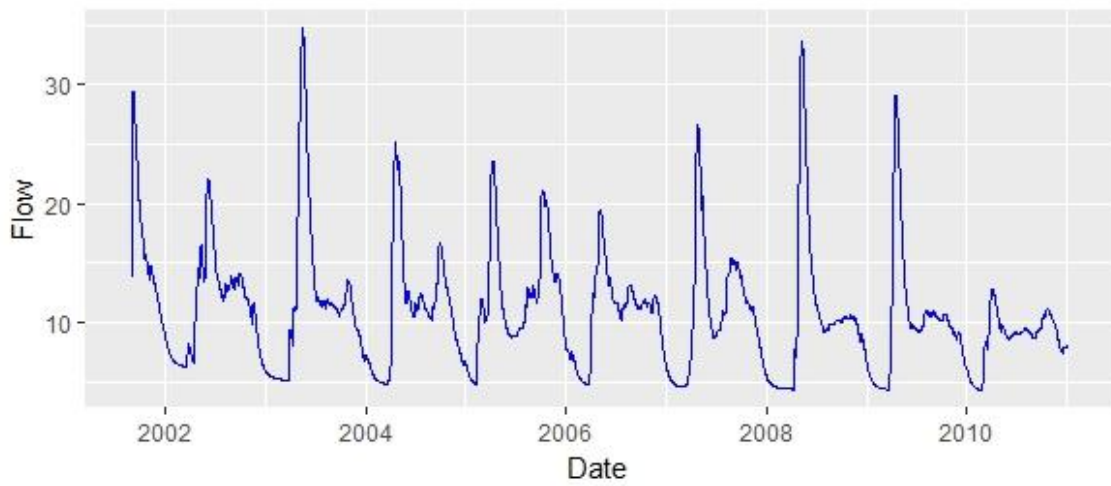


Figure 5. 34 Streamflow (September 2001 to December 2010) at outlet of Sub-basin 7

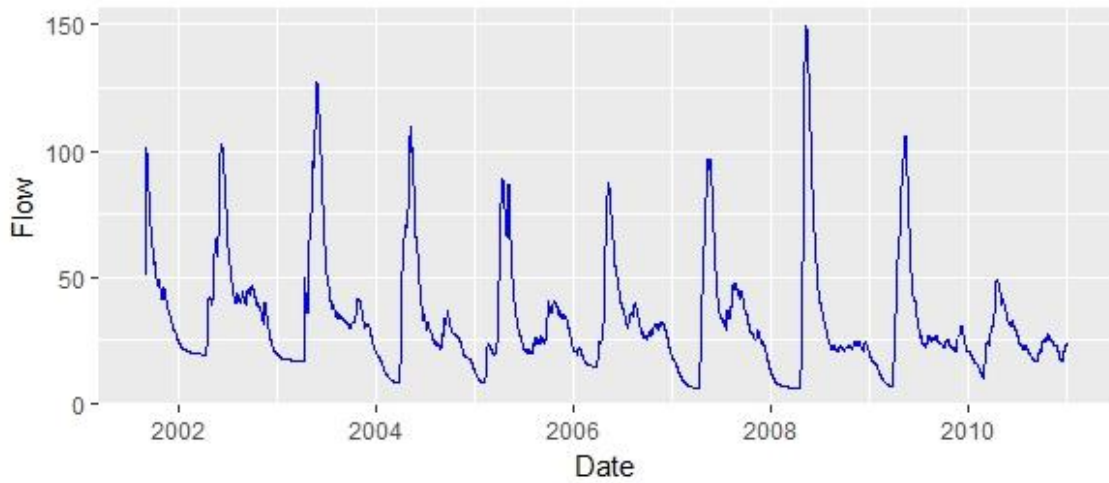


Figure 5. 35 Streamflow (September 2001 to December 2010) at outlet of Sub-basin 8

5.6 Winter snowpack prediction and comparison

Simulations of snow accumulation were performed by CRHM for HRB and the simulated Snow Water Equivalent (SWE) were compared with three paired forest sites of varying locations. The observed ground snow data were collected from Environment Canada Weather Stations and the Cormack Weather Station; Deer Lake Airport Weather Station and South Brook Pasadena Weather Station. The data from these were compared with the simulated data. The SWE is calculated by the following formulae from ground snow data (Fassnacht *et. al.*, 2003; Sturm, 2010),

$$SWE = h_s \frac{\rho_b}{\rho_w} \quad (5.4)$$

where h_s is ground snow depth and ρ_b is snow density; 0.3 g/cm^3 was considered for fresh snow and ρ_w is the density of the water (1 g/cm^3).

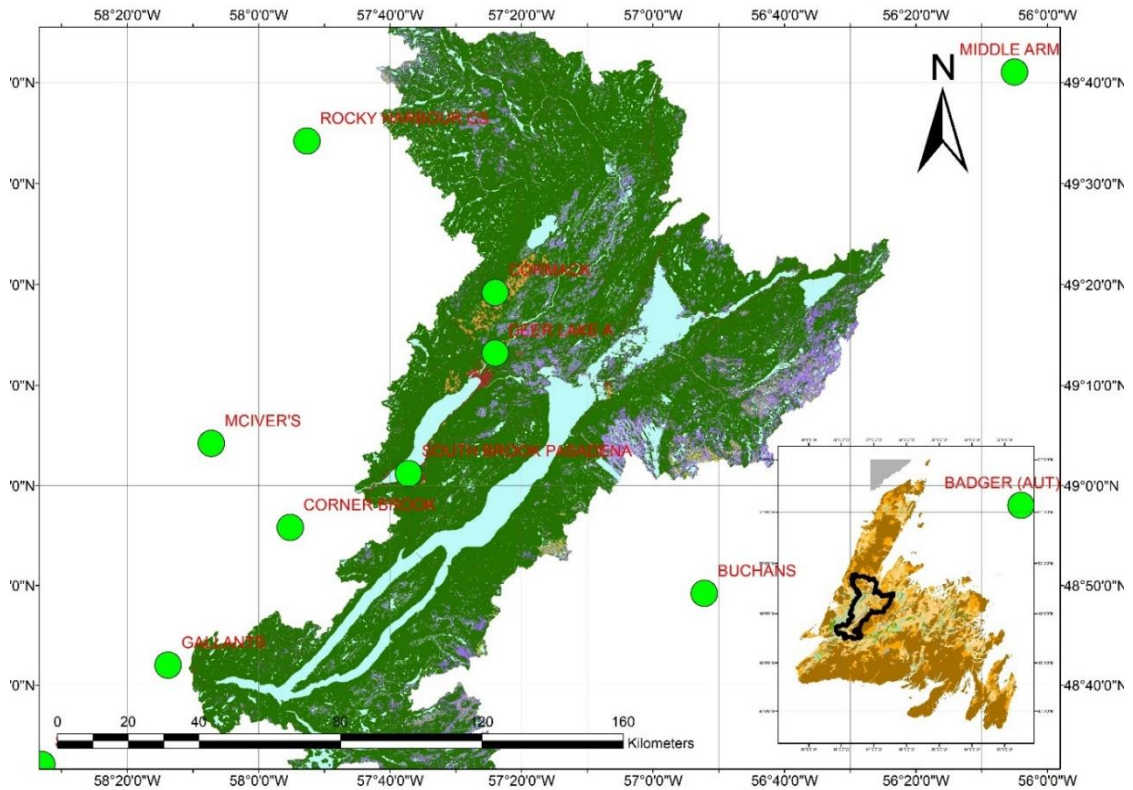


Figure 5. 36 Ground Snow Station over Humber River Basin

Figure 5.28 shows the observed station data around the river basin. In figure 5.29, observed and simulated SWE were plotted for forest sites of sub-basin 2. The simulated snow sublimation and snow depth for sub-basin 2 were also plotted in figure 5.30, while figure 5.31 illustrates the observations and simulations of SWE at Deer Lake Airport Weather Station for the forest site of sub-basin 9. Another representation of SWE data in figure 5.31 shows for the forest land cover of sub-basin 9 at South Brook Pasadena Weather Station.

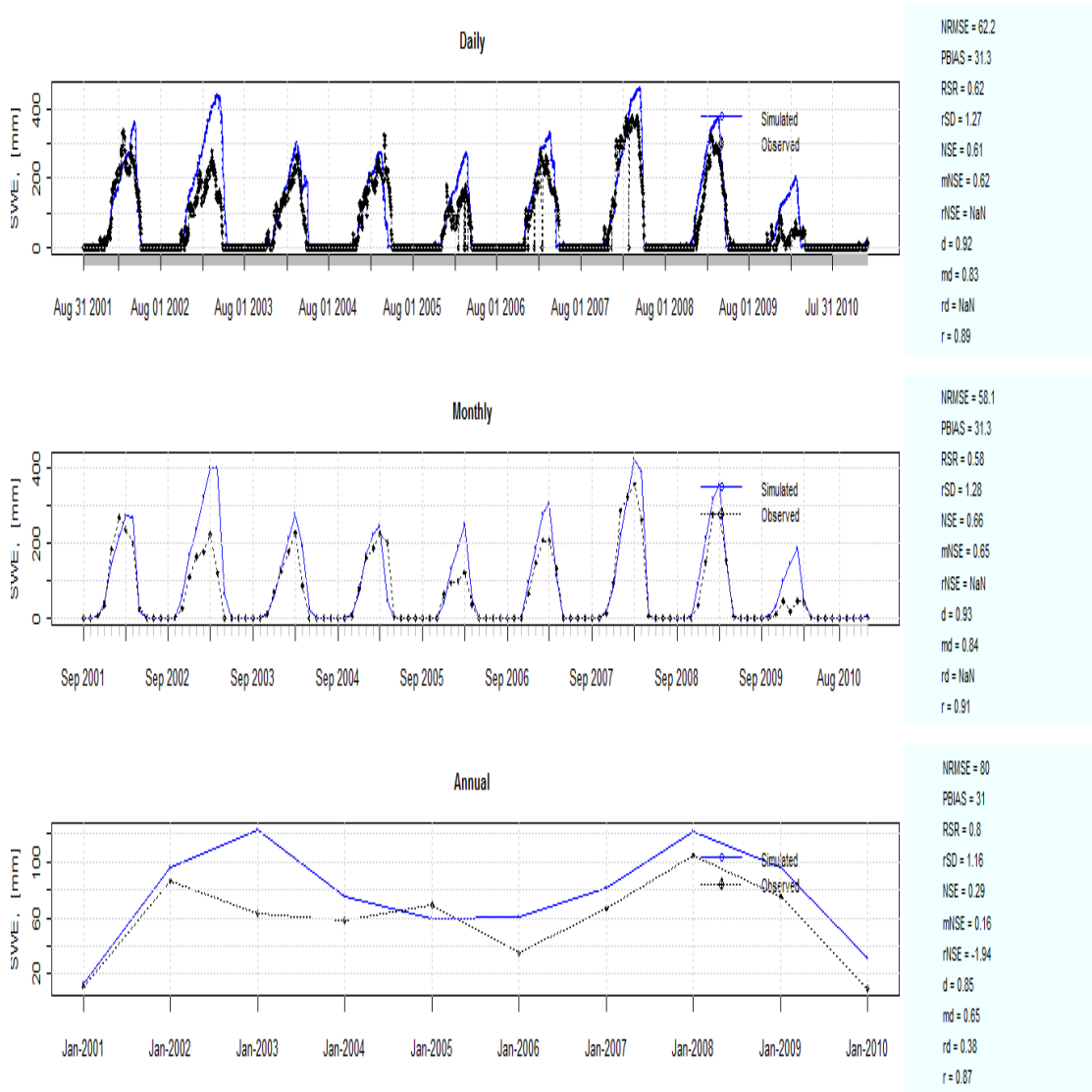


Figure 5. 37 Observed SWE (September 2001 to December 2010) at Cormack Weather Station (Daily, Monthly and Annual) at Forest HRU and Simulated SWE at Forest HRU of Sub-basin 2

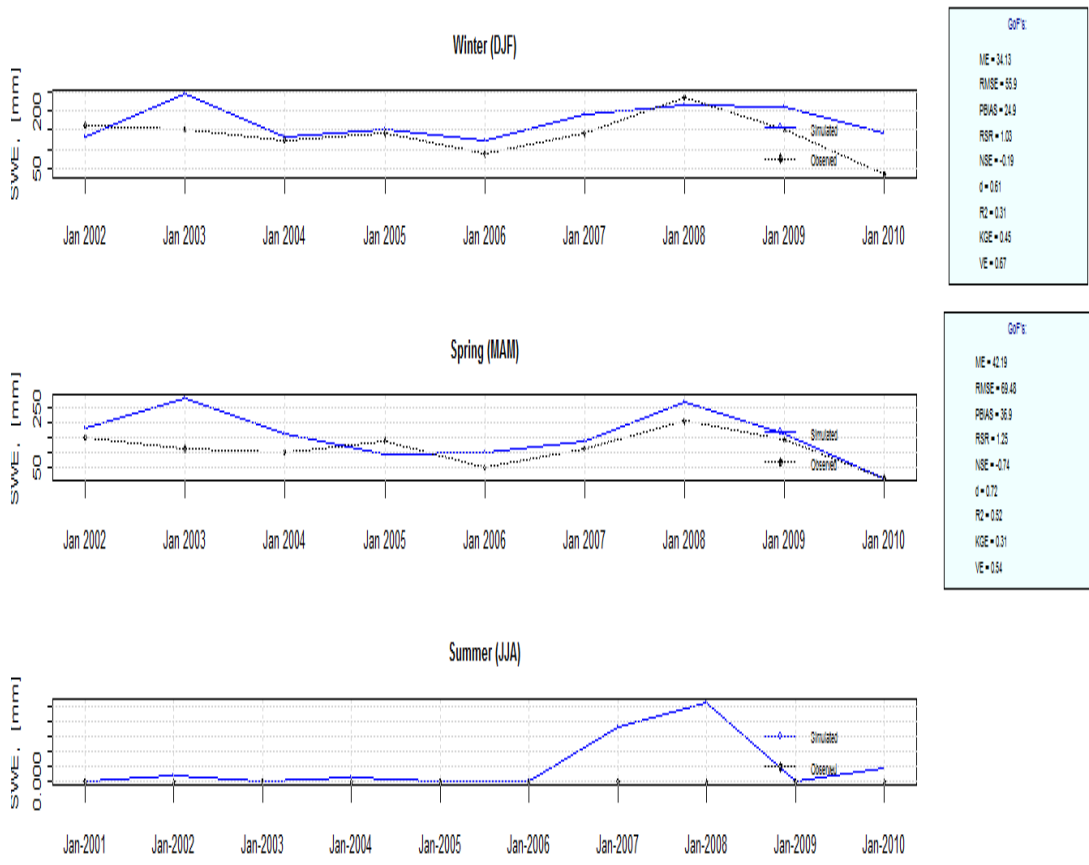


Figure 5. 38 Observed SWE (September 2001 to December 2010) at Cormack Weather Station (*Seasonal*) at Forest HRU and Simulated SWE at Forest HRU of Sub-basin 2

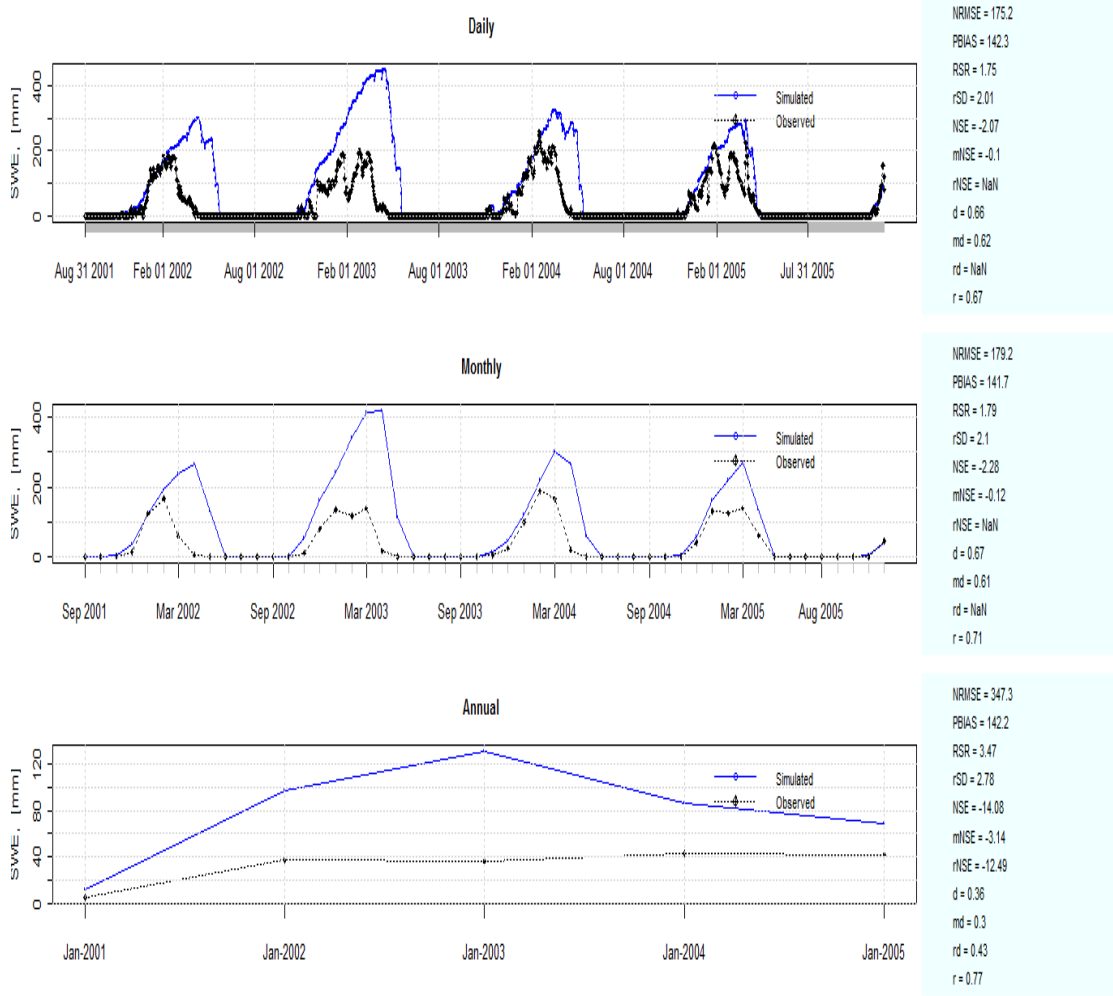


Figure 5. 39 Observed SWE (September 2001 to December 2005) at Deer Lake Airport Weather Station (Daily, Monthly and Annual) at Forest HRU and Simulated SWE at Forest HRU of Sub-basin 9

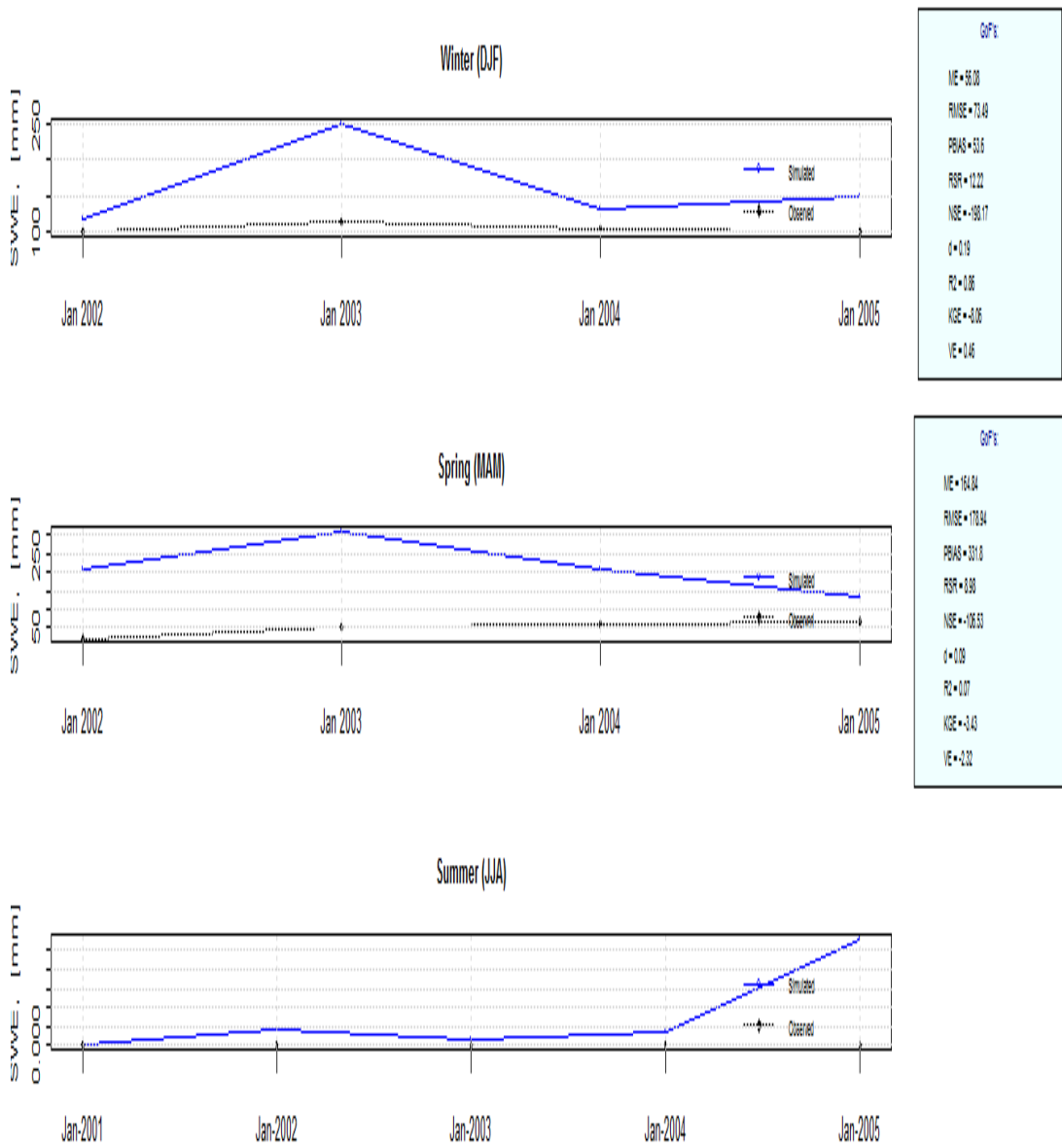


Figure 5. 40 Observed SWE (September 2001 to December 2005) at Deer Lake Airport Weather Station (Seasonal) at Forest HRU and Simulated SWE at Forest HRU of Sub-basin 9

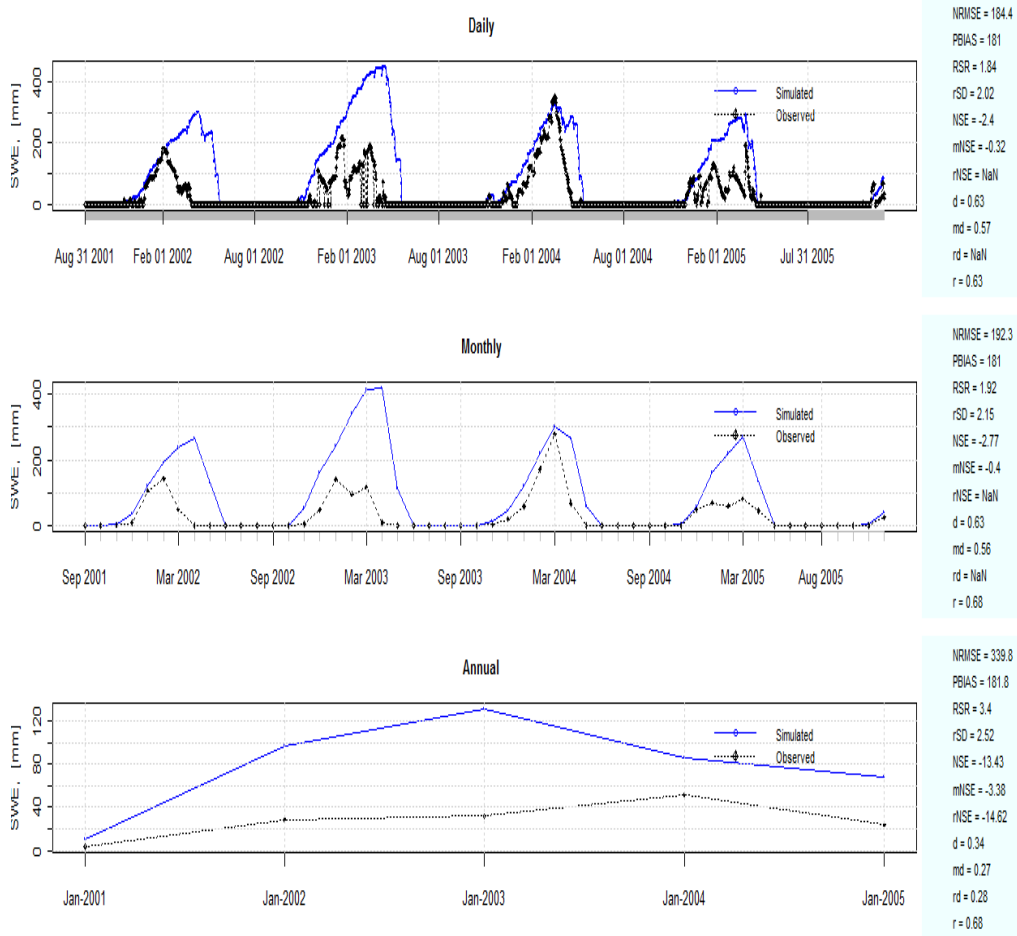


Figure 5. 41 Observed SWE (September 2001 to December 2010) at South Brook Pasadena Weather Station (Daily, Monthly and Annual) at Forest HRU and Simulated SWE at Forest HRU of Sub-basin 9

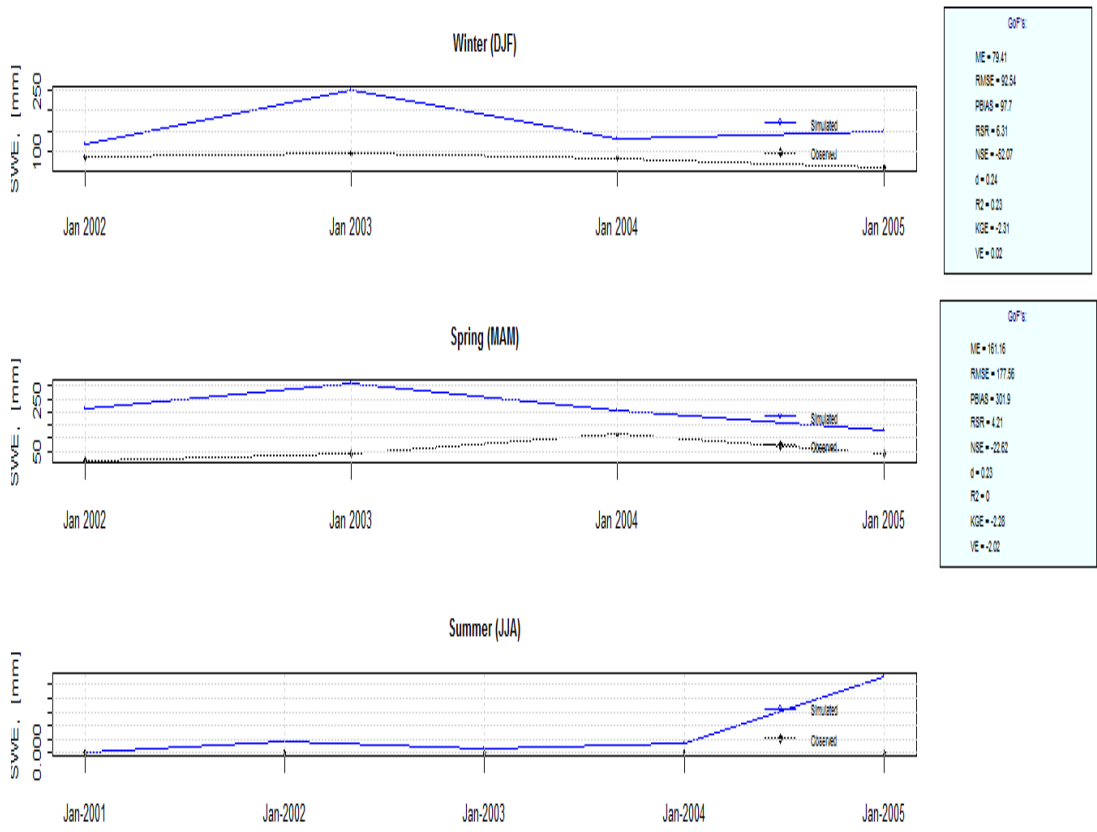


Figure 5. 42 Observed SWE (September 2001 to December 2010) at South Brook Pasadena Weather Station (Seasonal) at Forest HRU and Simulated SWE at Forest HRU of Sub-basin 9

Table 5. 7 Model bias index (MB), model efficiency index (ME), and root mean square error (RMSE) of simulated SWE

| Observation Station | MB | ME | RMSE |
|--------------------------------------|------|-------|------|
| Cormack Weather Station | 1.31 | 0.61 | 57 |
| Deer Lake Weather Station | 2.42 | -2.07 | 70.5 |
| South Brook Pasadena Weather Station | 2.81 | -2.4 | 74 |

The results from the model demonstrate that it was able to simulate the SWE regime for HRB boreal environments. The model performance is not good, however, for several reasons, such as soil and flow parameterization, and major snow-related processes, e.g. snow interception and sublimation from the forest canopy, transports

and sublimation from blowing snow. The RMSE for SWE predictions were overestimated for all the comparisons due to the unavailability of the snow survey data.

5.7 Discussion

The Cold Regions Hydrological Model platform (CRHM) was used to simulate the streamflow generated from snowmelt runoff for a large forest and wetland dominated boreal forest region basin, the Humber River Basin (7068 km²). Compared to other modelling efforts using for HRB, (Picco, 1997; Cai, 2010; Jasim, 2014), this study is the first attempt to predict the streamflow for such a large boreal basin using CRHM. The model showed the simulations of various components of the boreal region water balance, and the water in the wetlands and river channels generated from the redistribution of snow (Fang and Pomeroy, 2008) and subsequent snowmelt runoff.

The model was partially able to predict the timing and magnitude of the peak basin streamflow discharge derived from snowmelt. However, there are inadequacies in the spring basin streamflow hydrographs, at the recession limb. There was a small peak formed at the HRB bridge outlet and this peak was not observed at the hydrometric station. The predictions of streamflow were very similar, but the comparison is quite bad with outlet discharge. The simulations were able to effectively describe the cold region snow processes (Fang et. al., 2010) on a hydrological response unit based on various land cover information. However, large differences in the streamflow between the simulation and observation during the winter season existed at the HRB bridge outlet (**Figure 5.22**).

The model is also a little bit flashy at the HRB bridge point. The two big reservoirs, Grand Lake and Deer Lake, were not considered separately in the model. In addition, there were no measured soil moisture data of the study area. The soil moisture should increase during rainfall and snowmelt periods, slowly decreasing during dry periods due to evapotranspiration. A significant problem may lie with the baseflow and sub-surface flow of the HRB study area. Land cover changes have large effects on streamflow and the HRUs setup in CRHM for each sub-basin were based upon the supervised land use classification using AVHRR land use data and USGS waterbodies inventory data. The model accuracy is reduced for snowpack and streamflow simulation with observed data due to the model parameters from supervised land use characterization, but using these parameters reduced the computational time. It is certainly a challenge faced by CRHM to balance the complexity of HRU setup with model simulation accurately, gives all the model parameters, and further research is needed to resolve this. On the other hand, forcing meteorological datasets had missing data, and which was filled in by Deer Lake Airport Weather Station. No correction was performed for forcing meteorological data. Although, hydrologic routing was performed between the sub-basins to distribute the surface runoff from the upper sub-basin to lower sub-basin and it is a potential source of error for the simulated results. The surface depression storage, available groundwater storage and moisture at the recharge layer were also taken from the Lower Smoky River Basin Report. It may also affect the sub-surface runoff of the large watershed (Pomeroy et. al., 2013).

The Muskingum routing method could not perform well for snow-choked channels. Other factors for the differences between model and simulation were processes such as

subsurface storage and runoff on hillslopes. These were simulated using a relatively simple three-layer model with great uncertainty and there was no measured value from the study area. All the soil parameters such as soil moisture, depression storage, groundwater storage capacity and the saturated hydraulic conductivity of various soil layers were also collected from the Lower Smoky River, a boreal river basin. The area of the river basin is too large and the sub-basin's area were relatively high for CRHM simulations.

The land characterization is perfect for the basin but lots of HRU parameters did not have field observations. Accurate hillslope routing within the HRU is important to generate the sub-basin hydrograph, and an error in the hillslope routing parameters makes a great contribution to the difference in the hydrograph. In addition, the hydrograph was not fitted by calibration with other subsurface parameters to improve the model performance. The model performed much better in predicting streamflow discharge for sub-basin 2 and sub-basin 4 compared to the simulations of streamflow discharge for the basin outlet.

Chapter 6 Conclusion and Recommendation

This study represents the application of a new modelling strategy in cold region environments for predicting snowmelt runoff with limited data. The results obtained from the study were described in chapter 5. That chapter described the accuracy of the model set-up and comparison of the observed and simulated streamflow hydrographs in terms of the model objective function. The current chapter exhibits the conclusions determined from the model results and offer recommendations for further study.

6.1 Conclusions

This thesis highlights the development of a modelling strategy for snowmelt runoff in a large river basin of boreal forest regions. The CRHM model was set up as a base model to assess the impact of climate change and extreme events for future studies in the Humber River basin (NL). The model was then calibrated and validated with observed hydrometric data discussed in Chapter 5. The main outcomes of this study are summarized below:

1. Catchment delineation was performed in an iterative way. The catchment boundary was selected from the delineation of the catchment. The streamflow gauges were not used for catchment delineation for two reasons. The first reason is the CRHM model was developed as a non-calibrated model. The second reason was the catchment characteristics, such as the stream drainage network, the gauges location and the DEM data, jointly could not delineate the minimum number of sub-basins properly.

2. The classified Land Cover data showed the land cover heterogeneity, and all types of land cover area (HRU) were considered for developing the basin model. The land slope, land aspect and land elevation were also accounted for in the model.
3. Environment Canada weather stations data were used as observation data to set up the model. No gridded data were used for the model. The precipitation data were estimated by Thiessen Polygon over the sub-basins. The datasets were able to produce hydrographs but failed to match perfectly with the observed hydrographs in the timing of peak discharges at Upper Humber River at Reidville and Sheffield Brook Near Trans-Canada Highway. The results were influenced by the lower estimation of precipitation, i.e., rainfall or snowmelt, or both in the forcing data. According to simulated streamflow results, the rainfall data might not be good or at least not representative of the large river basin for the CRHM model. In addition, the modelled basin outlet points in sub-basins are far from the gauges, making the results worse. Again, the base flow was matched properly with the observed data. However, this is not crucial for snowpack simulation, so the model can be used for simulating the winter events.
4. Data gaps were filled by temporal and spatial interpolation and regression equations that were developed with Deer Lake Airport weather station as it has continuous data records. The data cannot, however, represent the whole study area perfectly for large catchment size.
5. No bias correction was introduced in the meteorological datasets, and solar radiation data were estimated by Annandale module.

6. Parameters were collected from the Lower Smoky River basin report and some parameters were optimized within their upper and lower limits. This creates a significant uncertainty of predicting accurate model results.
7. The water balance was checked, and the value of MB is pretty good over the sub-basins. Over a long period of time (several years), the total precipitation should equal the sum of the total runoff, and the total evaporation, because the change in storage is comparatively small.
8. Satisfactory results were obtained at gauge locations at Upper Humber River at Reidville and Sheffield Brook Near Trans-Canada Highway. The result at Humber River at Village Bridge is not satisfactory during winter and it underestimates the total model results. But, the fall and the spring peak discharges were predicted properly in the basin outlet. Furthermore, Grand Lake and Deer Lake were two large waterbodies within the watershed and those were not considered separately in the model, which hampers the overall model performance. In addition, the observed daily Streamflow data were plotted with simulated daily data acquired from hourly simulated streamflow data. Moreover, another problem occurred probably due to the partitioning of rainfall and snowmelt. This can be due to the problems with the soil moisture and the base flow. The soil moisture was checked, and it is very difficult to identify soil conditions such as wetness or dryness. Again, the soil moisture should increase during rainfall and snowmelt periods, slowly decreasing during dry periods due to evapotranspiration. There are no field measurements of soil moisture anywhere closest to the watershed.

9. Baseflow and sub-surface flow are other considerations for predicting better streamflow. The modelled streamflow and the observed streamflow were plotted against time during a period when there is no rainfall. Both curves were plotted as straight lines in a log scale in y-axis. The slopes were very different, and the model had the wrong value of soil parameter values. Furthermore, there was probably the wrong amount of water getting into the ground water reservoir, so, it was required that the model parameters be adjusted.
10. The initial model set-up was checked with observed streamflow data. Considerable streamflow was obtained at two selected stream gauge locations after model calibration and parameter optimization. Then the model was validated to satisfy the efficiency of the model set-up.
11. There was no optimization routine in the CRHM model as it is a non-calibrated model. So, an optimization routine was developed by SCE algorithm. SCE optimization routines did not work perfectly for this study and some parameters were manually optimized for better model results. There is a time limitation and it was not possible to make the model results fit better within these optimization schemes.
12. Snow survey data were collected from Environment Canada weather stations and the data records were not continuous. CRHM generates SWE, ground snow, blowing snow sublimation and lots more winter events within the HRU scale. The observed weather stations were located on the forest HRU, and simulated SWE over

forest HRU were plotted and compared. The overall results were not satisfactory due to the lack of measured snow survey data.

6.2 Recommendations

The present study developed a base model for Humber River Basin which can be further used for assessing the future climate scenario on the streamflow and various snowpack events. There was a time constraint and some other possibilities with the model were not assessed. The future extension of work for the large watershed with CRHM model are discussed below.

1. North American Regional Reanalysis (NARR) gridded data can be used to predict the winter snowpack events as weather station data could not simulate the result perfectly.
2. Only three stations' data were calibrated and validated for the study area. There were a few other gauge stations which can also be validated in the CRHM model.
3. Hydraulic routing will be needed to predict the winter peak discharges at Humber River at Village Bridge. The lake routing will consider the flow of Grand Lake and Deer Lake for simulating the winter peak flow.
4. Model calibration is not mandatory for the CRHM model. But when it is applied for large basin without measured parameter values, then calibration will be applicable. For getting better model results multi objective model calibration can be performed for simulating the peak discharges. More completed tasks would be

required to improve the calibration of the model. The re-estimation of present calibration parameters will also be recommended.

5. There was higher snow cover during winter, and the simulation starts from fall. The simulation can be started in winter by setting up initial condition.
6. The study was able to obtain a satisfactory model setup after calibration, and it can be used for future streamflow and snowpack simulation for future climate change predictions. The weather model datasets can be used for future winter snowpack and streamflow predictions.
7. The study will be applicable for estimating solar radiation data as there is no available solar radiation data on the study area.
8. Various types of probabilistic studies will be recommended on the basis of model results.
9. The model can be used for future flood forecasting studies in HRU scale because snowmelt runoff is very dominant over the large river basin.
10. The model can be used for blowing snow sublimation, ground snow evaluation, soil moisture evolution, surface and subsurface flow estimation.

References

- Altaf, F., Meraj, G., and Shakil A. (2013). Romshoo Morphometric Analysis to Infer Hydrological Behavior of Lidder Watershed, Western Himalaya, India. *Geography Journal*, 2013, 14.
- ArcGIS 10.1 Help. (n.d.). Retrieved from [\(http://resources.arcgis.com/en/help/main/10.1/index.html#/Fill/009z00000050000000/0/\)](http://resources.arcgis.com/en/help/main/10.1/index.html#/Fill/009z00000050000000/0/)
- Ariza-Villaverde, A.B., Jiménez-Hornero, F.J., and Gutiérrez de Ravé, E. (2015). Influence of DEM resolution on drainage network extraction: A multifractal analysis. *Geomorphology*, 241, 243–254.
- Armstrong R.N., Pomeroy, J. W., and Martz L.W. (2010). Estimating Evaporation in a Prairie Landscape under Drought Conditions. *Canadian Water Resources Journal*, 35, 173-186.
- Bera, A.K., Singh, V., Bankar, N., Salunkhe, S.S., and Sharma, J.R. (2014). Watershed Delineation in Flat Terrain of Thar Desert Region in North West India – A Semi Automated Approach Using DEM. *J Indian Soc Remote Sens*, 42(1), 187–199.
- Cai, H. (2010). Flood Forecasting on the Humber River using an Artificial Neural Network Approach. *Master of Engineering Memorial University of Newfoundland. Print. St. John's, NL, Canada.*

Chow, Ven. (Ed.), Hand Book of Applied Hydrology. McGraw Hill Book Company, New York.

Contour mapping. (n.d.). Retrieved from <https://www.britannica.com/science/contourmapping>

Dornes, P. F., Pomeroy, J. W., Pietroniro, A., Carey, S. K., and Quinton, W. L. (2008). Influence of landscape aggregation in modelling snow-cover ablation and snowmelt runoff in a sub-arctic mountainous environment. *Hydrological Science Journal*, 53, 725-740.

Dornes P.F. (2009). An approach for modelling snowcover ablation and snowmelt runoff in cold region environments. *Doctor of Philosophy, Centre for Hydrology, University of Saskatchewan. 117 Science Place, Saskatoon, SK S7N 5C8.*

Duan, Q. Y., Gupta, V. K., and Sorooshian, S. (1993). Shuffled complex evolution approach for effective and efficient global minimization. *Journal of Optimization Theory and Applications*, 76, 501-521.

Ellis, C. R., Pomeroy, J. W., Brown, T., and MacDonald, J. (2010). Simulation of snow accumulation and melt in Needleleaf forest environments. *Hydrol. Earth Syst. Sci.*, 14, 925–940.

Ellis, C. R., Pomeroy, J. W., Essery, R.L.H., and Link, T.E. (2011). Effects of needleleaf forest cover on radiation and snowmelt dynamics in the Canadian Rocky Mountains. *Can. J. For. Res.*, 41, 608–620.

Environment Canada National Climate Data and Information Archive weather stations.

Downloaded from

http://climate.weather.gc.ca/historical_data/search_historic_data_e.html)

Exploring Imagery and Elevation Data in GIS Applications. (n.d.). Retrieved from

<https://www.e-education.psu.edu/geog480/node/490>

Fang, X., and Pomeroy, J. W. (2007). Snowmelt runoff sensitivity analysis to drought on the Canadian prairies. *Hydrological Processes*, 21, 2594–2609.

Fang, X., Pomeroy, J.W., Westbrook, C.J., Guo, X., Minke, A.G. and Brown, T. (2010). Prediction of snowmelt derived streamflow in a wetland dominated prairie basin. *Hydrol. Earth Syst. Sci.*, 1, 1–16

Fang, X., Pomeroy, J.W., Ellis, C. R., MacDonald, M. K., DeBeer, C. M., and Brown, T. (2013). Multi-variable evaluation of hydrological model predictions for a headwater basin in the Canadian Rocky Mountains. *Hydrol. Earth Syst. Sci.*, 17, 1635–1659.

Fang, X., and Pomeroy, J. W. (2016). Impact of antecedent conditions on simulations of a flood in a mountain headwater basin. *Hydrological Processes*, 30, 2754–2772.

Fassnacht, S.R., Dressler, K.A., and Bales, R. C. (2003). Snow water equivalent interpolation for the Colorado River Basin from snow telemetry (SNOTEL) data. *Water Resources Research*, 39.

- Hadley, R.F., Schumm, S.A. (1961). Sediment sources and drainage basin characteristics in upper Cheyenne River Basin. *US Geol. Survey. Water-Supply Pap. 1531B,198.*
- Harder, P., Pomeroy, J.W., and Westbrook, C. (2015). Hydrological resilience of a Canadian Rockies headwaters basin subject to changing climate, extreme weather, and forest management. *Hydrological Processes,*
- Historical climate data. (n.d.). Retrieved from http://climate.weather.gc.ca/index_e.html
- Jarihani A.A., Callow J.N., McVicar T.R., Van Niel T.G., and Larsen J.R. (2015). Satellite-derived Digital Elevation Model (DEM) selection, preparation and correction for hydrodynamic modelling in large, low-gradient and data-sparse catchments. *Journal of Hydrology, 524, 489–506.*
- Jasim, F. (2014). Development of a Base Model for Flood Forecasting Studies in the HumberRiver Basin (NL) and Selection of an Appropriate Model Forcing Dataset. *Master of Engineering Memorial University of Newfoundland. Print. St. John's, NL, Canada.*
- Johnston, C.M., Dewald, T.G., Bondelid, T.R., Worstell, B.B., McKay, L.D., Rea1, A., Moore1, R.B., and Goodall, J.L. (2009). Evaluation of Catchment Delineation Methods for the Medium-Resolution National Hydrography Dataset. *Scientific Investigations Report,5233.*

- Krogh S.A., Pomeroy, J. W., and Mcphee J. (2013). Physically-based Mountain Hydrological Modelling Using Reanalysis Data in Patagonia. *Journal of Hydrometeorology*, 16, 172-193.
- Leavesley, G.H., Restrepo, P.J., Markstrom, S.L., Dixon, M., and Stannard, L.G. (1998). The Modular Modelling System (MMS): User's Manual. *Open-File Report 96-15, U.S. GEOLOGICAL SURVEY, USA*.
- Marsh, C., and Pomeroy, J.W. (n.d.). Cold regions hydrological model platform: CRHM brief introduction. *Centre of Hydrology, University of Saskatchewan, Saskatoon, SK, Canada*.
- Picco, R.C. (1997). A comparative study of flow forecasting in the Humber River Basin using a deterministic hydrologic model and a dynamic regression statistical model. *Master of Engineering Memorial University of Newfoundland. Print. St. John's, NL, Canada*.
- Pomeroy, J. W., Gray, D. M., Brown, T., Hedstrom, N. R., Quinton, W. L., Granger, R. J., and Carey, S. K. (2007). The cold regions hydrological model: a platform for basin process representation and model structure on physical evidence. *Hydrological Processes*, 21, 2650-2667.
- Pomeroy, J. W., Rowlands, A., Hardy, J., Link, T., Marks, D., Essery, R., Sicart, J.E., and Ellis, C. (2007). Spatial Variability of Shortwave Irradiance for Snowmelt in Forests. *Journal of Hydrometeorology*, 9, 1482-1490.

- Pomeroy, J.W., Fang, X., and Williams, B. (2009). Impacts of Climate Change on Saskatchewan's Water Resources. *Centre for Hydrology Report No. 6, Centre for Hydrology, University of Saskatchewan. 117 Science Place, Saskatoon, SK S7N 5C8.*
- Pomeroy, J.W., Semenova, O.M., Fang, X., Vinogradov, Y.B., Ellis, C., Vinogradova, T.A., MacDonald, M., Fisher, E.E., Dornes, P., Lebedeva, L., and Brown, T. (2010). Wolf Creek Cold Regions Model Set-up, Parameterization and Modelling Summary. *Centre for Hydrology Report No. 8, Centre for Hydrology, University of Saskatchewan. 117, Science Place, Saskatoon, SK S7N 5C8.*
- Pomeroy, J.W., Fang, X., and Ellis, C. R. (2012). Sensitivity of snowmelt hydrology in Marmot Creek, Alberta, to forest cover disturbance. *Hydrological Processes, 26, 1891–1904.*
- Pomeroy, J. W., Fang, X., Shook, K., Westbrook, C., and Brown, T. (2012). Informing the Vermilion River Watershed Plan through Application of the Cold Regions Hydrological Model Platform. *Centre for Hydrology Report No. 12, Centre for Hydrology, University of Saskatchewan. 117 Science Place, Saskatoon, SK S7N 5C8.*
- Pomeroy, J. W., Shook, K., Fang, X., Brown, T., and Marsh, C. (2013). Development of a Snowmelt Runoff Model for the Lower Smoky River. *Centre for Hydrology Report No. 13, Centre for Hydrology, University of Saskatchewan. 117 Science Place, Saskatoon, SK S7N 5C8.*

- Quinton, W.L., Baltzer, J.L. (2013). Changing surface water systems in the discontinuous permafrost zone: implications for streamflow. *Cold and Mountain Region Hydrological Systems Under Climate Change: Towards Improved Projections Proceedings of H02, IAHS-IAPSO-IASPEI Assembly, Gothenburg, Sweden,*
- Rasouli, K., Pomeroy, J. W., Janowicz, J. R., Carey, S.K., and Williams, T.J. (2014). Hydrological sensitivity of a northern mountain basin to climate change. *Hydrological Processes,*
- Roberts, J., Pryse-Phillips, A., and Snelgrove, K. (2012). Modelling the Potential Impacts of Climate Change on a Small Watershed in Labrador, Canada. *Canadian Water Resources Journal, 37(3), 231-251.*
- Rothwell, R., Hillman, G., and Pomeroy, J. W. (2016). Marmot Creek Experimental Watershed Study. *The Forestry Chronicle, 92, 32-36.*
- Serreze, M.C., Walsh, J.E., Chapin Iii, F.S., Osterkamp, T., Dyurgerov, M., Romanovsky, V., Oechel, W.C., Morison, J., Zhang, T. And Barry, R. G. (2000). Observational Evidence of Recent Change in The Northern High-Latitude Environment. *Climatic Change, 46, 159–207.*
- Shook, K., and Pomeroy, J. W. (2011). Synthesis of incoming shortwave radiation for hydrological simulation. *Journal of Hydrology Research, 42.6, 434–446.*
- Singh, P., Gupta, A., Singh, M. (2014). Hydrological inferences from watershed analysis for water resource management using remote sensing and GIS

techniques. *The Egyptian Journal of Remote Sensing and Space Sciences*, 17, 111–121.

Smith, K.G. (1950). Standards for grading texture of erosional topography. *Am. J. Sci.* 248, 655–668.

SRTM 90m Digital Elevation Database v4.1. (n.d.). Retrieved from (<http://www.cgiar-csi.org/data/srtm-90m-digital-elevation-database-v4-1>).

Sturm, M., Taras, B., Liston, G.E., Derksen, C., Jonas, T., and Lea, J. (2010). Estimating Snow Water Equivalent Using Snow Depth Data and Climate Classes. *Journal of Hydrometeorology*, 11, 1380-1394.

United States Geological Survey. (n.d.). Retrieved from <https://earthexplorer.usgs.gov/>

Whitfield, P., and Pomeroy, J. W. (2016). Changes to flood peaks of a mountain river: implications for analysis of the 2013 flood in the Upper Bow River, Canada. *Hydrological Processes*,

Zhou, J., Pomeroy, J. W., Zhang, W., Cheng, G., Wang, G., and Chen, C. (2014). Simulating cold regions hydrological processes using a modular model in the west of China. *Journal of Hydrology*, 509, 13–24.

Appendix

Appendix A Forms of Dynamic Regression Model

Table A. 1 Forms of Dynamic Regression Model for Humber River Basin (Picco, 1997)

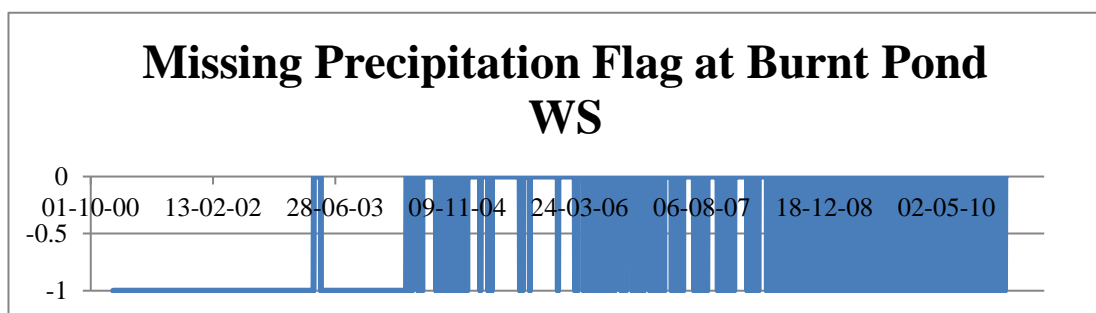
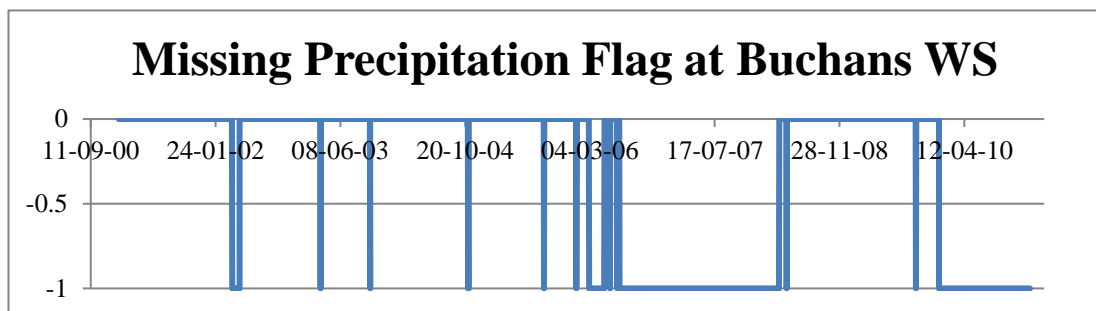
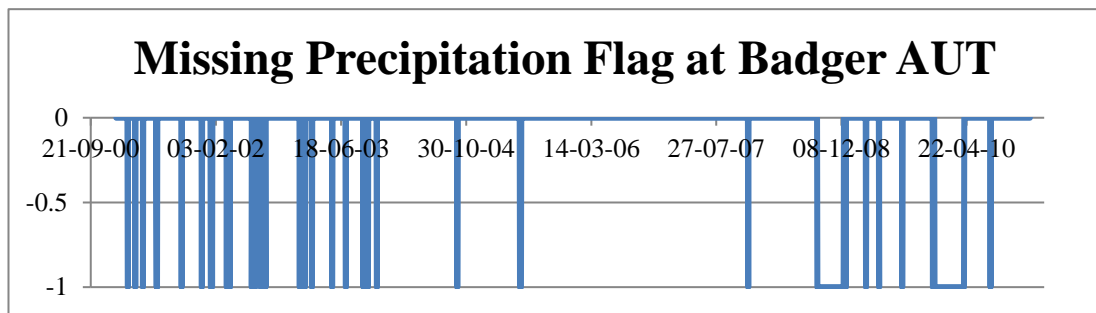
| Sub-basin Name | Form of Dynamic Regression Equation |
|--------------------------------------|--|
| Lewaseechjeech Brook | $_CONST + aPREGLGI + bFLOW[-1] + cFLOW[-2] + dFLOW[-3]$; Where $_CONST = 0.149490$; $a = 0.2442776$; $b = 1.664595$; $c = -1.046278$; $d = 0.336051$ |
| Sheffield Brook | $_CONST + aPREINDI + bFLOW[-1] + cFLOW[-2]$; Where $_CONST = 0.348126$; $a = 0.041432$; $b = 1.432156$; $c = -0.462627$ |
| Indian Brook Diversion | $_CONST + aPRECINDI + bFLOW[-1] + cFLOW[-2]$; Where $_CONST = 0.448615$; $a = 0.118321$; $b = 1.297039$; $c = -0.362822$ |
| Upper Humber River near Reidville | $_CONST + aPRESAND + bFLOW[-1] + cFLOW[-2] + dFLOBLAC + eAUTO[-1]$; Where $_CONST = 14.380586$; $a = -0.210896$; $b = 0.739059$; $c = -0.376750$; $d = 1.055177$; $e = 0.884608$ |
| Upper Humber River Above Black Brook | $_CONST + aPRECBLAC + bFLOW[-1] + cFLOW[-2]$; Where |

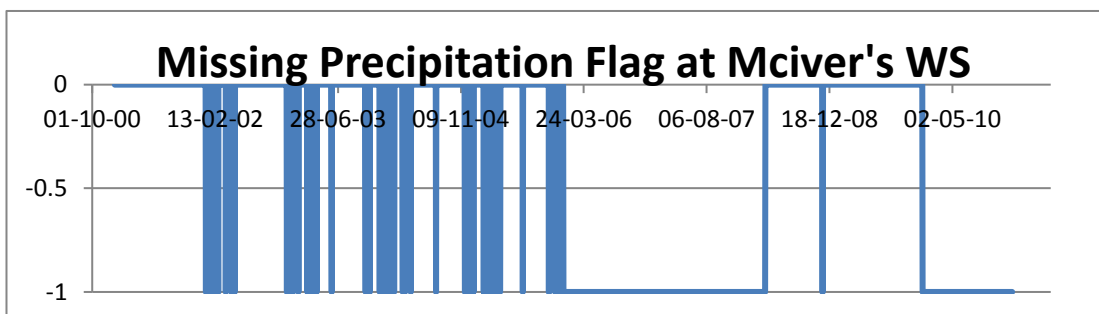
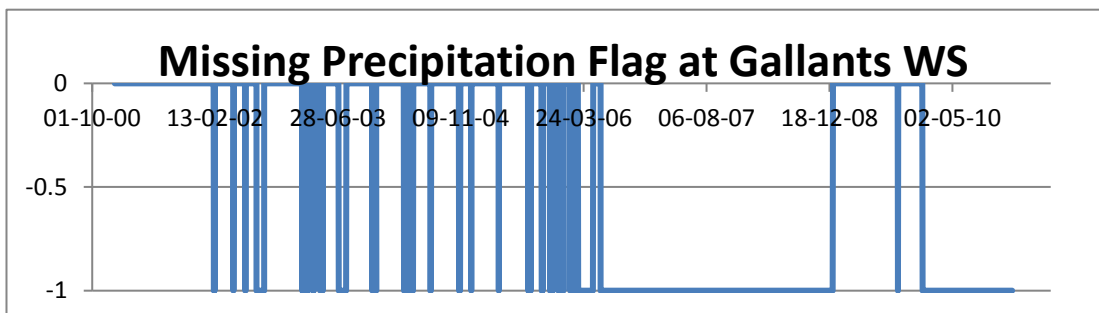
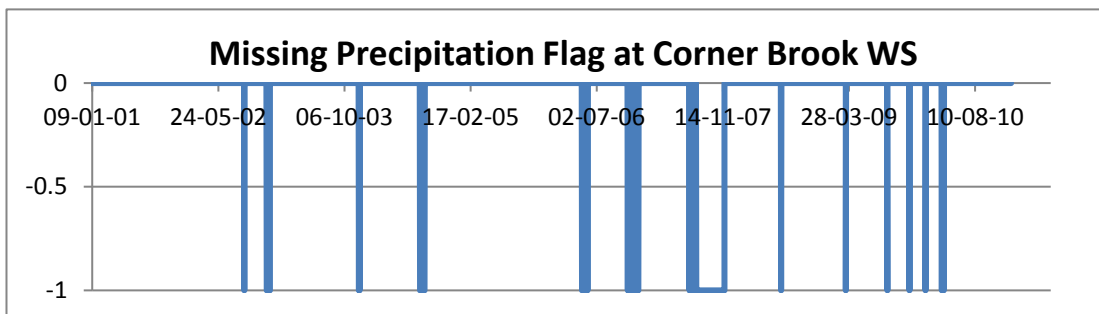
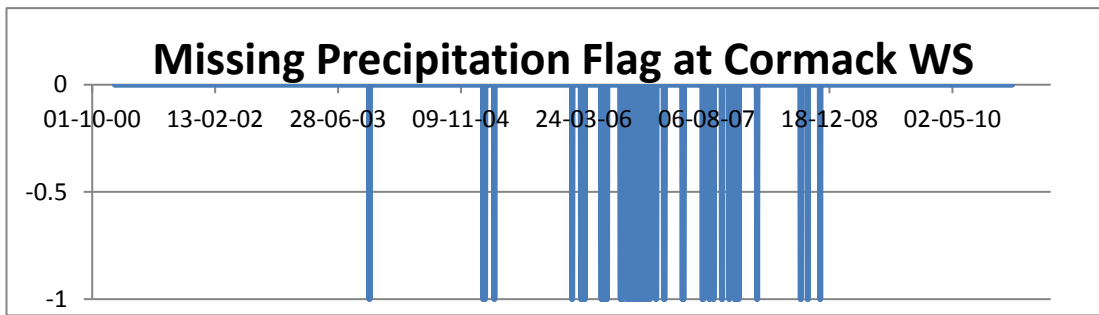
| Sub-basin Name | Form of Dynamic Regression Equation |
|---------------------------------------|---|
| | $_CONST = 1.254866; a = 0.558944; b = 1.238943; c = -0.315646$ |
| Humber River at Humber Village Bridge | $_CONST + aPREBLAC + bFLOW[-1] + cFLOREID + dFLOBLAC + eAUTO[-1];$ Where $_CONST = 21.697851; a = 0.187210; b = 0.859492; c = 0.196181; d = -0.055710; e = 0.525336$ |

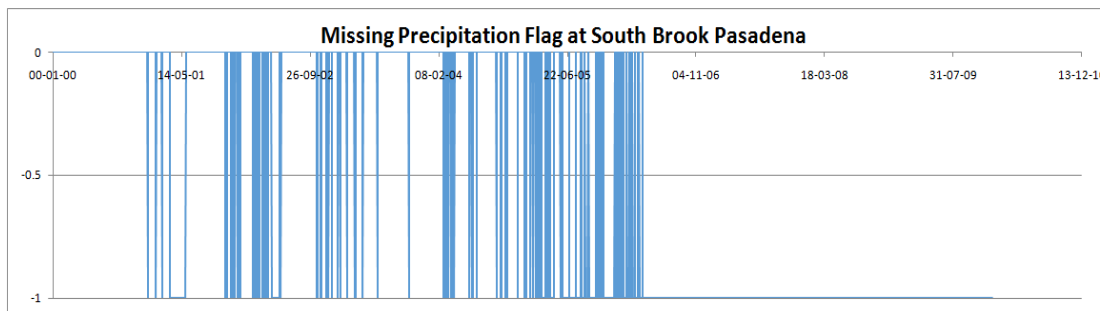
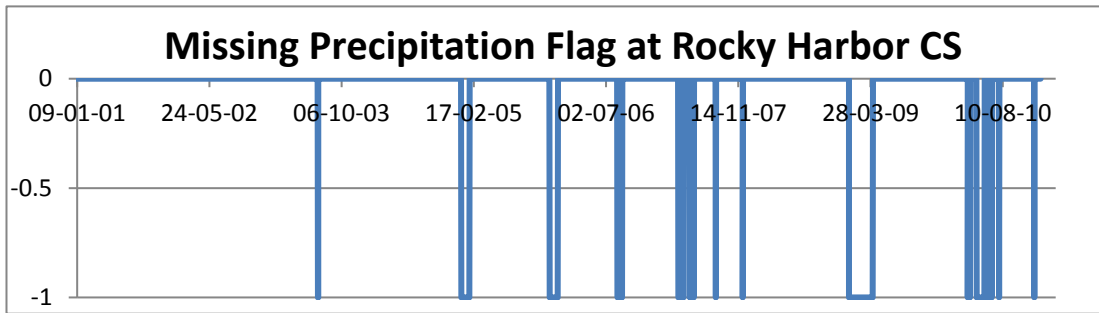
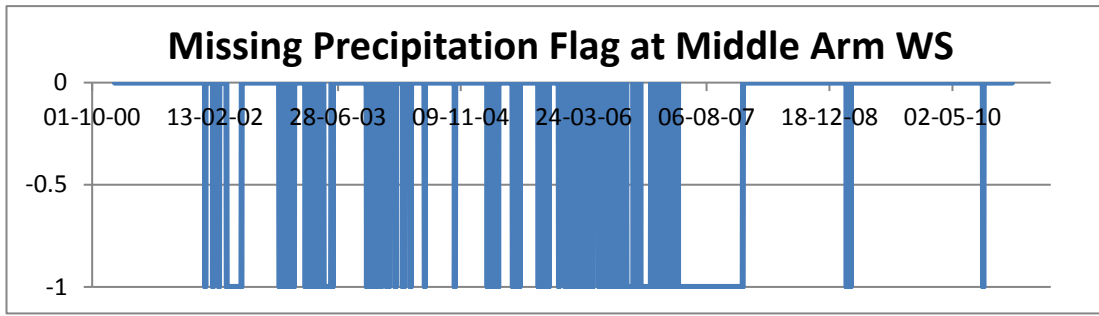
Here, *PREGLGI* = Precipitation at Grand Lake at Glover Island, *PREINDI* = Precipitation at Indian Brook Diversion, *PRESAND* = Precipitation at Sandy Lake at Howley Road, *PRECBLAC* = Precipitation at Upper Humber above Black Brook, *FLOBLAC* = Flow at Upper Humber above Black Brook and a, b, c, d and e are Dynamic regression coefficients.

Appendix B Missing precipitation data

Figures show the missing precipitation data at Badger AUT, Buchans, Burnt Pond, Cormack, Corner Brook, Gallants, Mcivers, Middle Arm WS, Rocky Harbour CS and South Brook Pasadena meteorological stations. Missing data is indicated by flag value of -1.

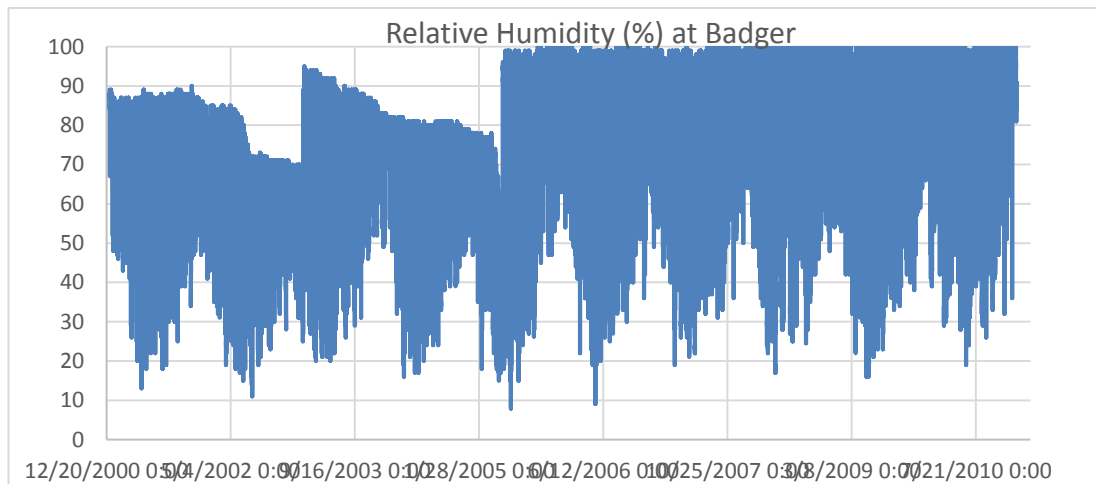
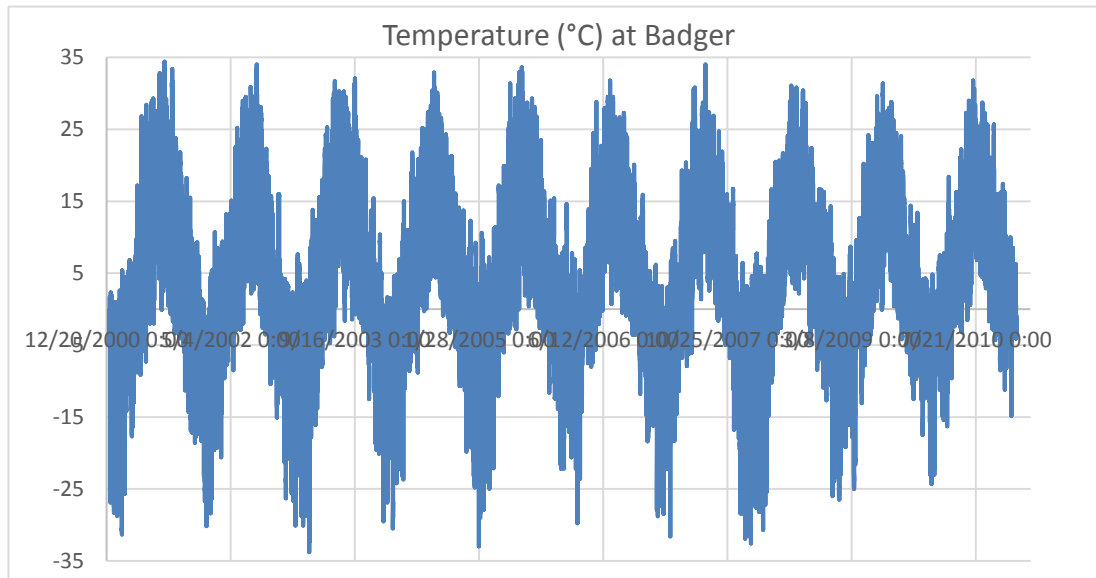


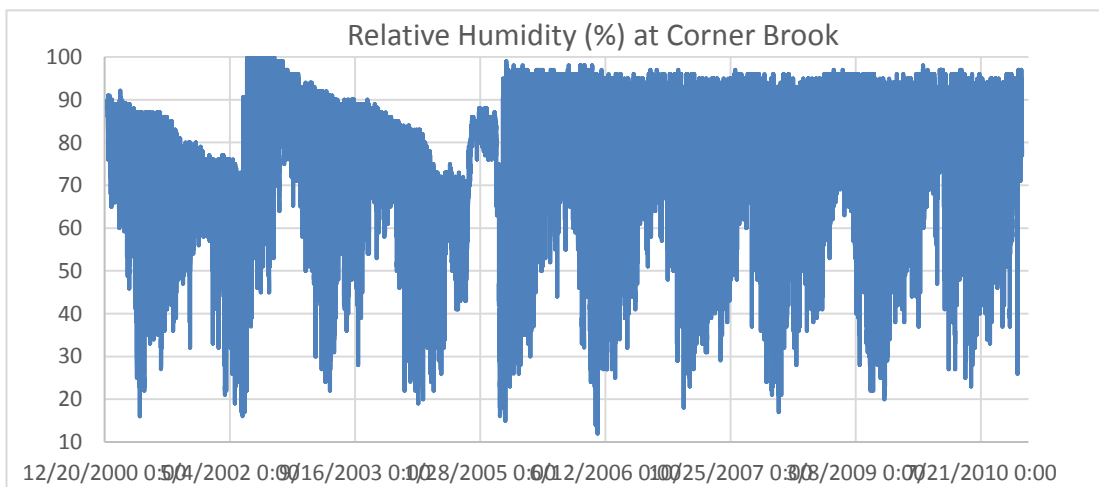
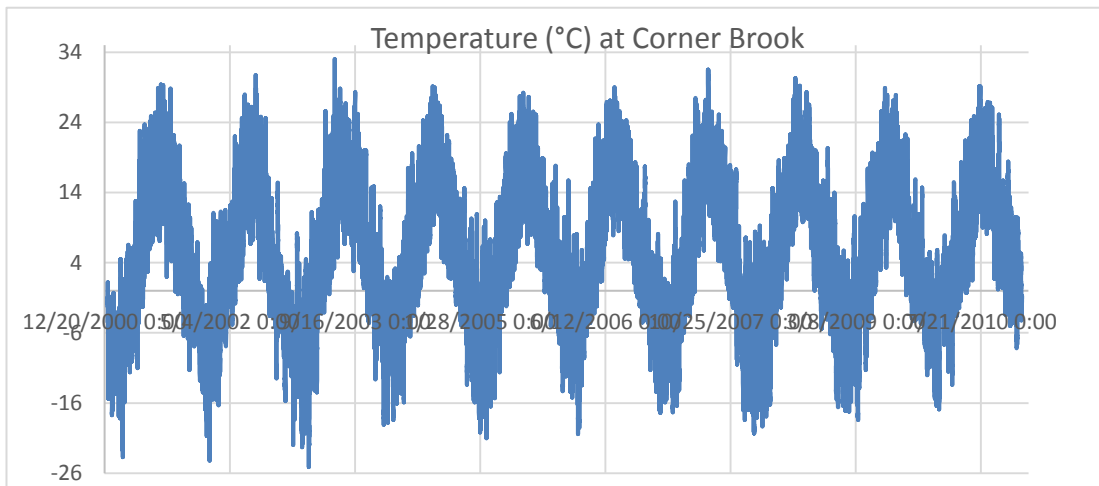
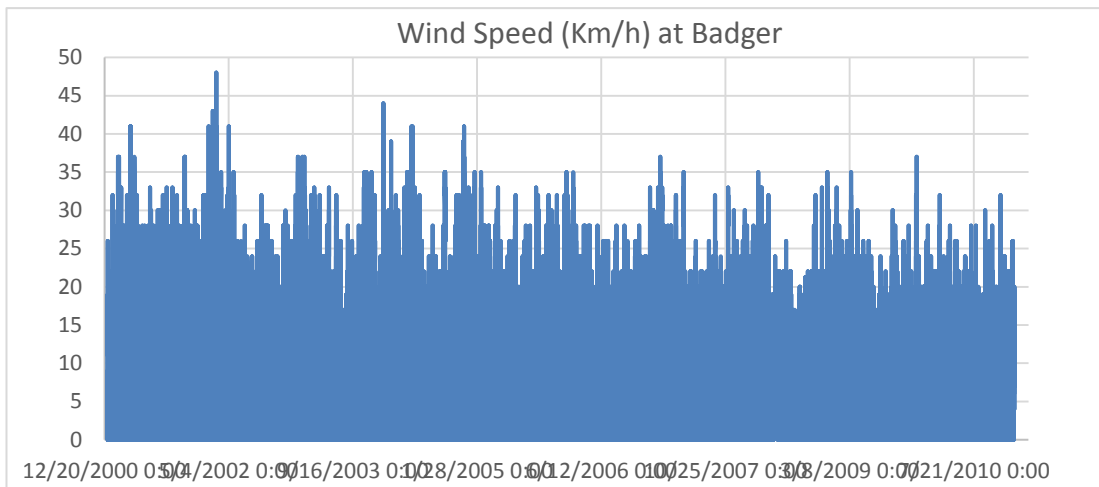


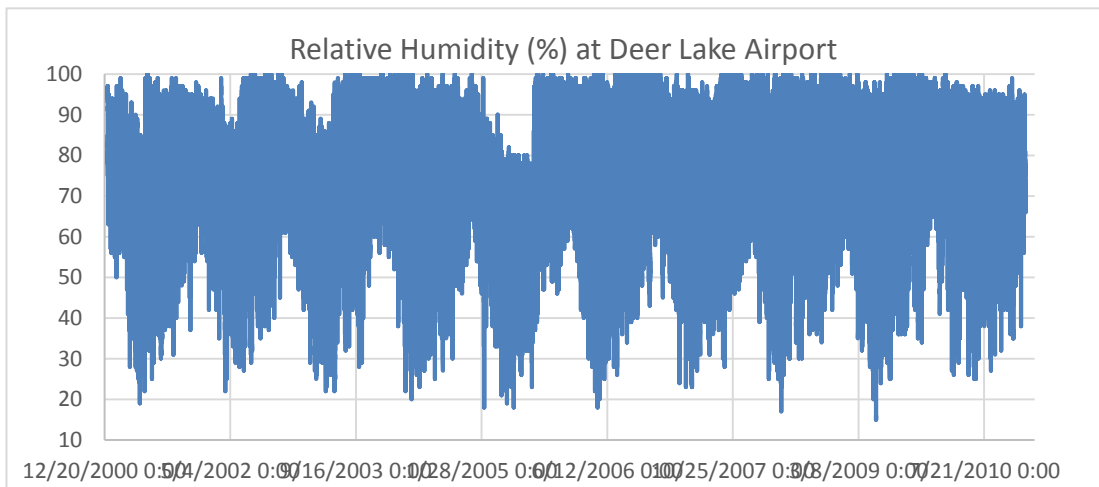
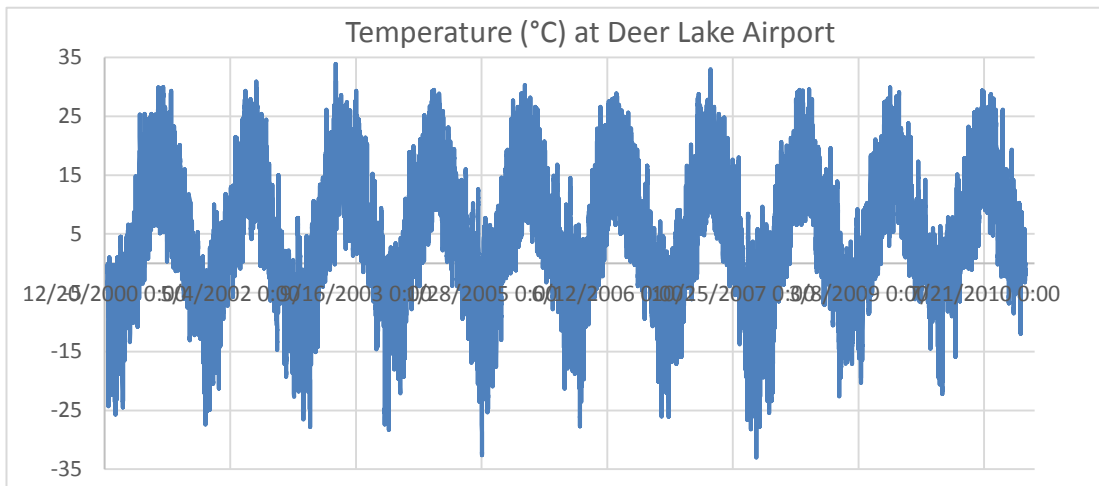
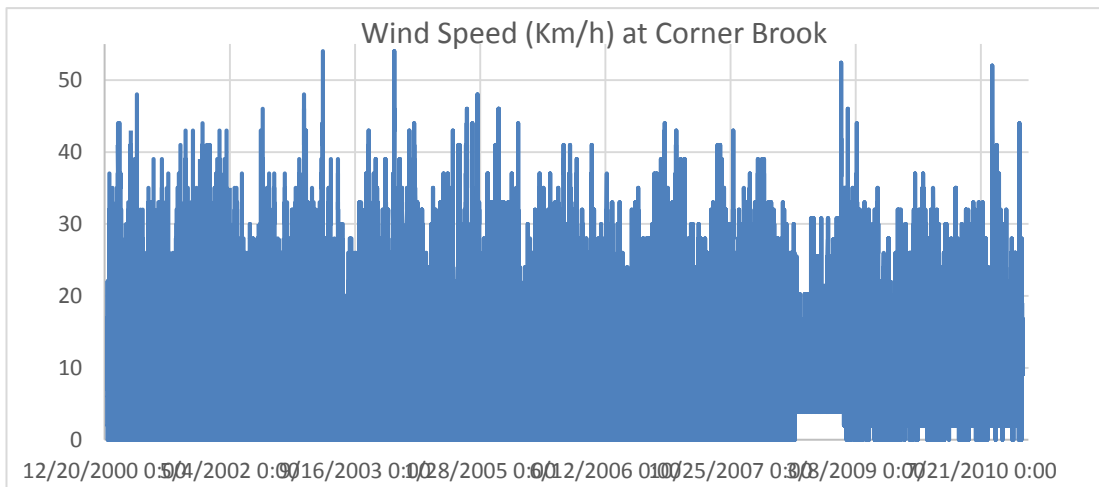


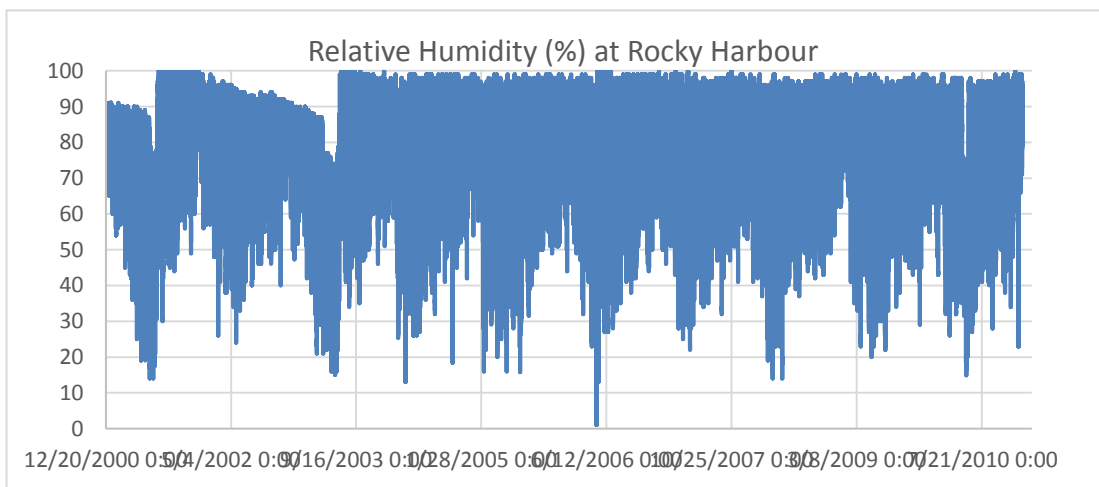
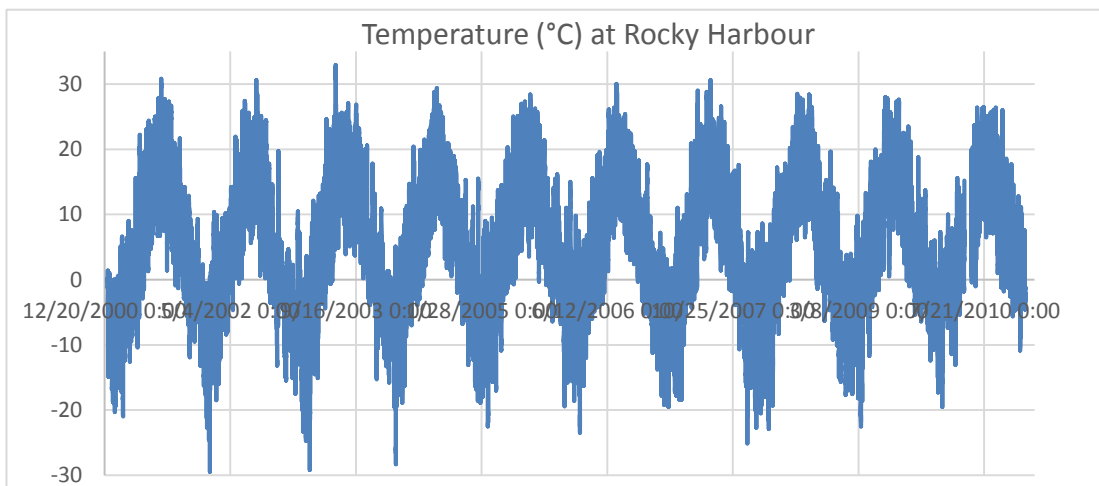
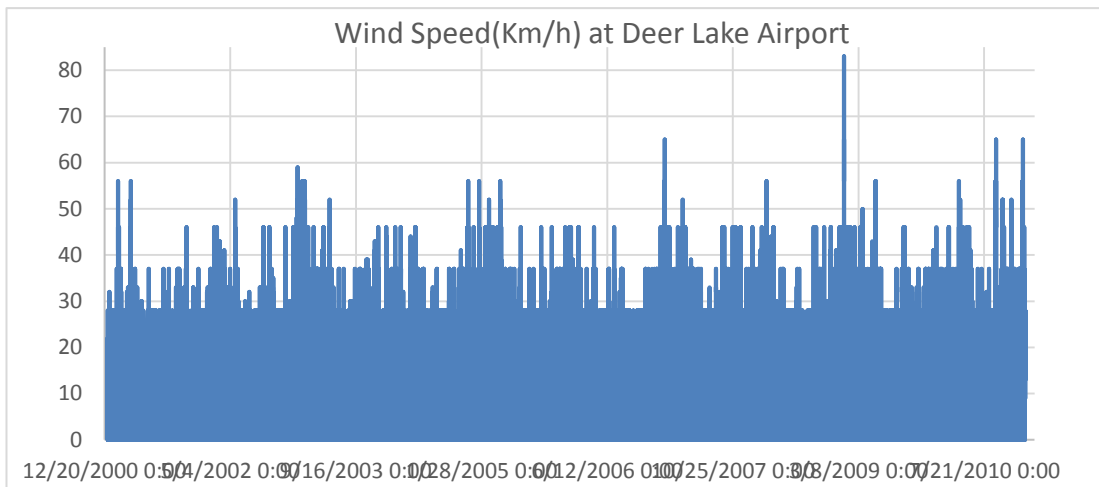
Appendix C Meteorological Observation of Humber River Basin

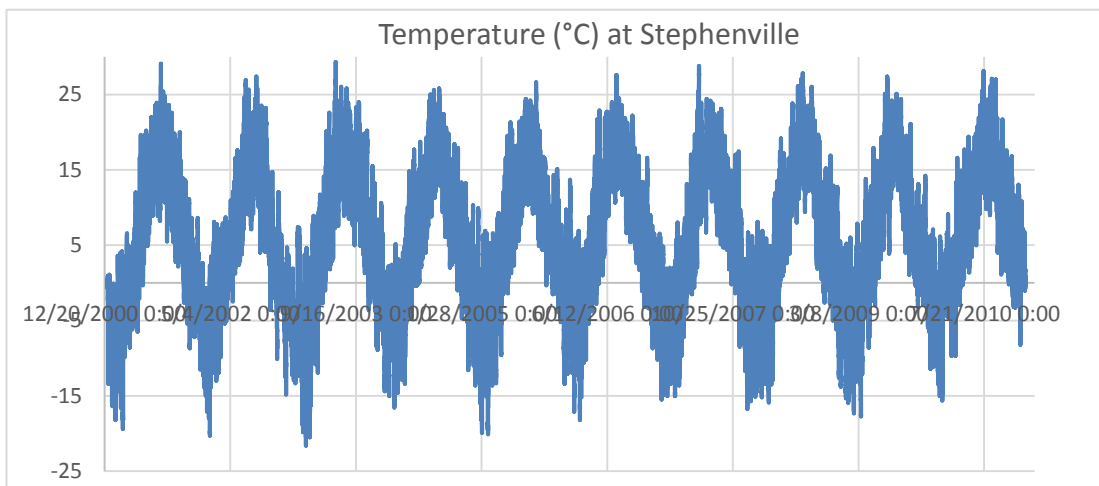
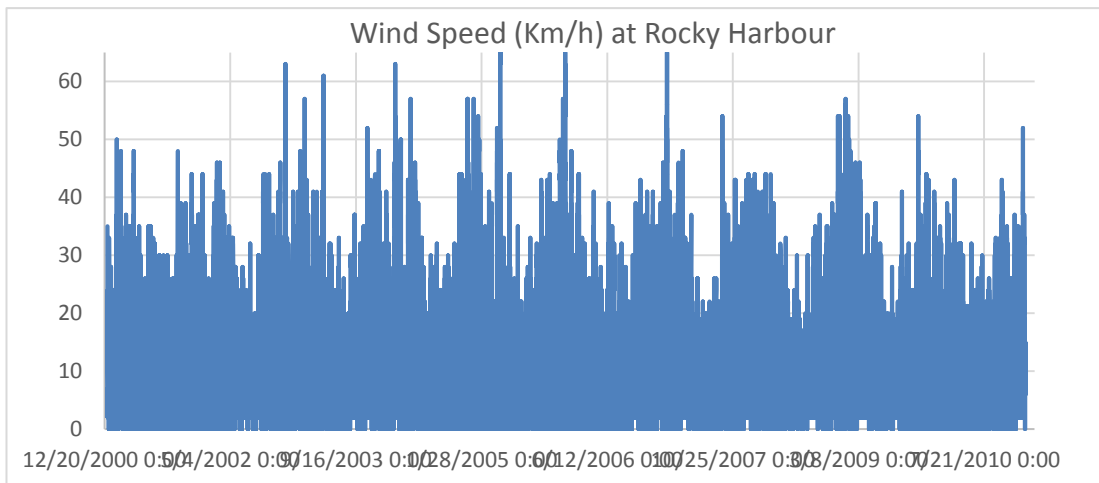
The continuous hourly records of temperature, relative humidity and wind speed are shown below

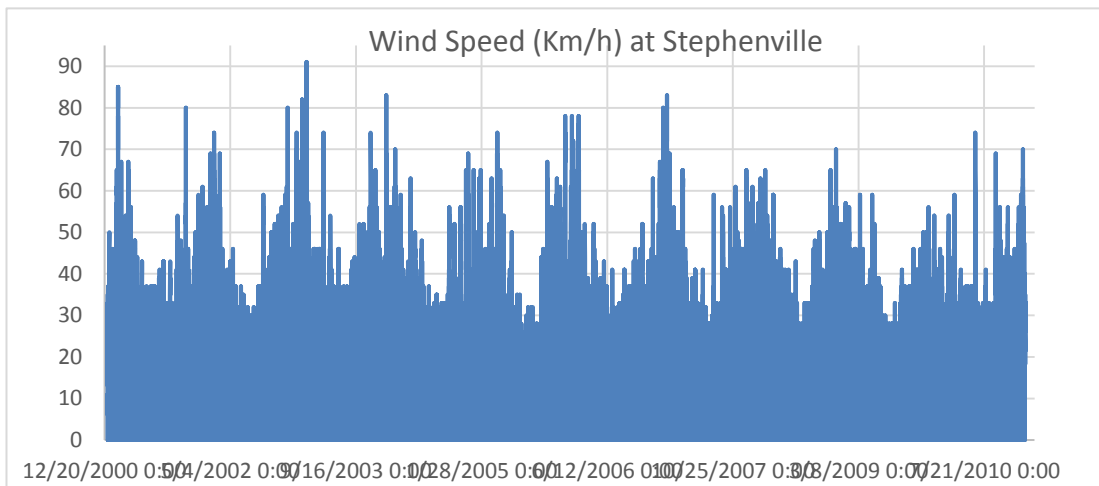
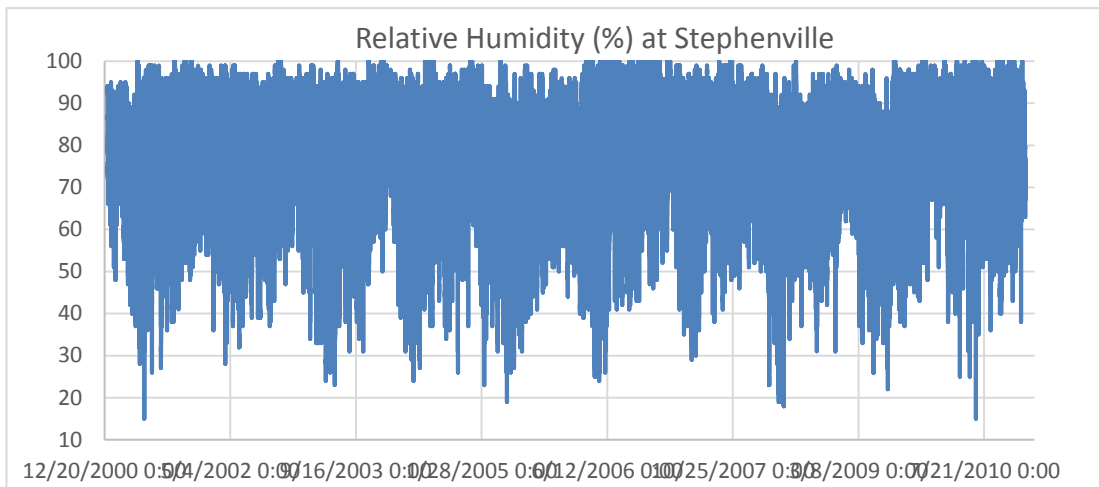




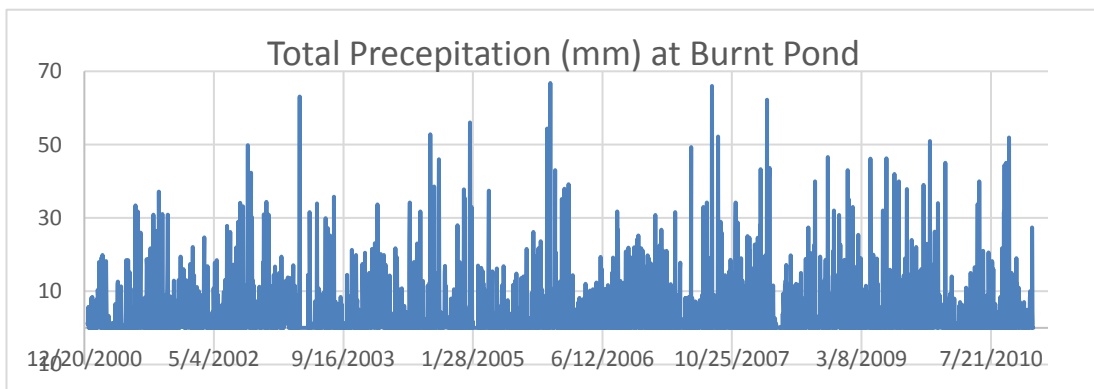
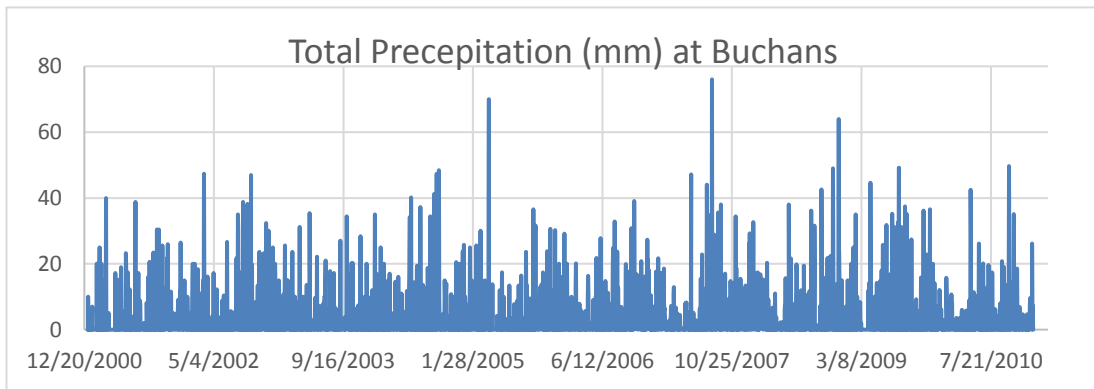
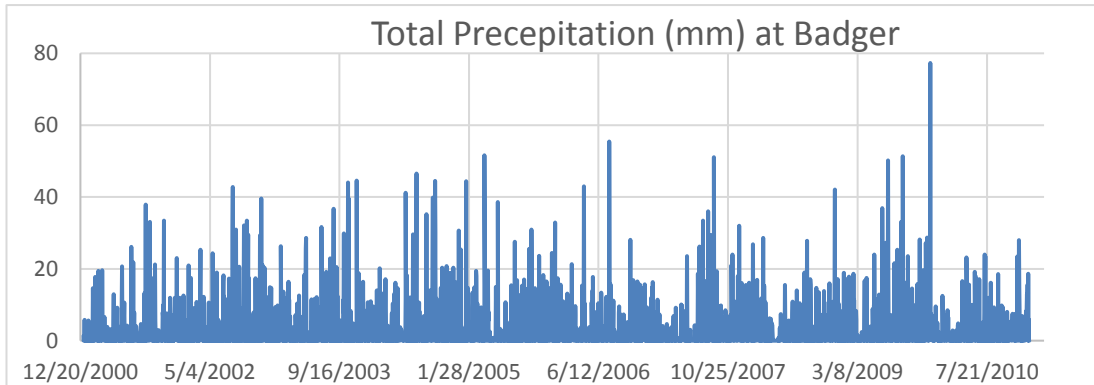


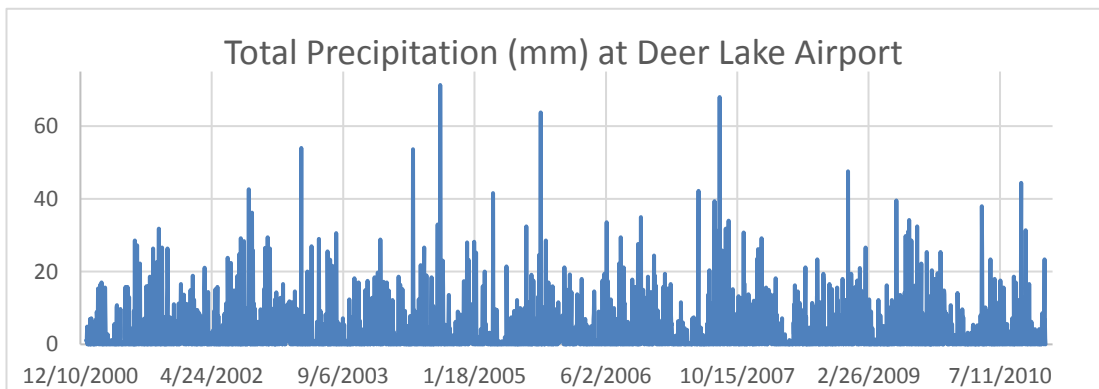
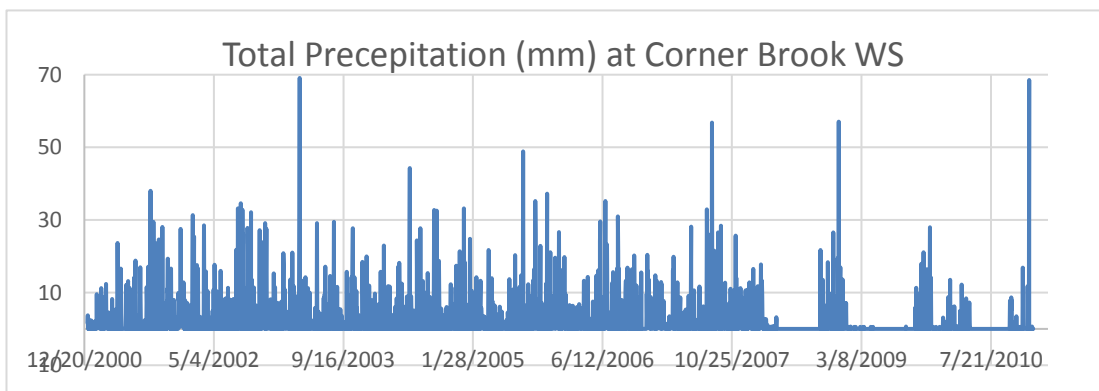
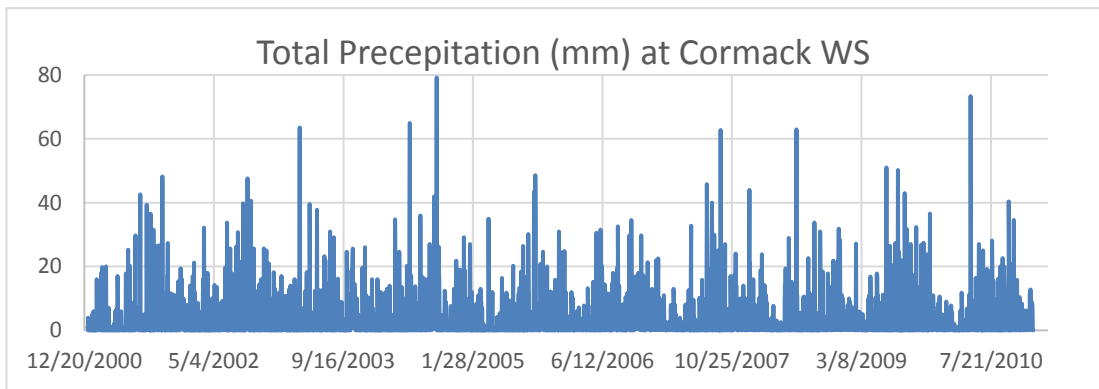


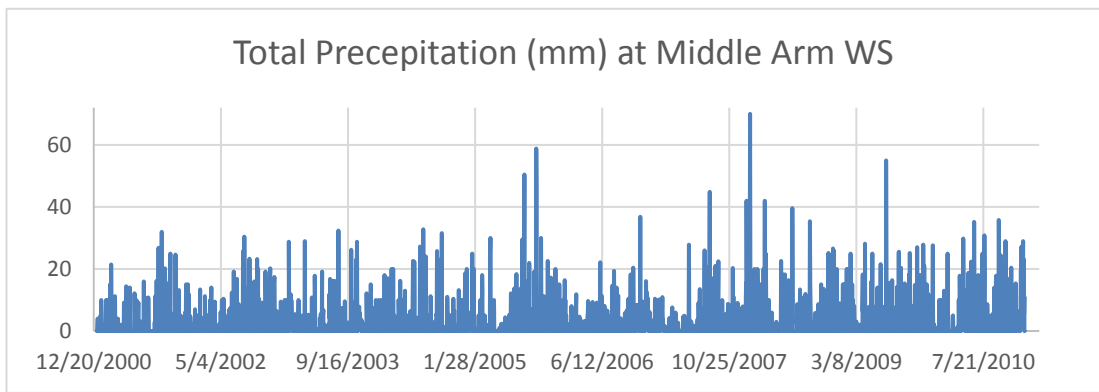
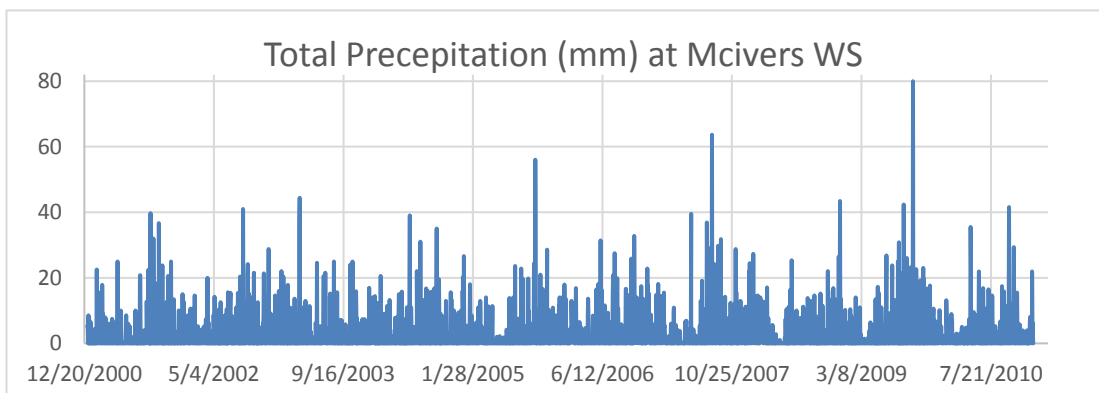
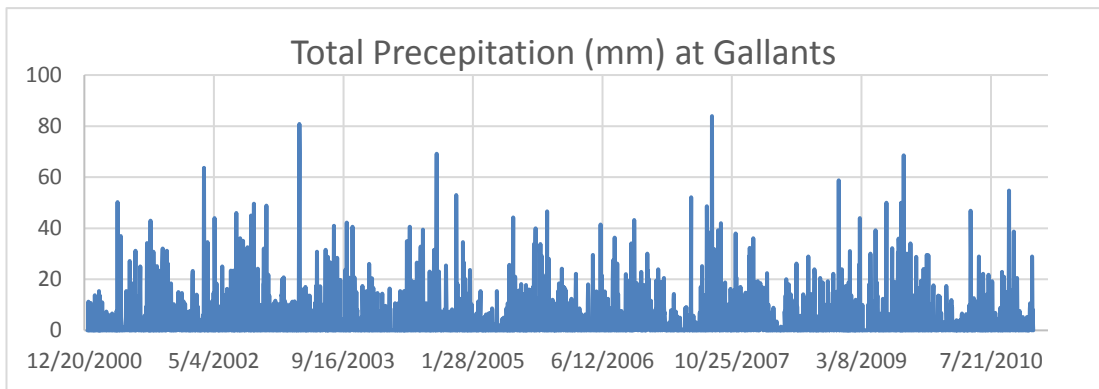


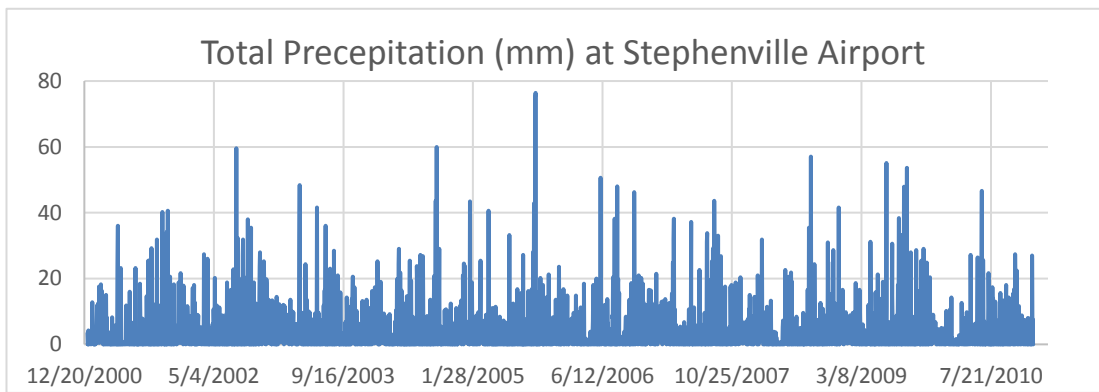
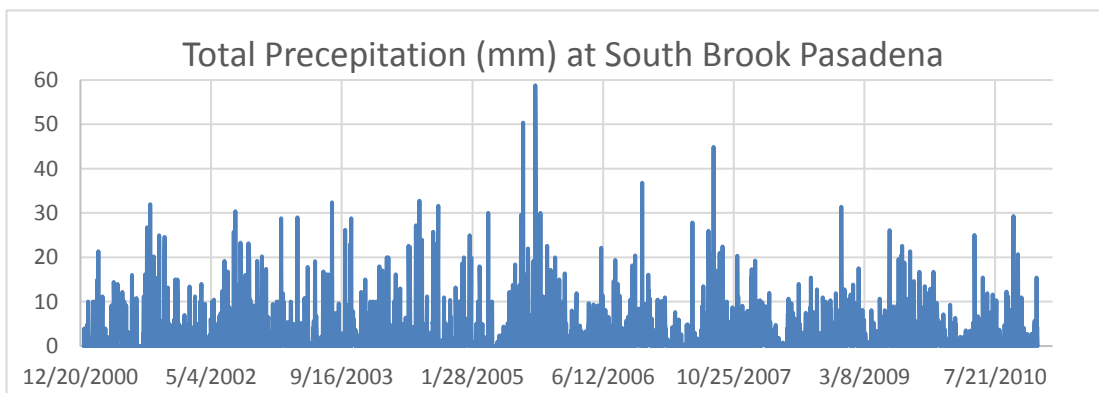
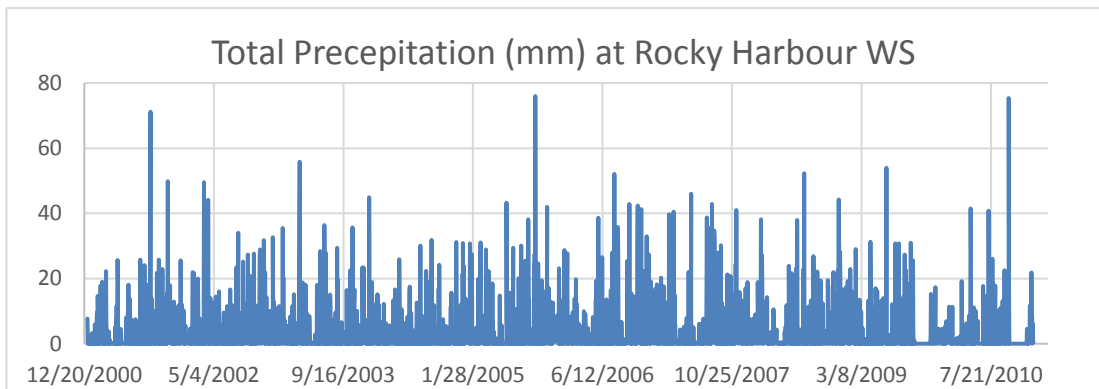


The Continuous daily records of Precipitation are shown below,

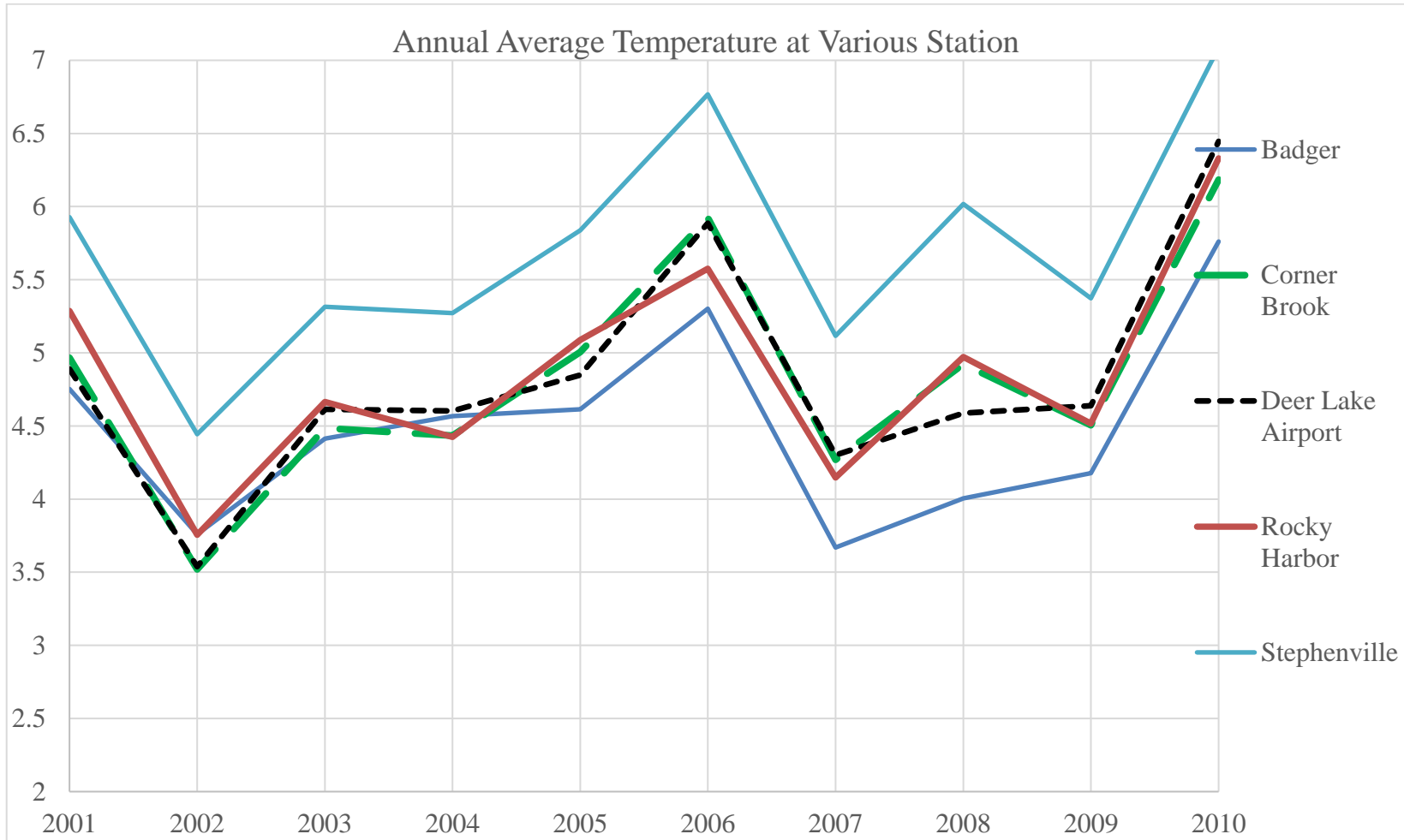


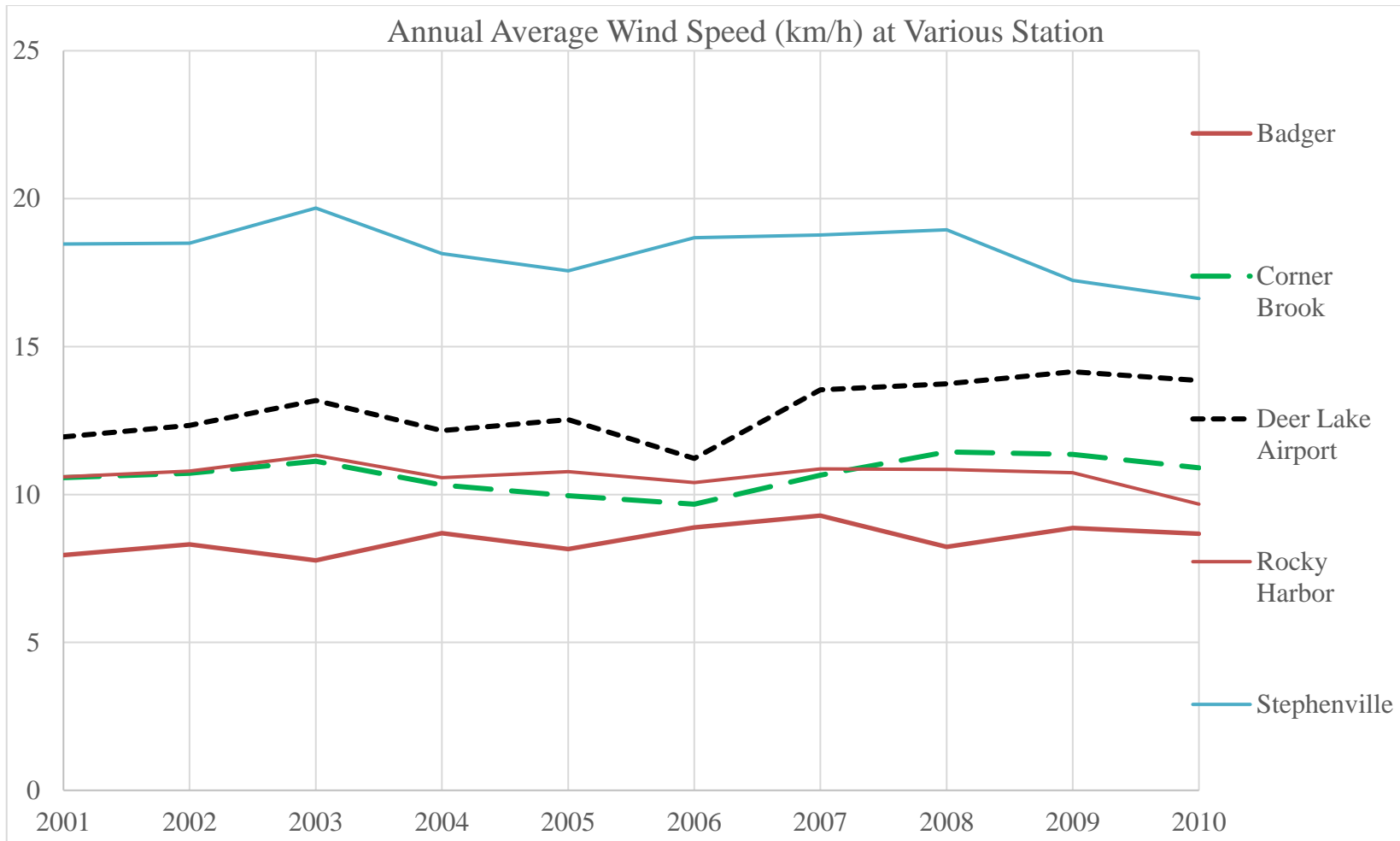


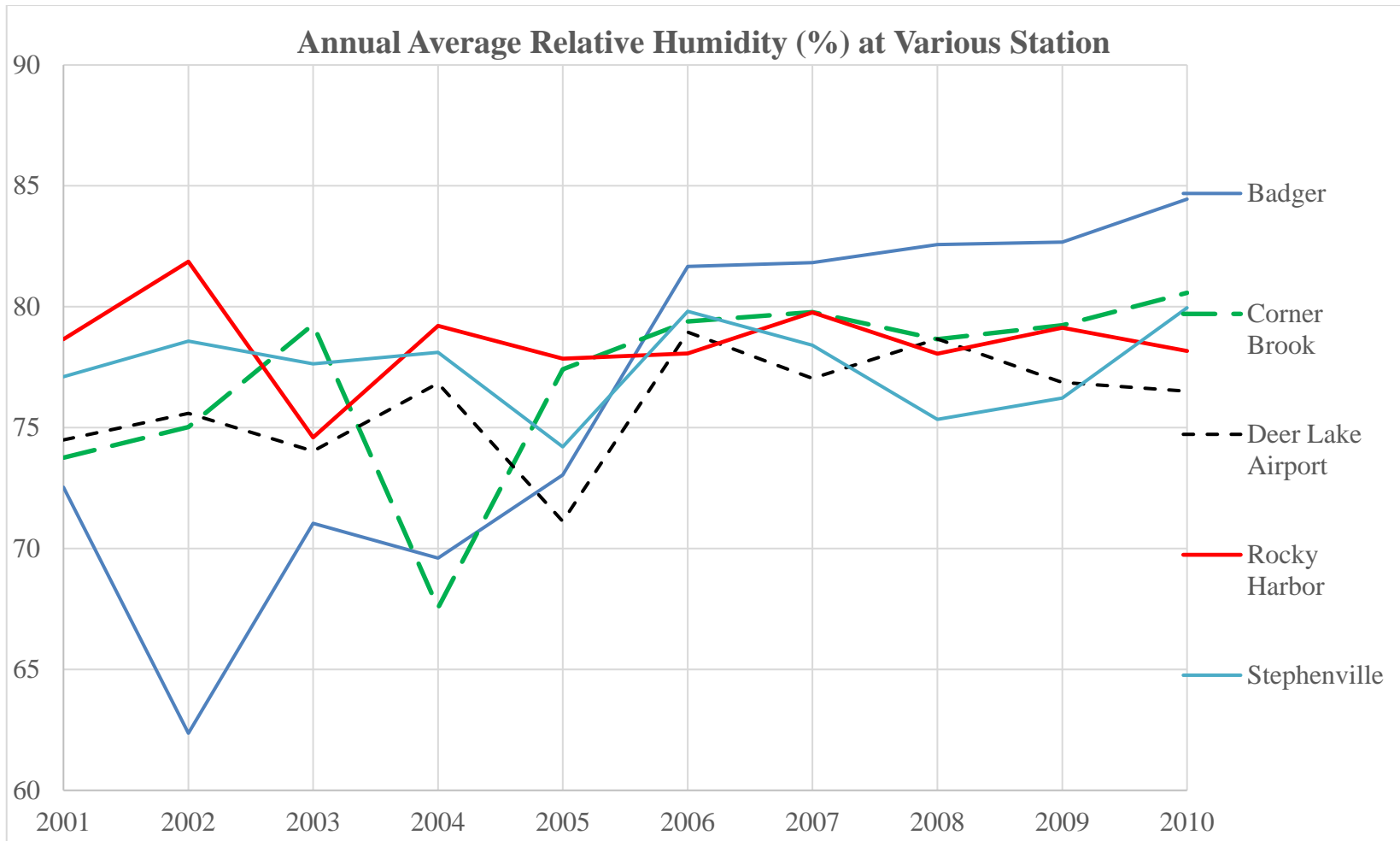


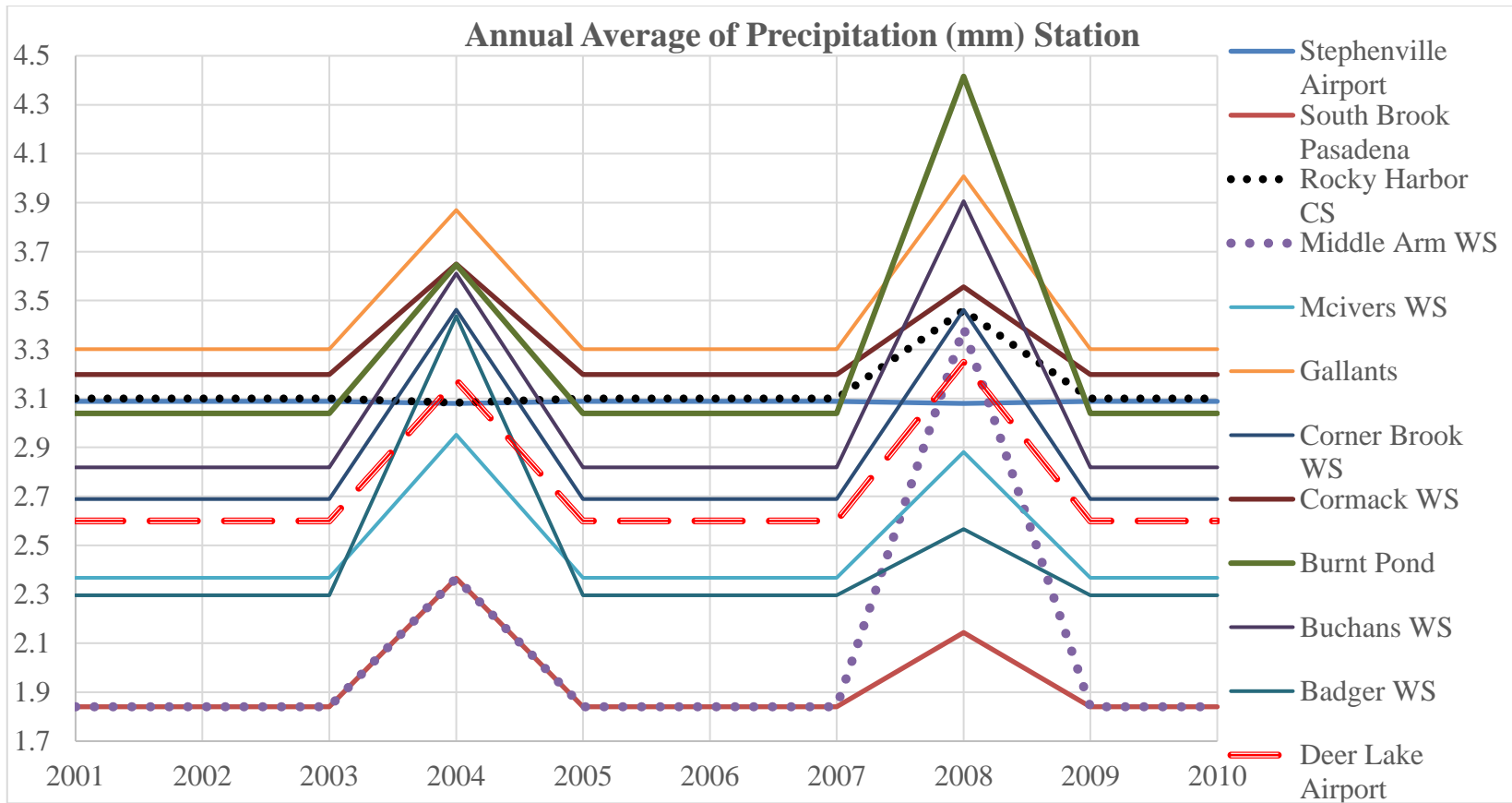


Appendix D Annual Averages of Meteorological Observation Stations



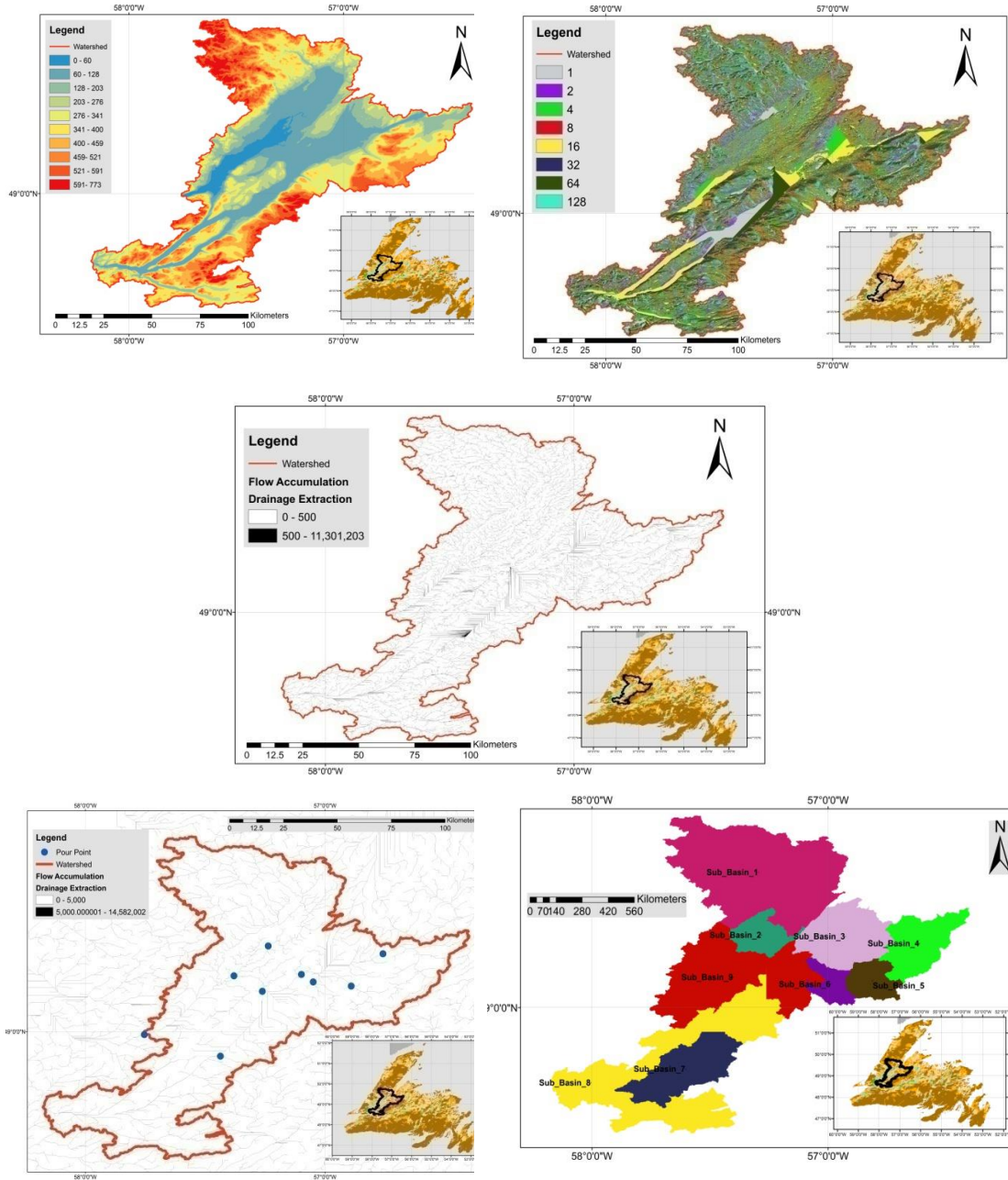






Appendix E Watershed Delineation

Watershed Delineation methodology: DEM, Flow Direction, Flow Accumulation, Accumulated Flow, Pour Point Selection, and Watershed Delineation to generate sub-basin



Appendix F Area of Hydrological Response Unit and Sub-basins Structure and Parameterization

Table F. 1 HRU areas for the sub-basin 1

| HRU | Area (Km²) | (%) |
|---------------------|------------------------------|------------|
| Cropland | 0.83 | 0.04 |
| Forest | 1494.16 | 80.02 |
| Forest Wetland | 79.33 | 4.25 |
| Grassland Unmanaged | 6.65 | 0.36 |
| Other land | 13.96 | 0.75 |
| Roads | 6.14 | 0.33 |
| Settlement | 2.00 | 0.11 |
| Treed Wetland | 16.77 | 0.90 |
| Trees | 2.61 | 0.14 |
| Water | 140.89 | 7.55 |
| Wetland | 4.52 | 0.24 |
| Wetland Herb | 11.52 | 0.62 |
| Wetland Shrub | 87.94 | 4.71 |

Table F. 2 HRU areas for the sub-basin 2.

| HRU | Area (Km²) | (%) |
|---------------------|------------------------------|------------|
| Cropland | 17.65 | 6.86 |
| Forest | 162.99 | 63.34 |
| Forest Wetland | 36.24 | 14.08 |
| Grassland Unmanaged | 0.00 | 0.00 |
| Other land | 0.23 | 0.09 |
| Roads | 1.52 | 0.59 |
| Settlement | 0.36 | 0.14 |
| Treed Wetland | 3.14 | 1.22 |
| Trees | 0.32 | 0.12 |
| Water | 7.09 | 2.76 |
| Wetland | 3.45 | 1.34 |
| Wetland Herb | 1.56 | 0.61 |
| Wetland Shrub | 22.77 | 8.85 |

Table F. 3 HRU areas for the sub-basin 3

| HRU | Area (Km²) | (%) |
|---------------------|------------------------------|------------|
| Forest | 426.94 | 66.92 |
| Forest Wetland | 30.47 | 4.78 |
| Grassland Unmanaged | 0.70 | 0.11 |
| Other land | 5.51 | 0.86 |
| Roads | 3.43 | 0.54 |
| Settlement | 3.55 | 0.56 |
| Treed Wetland | 4.93 | 0.77 |
| Trees | 0.84 | 0.13 |
| Water | 129.29 | 20.27 |
| Wetland | 2.08 | 0.33 |
| Wetland Herb | 2.42 | 0.38 |
| Wetland Shrub | 27.81 | 4.36 |

Table F. 4 HRU areas for the sub-basin 4

| HRU | Area (Km²) | (%) |
|---------------------|------------------------------|------------|
| Forest | 281.05 | 57.41 |
| Forest Wetland | 3.99 | 0.82 |
| Grassland Unmanaged | 6.20 | 1.27 |
| Other land | 21.55 | 4.40 |
| Roads | 1.94 | 0.40 |
| Settlement | 1.22 | 0.25 |
| Treed Wetland | 5.48 | 1.12 |
| Trees | 5.67 | 1.16 |
| Water | 60.78 | 12.41 |
| Wetland | 22.06 | 4.51 |
| Wetland Herb | 7.55 | 1.54 |
| Wetland Shrub | 72.05 | 14.72 |

Table F. 5 HRU areas for the sub-basin 5

| HRU | Area (Km²) | (%) |
|---------------------|------------------------------|------------|
| Forest | 150.81 | 63.49 |
| Forest Wetland | 2.27 | 0.95 |
| Grassland Unmanaged | 7.98 | 3.36 |
| Other land | 8.52 | 3.59 |
| Settlement | 0.58 | 0.24 |
| Treed Wetland | 3.39 | 1.43 |
| Trees | 2.18 | 0.92 |

| HRU | Area (Km²) | (%) |
|---------------|------------------------------|------------|
| Water | 16.25 | 6.84 |
| Wetland | 5.02 | 2.11 |
| Wetland Herb | 3.56 | 1.50 |
| Wetland Shrub | 36.99 | 15.57 |

Table F. 6 HRU areas for the sub-basin 6

| HRU | Area (Km²) | (%) |
|---------------------|------------------------------|------------|
| Forest | 90.77 | 50.19 |
| Forest Wetland | 3.93 | 2.18 |
| Grassland Unmanaged | 5.55 | 3.07 |
| Other land | 5.36 | 2.96 |
| Roads | 0.08 | 0.05 |
| Settlement | 0.61 | 0.34 |
| Treed Wetland | 3.71 | 2.05 |
| Trees | 2.14 | 1.18 |
| Water | 35.70 | 19.74 |
| Wetland | 4.08 | 2.26 |
| Wetland Herb | 2.49 | 1.38 |
| Wetland Shrub | 26.43 | 14.62 |

Table F. 7 HRU areas for the sub-basin 7

| HRU | Area (Km²) | (%) |
|---------------------|------------------------------|------------|
| Forest | 456.89 | 73.74 |
| Forest Wetland | 36.30 | 5.86 |
| Grassland Unmanaged | 2.50 | 0.40 |
| Other land | 3.64 | 0.59 |
| Settlement | 0.42 | 0.07 |
| Treed Wetland | 4.91 | 0.79 |
| Trees | 1.03 | 0.17 |
| Water | 82.84 | 13.37 |
| Wetland | 0.97 | 0.16 |
| Wetland Herb | 2.33 | 0.38 |
| Wetland Shrub | 27.75 | 4.48 |

Table F. 8 HRU areas for the sub-basin 8

| HRU | Area (Km²) | (%) |
|------------|------------------------------|------------|
| Cropland | 0.13 | 0.01 |
| Forest | 1070.58 | 54.98 |

| HRU | Area (Km²) | (%) |
|---------------------|------------------------------|------------|
| Forest Wetland | 31.93 | 1.64 |
| Grassland Unmanaged | 426.47 | 21.90 |
| Other land | 22.36 | 1.15 |
| Roads | 4.19 | 0.22 |
| Settlement | 0.85 | 0.04 |
| Treed Wetland | 10.73 | 0.55 |
| Trees | 3.02 | 0.16 |
| Water | 304.19 | 15.62 |
| Wetland | 2.91 | 0.15 |
| Wetland Herb | 8.09 | 0.42 |
| Wetland Shrub | 61.94 | 3.18 |

Table F. 9 HRU areas for the sub-basin 9

| HRU | Area (Km²) | (%) |
|---------------------|------------------------------|------------|
| Cropland | 17.13 | 1.37 |
| Forest | 848.98 | 68.11 |
| Forest Wetland | 39.98 | 3.21 |
| Grassland Unmanaged | 0.31 | 0.03 |
| Other land | 10.20 | 0.82 |
| Roads | 13.48 | 1.08 |
| Settlement | 17.50 | 1.40 |
| Treed Wetland | 11.15 | 0.89 |
| Trees | 1.78 | 0.14 |
| Water | 216.50 | 17.37 |
| Wetland | 6.02 | 0.48 |
| Wetland Herb | 3.97 | 0.32 |
| Wetland Shrub | 59.42 | 4.77 |

Table F. 10 HRU elevation, aspect and slope for the sub-basin 1

| HRU | Aspect (°) | Slope (°) | Elevation (m) |
|---------------------|-------------------|------------------|----------------------|
| Cropland | 240 | 6 | 100 |
| Forest | 170 | 8 | 220 |
| Forest Wetland | 112 | 4 | 130 |
| Grassland Unmanaged | 112 | 10 | 140 |
| Other land | 112 | 6 | 200 |
| Roads | 112 | 10 | 200 |
| Settlement | 240 | 10 | 200 |
| Treed Wetland | 200 | 4 | 200 |
| Trees | 180 | 6 | 200 |

| HRU | Aspect (°) | Slope (°) | Elevation (m) |
|---------------|-------------------|------------------|----------------------|
| Water | 56 | 3 | 124 |
| Wetland | 112 | 6 | 140 |
| Wetland Herb | 112 | 6 | 140 |
| Wetland Shrub | 112 | 10 | 140 |

Table F. 11 HRU elevation, aspect and slope for the sub-basin 2

| HRU | Aspect (°) | Slope (°) | Elevation (m) |
|---------------------|-------------------|------------------|----------------------|
| Cropland | 200 | 4 | 100 |
| Forest | 250 | 6 | 60 |
| Forest Wetland | 220 | 5 | 70 |
| Grassland Unmanaged | 200 | 4 | 126 |
| Other land | 200 | 4 | 50 |
| Roads | 200 | 4 | 80 |
| Settlement | 200 | 4 | 200 |
| Treed Wetland | 200 | 4 | 60 |
| Trees | 200 | 4 | 70 |
| Water | 60 | 6 | 30 |
| Wetland | 160 | 4 | 60 |
| Wetland Herb | 180 | 4 | 50 |
| Wetland Shrub | 200 | 4 | 60 |

Table F. 12 HRU elevation, aspect and slope for the sub-basin 3

| HRU | Aspect (°) | Slope (°) | Elevation (m) |
|---------------------|-------------------|------------------|----------------------|
| Forest | 250 | 10 | 200 |
| Forest Wetland | 180 | 4 | 140 |
| Grassland Unmanaged | 200 | 6 | 150 |
| Other land | 200 | 10 | 100 |
| Roads | 200 | 8 | 160 |
| Settlement | 250 | 10 | 200 |
| Treed Wetland | 200 | 6 | 130 |
| Trees | 220 | 10 | 120 |
| Water | 60 | 4 | 100 |
| Wetland | 180 | 4 | 120 |
| Wetland Herb | 160 | 4 | 140 |
| Wetland Shrub | 180 | 5 | 120 |

Table F. 13 HRU elevation, aspect and slope for the sub-basin 4

| HRU | Aspect (°) | Slope (°) | Elevation (m) |
|---------------------|-------------------|------------------|----------------------|
| Forest | 180 | 10 | 200 |
| Forest Wetland | 140 | 4 | 200 |
| Grassland Unmanaged | 220 | 4 | 200 |
| Other land | 200 | 8 | 200 |
| Roads | 220 | 6 | 180 |
| Settlement | 300 | 8 | 180 |
| Treed Wetland | 220 | 6 | 200 |
| Trees | 180 | 8 | 200 |
| Water | 60 | 4 | 200 |
| Wetland | 180 | 5 | 180 |
| Wetland Herb | 180 | 6 | 180 |
| Wetland Shrub | 200 | 7 | 180 |

Table F. 14 HRU elevation, aspect and slope for the sub-basin 5

| HRU | Aspect (°) | Slope (°) | Elevation (m) |
|---------------------|-------------------|------------------|----------------------|
| Forest | 220 | 9 | 200 |
| Forest Wetland | 200 | 4 | 200 |
| Grassland Unmanaged | 220 | 4 | 200 |
| Other land | 160 | 6 | 200 |
| Settlement | 160 | 10 | 200 |
| Treed Wetland | 180 | 6 | 200 |
| Trees | 200 | 7 | 200 |
| Water | 60 | 4 | 200 |
| Wetland | 200 | 4 | 200 |
| Wetland Herb | 180 | 4 | 200 |
| Wetland Shrub | 160 | 5 | 200 |

Table F. 15 HRU elevation, aspect and slope for the sub-basin 6

| HRU | Aspect (°) | Slope (°) | Elevation (m) |
|---------------------|-------------------|------------------|----------------------|
| Forest | 260 | 9 | 190 |
| Forest Wetland | 200 | 4 | 150 |
| Grassland Unmanaged | 240 | 6 | 190 |
| Other land | 240 | 8 | 190 |
| Roads | 180 | 4 | 100 |
| Settlement | 250 | 4 | 220 |
| Treed Wetland | 220 | 4 | 190 |
| Trees | 180 | 4 | 200 |
| Water | 60 | 4 | 180 |
| Wetland | 160 | 4 | 180 |

| HRU | Aspect (°) | Slope (°) | Elevation (m) |
|---------------|-------------------|------------------|----------------------|
| Wetland Herb | 180 | 4 | 200 |
| Wetland Shrub | 180 | 5 | 200 |

Table F. 16 HRU elevation, aspect and slope for the sub-basin 7

| HRU | Aspect (°) | Slope (°) | Elevation (m) |
|---------------------|-------------------|------------------|----------------------|
| Forest | 240 | 10 | 200 |
| Forest Wetland | 200 | 8 | 190 |
| Grassland Unmanaged | 150 | 6 | 190 |
| Other land | 200 | 6 | 190 |
| Settlement | 220 | 5 | 200 |
| Treed Wetland | 180 | 4 | 200 |
| Trees | 200 | 4 | 210 |
| Water | 50 | 4 | 50 |
| Wetland | 180 | 5 | 180 |
| Wetland Herb | 180 | 4 | 180 |
| Wetland Shrub | 180 | 4 | 180 |

Table F. 17 HRU elevation, aspect and slope for the sub-basin 8

| HRU | Aspect (°) | Slope (°) | Elevation (m) |
|---------------------|-------------------|------------------|----------------------|
| Cropland | 60 | 7 | 200 |
| Forest | 160 | 10 | 200 |
| Forest Wetland | 140 | 7 | 190 |
| Grassland Unmanaged | 120 | 4 | 190 |
| Other land | 160 | 7 | 190 |
| Roads | 200 | 10 | 200 |
| Settlement | 140 | 12 | 200 |
| Treed Wetland | 200 | 6 | 200 |
| Trees | 160 | 9 | 200 |
| Water | 60 | 4 | 90 |
| Wetland | 120 | 8 | 180 |
| Wetland Herb | 140 | 5 | 180 |
| Wetland Shrub | 120 | 6 | 180 |

Table F. 18 HRU elevation, aspect and slope for the sub-basin 9

| HRU | Aspect (°) | Slope (°) | Elevation (m) |
|----------------|-------------------|------------------|----------------------|
| Cropland | 120 | 4 | 60 |
| Forest | 180 | 10 | 120 |
| Forest Wetland | 120 | 4 | 120 |

| HRU | Aspect (°) | Slope (°) | Elevation (m) |
|---------------------|-------------------|------------------|----------------------|
| Grassland Unmanaged | 220 | 7 | 40 |
| Other land | 180 | 7 | 120 |
| Roads | 240 | 8 | 140 |
| Settlement | 240 | 5 | 60 |
| Treed Wetland | 220 | 5 | 120 |
| Trees | 220 | 5 | 80 |
| Water | 60 | 4 | 70 |
| Wetland | 200 | 4 | 70 |
| Wetland Herb | 200 | 4 | 80 |
| Wetland Shrub | 220 | 4 | 100 |

Table F. 19 Blowing snow module parameters in the Humber River Basin (HRB) (Pomeroy et. al., 2013)

| HRU | Fetch Distance (m) | Vegetation Height (m) | Stalk Diameter (m) | Stalk Density (#/m²) | Distribution Factor (dimensionless) |
|---------------------|---------------------------|------------------------------|---------------------------|--|--|
| Cropland | 1000 | 0.15 | 0.003 | 150 | 1 |
| Forest | 300 | 15 | 0.6 | 1.5 | 5 |
| Forest Wetland | 300 | 15 | 0.6 | 1.5 | 5 |
| Grassland Unmanaged | 1000 | 0.7 | 0.003 | 150 | 2 |
| Other land | 300 | 0.001 | 0.003 | 1 | 1 |
| Roads | 300 | 0.001 | 0.003 | 1 | 1 |
| Settlement | 300 | 0.001 | 0.003 | 1 | 1 |
| Treed Wetland | 300 | 15 | 0.6 | 1.5 | 5 |
| Trees | 300 | 15 | 0.6 | 1.5 | 5 |
| Water | 300 | 0.001 | 0.003 | 1 | 5 |
| Wetland | 300 | 1.5 | 0.05 | 50 | 5 |
| Wetland Herb | 300 | 1.5 | 0.05 | 50 | 5 |
| Wetland Shrub | 300 | 1.5 | 0.05 | 50 | 5 |

Table F. 20 Albedo and canopy parameters in the Humber River Basin (HRB) (Pomeroy et. al., 2013)

| HRU | Albedo Parameter | | | Canopy Parameter |
|------------------------|---------------------------------------|--------------------------------|--|---|
| | Albedo Bare Ground (dimensionless) | Albedo Snow (dimensionless) | Leaf Area Index (LAI) (dimensionless) | Canopy Snow Interception Capacity (kg/m ²) |
| Cropland | 0.180 | 0.85 | 0.1 | 0 |
| Forest | 0.145 | 0.85 | 0.54 | 6.3 |
| Forest Wetland | 0.145 | 0.85 | 0.54 | 6.3 |
| Grassland Unmanaged | 0.170 | 0.85 | 0.1 | 0 |
| Other land | 0.152 | 0.85 | 0.1 | 0 |
| Roads | 0.152 | 0.85 | 0.1 | 0 |
| Settlement | 0.152 | 0.85 | 0.1 | 0 |
| Treed Wetland | 0.110 | 0.85 | 0.54 | 0 |
| Trees | 0.145 | 0.85 | 0.54 | 6.3 |
| Water | 0.000 | 0.85 | 0.1 | 0 |
| Wetland | 0.110 | 0.85 | 0.1 | 0 |
| Wetland Herb | 0.110 | 0.85 | 0.1 | 0 |
| Wetland Shrub | 0.110 | 0.85 | 0.1 | 0 |

Table F. 21 Soil parameters in the Humber River Basin (HRB). K_{s_gw} , K_{s_Upper} and K_{s_lower} are the saturated hydraulic conductivity in the groundwater, upper and lower of soil layers, respectively. λ is the pore size distribution index. $Soil_{rechr_max}$, $Soil_{moist_max}$ and gw_{max} are the water storage capacity for the recharge, soil of both recharge and lower and groundwater layers, respectively. Sd_{max} is the depressional storage capacity. (Pomeroy et. al., 2013)

| HRU | Saturated hydraulic conductivity in groundwater K_{s_gw} (m/s) | Saturated hydraulic conductivity in upper soil layer K_{s_Upper} (m/s) | Saturated hydraulic conductivity in lower soil layer K_{s_lower} (m/s) | Pore size distribution index λ (dimensionless) | Water storage capacity recharge, $Soil_{rechr_max}$ (mm) | Water storage capacity soil of both recharge and lower $Soil_{moist_max}$ (mm) | Water storage capacity groundwater layers gw_{max} (mm) | Sd_{max} (m) |
|---------------------|---|---|---|--|---|---|---|----------------|
| Cropland | 1.28×10^{-6} to 6.95×10^{-6} | 1.28×10^{-6} to 6.95×10^{-6} | 1.28×10^{-6} to 6.95×10^{-6} | 0.088 to 0.186 | 98 to 135 | 380 to 578 | 500 | 67 |
| Forest | 3.4×10^{-6} | 2.5×10^{-4} | 3.4×10^{-6} | 0.096 | 90 to 97 | 397 to 695 | 500 | 86 |
| Forest Wetland | 3.4×10^{-6} | 2.5×10^{-4} | 3.4×10^{-6} | 0.096 | N/A | N/A | 500 | 86 |
| Grassland Unmanaged | 1.28×10^{-6} | 1.28×10^{-6} | 1.28×10^{-6} | 0.088 | 117 to 135 | 397 to 578 | 500 | 97 |
| Other land | 1.28×10^{-6} | 1.28×10^{-6} | 1.28×10^{-6} | 0.088 | 10 | 20 | 500 | 0 |
| Roads | 1.28×10^{-6} | 1.28×10^{-6} | 1.28×10^{-6} | 0.088 | 10 | 20 | 500 | 0 |
| Settlement | 1.28×10^{-6} | 1.28×10^{-6} | 1.28×10^{-6} | 0.088 | 10 | 20 | 500 | 0 |
| Treed Wetland | 1.28×10^{-6} | 2.5×10^{-4} | 3.4×10^{-6} | 0.096 | N/A | N/A | 500 | 86 |
| Trees | 3.4×10^{-6} | 2.5×10^{-4} | 3.4×10^{-6} | 0.096 | 117 to 135 | 397 to 695 | 500 | 86 |
| Water | 1.28×10^{-6} | 1.28×10^{-6} | 1.28×10^{-6} | 0.088 | N/A | N/A | 500 | 500 |

| HRU | Saturated hydraulic conductivity in groundwater K_{s_gw} (m/s) | Saturated hydraulic conductivity in upper soil layer K_{s_Upper}(m/s) | Saturated hydraulic conductivity in lower soil layer K_{s_lower} (m/s) | Pore size distribution index λ (dimensionless) | Water storage capacity recharge, $Soil_{rechr_max}$(mm) | Water storage capacity soil of both recharge and lower $Soil_{moist_max}$(mm) | Water storage capacity groundwater layers g_{wmax} (mm) | S_{dmax}(m) |
|---------------|---|--|---|--|--|--|---|---------------------------------|
| Wetland | 1.28×10^{-6} | 1.28×10^{-6} | 1.28×10^{-6} | 0.088 | N/A | N/A | 500 | 500 |
| Wetland Herb | 1.28×10^{-6} | 2.5×10^{-4} | 3.4×10^{-6} | 0.088 | N/A | N/A | 500 | 500 |
| Wetland Shrub | 1.28×10^{-6} | 2.5×10^{-4} | 3.4×10^{-6} | 0.088 | N/A | N/A | 500 | 500 |

Appendix G CRHM Hydrological Module for Humber River Basin

To simulate the dominant hydrological processes for the watershed, a set of physically-based modules were constructed based on the modellers experience in western Canada. The modules were developed to predict, forecast, and simulate the hydrological cycle of the region in a physically-based manner. Figure 4.7 shows the schematic setup of these modules, which will be discussed in the following sections (Pomeroy et al., 2013; Fang et. al., 2010).

Basin module

The basin module sets the basin and HRU physical, the soil, and land cover characteristics such as the basin name, the HRU name, area, latitude, elevation, aspect, slope etc.

Observation module

The observation module set up the meteorological observations from the point of collection. The corrected air temperature, the relative humidity, the amount and phase of precipitation for elevation, as well as the correction of shortwave and longwave irradiance for topography were included in the module. It also reads the meteorological data (temperature, wind speed, relative humidity, vapour pressure, precipitation, and radiation) which is used to operate CRHM, adjust the temperature in response to the environmental lapse rate and precipitation with elevation and wind-induced under catch, and provide these inputs to other modules.

Radiation module

Theoretical global radiation, direct and diffuse solar radiation, as well as maximum sunshine hours were estimated by using the Radiation module based on latitude, elevation, ground slope, and azimuth. The model also provides radiation inputs to the sunshine hour module, the energy-budget snowmelt module, and the net all-wave radiation module. The Annandale model incorporates the effects of altitude on transmittance for mountain applications shown in Equation (Garnier and Ohmura, 1970).

$$\tau_D = K_{RS}(1 + 2.7 \times 10^{-5} Alt \Delta T^{0.5}) \quad (E.1)$$

where k_{RS} = adjustment coefficient, 0.16 for interior locations, 0.19 for coastal regions, and Alt = site altitude (m).

Solar radiation, Q_{si} is directly estimated by using theoretical components to predict the Sun's position relative to a given location and empirical relationships (which estimate the effects of the Earth's atmosphere). Q_{si} can be expressed as the sum of direct beam (Q_{dr}) and diffuse sky (Q_{df}) radiation as,

$$Q_{si} = Q_{dr} + Q_{df} \quad (E.2)$$

For the prairies, the daily, clear-sky diffuse shortwave radiation (Q_{dfOD}) in MJ/ (m² day) can be estimated from the relationship (Granger & Gray)

$$Q_{dfOD} = \frac{3.5(\frac{P}{P_o}) \cos(X^{\wedge}S)}{p} + 0.45 \sin\left(\frac{(172-d)2\pi}{365}\right) \quad (E.3)$$

Sunshine hour module

The maximum sunshine hours values represent the generating inputs to the energy-balance snowmelt module and the net all-wave radiation module. Sunshine hours were estimated from incoming short-wave radiation.

Short-wave radiation module

The short-wave radiation module estimates the incident short-wave incoming solar radiation, using temperature, and adjusts the incident short-wave to a slope. The measured incoming short-wave radiation, from the observation module, and the calculated direct and diffuse solar radiation, from the radiation module, were used to calculate the ratio for adjusting the short-wave radiation on the slope (Annandale *et al.*, 2002).

In CRHM, net shortwave radiation to forest snow ($K * _f$) is equal to the above-canopy irradiance ($K \downarrow$) transmitted through the canopy less the amount reflected from snow, which is expressed as

$$K * _f = K \downarrow \tau (1 - \alpha_s) \quad (\text{E.4})$$

where α_s is the snow surface albedo, the decay is a function of time to a snowfall event, and τ is the forest shortwave transmittance (Pomeroy *et al.*, 2009).

$$\tau = e^{-\frac{1.081\theta \cos(\theta)LAI'}{\sin(\theta)}} \quad (\text{E.5})$$

where θ (radians) is the solar angle above the horizon.

Long-wave radiation module

The module estimates incoming long-wave radiation by using short-wave radiation. This is an input of energy-balance snowmelt module (Sicart et al., 2006). Thermal emissions from the canopy are related to the longwave irradiance to forest snow ($L \downarrow_f$). Simulation of ($L \downarrow_f$) is made as the sum of sky and forest longwave emissions weighted by the sky view factor (v), i.e.

$$L \downarrow_f = vL \downarrow + (1 - v)\varepsilon_f\sigma T_f^4 \quad (\text{E.6})$$

where ε_f is the forest thermal emissivity, σ is the Stefan-Boltzmann constant ($\text{Wm}^{-2}\text{K}^{-4}$), and T_f is the forest temperature (K). Longwave emittance from snow ($L \uparrow$) is determined by

$$L \uparrow = \varepsilon_s\sigma T_s^4 \quad (\text{E.7})$$

where ε_s is the thermal emissivity of snow, and T_s is the snow surface temperature (K) which is resolved using the longwave psychrometric formulation by Pomeroy and Essery (2010)

$$T_s = T_a + \frac{\varepsilon_s(L \downarrow - \sigma T_a^4) + \lambda_s(\omega_a - \omega_s)\rho_a/r_a}{4\varepsilon_s\sigma T_a^3 + (c_p + \lambda_s\Delta)\rho_a/r_a} \quad (\text{E.8})$$

where ω_a and ω_s are the specific and the saturation mixing ratios, ρ_a is the air density (kgm^{-3}), c_p is the specific heat capacity of air ($\text{J kg}^{-1}\text{K}^{-1}$), λ_s is the latent heat of sublimation (MJ kg^{-1}), r_a is the aerodynamic resistance (sm^{-1}), and Δ is the slope of the saturation vapour pressure curve (KPaK^{-1}).

All-wave radiation module

There was another module which calculates the net all-wave radiation from short-wave radiation for input to the evaporation module for snow-free conditions (Granger and Gray, 1990).

Albedo module

Snow albedo was estimated throughout the winter by the albedo module into the melt period, indicating the beginning of melt for the energy-balance snowmelt module (Gray and Landine, 1987). During continuous melt, the shape of the albedo-depletion curve is 'S'-shaped and the period of rapid decrease in albedo is preceded and followed by one or two days when the rate of change is slower. The decrease during rapid, continuous melt is approximated by the equation,

$$A(t) = A_i - 0.07t \quad (\text{E.9})$$

where $A(t)$ is the albedo after 't'-days of continuous depletion and A_i is the albedo of the snow surface at the start of 'active' melt. The period of ablation of shallow arctic and prairie snow covers, under continuous melting, often spans only 4 to 7 seven days. Therefore, slope corrections have been applied to incoming direct and diffuse shortwave radiation and albedo has been calculated, during which the melt period Q_n is calculated as a linear function of the daily net short-wave radiation, Q_0 the albedo, and the sunshine ratio by the expression,

$$Q_n = -0.53 + 0.47Q_0 \left(0.52 + 0.52 \left(\frac{n}{N} \right) \right) (1 - A(t)) \quad (\text{E.10})$$

Equation (4.10) has a correlation coefficient of 0.87 and a standard error of estimate of $1.55 \text{ MJ m}^{-2} \text{ d}^{-1}$. The ratio $\frac{n}{N}$ is that of the actual hours to potential hours of bright sunshine. CRHM has an algorithm to estimate $\frac{n}{N}$ from observed incoming shortwave radiation, as ‘sunshine hours’ have not been recorded in meteorological records (Gray and Landine, 1988).

Canopy module

The snowfall and rainfall intercepted by the forest canopy were calculated by the canopy module. Additionally, the snowfall and rainfall interception were calculated through under-canopy snowfall and rainfall and calculates short-wave and long-wave sub-canopy radiation. This module has options for open environments (no canopy adjustment of snow mass and energy), small forest clearing environments (adjustment of snow mass and energy based on diameter of the clearing and surrounding forest height), and forest environments (adjustment of snow mass and energy from forest canopy) (Ellis et al., 2010).

Various physical factors, including tree species, forest density, and the antecedent intercepted snowload ($I_{s,o}$) (kgm^{-2}) were related to the amount of snowfall intercepted. In CRHM, a dynamic canopy snow-balance is calculated, in which the amount of snow interception (I_s) is calculated by

$$I_s = (I_s^* - I_{s,o}) \left(1 - e^{-\frac{C_l \rho_s t}{I_s^*}}\right) \quad (\text{E.11})$$

where C_l is the “canopy-leaf contact area” per unit ground, and I_s^* is the species-specific maximum intercepted snowload (kgm^{-2}), which is determined as a function of the mean

and maximum snowload per unit area of branch, S (kgm^{-2}), the density of falling snow, ρ_s (kgm^{-3}), and LAI' by

$$I_s^* = \bar{S} \left(0.27 + \frac{46}{\rho_s} \right) LAI' \quad (\text{E.12})$$

The sublimation of intercepted snow is estimated by the sublimation rate coefficient for intercepted snow, V_i (s^{-1}), is multiplied by the intercepted snowload to give the canopy sublimation flux, q_e ($\text{kgm}^{-2} \text{s}^{-1}$), i.e.

$$q_e = V_i I_s \quad (\text{E.13})$$

Here, V_i is determined by adjusting the sublimation flux for a 500 μm radius ice-sphere, V_s (s^{-1}), by the intercepted snow exposure coefficient, C_e i.e.

$$V_i = V_s C_e \quad (\text{E.14})$$

$$C_e = k \left(\frac{I_s}{I_{*s}} \right)^{-F} \quad (\text{E.15})$$

where k is a dimensionless coefficient indexing the shape of intercepted snow (i.e. age and structure) and F is an exponent value of approximately 0.4.

The ventilation wind speed, of intercepted snow, may be set as an observed within-canopy wind speed or approximated from the above-canopy wind speed by the following equation,

$$\mu_\xi = u_h e^{-\psi \xi} \quad (\text{E.16})$$

where $\mu_{\xi}(\text{ms}^{-1})$ is the estimated within-canopy wind speed, at a fraction ξ of the entire forest depth, u_h is the wind speed at the canopy top (ms^{-1}), and considered as the canopy wind speed extinction coefficient (κ), which is determined as a linear function of LAI' for various needleleaf species. The unloading of intercepted snow, to the sub-canopy snowpack, is calculated as an exponential function of time (Hedstrom and Pomeroy, 1998).

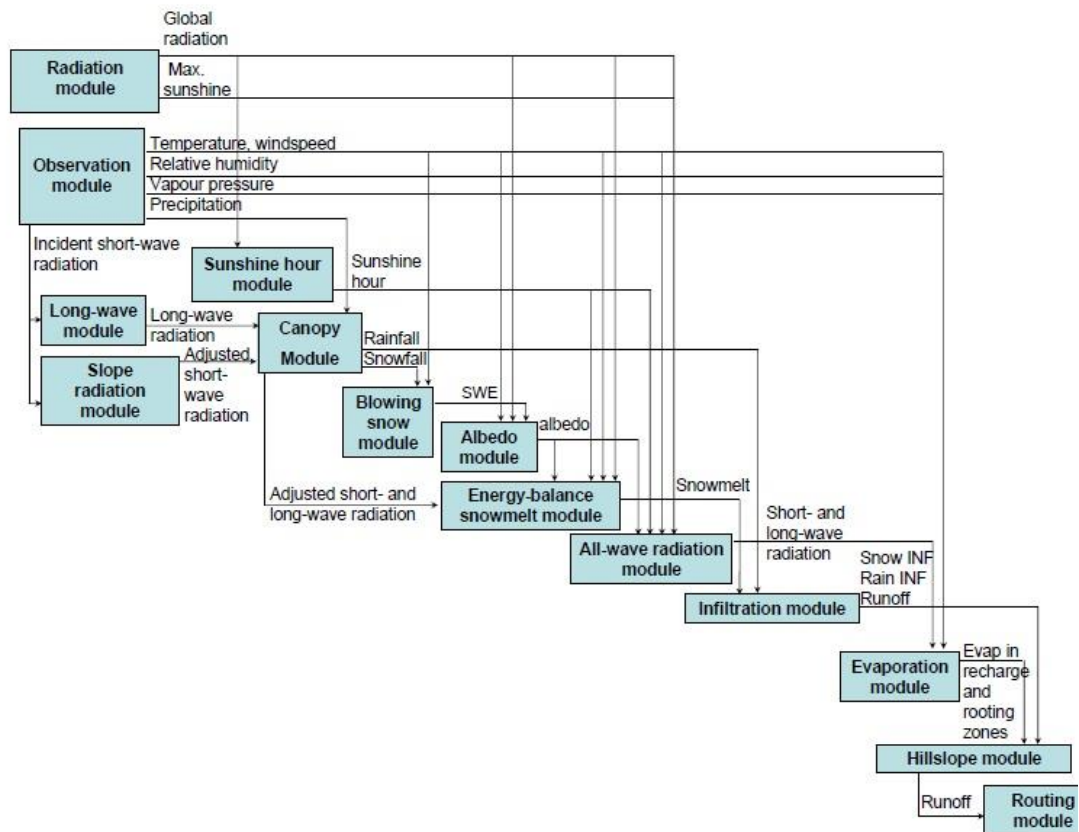


Figure E.1 Flowchart of physically-based hydrological modules used in the Humber River Basin Model (HRB).

Blowing snow module

This module simulates the inter-HRU wind redistribution of snow transport and blowing snow sublimation losses throughout the winter period. Blowing snow was found to be a major transport mechanism for snow, with redistribution causing snow water equivalent (*SWE*), accumulation on various landscape types within a basin with different accumulation level (Pomeroy et al., 2007).

$$\frac{dSWE}{dt}(x) = P - p \left[\nabla F(x) + \frac{\int E_B(x) dx}{x} \right] - E - M \quad (E.17)$$

Where $dSWE/dt$ is surface snow accumulation rate ($\text{kg m}^{-2} \text{s}^{-1}$), P is the snowfall rate ($\text{kg m}^{-2} \text{s}^{-1}$), p is the probability of blowing snow occurrence within the HRU, F is the downwind transport rate ($\text{kg m}^{-1} \text{s}^{-1}$), E is the snow surface sublimation rate ($\text{kg m}^{-1} \text{s}^{-1}$), E_B is the blowing snow sublimation rate ($\text{kg m}^{-1} \text{s}^{-1}$), and M is the snow melt rate ($\text{kg m}^{-2} \text{s}^{-1}$) (Pomeroy et al., 2007).

Snow mass-balance module

In CRHM, a single defined spatial unit, with changes in mass through a divergence of incoming and outgoing fluxes is considered as snow. Additionally, in clearing environments, the snow water equivalent (*SWE*) (kgm^{-2}) on the ground may be expressed in the following mass-balance of vertical and horizontal snow gains and losses, (Ellis et al., 2010)

$$SWE = SWE_0 + (P_s + P_r + H_{in} - H_{out} - S - M)t \quad (E.18)$$

where t is the time step in the model calculation, SWE_0 is the antecedent snow water equivalent (kgm^{-2}), P_s and P_r are the respective snowfall and rainfall rates, H_{in} is the

incoming horizontal snow transport rate, H_{out} is the outgoing horizontal snow transport rate, S is the sublimation loss rate, and M is the melt loss rate (all units $\text{kgm}^{-2}\text{t}^{-1}$) (Ellis et al., 2010).

In forest environments Eq. (1) is modified to

$$SWE = SWE_0 + (P_s - (I_s - U_l) + P_r - (I_r - R_d) - M)t \quad (\text{E.19})$$

where I_s is the canopy snowfall interception rate, U_l is the rate of canopy snow unloading, I_r is the canopy rainfall interception rate, and R_d is the rate of canopy rain drip (all units $\text{kgm}^{-2}\text{t}^{-1}$). The amount of snowfall intercepted by the canopy is dependent on various physical factors, including tree species, forest density, and the antecedent intercepted snowload (kgm^{-2}) (Ellis et al., 2010).

Rainfall interception and evaporation module

For snow forest interactions, winter rainfall may represent substantial water and energy inputs to snow. In this regard, the fraction of rainfall to sub-canopy snow, received directly through fall, is assumed to be inversely proportional to the fractional horizontal canopy coverage (C_c) (Ellis et al., 2010). Rainfall which is intercepted by the canopy may be lost through evaporation (E) ($\text{kgm}^{-2}\text{t}^{-1}$) or dripped to the sub-canopy, if the canopy rain storage (C_R) (mm) exceeds the maximum canopy storage (S_{max}). Additionally, the direct through fall and drip, to the sub-canopy, are added to the water equivalent of the snowpack. Evaporation from a fully-wetted canopy (E_p) ($\text{kgm}^{-2}\text{t}^{-1}$) is calculated by using the Penman-Monteith combination equation (Ellis et al., 2010).

$$E = C_c E_p \text{ for } C_R = S_{max} \quad (\text{E.20})$$

Again, in partially-wetted canopies E is reduced in proportion to the degree of canopy saturation, (Ellis et al., 2010).

$$E = \frac{C_c E_p C_R}{S_{max}} \text{ for } C_R < S_{max} \quad (\text{E.21})$$

Snow energy-balance module/ Energy-Budget Snowmelt Model

The energy balance of radiation, sensible heat, latent heat, ground heat, advection from rainfall, and change in internal energy was determined by the snow energy-balance module (Gray and Landine, 1988). In CRHM, the sum of radiative, turbulent, advective, and conductive energy fluxes to snow determined by following the equation, (Ellis et al., 2010).

$$K_* + L_* + Q_h + Q_e + Q_g + Q_p = \frac{dU}{dt} + Q_m = Q_* \quad (\text{E.22})$$

where energy for snowmelt (Q_m), the change in internal energy of snow ($\frac{dU}{dt}$), K_* , and L_* all represent net shortwave and long wave radiations, Q_h and Q_e are the net sensible and latent heat turbulent fluxes, Q_g is the net ground heat flux, and Q_p is the energy from rainfall advection (all units $\text{MJm}^{-2}\text{t}^{-1}$). The amount of melt (M) is calculated from Q_m by the following equation, (Ellis et al., 2010).

$$M = \frac{Q_m}{\rho_w B \gamma_f} \quad (\text{E.23})$$

where ρ_w is the density of water (kgm^{-3}), B is the fraction of ice in wet snow (0.95–0.97), and γ_f is the latent heat of fusion for ice (MJ kg^{-1}). When, Q_m is in (W m^{-2}), daily melt, M (mm day^{-1}) the relation can be approximated as,

$$M = 0.270Q_m \quad (\text{E.24})$$

Infiltration to frozen soils module

This module evaluates frozen soil infiltration (*INF*), during snowmelt and over-winter soil moisture changes. The infiltration algorithm estimates snowmelt infiltration into frozen soils and the Ayers' infiltration model (Ayers, 1959) estimates rainfall infiltration into unfrozen soils based on soil texture and ground cover. When snowmelt or rainfall exceeds the infiltration rate, surface runoff forms. The above mentioned algorithms were based upon 15 years of study on the snow hydrology of the prairie region of Canada (Gray *et al.*, 1986). The infiltration potential of frozen soils may be grouped in three broad categories, namely: restricted, limited, and unlimited. The derivation of equations defining the relationship between total snowmelt infiltration (*INF*, mm) and premelt *SWE* (mm) based on θ_p ,

$$INF = 5(1 - \theta_p)SWE^{0.584} \quad (\text{E.25})$$

Evaporation module/ Evapotranspiration module

Evapotranspiration is estimated by the following equation,

$$E = \frac{Q_E}{L_v} \quad (\text{E.26})$$

where *E* is Evapotranspiration, L_v is the latent heat of vapourization and Q_E is the evaporative heat flux. Again, Q_E is calculated using the algorithm of Granger and Pomeroy (1997), which is an extension of the Penman equation to unsaturated conditions under conditions with minimal advection Granger and Gray (1989).

$$Q_E = \frac{G(s(Q^* - Q_G) + C v d d_a / r_a)}{sG + \gamma} \quad (\text{E.27})$$

where C is the specific heat capacity of air ($\text{J kg}^{-1} \text{K}^{-1}$), $v d d_a$ is the vapour density deficit (kg m^{-3}), r_a is the aerodynamic resistance (s m^{-1}), s is the slope of the saturation vapour of density curve ($\text{kg m}^{-3} \text{K}^{-1}$), γ is the psychrometric constant ($\text{kg m}^{-3} \text{K}^{-1}$), G is the relative (saturated) evaporation (dimensionless), and D is the relative drying power (dimensionless). The terms G and D are found from

$$G = 1 / (0.793 + 0.2 \exp(4.902D)) + 0.006D \quad (\text{E.28})$$

$$D = \frac{L_v v d d_a / r_a}{(L_v v d d_a / r_a) + Q^* - Q_G} \quad (\text{E.29})$$

Soil moisture balance module

Soil moisture is required for running the multiple-year simulation for both frozen and unfrozen periods. Additionally, the maximum soil moisture storage, in the soil column was used to estimate the fall soil moisture status, which is an input for the initial fall soil saturation for the infiltration module. When snow cover is present, the input for this module is the infiltration (INF) generated by the snowmelt infiltration module. From the end of snow melt until late fall, INF is generated by the runoff module. The soil is handled as two layers. The top layer is called the recharge layer and represents the top soil and the lower soil layer is the recharge layer of surface infiltration. Evaporation (E_{SURFACE}) can only occur from the recharge layer; however water for transpiration ($Trans$) is withdrawn from the entire soil depth. Excess water from both soil layers satisfies the ground water flow (GW) before being discharged to the sub-surface flow (SSR). Field capacity is specified as a parameter representing the

maximum soil moisture (θ) capacity for the two layers. The wilting point (transpiration =0) occurs when the state variables soil recharge and the soil moisture content is equal to zero. The mass balance for the soil moisture module is

$$INF - GW - SSR - E_{SURFACE} - Trans - \Delta\theta = 0 \quad (E.30)$$

Soil & Hillslope module

This module was developed for calculating sub-surface flow and simulating groundwater-surface water interactions using physically-based parameters. This module was revised from an original soil moisture balance routine and calculates the soil moisture balance, groundwater storage, subsurface and groundwater discharge, depressional storage, and runoff for control volumes of two soil layers, a groundwater layer, and surface depressions. Evaporation does not withdraw soil moisture until canopy interception and surface water storage are exhausted. Groundwater recharge occurs through percolation from the soil layers or directly from depressional storage through macropores. Subsurface discharge occurs through horizontal drainage from either soil layer, groundwater discharge takes place through horizontal drainage in the groundwater layer. Surface runoff occurs if snowmelt or rainfall inputs exceed subsurface withdrawals from saturated soils or if the rate of snowmelt or rainfall exceeds the infiltration rate. The drainage factors for lateral flow in soil layers and groundwater layers (i.e. subsurface and groundwater discharges) as well as the vertical flow of excess soil water to groundwater (i.e. groundwater recharge) are estimated based on Darcy's flux. The Brooks and Corey (1964) relationship is used to calculate the unsaturated hydraulic conductivity.

Flow modules

These modules calculate subsurface drainage from hillslopes in organic-covered terrain, saturated permafrost, and relatively impermeable substrates, such as bedrock, dense clay, or transient ice lenses. This is based on Darcy's law. These studies formed the basis of a mass transport algorithm, where lateral subsurface runoff from each HRU, is computed from the HRU slope, and the transmission properties of the soils in the saturated layers (Quinton *et al.*, 2004). Since the frost table is relatively impermeable, the elevation of the saturated layer depends on the degree of soil thaw. The mass flow algorithm was therefore coupled to a heat flow routine to estimate the subsurface runoff from hillslopes during soil thawing. The cumulative average daily heat flux into the ground $\sum Q_g$ is estimated from its strong linear association with the cumulative average daily ground surface temperature $\sum T_s$. The modules then compute the fraction of $\sum Q_g$ used to lower the frost table $\sum Q_i$ based on the soil thermo-physical properties of the peat matrix at the thawing front. The increase in the depth to the impermeable frost table is then computed by converting $\sum Q_i$ into the equivalent cumulative depth of thaw dt .

$$\sum dt = \left(\frac{Q_i}{\rho_I h_f}\right) f_i \quad (\text{E.31})$$

where Q_i is in units of J m^{-2} , ρ_I is the density of ice, h_f is the latent heat of fusion, and f_i is the volume fraction of ice at the frost table, and f_i is equivalent to the porosity, ϕ (i.e. the soil is assumed to be saturated with ice).

Routing module

A routing module handles the movement of runoff, subsurface flow, and groundwater flow between HRU. The Muskingum routing method is based on a variable discharge-storage relationship (Chow, 1964) and is used to route runoff between HRUs in the sub-basins. The routing storage constant is estimated from the average distance from the HRU to the main channel and the average flow velocity; which is calculated by Manning's equation (Chow, 1959) based on the average HRU distance to the main channel, the average change in HRU elevation, and the overland flow depth and HRU roughness.

Appendix H List of Symbols

| | |
|------------|---|
| B | Fraction of ice in wet snow [] |
| C | Celsius [°] |
| C_{τ} | Fraction of horizontal canopy coverage [] |
| C_e | Intercepted snow exposure coefficient [] |
| C_l | “canopy-leaf contact area” per unit ground [] |
| C_p | Specific heat capacity of air [$\text{J kg}^{-1} \text{K}^{-1}$] |
| C_R | Canopy rain depth [mm] |
| E | Evaporation from a partially-wetted canopy [$\text{kgm}^{-2} \text{t}^{-1}$] |
| E_p | Evaporation from a fully-wetted canopy [$\text{kgm}^{-2} \text{t}^{-1}$] |
| e_a | Vapour pressure [kPa] |
| e_a | Mean mean daily vapour pressure [kPa] |
| F | Exponent value [] |
| h | Forest height [m] |
| H_{in} | Incoming horizontal snow transport rate [$\text{kgm}^{-2} \text{t}^{-1}$] |
| H_{out} | Outgoing horizontal snow transport rate [$\text{kgm}^{-2} \text{t}^{-1}$] hour [] |
| I_r | Canopy rainfall interception rate [$\text{kgm}^{-2} \text{t}^{-1}$] |

| | |
|-----------|---|
| $I_{r,o}$ | Canopy intercepted rainload [kgm^{-2}] |
| I_s | Canopy snowfall interception rate [$\text{kgm}^{-2} \text{t}^{-1}$] |
| $I_{s,o}$ | Canopy intercepted snowload [kgm^{-2}] |
| I_s^* | Species-specific maximum intercepted snowload [kgm^{-2}] |
| K | Intercepted snow shape coefficient [] |
| K | Degrees Kelvin [] |
| K | Shortwave irradiance [$\text{MJm}^{-2}\text{t}^{-1}$ or Wm^{-2}] |
| K_f | Sub-canopy shortwave irradiance [$\text{MJm}^{-2} \text{t}^{-1}$ or Wm^{-2}] |
| K | Reflected shortwave irradiance [$\text{MJm}^{-2}\text{t}^{-1}$ or Wm^{-2}] |
| K | Net shortwave radiation [$\text{MJm}^{-2}\text{t}^{-1}$ or Wm^{-2}] |
| L | Longwave irradiance [$\text{MJm}^{-2}\text{t}^{-1}$ or Wm^{-2}] |
| L_f | Sub-canopy longwave irradiance [$\text{MJm}^{-2}\text{t}^{-1}$ or Wm^{-2}] |
| L | Surface longwave exitance [$\text{MJm}^{-2}\text{t}^{-1}$ or Wm^{-2}] |
| L | Net longwave radiation [$\text{MJm}^{-2}\text{t}^{-1}$ or Wm^{-2}] |
| LAI' | Effective leaf area index [] |
| M | Snowmelt rate [$\text{kgm}^{-2} \text{t}^{-1}$] |

| | |
|----------|---|
| MB | Model bias index [] |
| ME | Model efficiency index [] |
| NSE | Nash-Sutcliffe efficiency [] |
| n | Number [] |
| P | Precipitation rate [$\text{kgm}^{-2} \text{t}^{-1}$] |
| P_r | Rainfall rate [$\text{kgm}^{-2} \text{t}^{-1}$] |
| P_s | Snowfall rate [$\text{kgm}^{-2} \text{t}^{-1}$] |
| Q_e | Canopy sublimation rate [$\text{kgm}^{-2} \text{t}^{-1}$] |
| Q_e | Net latent heat flux [$\text{MJm}^{-2}\text{t}^{-1}$ or Wm^{-2}] |
| Q_g | Net ground heat flux [$\text{MJm}^{-2}\text{t}^{-1}$ or Wm^{-2}] |
| Q_h | Net sensible heat flux [$\text{MJm}^{-2}\text{t}^{-1}$ or Wm^{-2}] |
| Q_m | Snowmelt energy [$\text{MJm}^{-2}\text{t}^{-1}$ or Wm^{-2}] |
| Q_n | Total net radiation to snow [$\text{MJm}^{-2}\text{t}^{-1}$ or Wm^{-2}] |
| Q_{nf} | Total net radiation to forest snow [$\text{MJm}^{-2}\text{t}^{-1}$ or Wm^{-2}] |
| Q_p | Energy from rainfall advection [$\text{MJm}^{-2}\text{t}^{-1}$ or Wm^{-2}] |
| Q^* | Net energy to snow [$\text{MJm}^{-2}\text{t}^{-1}$ or Wm^{-2}] |

| | |
|-----------|--|
| r_a | Aerodynamic resistance [sm^{-1}] |
| R_d | Canopy rain drip rate [$\text{kgm}^{-2} \text{t}^{-1}$] |
| RH | Relative humidity [%] |
| $RMSE$ | Root mean square error [unit variable] |
| S | Sublimation loss rate [$\text{kgm}^{-2} \text{t}^{-1}$] |
| S | Mean maximum snow load per unit area of branch [kgm^{-2}] |
| SWE | Snow water equivalent [kgm^{-2}] |
| SWE_O | Antecedent snow water equivalent [kgm^{-2}] |
| t | Time-step [variable] |
| T_a | Air temperature [°C or K] |
| T_b | Threshold ice-bulb temperature for snow unloading [°C] |
| T_f | Forest temperature [K] |
| T_{max} | Maximum daily air temperature [°C] |
| T_r | Rainfall temperature [°C] |
| u | Wind speed [ms^{-1}] |
| uh | Wind speed at canopy top [ms^{-1}] |

| | |
|-----------------|---|
| U_{mean} | Mean daily wind speed [ms^{-1}] |
| u_z | Within-canopy wind speed at depth z from canopy top [ms^{-1}] |
| U | Internal (stored) snow energy [$\text{MJm}^{-2}\text{t}^{-1}$] |
| U_L | Canopy snow unloading rate [$\text{kgm}^{-2}\text{t}^{-1}$] |
| V_i | Sublimation rate of intercepted snow [s^{-1}] |
| V_s | Simulated sublimation flux for a $500\mu\text{m}$ radius ice-sphere [s^{-1}] |
| x_{avg} | Average observed value [] |
| x_{obs} | Observed value [] |
| x_{sim} | Simulated value [] |
| α_s | Snow albedo [] |
| λ_f | Latent heat of fusion [MJ kg^{-1}] |
| λ_s | Latent heat of sublimation [MJ kg^{-1}] |
| D | Slope of saturation vapour pressure curve [kPaK^{-1}] |
| ε_f | Thermal emissivity of forest cover [] |
| ε_s | Thermal emissivity of snow [] |
| θ | Solar elevation angle [radians] |

| | |
|------------|---|
| ζ | Depth from canopy top (as a fraction of forest height) [] |
| ρ_a | Density of air [kgm^{-3}] |
| ρ_s | Density of snowfall [kgm^{-3}] |
| ρ_w | Density of water [kgm^{-3}] |
| σ | Stefan-Boltzmann constant [$\text{Wm}^{-2}\text{K}^{-4}$] |
| τ | Forest shortwave transmittance [] |
| ν | Sky view factor [] |
| ψ | Canopy wind speed extinction coefficient [] |
| ω_a | Specific mixing ratio of air [] |
| ω_s | Saturation mixing ratio of air [] |